Reactivity of copper(II) complexes with NO_X (X=1, 2): Development of NO_2 sensors

A Dissertation submitted to the
Indian Institute of Technology Guwahati as
Partial fulfillment for the Degree of
Doctor of Philosophy in Chemistry

Submitted by

Vikash Kumar
(Roll No. 10612227)

Supervisor

Prof. Biplab Mondal

Department of Chemistry
Indian Institute of Technology Guwahati

July, 2015

Dedicated to My Family
&
Friends…..

Statement

I hereby declare that this thesis entitled "**Reactivity of copper(II) complexes with NO_X (X=1, 2): Development of NO_2 sensors**" is the outcome of research work carried out by me under the supervision of Prof. Biplab Mondal, in the Department of Chemistry, Indian Institute of Technology Guwahati, India.

In keeping with the general practice of reporting scientific observations, due acknowledgements have been made whenever work described here has been based on the findings of other investigators.

July, 2015 **Vikash Kumar**

Certificate

This is to certify that Mr Vikash Kumar has been working under my supervision since July, 2010 as a regular Ph. D. Student in the Department of Chemistry, Indian Institute of Technology, Guwahati. I am forwarding his thesis entitled **"Reactivity of copper(II) complexes with NO_X (X=1, 2): Development of NO_2 sensors"** being submitted for the Ph. D. degree.

I certify that he has fulfilled all the requirements according to the rules of this institute regarding the investigations embodied in his thesis and this work has not been submitted elsewhere for a degree.

July, 2015 **Biplab Mondal**

Acknowledgements

This work would not have been possible without many people. In particular, I would like to express my deepest gratitude to:

First and foremost, I feel it as a great privilege in expressing my deepest and most sincere gratitude to my supervisor Prof. Biplab Mondal, for providing me the opportunity to conduct research in his group and giving me freedom in defining and carrying out my Ph.D; for his patience in correcting and reviewing my muddled drafts and helping me to improve my writing skills. My heart felt thanks to you sir for the unlimited support and patience shown to me. He has also created an indispensable environment for me to conduct my project work.

I am also thankful to my doctoral committee Chairman and members Prof. Bhisma K. Patel, Dr. Debasis Manna and Dr. Subhradip Ghosh for sparing their precious time to evaluate the progress of my work. I would also like to thank to other faculty members for their kind help in carrying out this work. I am also grateful to all the technical staff of the department without whose help I could not have completed this thesis.

I would like to acknowledge CSIR, India for financial support and IIT Guwahati for all the facilities that were made available to me. I thank CIF, IIT Guwahati for providing the facility of X-ray single crystal, LC-MS, X-band EPR and NMR facility.

It is an immense pleasure to thank my present lab mates Kanhu, Somnath, Hemanta, Kuldeep, Soumen and Baishakhi for their support and help as well as for making a pleasant environment in the laboratory to work. Thanks once again all of you for making my leisure time interesting and joyful. Also my sincere thanks to my lab seniors, Dr. Amardeep Singh, Dr. Moushumi Sarma, Dr. Pankaj Kumar and Dr. Aswini Kalita for their enormous help and support in my PhD life. I thank all the masters and summer research fellows of my lab, Tulika, Pritam, Ivy, Narayani, Najmul, Soham, Sayantani, Arpan, Hemrupa, Tarali,

Ayushree, Nimisha, Samarjit, Bhagyasmeeta, Arnab, Rini, Munmi, Dikshita, Banashree and Shyamalee to whom I have the opportunity to work.

My special thanks to my friends of IIT Guwahati Dr. N. K. Chatainya, Dr. Kiran Indukuri, Dr. B. Lakshman, Ajaz Ahmad Dar, Najbul, Sukhomoy, Jayanta, Rajesh, K. Radhakrishnan for their help and support during this long time of my research.

I am very grateful to my parents, my sisters, brother-in-laws, nephew and niece for their endless moral support, encouragement and motivation at difficult times.

Last but not least, I am greatly indebted to my wife Neha and my son Parth. They form the backbone and origin of my happiness. I would like to thank all others who are associated with my work directly or indirectly at IIT Guwahati for their help.

Vikash Kumar

Contents

Synopsis

The thesis entitled, "**Reactivity of copper(II) complexes with NO_X (X=1, 2): Development of NO_2 sensors**" is divided into six chapters.

Chapter 1: Introduction

Nitric oxide (NO) has attracted the attention of scientists since its discovery as an essential component in many physiological processes such as blood pressure control, neurotransmission and immune response etc.[1] Most of the roles played by NO in biology are attributed to the formation of nitrosyl complexes of the metallo-proteins, mostly iron or copper.[2] Subsequent reports have identified a number of disease states involving NO imbalances and such observations have stimulated extensive research activity into the chemistry, biology, and pharmacology of NO.[2, 3] For instance, in bioregulatory purposes, less than 1 μM concentration of NO has been reported to be produced in endothelium cells for blood pressure control;[4] however, during immune response, NO is produced at much higher concentration and under these conditions, reactive nitrogen species such as peroxynitrite anion [$ONOO^-$] and nitrogen dioxide (NO_2) may form which have immense physiological importance.[5] NO_2 is a strong lipophilic oxidant which can trigger lipid auto-oxidation[6] and oxidative nitration of aromatic amino acids, particularly tyrosine.[7] Protein tyrosine nitration has been observed in connection with numerous human diseases including neurodegenerative conditions.[8-15] NO_2 can be generated *via* several mechanisms in biological system, including the oxidation of NO by oxygen,[5] the decomposition of $ONOO^-$,[16] and the oxidation of nitrite (NO_2^-) by hydrogen peroxide (H_2O_2) catalyzed with peroxidases.[17] The reaction of metmyoglobin (metMb) with peroxynitrite leads to the formation of $Fe(III)^-OO$-NO, is the same species as is postulated for the reaction of oxyMb with NO.[18] Thus, the reactivity of NO and NO_2 with transition metal ions is of immense importance to understand the basic

chemistry involved in their generation and activation in biological processes. Thus thesis is focused on the study the NO_x reactivity of Cu(II) complexes with NO and NO_2.

First chapter of this thesis describes a general introduction of NO and NO_2 with respect to its structural and spectroscopic properties. Subsequent chapters will describe the reactivity of NO and NO_2 with various Cu(II) complexes, and finally the development of NO_2 sensors based on Cu(II) complexes.

Chapter 2: Nitric oxide reactivity of copper(II) complexes of tridentate amine ligands and role of chelate ring size

In our laboratory we have been involved in studying the NO reactivity of Cu(II) complexes of various N-donor ligands. In continuation of those studies, two copper (II) complexes, **2.1** and **2.2** with ligands $\mathbf{L_1}$ and $\mathbf{L_2}$, [$\mathbf{L_1}$ = N^1-(3-(dimethylamino)propyl)propane-1,3-diamine, $\mathbf{L_2}$ = N^1-(3-(dimethylamino)propyl)-N^3,N^3-dimethylpropane-1,3-diamine], respectively, have been synthesized. Complexes were characterized by various analytical techniques. The complexes **2.1** and **2.2** exhibited a broad *d-d* band having λ_{max} at 645 nm (ε, 108 M^{-1} cm^{-1}) and 692 nm (ε, 163 M^{-1} cm^{-1}) respectively. Both the complexes displayed one electron paramagnetism and characteristic signals in X-band EPR spectroscopy.

The NO reactivity of these complexes was studied in acetonitrile solvent. Unlike many other systems, the formation of [Cu^{II}-NO] intermediate was not observed for the present set of complexes. However, the intensity of the *d-d* band was found to decay gradually with time to a colorless solution (Figure 1a and 1b) suggesting the reduction of Cu(II) centres by NO. The observed rate constant at 298 K are 2.271×10^{-3} and 7.51×10^{-3} s^{-1}, respectively.

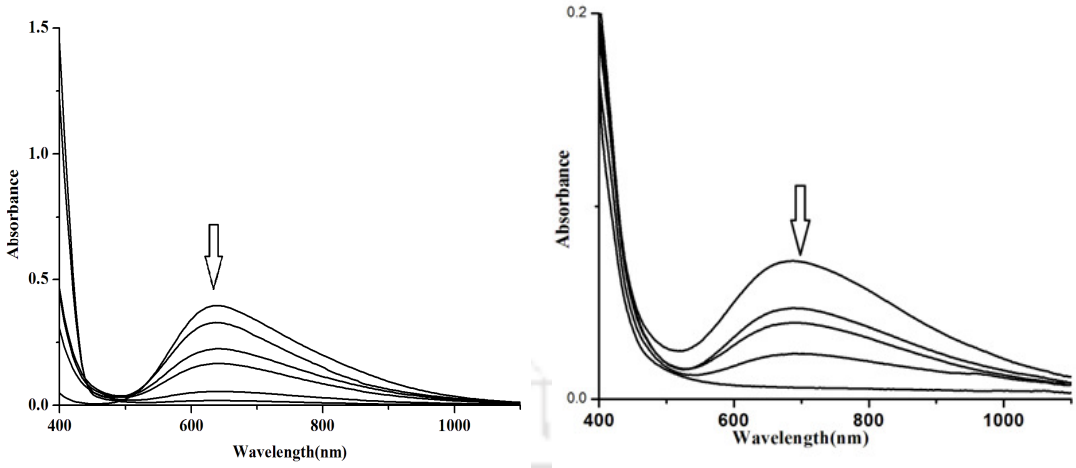

(a) **(b)**

Figure 1: UV-visible spectra of complexes (a) **2.1** and (b) **2.2** with NO in acetonitrile solvent at room temperature.

The reduction was further supported by ^{1}H-NMR and X-band EPR studies. The reduction was found to result with a simultaneous nitrosation at the secondary amine site of the ligands. The nitrosation products were isolated and characterized.

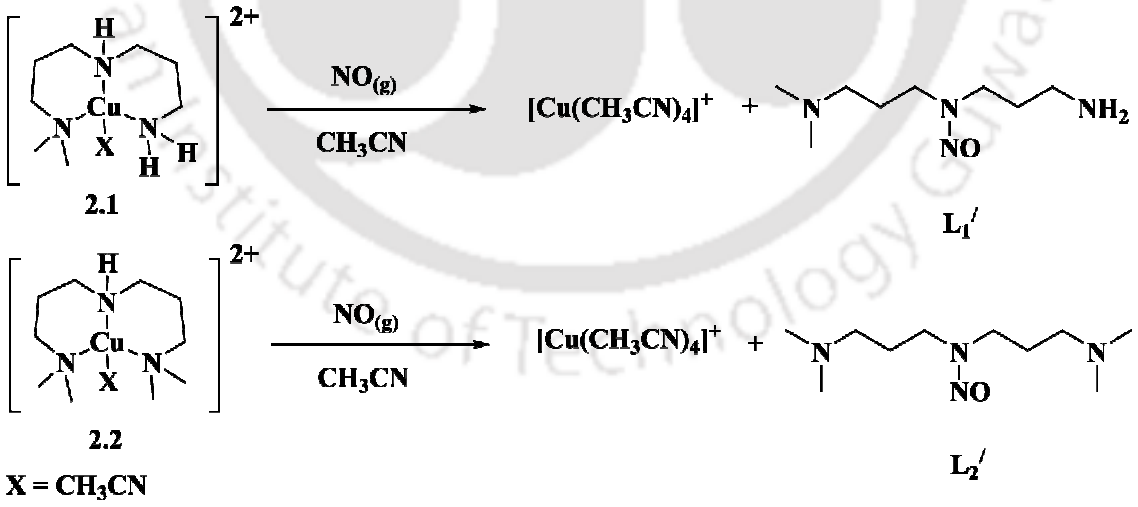

Scheme 1

Chapter 3: Phenol ring nitration induced by unprecedented reduction of the Cu(II) centre by nitrogen dioxide

Copper(II) complexes **3.1** and **3.2** were synthesized with ligand $\mathbf{L_3}$ [$\mathbf{L_3}$ = 2,4-di-tert-butyl-6-(((2-(dimethylamino)ethyl)(isopropyl)amino)methyl)phenol] and $\mathbf{L_4}$ [$\mathbf{L_4}$ = 6,6'-(((2-(dimethylamino)ethyl)azanediyl)*bis*(methylene))*bis*(2,4-di-*tert*-butylphenol)] as their acetate salt.

The single crystal structures of complexes **3.1** and **3.2** were determined. The perspective ORTEP view for **3.1** and **3.2** are shown in figure 2. In methanol solution complex **3.1** and **3.2** exhibit broad *d-d* band with λ_{max} at 675 nm and 702 nm, along with a relatively strong ligand to metal charge transfer absorption at 478 nm and 480 nm, respectively.

The addition of NO gas in the methanol solution of complex **3.1** was not found to react. However, addition of NO_2 gas into the degassed methanol solution of complex **3.1** was found to result in a color change to pale yellow.

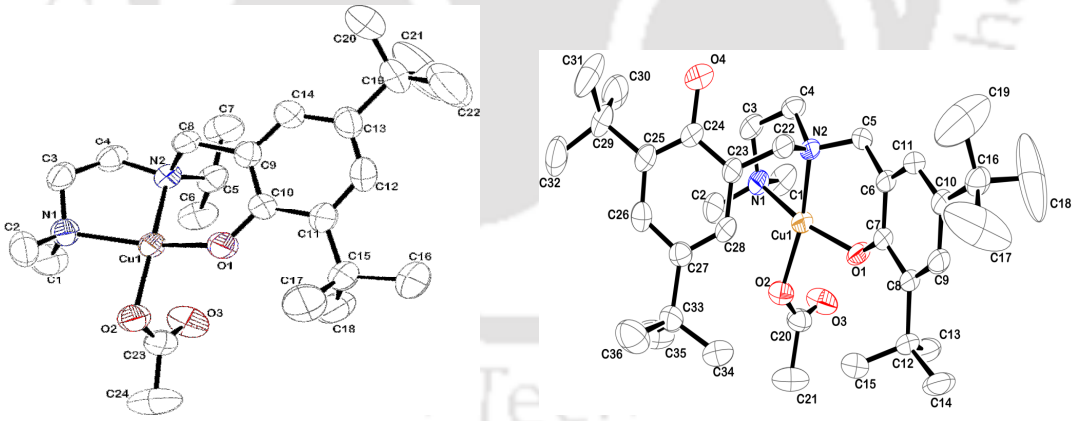

(a) **(b)**

Figure 2: ORTEP diagrams of complexes **3.1** and **3.2** (50% thermal ellipsoid plot, hydrogen atoms are omitted for clarity).

In the UV-visible spectra, the phenolato → Cu(II) charge transfer band at 478 nm as well as the *d–d* band were found to disappear upon reaction with NO_2. These observations are attributed to the reduction of the Cu(II) center by NO_2 (Figure 3). The reduction of Cu(II)

was further confirmed by the EPR silent nature of the colorless solution and from the ^{1}H-NMR spectral studies. Complex **3.2** was also found to behave in a similar way towards NO_2.

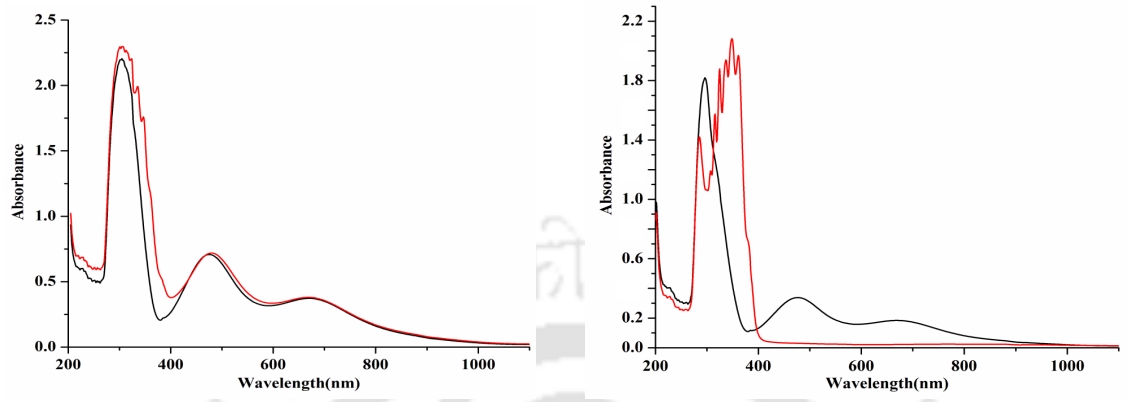

(a) **(b)**

Figure 3: UV-visible spectra of complex **3.1** (a) after purging NO and (b) **3.1** with NO_2 in methanol solution (complex **3.1** (black trace) and **3.1** after purging NO_2 (red trace).

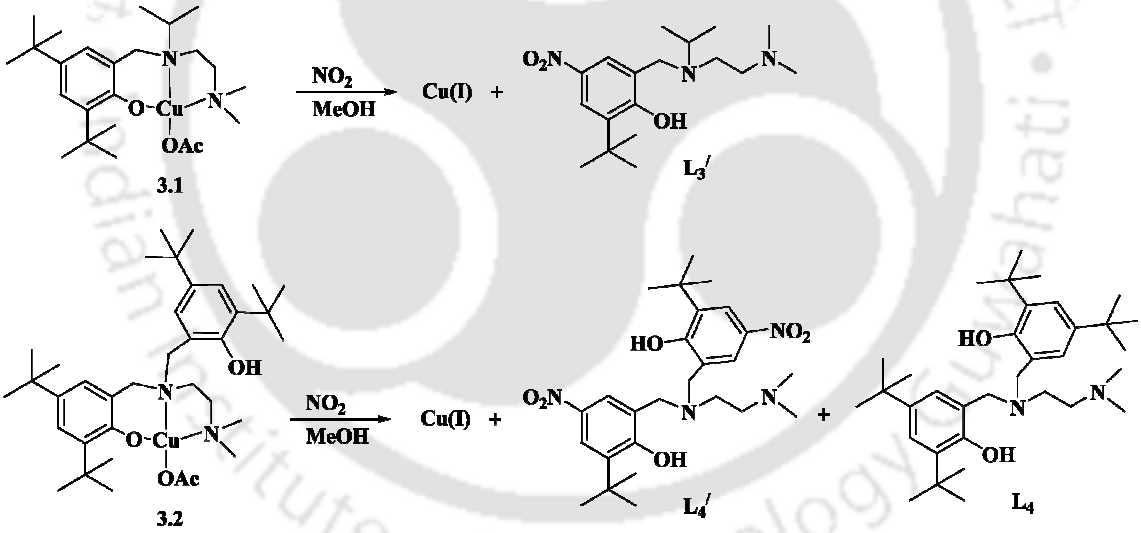

Scheme 2

The reduction was associated with simultaneous phenol ring nitration of the ligand framework. The phenol ring nitration takes place through an *ipso*-mechanism where the nitronium ion (NO_2^+), generated in the reduction of Cu(II) by NO_2, attacks at the 4-position of the phenol ring. This resulted in the corresponding 2-tertiary-butyl-4- nitrophenol.

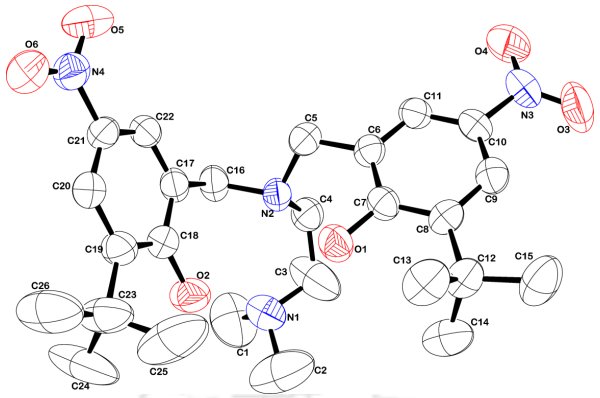

Figure 4: ORTEP diagram of modified ligand $\mathbf{L_4}'$ (50% thermal ellipsoid plot, hydrogen atoms are omitted for clarity).

The release of the tertiary-butyl cation in the process is confirmed from the presence of tertiary-butanol in the GC mass spectrum of the reaction mixture.

Chapter 4: Copper(II) mediated site specific phenol ring nitration by nitrogen dioxide

In this chapter, two Cu(II) complexes, **4.1** and **4.2** with $\mathbf{L_5}$ and $\mathbf{L_6}$ [$\mathbf{L_5}$ =2,6,6'-(((pyridin-2-ylmethyl)azanediyl)*bis*(methylene))*bis*(2,4-di-tert-butylphenol); $\mathbf{L_6}$ = 2,4-di-*tert*-butyl-6-(((3-(tert-butyl)-2-hydroxy-5-methylbenzyl)(pyridin-2-ylmethyl)amino)methyl)phenol], respectively, were synthesized and characterized. In the UV-visible spectroscopy, complex **4.1** displays an intense absorption band ~ 470 nm with weaker *d-d* transition near 675 nm in acetonitrile solution. The band centred at 470 nm is assigned as the phenolato → Cu(II) charge transfer; while the bands at lower wavelength are attributed to the intra-ligand transitions. In case of complex **4.2**, the transitions were found at 480 and 680 nm, respectively in acetonitrile. Addition of NO_2 in methanol solution of complexes **4.1** and **4.2**, resulted in green complexes, **4.3** and **4.4**, respectively. The complexes **4.3** and **4.4** were isolated as pure solid and characterized structurally. The ORTEP diagrams are shown in figure 5.

Since no indication of the reduction of Cu(II) centre in complexes **4.1** and **4.2** in methanol was observed in presence of NO_2, one could think of the possibility of a NO_2 induced

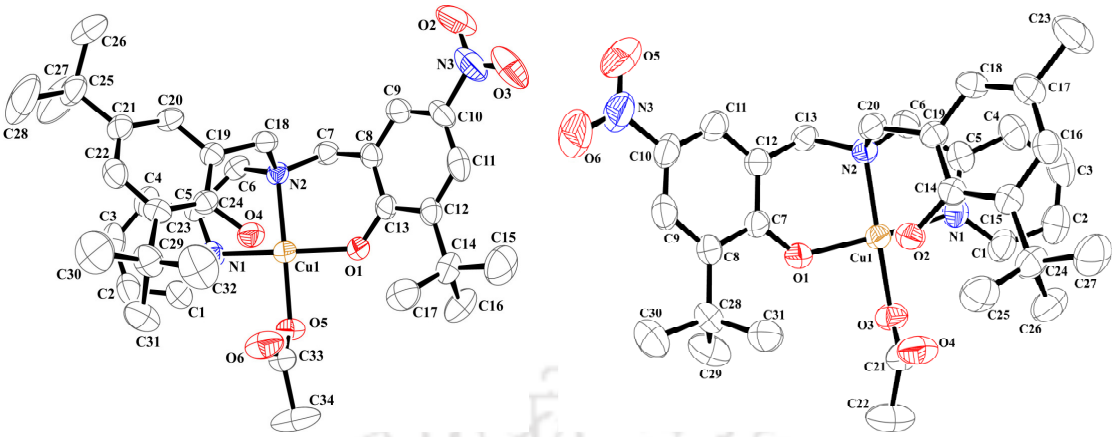

Figure 5: ORTEP diagrams of complexes **4.3** and **4.4** (50% thermal ellipsoid plot, hydrogen atoms are omitted for clarity).

phenoxyl radical formation in the reaction medium. However, in methanol solution, no intermediate was trapped in UV-visible spectroscopy even at -80 °C or in X-band EPR spectral study of the frozen reaction mixture. But in dry and degassed THF solution of complexes **4.1** and **4.2** at -80 °C temperature, addition of NO_2 resulted in a transient pale brown intermediate. In case of complex **4.1**, the phenolate →Cu(II) charge transfer band was immediately disappeared and a new bands at 365, 380 and 395 nm were appeared. On the other hand, addition of NO_2 in the THF solution of complex **4.1** at -80 °C followed by immediate freezing of the reaction mixture at 77 K, the solution became silent in X-band EPR spectroscopy suggesting the formation of a diamagnetic intermediate. This is attributed to the formation of corresponding phenoxyl radical complexes. It should be noted that the same compound **4.1** upon oxidation by Ce(IV) was reported to result in the phenoxyl radical complex.[19]

The presence of the *d-d* band in the UV-visible spectra of the reaction mixture ruled out the possibility of formation of Cu(I) species in the reaction. The crystal structures of the products i.e. complexes **4.3** and **4.4** revealed that in both the cases nitration occurred at the 4-position

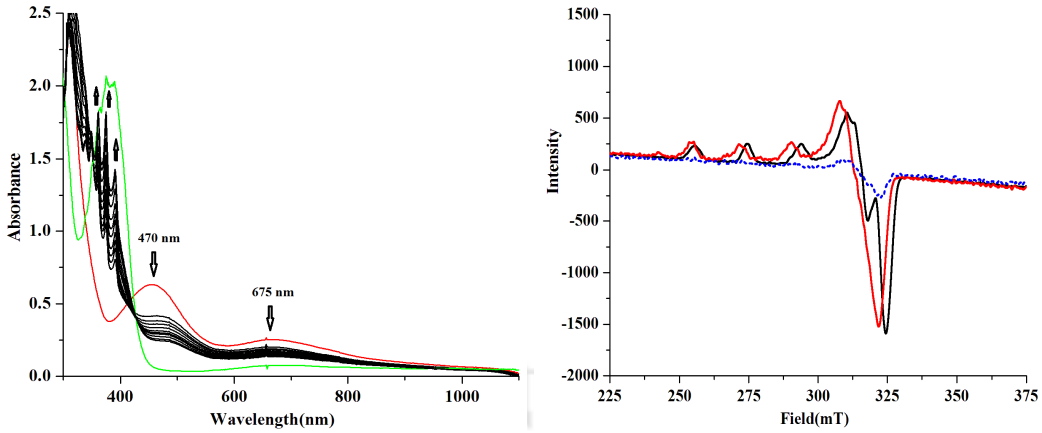

(a) **(b)**

Figure 6: (a) UV-visible spectra of complex **4.1** (red trace) after addition of NO_2 in dry THF medium at -80°C, (b) X-band EPR spectrum of complex **4.1** (black trace), phenoxyl radical intermediate (blue trace) and complex **4.3** (red trace) at 77 K in dry THF.

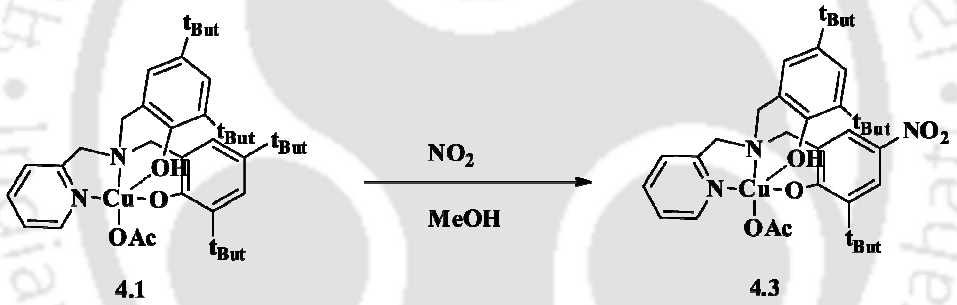

Scheme 3

of the phenolate ring which is coordinated to the Cu(II) centre at equatorial position. Since the free ligands were not observed to afford appreciable nitration in presence of NO_2, this supports the involvement of the Cu(II) centre in the radical formation mechanism; though exact role is not yet known. The selective nitration is perhaps because of the higher probability of Cu(II) induced formation of phenoxyl radical at the equatorial phenolate ring.

Chapter 5: A fluorescence turn-on probe for selective detection of nitrogen dioxide

In the previous chapter **3**, we observed that NO_2 selectively reduces the Cu(II) centres in complexes **3.1** and **3.2** over NO. This selective nature of reactivity of NO_2 instigates us to

develop the probe which can selectively detect NO_2. In this direction two Cu(II) complexes **5.1** and **5.2** with fluorophoric ligand $\mathbf{L_7}$ [$\mathbf{L_7}$ = 2-{[anthracen-9-ylmethyl-(2-dimethylamino-ethyl)-amino]-methyl}-4,6-di-tert-butyl-phenol]; $\mathbf{L_8}$ [$\mathbf{L_8}$ = 5-dimethylamino-naphthalene-1-sulfonic acid (3,5-di-tert-butyl-2-hydroxy-benzyl)-(2-dimethylamino-ethyl)-amide], respectively, were synthesized as their acetate salt. The single crystal structure of complex **5.1** was determined. The perspective ORTEP view for **5.1** is shown in figure 7.

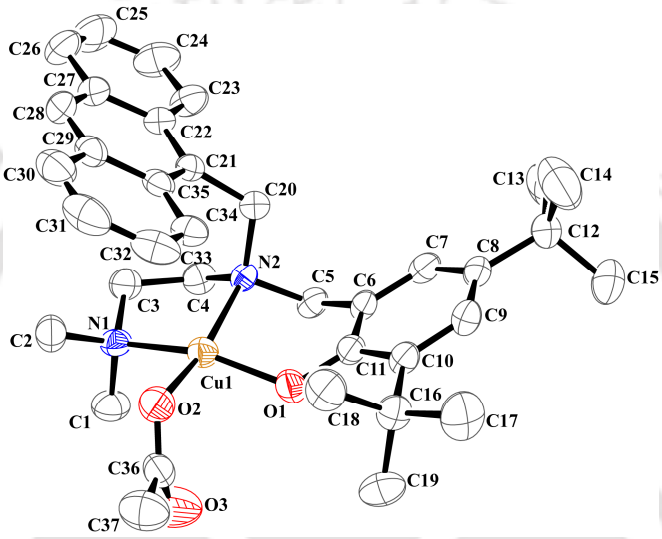

Figure 7: ORTEP diagram of complex **5.1** (50% thermal ellipsoid plot, hydrogen atoms are omitted for clarity).

In UV-visible spectrum, complexes **5.1** and **5.2** in methanol solution displayed the *d–d* transition at 665 nm and 685 nm, respectively. Both the complexes displayed one electron paramagnetism and characteristic signals in X-band EPR spectroscopy.

While NO is purged to the degassed methanol solution of the complexes, no change in fluorescence behavior was observed. This is in accord with earlier observation that the Cu(II) centre in these complexes does not react with NO. Addition of NO_2 to the degassed methanol solution of complexes **5.1** and **5.2** restored the quenched fluorescence intensity of the ligands (Figure 8). The restored emission intensity was found to be more in case of dansyl

fluorophore ($\mathbf{L_8}$) compared to $\mathbf{L_7}$. In case of complex **5.1**, the restored intensity was 3 ± 0.2 fold and in case complex **5.2**, it was 5 ± 0.2 fold.

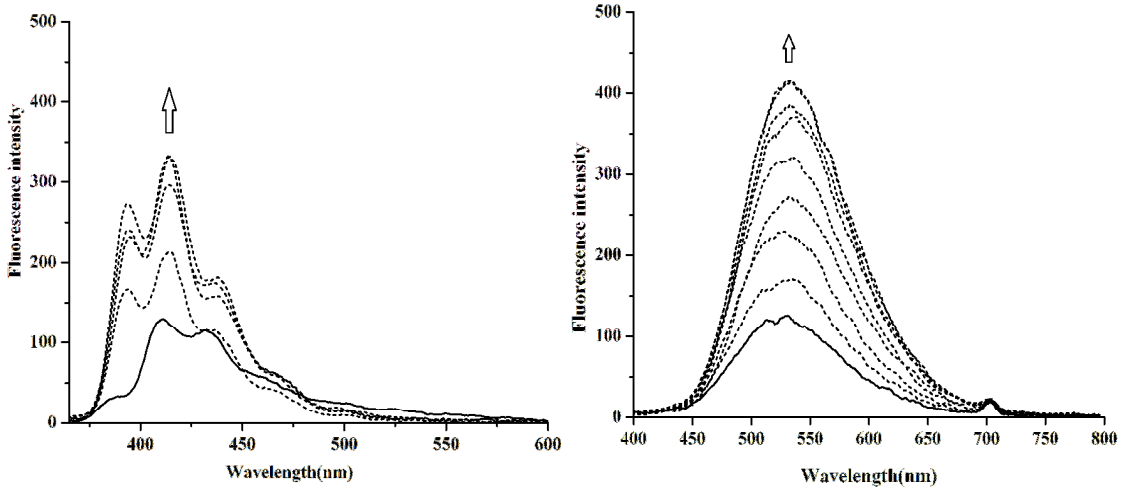

(a) **(b)**

Figure 8: Fluorescence responses (λ_{ex}, 350 nm) of deoxygenated methanol solution (20 μM) of complex **5.1** before (solid trace) and after (dashed trace) purging of NO_2 at 298 K. (b) Fluorescence responses (λ_{ex}, 354 nm) of deoxygenated methanol solution (20 μM) of complex **5.2** before (solid trace) and after (dashed trace) purging of NO_2 at 298 K.

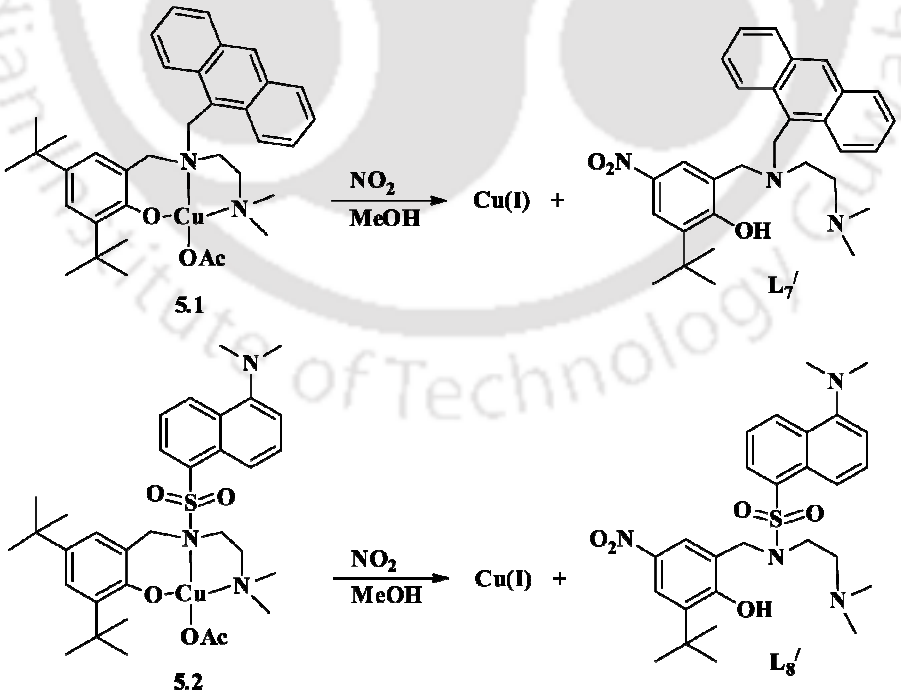

Scheme 4

The detection was observed even at 10 nmol concentration. Though addition of NO or O_2 alone in the degassed methanol solution of complexes did not make any difference, when NO was added in presence of O_2, the quenched fluorescence intensity of the respective ligands were restored.

The reduction was associated with a simultaneous phenol ring nitration of the ligand framework (Scheme 4). The nitrated ligands were isolated and characterized.

Chapter 6: A new NBD-based fluorogenic turn-on probe for selective detection of NO_2

In this chapter, Cu(II) complex **6.1** with tridentate ligands $\mathbf{L_9}$ [$\mathbf{L_9}$ = 7-nitro-N-(2-(pyridin-2-yl)ethyl)-N-(pyridin-2-ylmethyl)benzo[c][1,2,5]oxadiazol-4-amine], was synthesized as chloride salt. The complex was characterized by various spectroscopic techniques as well as by X-ray single crystal structure determination (Figure 9). The **6.1** exhibited a broad *d-d* band having λ_{max} at 768 nm (ε, 495 $M^{-1}cm^{-1}$) and the complex displayed one electron paramagnetism and characteristic signals in X-band EPR spectroscopy.

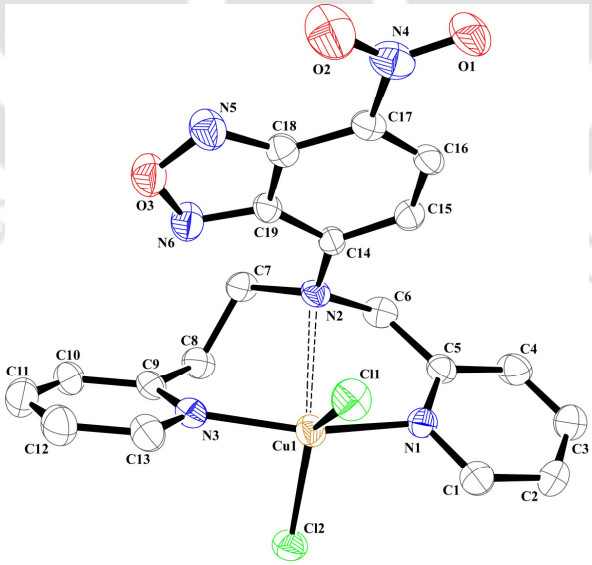

Figure 9: ORTEP diagram of complex **6.1** (50% thermal ellipsoid plot, solvent molecules are omitted for clarity).

Upon addition of NO_2 in degassed acetonitrile solution of complex **6.1**, rapid reduction of Cu(II) centre was observed. The reduction of Cu(II) centre has been monitored by UV-visible spectroscopy (Figure 10a). The *d-d* band centred at 768 nm disappears upon addition of NO_2 suggesting the formation of Cu(I) (Figure 10a). The reduction of Cu(II) in presence NO_2 has been further supported by the EPR silent nature of reaction mixture in X-band EPR study at room temperature (Figure 10b). Importantly, addition of NO in the degassed solution of complex **6.1** was not found to result in the reduction of the Cu(II) centre. However, addition of NO_2 was observed to reduce of Cu(II) with the formation of nitronium ion (NO_2^+). The nitronium ion (NO_2^+) generated in the reaction medium has an extremely short life time ($t_{1/2}$ ~ 1.4 ns) and it immediately gives nitrate and H^+ ions. These H^+ ions protonates $\mathbf{L_9}$ and the protonated ligand $(\mathbf{L_9H_2})^{2+}$ becomes free from the metal centre.

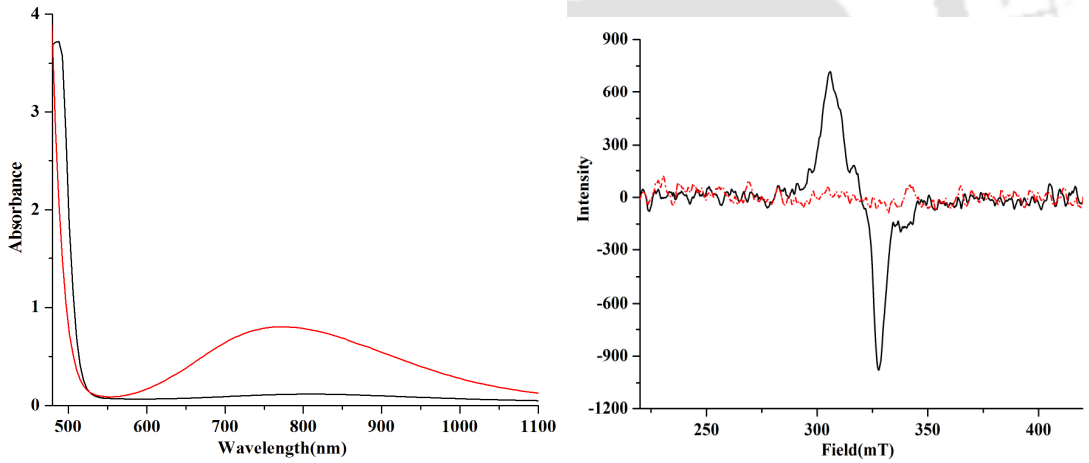

(a) **(b)**

Figure 10: (a) UV-visible spectra of complex **6.1** before (red trace) and after (black trace) purging NO_2 (b) X-band EPR spectra of complex **6.1** (black trace) and after purging NO_2 (red trace) at room temperature in acetonitrile medium.

The stretching band at ~1384 cm^{-1} in FT-IR spectrum reveals the formation of NO_3^- ions in the reaction mixture (Figure 11). The emission profile of $\mathbf{L_9}$ shows typical NBD based fluorescence at 536 nm. The fluorescence emission of $\mathbf{L_9}$ centred at 536 nm is found to

decrease (>90%) upon the addition of equivalent amount of Cu(II) ion in acetonitrile medium as shown in figure 12.

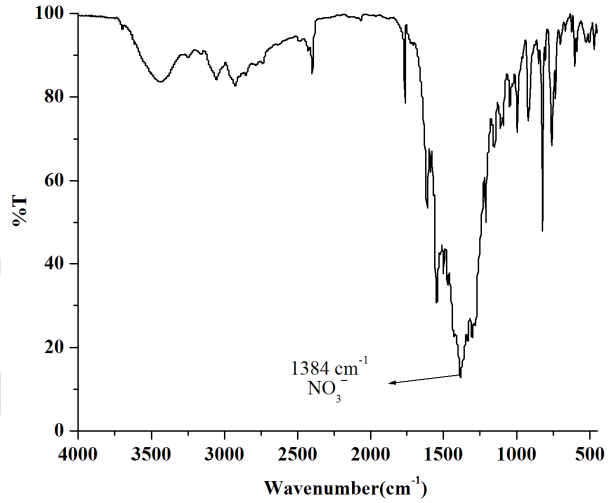

Figure 11: FT-IR spectrum of complex **6.1** after addition of NO_2 in acetonitrile medium.

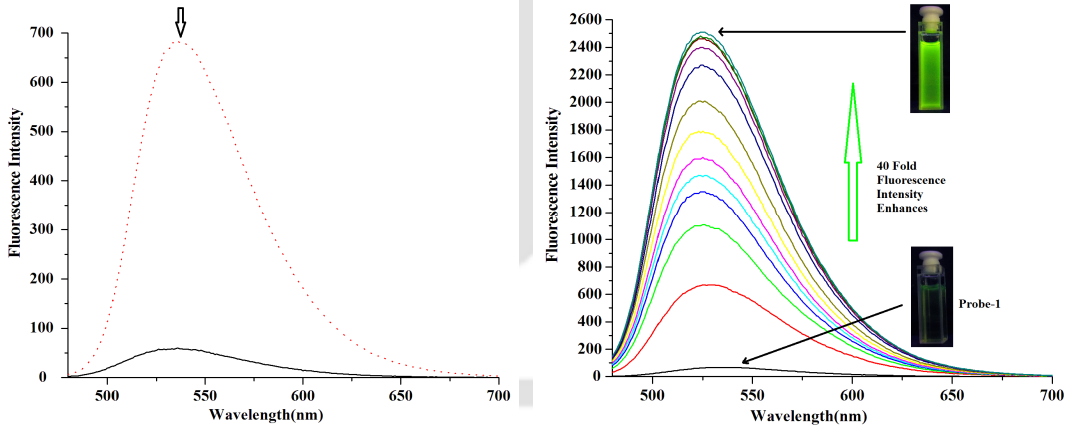

(a) **(b)**

Figure 12: (a) Fluorescence response (λ_{ex}, 470nm) for 5 μM solution of ligand $\mathbf{L_9}$ (dotted trace), and after addition of one equivalent of $CuCl_2.2H_2O$ (solid trace) (b) Fluorescence response (λ_{ex}, 470 nm) for 5 μM solution of deoxygenated solution of complex **6.1**(black trace) before and after addition of NO_2 in acetonitrile medium.

Addition of NO_2 gas in the 5 μM acetonitrile solution of complex **6.1** immediately resulted the enhancement in fluorescence intensity; within few seconds the fluorescence intensity reaches up to 40 (±1) folds.

The selectivity of complex **6.1** towards common reactive oxygen species (NO, NO_2, OH^-, O_2^-, O_2, NO_2^- and NO_3^-) in acetonitrile medium has been evaluated (Figure 13). Only NO_2 was found to increase the fluorescence intensity up to 40(±1) fold.

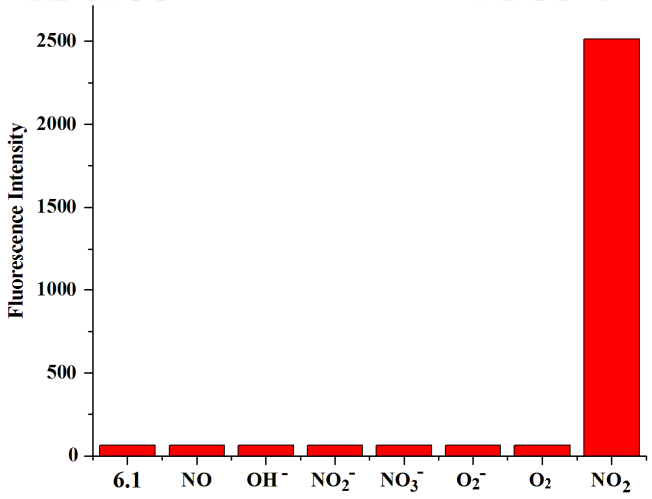

Figure 13: Fluorescence response of complex **6.1** selectively towards various ions/anions medium at room temperature in acetonitrile medium.

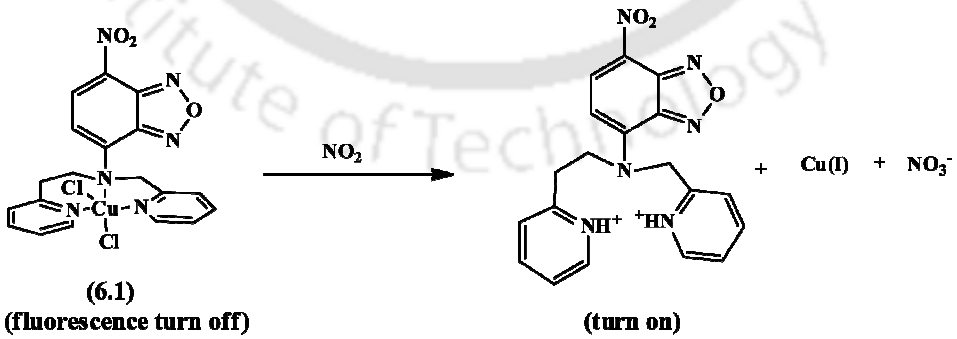

(6.1)
(fluorescence turn off)

(turn on)

Scheme 5

From the present study, it has been observed that complex **6.1** selectively reacts with NO_2, to turn on the quenched fluorescence intensity of the fluorogenic ligand. Thus, it can be used as selective sensor for NO_2.

References

1. Moncada, S.; Palmer, R. M. J.; Higgs, E. A. *Pharmacol. Rev.* **1991**, *43*, 109.
2. *Nitric Oxide: Biology and Pathobiology*; Ignarro, L. J., Ed.; Academic Press: San Diego, 2000.
3. *Nitric Oxide and Infection*; Fang, F. C., Ed.; Kluwer Academic/ Plenum Publishers: New York, 1999.
4. Ghosh, S.; Dey, A.; Usov, O. M.; Sun, Y.; Grigoryants, V. M.; Scholes, C. P.; Solomon, E. I. *J. Am. Chem. Soc*. **2007**, *129*, 10310.
5. Olbregts, J. *Int. J. Chem. Kinet.* **1985,** *17,* 835.
6. Cosby, K.; Partovi, K. S.; Crawford, J. H.; Patel, R. P.; Reiter, C. D.; Martyr, S.; Yanq, B. K.; Waclawiw, M. A.; Zalos, G.; Xu, X.; Huang, K. T.; Shields, H.; Kim-Shapiro, D. B.; Schechter, A. N.; Cannon, R. O.; Gladvin, M. T. *Nat. Med.* **2003,** *9,* 1498 – 1505.
7. Kirsch, M.; Korth, H. G.; Sustmann, R.; de Groot, H. *Biol. Chem.* **2002,** *383,* 389.
8. Beckman, J. S. *Arch. Biochem. Biophys.* **2009**, *484*, 114.
9. Ischiropoulos, H. *Arch. Biochem. Biophys.* **2009**, *484*, 117.
10. Ferrer-Sueta, G.; Radi, R. *ACS Chem. Biol.* **2009**, *4*, 161.

11. Abello, N.; Kerstjens, H. A. M.; Postma, D. S.; Bischoff, R. *J. Proteome Res.* **2009**, *8*, 3222.

12. Radi, R. *Proc. Natl. Acad. Sci. U.S.A.* **2004**, *101*, 4003.

13. Ischiropoulos, H. *Arch. Biochem. Biophys.* **1998**, *356*, 1.

14. Reynolds, M. R.; Berry, R. W.; Binder, L. I. *Biochemistry* **2007**, *46*, 7325.

15. Ascenzi, P.; di Masi, A.; Sciorati, C.; Clementi, E. *BioFactors* **2010**, *36*, 264.

16. Su, J.; Groves, J. T. *J. Am. Chem. Soc.* **2009,** *131,* 12979.

17. Bian, K.; Gao, Z. H.; Weisbrodt, N.; Murad, F. *Proc. Natl. Acad. Sci. U.S.A.* **2003,** *100,* 5712.

18. (a) Doyle, M. P.; Hoekstra, J. W. *J. Inorg. Biochem*. **1981**, *14*, 351. (b) Wade, R. S.; Castro, C. E. *Chem. Res. Toxicol*. **1996**, *9*, 1382.

19. Thomas, F.; Gellon, G.; Gautier- Luneau, I.; Saint-Aman, E.; Pierre, J. L. *Angew. Chem. Int. Ed.* **2002**, *41*, 3047.

Chapter 1

Introduction

1.1 General aspects of nitric oxide

Nitric oxide (NO) is one of the simplest molecule and chemists have studied its structure and reactivity for many years. In the past decade NO has attracted the attention of scientists as it is found to be an essential component in many physiological processes.[1] The activities of NO are now known to include roles in blood pressure control, neurotransmission, and immune response. Subsequent reports have identified a number of disease states involving NO imbalances and such observations have stimulated extensive research activity into the chemistry, biology, and pharmacology of NO. [2, 3] Most of the roles played by NO in biology is attributed to the formation of nitrosyl complexes of the metallo-proteins, mostly iron or copper. The best characterized example is the ferro-heme enzyme soluble guanylyl cyclise (sGC) .[4] Formation of a nitrosyl complex with Fe (II) leads to labilization of a *trans* axial (proximal) histidine ligand in the protein backbone, and the resulting change in the protein conformation is believed to activate the enzyme for catalytic formation of the secondary messenger cyclic-guanylyl monophosphate (cGMP) from guanylyl triphosphate (GTP). The enzymatic formation of cGMP leads to relaxation of smooth muscle tissue of blood vessels, hence lowering blood pressure. For bioregulatory purposes, NO concentrations generated are low and less than 1 μM have been reported to be generated in endothelium cells for blood pressure control .[5] Another example includes the catalytic cycle of bacterial copper containing nitrite reductase (Cu-NiRs) where a [Cu^{I}-NO^{+} ↔ Cu^{II}-NO] intermediate is known to involve in the conversion of NO_2^- to NO or, in some cases to N_2O (Scheme 1.1). [6-10]

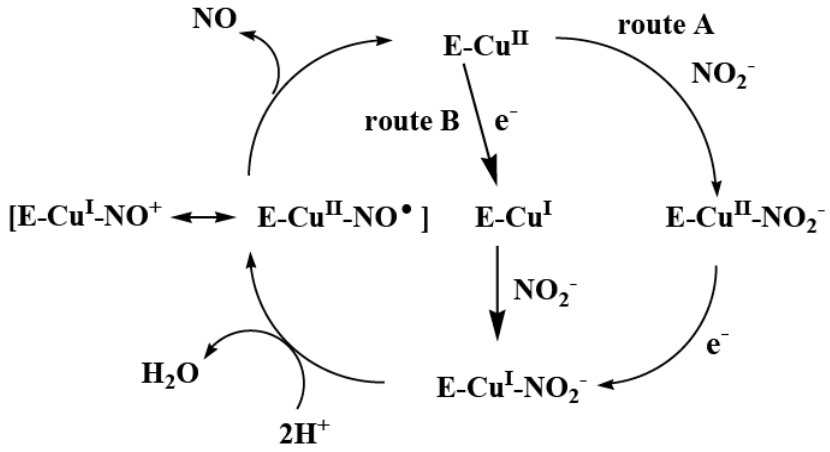

Scheme 1.1

Upon binding with a metal centre, the character of the NO ligand ranges from that of a nitrosyl cation (NO^+), which binds to the metal with an M-NO angle of ~180°, to that of a nitroxyl anion (NO^-), for which a bond angle of ~120°. The ability to form a stable NO complex and the structure of that species depend strongly on the oxidation state of the metal.[15] The binding of NO in these complexes is similar to the coordination of dioxygen to such metal centers, although the nitrosyl products are far more stable and easy to characterize than are their superoxo (O_2^-) analogues. The nitroprusside anion, $[Fe(CN)_5(NO)]^{2-}$ is perhaps the earliest discovered nitrosyl complex, and it remains the subject of intense research efforts.[11-14]

1.2 Copper (II) - nitrosyl

Several theoretical and matrix-isolation studies on Cu(II) – nitrosyl complexes have been reported.[15, 16] These investigations have suggested that N-bound nitrosyls are more stable than O-bound nitrosyls. Copper-containing zeolites have been found to form mono- and dinitrosyl species when exposed to NO.[17,18] Alcoholic solutions of CuX_2 (X = Cl, Br, F) were reported to absorb NO, generating deeply colored solutions that exhibit strong ν_{NO} in their solution IR spectra, but the structures of these are not known.[19-21] Another $\{CuNO\}^{10}$ complex reported is

$[Cu(NO)(H_2SO_4)_n]^{2+}$, though not properly characterized.[22] The lack of structural data for these complexes highlights the need for new Cu(II) - nitrosyls to be isolated and characterized. Cao and coworkers reported the formation of air-stable Cu(II)-nitrosyl and dinitrosyl species in the reaction of Cu(II)dithiocarbamates with NO in aqueous solution.[23] This was, perhaps, the first report of formation of air stable [Cu^{II}-NO] complex (Scheme 1.2).

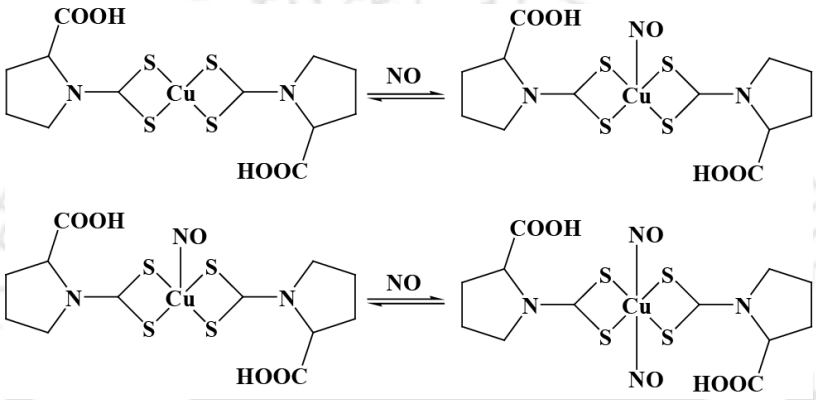

Scheme 1.2

In recent reports of reaction of NO with $[Cu(TEAEA)(CH_3CN)]^{2+}$, **1.1** and $[Cu(TIAEA)(CH_3CN)]^{2+}$, **1.2** { TEAEA = *tris*(2-ethylaminoethyl)amine; TIAEA = *tris* (2-isopropyl aminoethyl)amine} complexes , reduction of Cu(II) centre has been reported to

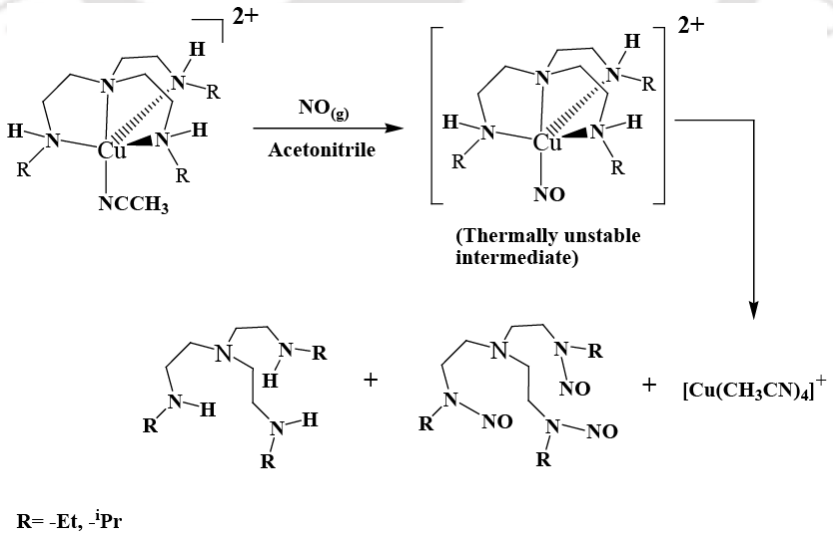

Scheme 1.3

proceed through the formation of a thermally unstable [Cu^{II}-NO] intermediate (Scheme 1.3).[24] The reaction was monitored by UV-visible, EPR and solution FT-IR spectroscopic studies. Spectral evidences for the formation [Cu^{II}-NO] intermediate has been reported in the reaction of NO with $[Cu(TAEA)(CH_3CN)]^{2+}$, **1.3** $[Cu(PYMEA)_2]^{2+}$, **1.4** and $[Cu(BAEA)(CH_3CN)]^{2+}$, **1.5** {TAEA = *tris*(2- aminoethyl)amine; PYMEA = pyridine-2-methylamine and BAEA = *bis*(2-amino ethyl)amine}complexes.[24,25]

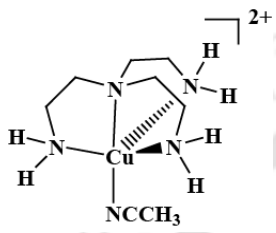

1.3

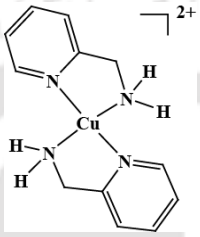

1.4

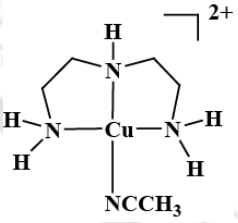

1.5

In the FT-IR spectra of the acetonitrile solutions of complexes **1.3**, **1.4** and **1.5** after addition of NO a new intense and sharp band appeared at ~1650 , 1642 and 1635 cm^{-1} , respectively. These were assigned as stretching of NO (ν_{NO}) coordinated to the copper (II) center.[24, 26]

1.3 General aspects of nitrogen dioxide

On the other hand, nitrogen dioxide (NO_2) is a simple triatomic, brown colored gas. The roles of NO_2 in mammalian biology are drawing increasing attention.[27-30] NO_2 is a strong lipophilic oxidant. It can trigger lipid auto-oxidation[31] and oxidative nitration of aromatic amino acids, particularly tyrosine.[32] Protein tyrosine nitration has been observed in connection with numerous diseases including neurodegenerative conditions, cardiovascular disorders, diabetes, and Alzheimer's disease.[33-40] Recent evidence suggests that protein nitration is an early event disease development, emphasizing its role in the etiology of these disorders.[39,41-43] It can be used as a diagnostic biomarker for several diseases states.[39,41-43]

NO_2 can be generated *via* several mechanisms in biological system, including the oxidation of NO by O_2,[44] the decomposition of $ONOO^-$,[45] and the oxidation of nitrite (NO_2^-) by hydrogen peroxide (H_2O_2) catalyzed with peroxidases.[46]

For instance, the reaction of metmyoglobin (metMb) with peroxynitrite (PN) leads to the formation of metMb-PN adduct, $Fe^{(III)}OO\text{-}NO^-$; Groves et al. reported that metMb catalyzes the decomposition of peroxynitrite to afford both nitrate and NO_2.[48]

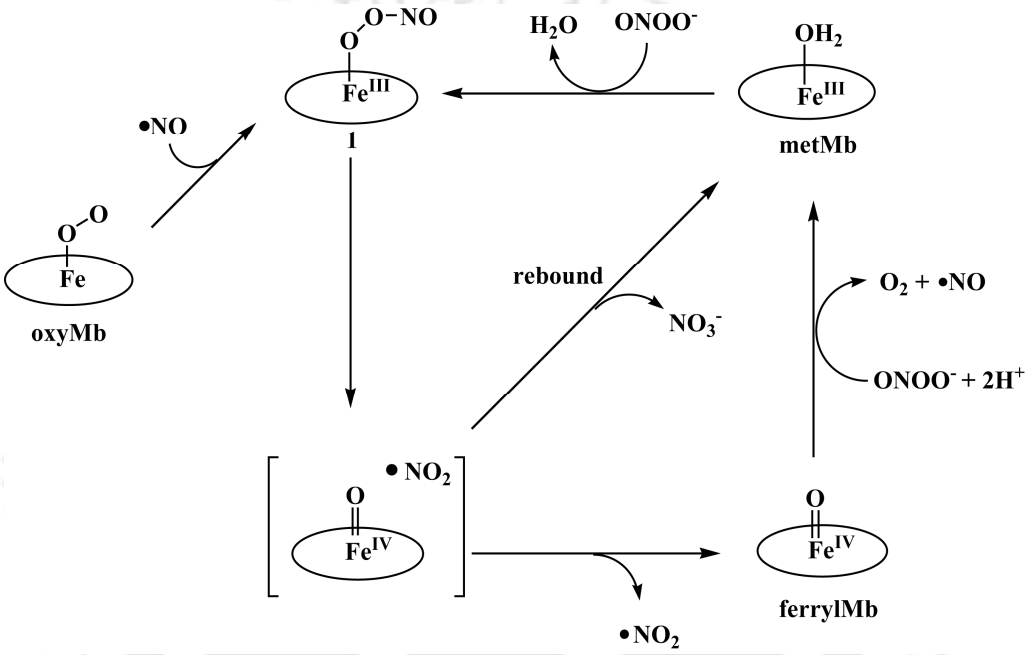

Scheme 1.4

Mitochondrial protein tyrosine nitration induced by MnSOD is a well-documented phenomenon under both basal and disease conditions.[49,50] Peroxynitrite-dependent MnSOD induced nitration results in a gradual alteration of mitochondrial redox homeostasis, which in turn further results in more enzyme inactivation, ultimately leading to mitochondrial dysfunction. In MnSOD induced tyrosine nitration Radi et al. proposed that this nitration involves three redox steps as follows. Where NO_2 and tyrosyl radical form and combine in subsequent step.[54]

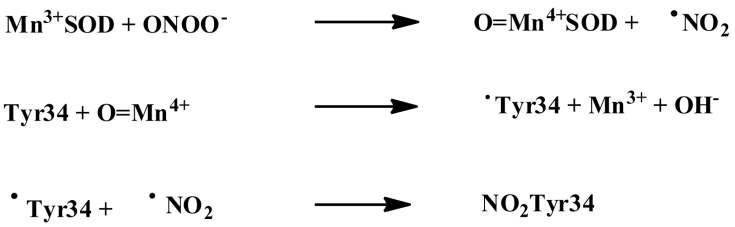

Scheme 1.5

Recent investigations have established that activation of various heme peroxidases (MPO or LPO) by H_2O_2 can promote oxidation of NO_2^- to the formation of NO_2 as intermediates that is capable of nitrating aromatic substrates and proteins.[55]

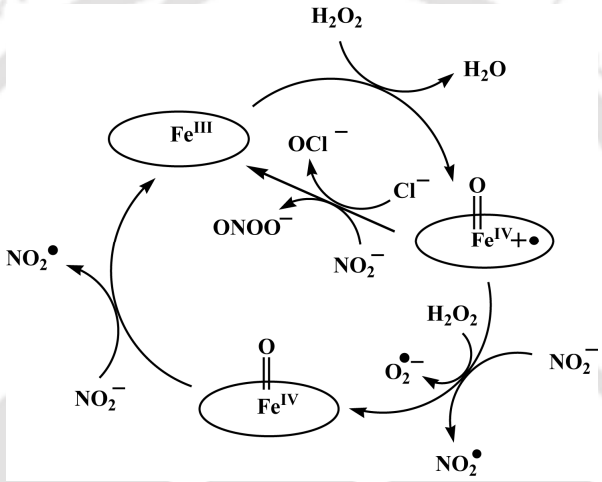

Scheme 1.6

Superoxide reacts with nitric oxide at a rate of 6.7×10^9 M^{-1} s^{-1}, to form the powerful oxidant peroxinitrite ($ONOO^-$).[56]

Girault et al has reported tyrosine nitration catalysed by cupric ions through a Fenton-like catalytic pathway which eventually leads to the formation of NO_2 and tyrosyl radical (Scheme 1.7).[57]

Recent evidences indicates that the mechanism of protein tyrosine nitration in biological systems is mediated by free radical reactions, implying the intermediacy of $Tyr^•$ and subsequent reactions with either NO or NO_2 (Scheme 1.8). There is no direct bimolecular

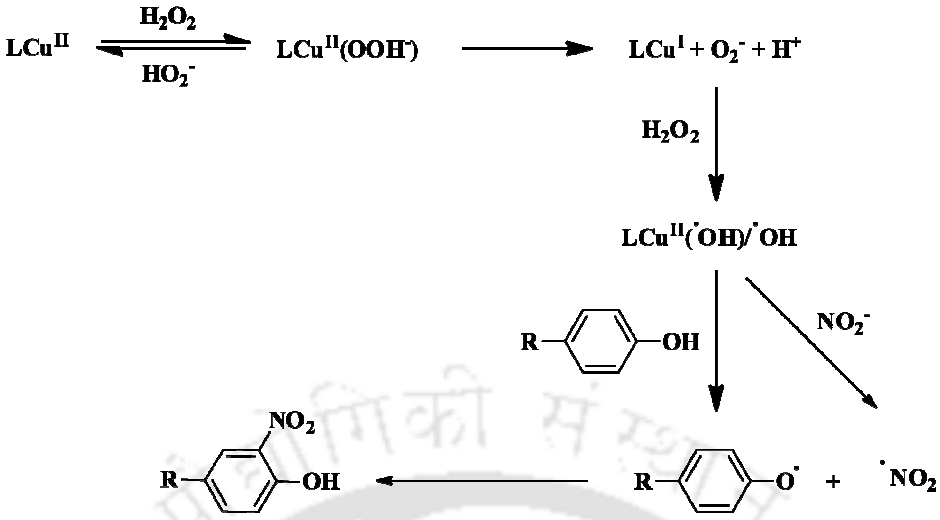

Scheme 1.7

reaction of tyrosine with peroxynitrite but rather a reaction with peroxynitrite-derived secondary species like NO_2 (Scheme 1.8).[54]

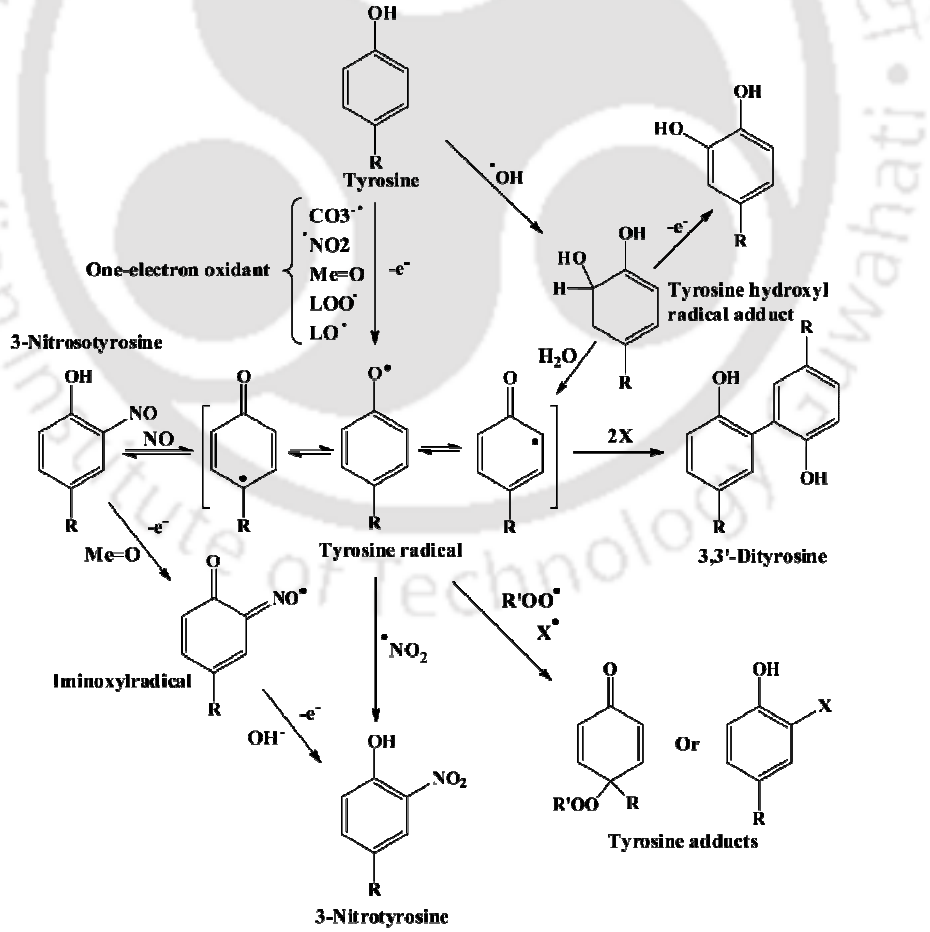

Scheme 1.8: The free radical pathways of tyrosine nitration.

Thus, NO_2 is identified as the key player in tyrosine nitration. Hence, its activation by metal ions has attracted enormous interest from chemists and biochemists.

1.4 Detection of nitrogen dioxide

Since NO_2 is believed to play the key roles in tyrosine nitration, a probe to detect NO_2 with spatio-temporal resolution is very much desirable to understand its reactivity in physiological process. However, there is a lack of selective fluorescent probes for convenient detection of NO_2. Most of the reported fluorescent probes are for NO detection. While probes based on transition-metal complexes contain a NO-reactive metal as a fluorescence quencher,[58–62] organic-dye-based probes detect NO indirectly through oxidation of aromatic amines by N_2O_3,[63,64] which is produced via oxidation of NO by O_2.[65,66]

Recently Huang et at reported the first example of metal based highly selective NO_2 sensor.

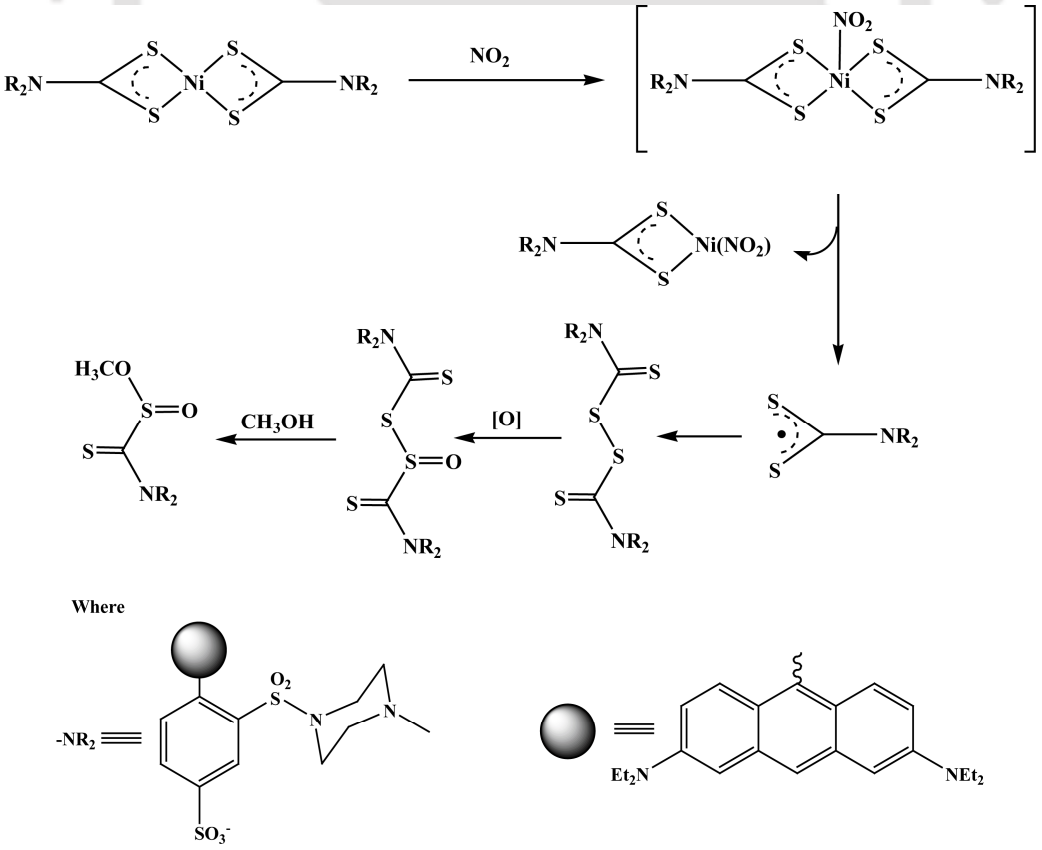

Scheme 1.9

They have synthesized complexes of Ni(II) with dithiocarbamate ligands derived from the *ortho* and *para* isomers of sulforhodamine B fluorophores. The *ortho* isomer showed much greater fluorescence increase in compare with *para* isomer, where mechanism behind the fluorescence quenching involves photoinduced electron transfer (PET) from the electron donor, Ni(II), to the sulforhodamine B excited state (Scheme 1.9). [67]

These results instigate us to study the NO and NO_2 reactivity of Cu(II) complexes with various

ligand frameworks with the target to establish the role of NO_2 in phenol ring nitration. The results presented in the proceeding chapters of the thesis will preliminary focus on:

- To study the role of chelate ring size on [Cu^{II}-NO] intermediate in reduction of Cu(II) by NO.
- Phenol ring nitration induced by reduction of Cu(II) centre by NO_2 .
- Cu(II) mediated site specific phenol ring nitration by NO_2.
- Development of a fluorescence turn-on probe for selective detection of NO_2.
- Development of a new NBD-based fluorogenic turn-on probe for selective detection of NO_2.

1.5 References

20. Moncada, S.; Palmer, R. M. J.; Higgs, E. A. *Pharmacol. Rev.* **1991**, *43*, 109.
21. *Nitric Oxide: Biology and Pathobiology*; Ignarro, L. J., Ed.; Academic Press: San Diego, 2000.

22. *Nitric Oxide and Infection*; Fang, F. C., Ed.; Kluwer Academic/ Plenum Publishers: New York, 1999.

23. (a) Kim, S.; Deinum, G.; Gardner, M. T.; Marletta, M. A.; Babcock, G. T. *J. Am. Chem. Soc.* **1996**, *118*, 8769 and references therein. (b) Burstyn, J. N.; Yu, A. E.; Dierks, E. A.; Hawkins, B. K.; Dawson, J. H. *Biochemistry* **1995**, *34*, 5896.

24. Ghosh, S.; Dey, A.; Usov, O. M.; Sun, Y.; Grigoryants, V. M.; Scholes, C. P.; Solomon, E. I. *J. Am. Chem. Soc*. **2007**, *129*, 10310.

25. Malinski, T.; Czuchajowski, C. *Methods in Nitric Oxide Research*; Feelisch M., Stamler, J. S., Eds.; John Wiley and Sons: Chichester, England, 1996; Chapter 22.

26. Tolman, W. B. *Adv. Chem. Ser.* **1995**, *246*, 195.

27. Ferguson, S. J. *Curr. Opin. Chem. Biol.* **1998**, *2*, 182.

28. Richardson, D. J.; Watmough, N. J. *Curr. Opin. Chem. Biol.* **1999**, *3*, 207.

29. Moura, I.; Moura, J. J. G. *Curr. Opin. Chem. Biol.* **2001**, *5*, 168.

30. Haskin, C. J.; Ravi, N.; Lynch, J. B.; Munck, E.; Que, L., Jr. *Biochemistry* **1995**, *34*, 11090.

31. Estrin, D. A.; Baraldo, L. M.; Slep, L. D.; Barja, B. C.; Olabe, J. A.; Paglieri, L.; Corongiu, G. *Inorg. Chem.* **1996**, *35*, 3897.

32. Nikol'skii, A. B.; Kotov, V. Y.; Vitalii, Y. *Mendeleev Commun.* **1995**, *4*, 139.

33. Go´mez, J. A.; Guenzburger, D. *Chem. Phys.* **2000**, *253*, 73.

34. Zhou, M. F.; Andrews, L. *J. Phys. Chem. A* **2000**, *104*, 2618.

35. Dobos, S.; Cesaro, S. N. *High Temp. Mater. Sci.* **1997**, *37*, 81.

36. Spoto, G.; Bordiga, S.; Scarano, D.; Zecchina, A. *Catal. Lett.* **1992**, *13*, 39.

37. Spoto, G.; Zecchina, A.; Bordiga, S.; Ricchiardi, G.; Martra, G.; Leofanti, G.; Petrini, G. *Appl. Catal. B* **1994**, *3*, 151.

38. Kohlschuetter, V.; Kutscheroff, M. *Chem. Ber.* **1904**, *37*, 3044.

39. Fraser, R. T. M.; Dasent, W. E. *J. Am. Chem. Soc.* **1960**, *82*, 348.

40. Fraser, R. T. M. *J. Inorg. Nucl. Chem.* **1961**, *17*, 265.

41. Tsumore, N.; Xu, Q. *Bull. Chem. Soc. Jpn.* **2002**, 75, 1861.

42. Diaz, A.; Ortiz, M.; Sanchez, I.; Cao, R.; Mederos, A.; Sanchiz, J.; Brito, F. *J. Inorg. Biochem.* **2003**, *95*, 283.

43. Sarma, M.; Singh, A.; Mondal, B. *Inorg. Chim. Acta* **2010**, *363*, 63.

44. Sarma, M.; Mondal, B. *Inorg. Chem.* **2011**, *50*, 3206.

45. Tennyson, A. G.; Lippard, S. J. *Chemistry & Biology* **2011**, *18,* 1211.

46. (a) Kirsch, M.; Korth, H. G.; Sustmann, R.; Groot, H. D. *Biol. Chem.* **2002**, *383,* 389. (b) Pfeiffer, S.; Mayer, B.; Hemmens, B. *Angew. Chem.* **1999**, *111,* 1824; *Angew. Chem.* **1999**, *38,* 1714.

47. Espey, M. G.; Xavier, S.; Thomas, D. D.; Miranda, K. M.; Wink, D. A. *Proc. Natl. Acad. Sci. U.S.A.* **2002**, *99,* 3481.

48. Pfeiffer, S.; Lass, A.; Schmidt, K.; Mayer, B. *FASEB J.* **2001**, *15,* 2355.

49. (a) Bryan, N. S.; Rassaf, T.; Maloney, R. E.; Rodriguez, C. M.; Saijo, F.; Rodriguez, J. R.; Feelisch, M. *Proc. Natl. Acad. Sci. U.S.A.* **2004**, *101,* 4308; (b) Rassaf, T.; Feelisch, M.; Kelm, M. *Free Radical Biol. Med.* **2004**, *36,* 413.

50. Cosby, K.; Partovi, K. S.; Crawford, J. H.; Patel, R. P.; Reiter, C. D.; Martyr, S.; Yanq, B. K.; Waclawiw, M. A.; Zalos, G.; Xu, X.; Huang, K. T.; Shields, H.; Kim-Shapiro, D. B.; Schechter, A. N.; Cannon, R. O.; Gladvin, M. T. *Nat. Med.* **2003**, *9,* 1498.

51. Kirsch, M.; Korth, H. G.; Sustmann, R.; de Groot, H. *Biol. Chem.* **2002**, *383,* 389.

52. Beckman, J. S. *Arch. Biochem. Biophys.* **2009**, *484*, 114.

53. Ischiropoulos, H. *Arch. Biochem. Biophys.* **2009**, *484*, 117.

54. Ferrer-Sueta, G.; Radi, R. *ACS Chem. Biol.* **2009**, *4*, 161.

55. Abello, N.; Kerstjens, H. A. M.; Postma, D. S.; Bischoff, R. *J. Proteome Res.* **2009**, *8*, 3222.

56. Radi, R. *Proc. Natl. Acad. Sci. U.S.A.* **2004**, *101*, 4003.

57. Ischiropoulos, H. *Arch. Biochem. Biophys.* **1998**, *356*, 1.

58. Reynolds, M. R.; Berry, R. W.; Binder, L. I. *Biochemistry* **2007**, *46*, 7325.

59. Ascenzi, P.; di Masi, A.; Sciorati, C.; Clementi, E. *BioFactors* **2010**, *36*, 264.

60. Reyes, J. F.; Reynolds, M. R.; Horowitz, P. M.; Fu, Y. F.; Guillozet- Bongaarts, A. L.; Berry, R.; Binder, L. I. *Neurobiol. Dis.* **2008**, *31*, 198.

61. Wattanapitayakul, S. K.; Weinstein, D. M.; Holycross, B. J.; Bauer, J. A. *FASEB J.* **2000**, *14*, 271.

62. Cruthirds, D. L.; Novak, L.; Akhi, K. M.; Sanders, P. W.; Thompson, J. A.; MacMillan-Crow, L. A. *Arch. Biochem. Biophys.* **2003**, *412*, 27.

63. Olbregts, J. *Int. J. Chem. Kinet.* **1985**, *17,* 835.

64. Su, J.; Groves, J. T. *J. Am. Chem. Soc.* **2009**, *131,* 12979.

65. Bian, K.; Gao, Z. H.; Weisbrodt, N.; Murad, F. *Proc. Natl. Acad. Sci. U.S.A.* **2003**, *100,* 5712.

66. (a) Doyle, M. P.; Hoekstra, J. W. *J. Inorg. Biochem.* **1981**, *14*, 351. (b) Wade, R. S.; Castro, C. E. *Chem. Res. Toxicol*. **1996**, *9*, 1382.

67. Bourassa, J. L.; Ives, E. P.; Marqueling, A. L.; shimanovich, R.; Groves, J. T. *J. Am. Chem. Soc.* **2001**, *123,* 5142.

68. Castro, L.; Demicheli, V.; Tortora, V.; Radi, *R. Free Radical Res.* **2011**, *45,* 37.

69. Radi, R.; Cassina, A.; Hodara, R.; Quijano, C.; Castro, L. *Free Radical Biol. Med.* **2002**, *33,* 1451.

70. MacMillan-Crow, L. A.; Crow, J. P.; Kerby, J.D.; Beckman, J. S.; Thompson, J. *Proc. Natl. Acad. Sci. U.S.A.* **1996**, *93,* 11853.

71. Quijano, C.; Hernandez-Saavedra, D.; Castro, L.; McCord, J. M.; Freeman, B. A.; Radi, R. *J. Biol. Chem*. **2001**, *276,* 11631.

72. Yamakura, F.; Taka, H.; Fujimura, T.; Murayama, K. *J. Biol. Chem.* **1998**, *273,* 14085.

73. Radi, R. *A. Chem. Rev.* **2013**, *46(2),* 550.

74. Vliet, A. V.; Eiserich, J. P.; Halliwell, B.; Cross, C. E. *J. Biol. Chem.* **1997**, *272,* 7617.

75. Eiserich, J. P.; Cross, C. E.; Halliwell, B.; Vliet, A. V. *J. Biol. Chem.* **1996**, *271,* 19199.

76. Qiao, L.; Lu, Y.; Liu, Baohong.; Grault, H. H. *J. Am. Chem. Soc.* **2011**, *133,* 19823.

77. Mondal, B.; Kumar, P.; Ghosh, P.; Kalita, A. *Chem. Commun*. **2011**, *47*, 2964.

78. Hu, X.; Wang, J.; Zhu, X.; Dong, D.; Zhang, X.; Wu, S.; Duan, C. *Chem. Commun*. **2011**, 47, 11507.

79. Rosenthal, J.; Lippard, S. J. *J. Am. Chem. Soc.* **2010**, *132*, 5536.

80. Lim, M. H.; Lippard, S. J. *Acc. Chem. Res.* **2007**, *40*, 41.

81. Wang, S. H.; Han, M. Y.; Huang, D. J. *J. Am. Chem. Soc.* **2009**, *131*, 11692.

82. Terai, T.; Urano, Y.; Izumi, S.; Kojima, H.; Nagano, T. *Chem. Commun.* **2012**, *48*, 2840.

83. Kojima, H.; Nakatsubo, N.; Kikuchi, K.; Kawahara, S.; Kirino, Y.; Nagoshi, H.; Hirata, Y.; Nagano, T. *Anal. Chem*. **1998**, *70*, 2446.

84. Chen, Y.; Guo, W.; Ye, Z.; Wang, G.; Yuan, J. *Chem. Commun*. **2011**, *47*, 6266.

85. Yang, Y.; Seidlits, S. K.; Adams, M. M.; Lynch, V. M.; Schmidt, C. E.; Anslyn, E. V.; Shear, J. B. *J. Am. Chem. Soc.* **2010**, *132*, 13114.

86. Yan, Y.; Krishnakumar, S.; Yu, H.; Ramishetti, S.; Deng, L. W.; Wang, S.; Huang, L.; Huang, D. *J. Am. Chem. Soc*. **2013**, *135,* 5312.

Chapter 2

Nitric oxide reactivity of copper(II) complexes of tridentet amine ligands and role of chelate ring size

Abstract

Two copper complexes, **2.1** and **2.2**, with tridentate N-donor ligands, $\mathbf{L_1}$ and $\mathbf{L_2}$ [$\mathbf{L_1}$ = N^1-(3-(dimethylamino)propyl)propane-1,3-diamine; $\mathbf{L_2}$ = N^1-(3-(dimethylamino)propyl)-N^3,N^3-dimethylpropane-1,3-diamine], respectively, have been synthesized and characterized. On exposure to nitric oxide (NO), the Cu(II) centres in complexes **2.1** and **2.2** were found to undergo reduction in acetonitrile medium. In acetonitrile medium the reduction was accompanied by a simultaneous N-nitrosation on the secondary amine centre on the ligand frameworks. The final organic products, in both the cases, were isolated and characterized by various spectroscopic studies.

2.1 Introduction

Activation of NO by transition metal ions has been a subject of interest for chemists and biochemists since its discovery to play various roles in mammalian biology.[1–6] Some of these activities are attributed to the formation of nitrosyl complexes of iron and copper-proteins.[1–3] Iron–nitrosyls, both in protein and synthetic model systems have been studied extensively.[7–13] The reduction of Cu(II) centres in some proteins, such as cytochrome c oxidase and laccase, to Cu(I) by nitric oxide though known for a long time, has not been studied as extensively as iron.[14–17] In recent years, however, this has been exemplified by a number of model Cu(II) complexes. For instance, Cu(II) centres in $[Cu(dmp)_2(X)]^{2+}$ (dmp = 2,9-dimethyl-1,10-phenanthroline, X = solvent) and analogous complexes were reported to undergo reduction by NO. From the detailed mechanistic study, reduction has been proposed to proceed through an inner-sphere pathway though the formation of $[Cu^{II}–NO]$ has not been observed even in the early stage of the reaction. It is observed that the reduction was accompanied by the nitrosation of the solvent resulting in methylnitrite or NO_2^- in the case of methanol or water, respectively (eqn (1)).[18,19]

$$[Cu(dmp)_2(X)]^{2+} + NO + CH_3OH \longrightarrow [Cu(dmp)_2]^{+} + CH_3ONO + H^{+} \qquad (1)$$

In methanol solution, the Cu(II) centre of the $[Cu^{II}(DAC)]^{2+}$ {DAC = 1,8-*bis(*9-anthracylmethyl) derivative of the macrocyclic tetraamine cyclam (1,4,8,11-tetraazacyclotetradecane)} was observed to be reduced by NO with a concomitant nitrosation of the ligand.[20] Detailed quantitative and theoretical studies suggested that the reaction proceeds through a pathway analogous to the inner-sphere mechanism for electron transfer between two metal centres through a bridging ligand where NO is the reductant, Cu(II) the oxidant and the coordinated anion behaves as the bridging ligand (Scheme 2.1).

The coordination preference of Cu(I) and the decreased donor ability of the nitrosated ligand resulted in the demetallation of the macrocyclic ring after the reduction. A similar mechanistic

pathway was reported by Armor et al. in the reaction of $[Ru(NH_3)_6]^{3+}$ with NO in alkaline solution resulting in the Ru(II)–dinitrogen complex, $[Ru(NH_3)_5(N_2)]^{2+}$.[21] Nitrosation of a coordinated amide ligand with the concomitant reduction of Ru(III) to Ru(II) leads to the formation of a coordinated nitroso amine, which on subsequent dehydration results in the coordinated dinitrogen complex.

Wayland and others suggested an alternative mechanism, more close to that of ferriheme reduction, which involves the initial NO coordination to the Cu(II) centre to form $[Cu^{II}–NO \leftrightarrow Cu^{I}–NO^{+}]$.[22] In successive steps, amine deprotonation and migration of NO^{+} to the coordinated amide would result into the nitrosoamine. Subsequently, demetallation from the ligand will occur.

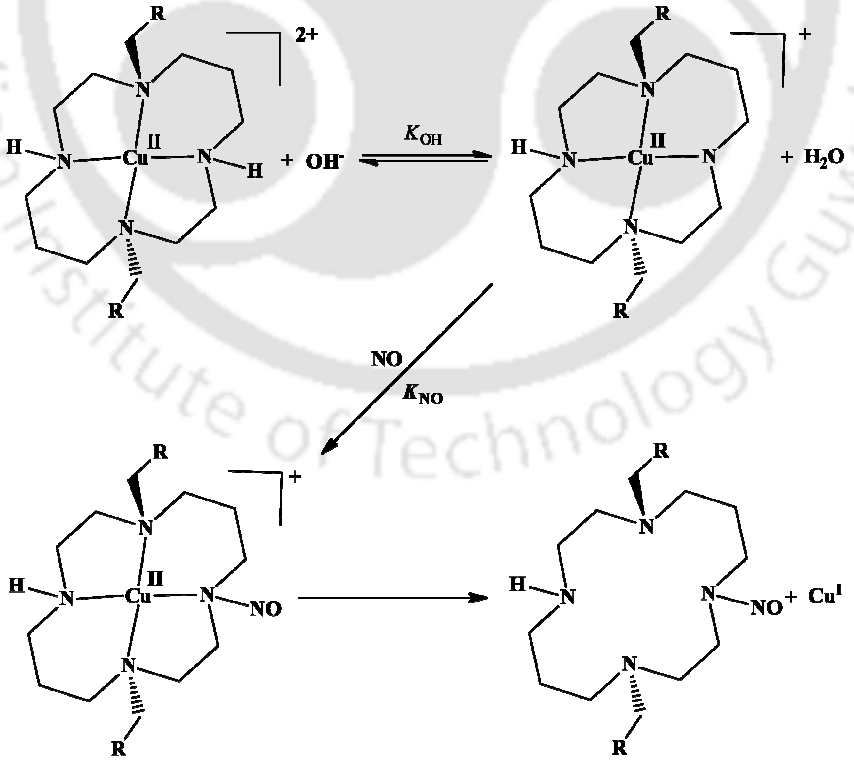

Scheme 2.1

In our recent studies, with $[Cu^{II}(tren)(CH_3CN)]^{2+}$, $[Cu^{II}(taea)(CH_3CN)]^{2+}$, $[Cu^{II}(tiaea)(CH_3CN)]^{2+}$, $[Cu(pymea)_2]^{2+}$ and $[Cu^{II}(baea)(CH_3CN)]^{2+}$ [tren = *tris*-(2-aminoethyl)amine; taea = *tris*-(2-ethylaminoethyl)amine; tiaea = *tris*-(2-isopropylaminoethyl)-

amine; pymea = pyridine-2-methylamine and baea = *bis*-(2-aminoethyl)amine], the reduction was found to proceed through the formation of a thermally unstable [Cu^{II}–NO] intermediate.[23] It should be noted that in the case of Cu(II) complexes of ppmea and mimpea [ppmea, 2-(pyridin-2-yl)-N-((pyridin-2-yl)methyl)-ethaneamine; mimpea, N-((methyl-1H-imidazol-2-yl)methyl)-2-

(pyridine-2-yl)ethanamine], any indication of the formation of a [Cu^{II}–NO] inner-sphere complex has not been observed prior to the reduction.[24] This is attributed to the much lower values of the equilibrium constants, K_{NO} (eqn (2)) as reported earlier in the case of $[Cu(dmp)_2(X)]^{2+}$.[19]

$$[(L)_2Cu^{II}]^{2+} + NO \underset{}{\overset{K_{NO}}{\rightleftharpoons}} [(L)_2Cu^{II}(NO)]^{2+} \qquad (2)$$

This difference in mechanistic pathway is, mostly, because of the difference in ligand environment. This has been exemplified in the cases of $[Cu(mtad)]^{2+}$ and $[Cu(tmd)_2]^{2+}$ [mtad = 5,5,7,12,12,14-hexamethyl-1,4,8,11-tetraazacyclotetradecane, tmd = 5,5,7-trimethyl-[1,4]-diazepane].[25] It was found that in case of $[Cu(mtad)]^{2+}$, the reduction takes place in methanol medium in the presence of sodium methoxide through a deprotonation pathway as reported earlier in the case of $[Cu(DAC)]^{2+}$. On the other hand, the reduction was observed to be very facile in dry acetonitrile in the case of $[Cu(tmd)_2]^{2+}$ and proceeds through a [Cu^{II}–NO] intermediate. Thus, it was noticed that though the copper(II) complexes with macrocyclic ligands prefer a deprotonation pathway, ones with non-macrocyclic ligands prefer a [Cu^{II}–NO] intermediate pathway which is similar to that observed in the ferriheme reduction. DFT

calculations also suggested the facile formation of a [Cu^{II}–NO] intermediate for $[Cu(mtad)]^{2+}$. Hence, it is logical to believe that the ligand frameworks have a significant role to control the mechanistic pathway for the reduction of Cu(II) by NO.

In this direction, as a continuation of our earlier work, two Cu(II) complexes with ligands $\mathbf{L_1}$ and $\mathbf{L_2}$ [$\mathbf{L_1}$ = N^1-(3-(dimethylamino)propyl)propane-1,3-diamine, $\mathbf{L_2}$ = N^1-(3-(dimethylamino)propyl)-N^3,N^3-dimethylpropane-1,3-diamine] (Figure 2.1) have been prepared and their NO reactivity have been studied.

Figure 2.1: Ligands used for the present study.

2.2 Results and discussion

Complexes **2.1** and **2.2** were synthesized by the reaction of copper(II) perchlorate hexahydrate with the respective ligands in a 1 : 1 ratio. Both the complexes were isolated as solid. They displayed satisfactory elemental analyses (Experimental section). They were characterized by various spectroscopic methods (Experimental section and Appendix I). The *d–d* transition for complexes **2.1** and **2.2** appears with λ_{max} at 645 nm (ε, 108 M^{-1} cm^{-1}) and 692 nm (ε, 163 M^{-1} cm^{-1}), respectively, in acetonitrile solvent. This shift in λ_{max} in the cases of complexes **2.1** and **2.2** is due to the increasing order of covalent character of the σ-bond on moving from an H to an ethyl group at the N-substitution.[26] Both the complexes displayed axial EPR spectra at room temperature, characteristic for the square planar copper(II) complexes having a $d_{x^2-y^2}$ ground state.[27] The complexes were found to exhibit one electron paramagnetism at room temperature.

2.3 Nitric oxide reactivity

Purging of excess NO to the degassed acetonitrile solution of complexes **2.1** and **2.2** resulted in the rapid reduction of the Cu(II) centre to Cu(I). The reduction was monitored by UV-visible spectroscopy and figures 2.3(a) and (b) represent the observed spectral change during the reaction. The *d-d* bands at 645 and 692 nm in the case of complexes **2.1** and **2.2**, respectively, were found to diminish in intensity suggesting the reduction of Cu(II) centre to Cu(I) (Figure 2.2). In the presence of excess NO, the reduction of Cu(II) to Cu(I) was found to follow simple first-order kinetics in acetonitrile medium and the rate behaviour was observed to be independent of the initial concentration of the complexes. The observed rate constants at 298 K for complexes **2.1** and **2.2** are 2.271×10^{-3} and 7.51×10^{-3} s^{-1}, respectively. The striking difference between the these two cases and the present ones is, in the case of $[Cu(dmp)_2(H_2O)]^{2+}$ and $[Cu(phen)_2(H_2O)]^{2+}$, the reduction was observed only in presence of

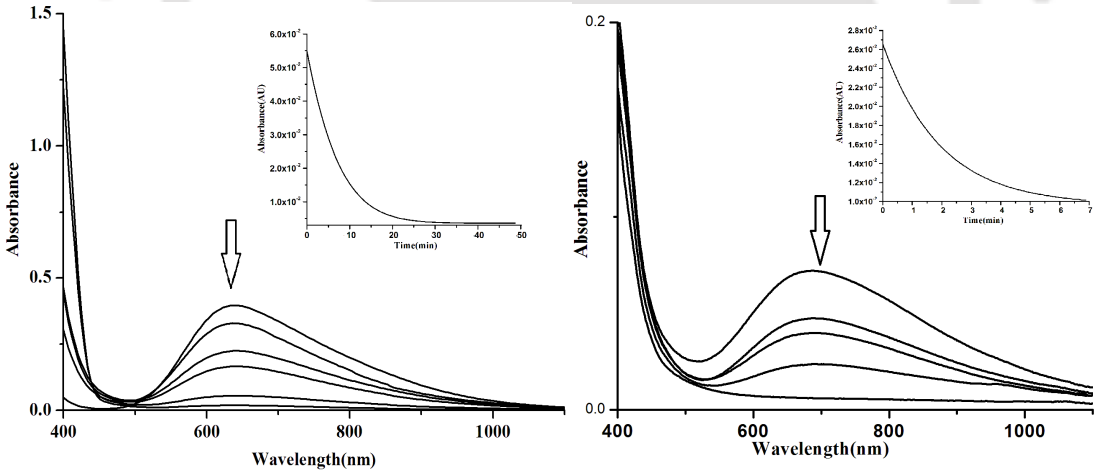

Figure 2.2: UV-visible spectra of complexes (a) **2.1** and (b) **2.2** with NO in acetonitrile solvent at room temperature. Inset: Time-scan plot for the reduction of Cu(II) centre at room temperature.

a protic solvent, but not in pure acetonitrile and dichloromethane.[29,18] On the other hand, the Cu(II) centres in $[Cu(tren)(CH_3CN)]^{2+}$, $[Cu(tiaea)(CH_3CN)]^{2+}$ and $[Cu(teaea)(CH_3CN)]^{2+}$

[tren = *tris*(2- aminoethyl)amine; tiaea = *tris*(2-isopropylaminoethyl)amine and teaea = *tris*(2-ethylaminoethyl)amine] were found to undergo reduction in the presence of NO in pure

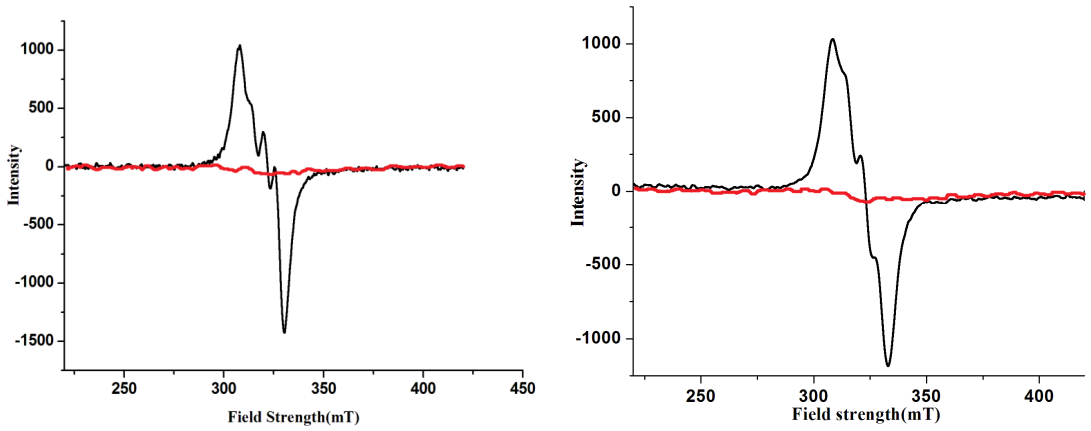

(a) **(b)**

Figure 2.3: X-band EPR spectra of complexes (a) **2.1** and (b) **2.2** before (black trace) and after (red trace) reaction with NO in acetonitrile solution at room temperature.

acetonitrile also.[23a, b] In these cases, the reduction was accompanied with either the N-nitrosation or the diazotization of the primary amine centre of the ligand followed by ligand transformation.[23a, b] In the present cases, the reduction in acetonitrile medium, led to the N-nitrosation of the ligand (Scheme 2.2).

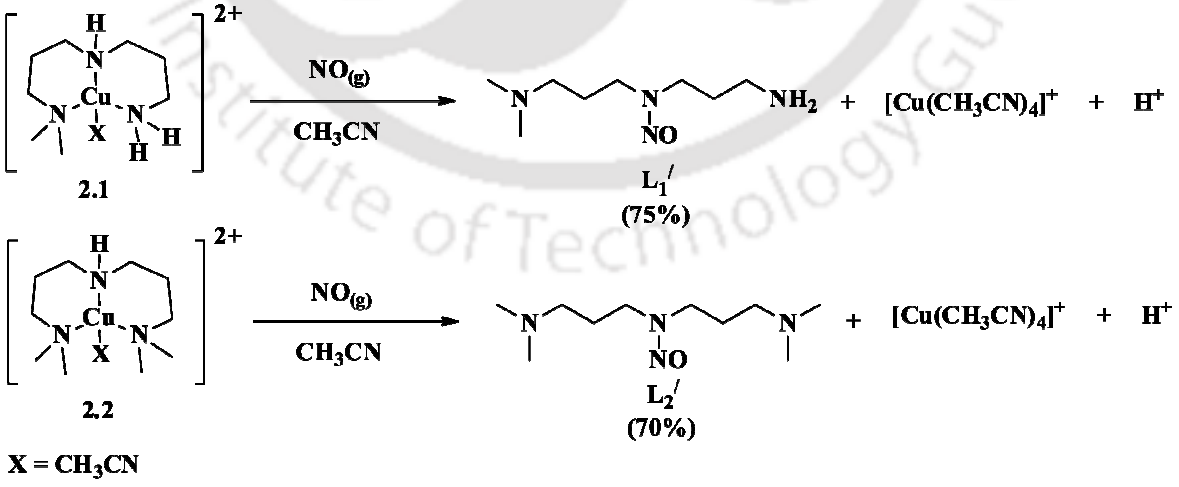

Scheme 2.2

The N-nitrosation was reported in case of $[Cu(DAC)]^{2+}$ also (DAC = 1,8-*bis*(9-anthracylmethyl)-derivative of the macrocyclic tetraamine cyclam).[20,11a] The reduction of Cu(II) centres by NO in complexes **2.1** and **2.2** can be rationalized by an inner-sphere mechanism involving three steps: (i) reversible displacement of the solvent by NO from the coordination sphere of copper(II) leading to the formation of a inner-sphere $[Cu^{II}–NO]$ intermediate; (ii) nucleophilic attack of H_2O or CH_3OH (in the case of water and methanol media) or the generation of highly electrophilic NO^+ owing to $[Cu^{II}–NO \leftrightarrow Cu^{I}–NO^+]$ charge distribution followed by the (iii) release of NO_2^- (or CH_3ONO) or N-nitrosated ligand. Step three, perhaps, became more facile owing to the geometrical preference of Cu(I) complexes for tetrahedral coordination. In our earlier studies with $[Cu(tren)(CH_3CN)]^{2+}$, $[Cu(tiaea)(CH_3CN)]^{2+}$ and $[Cu(teaea)(CH_3CN)]^{2+}$ the formation of the transient $[Cu^{II}–NO]$ intermediate complex was observed. [23a, b] Similar instances of nucleophilic attack at the coordinated NO were reported in the reaction of hydroxide ion in $[Ru^{II}–NO]$ to result in the corresponding nitro complexes and also the in the reaction of alcohols with $Ir^{III}–NO$ to yield alkyl nitrite complexes.[30,31]

In the present cases, we have not observed any indication of the formation of an $[Cu^{II}–NO]$ inner-sphere complex (Figure 2.2). Similarly, with $[Cu(dmp)_2(H_2O)]^{2+}$ and $[Cu(phen)_2(H_2O)]^{2+}$, even at the early stage of mixing no spectral change for the inner-sphere complex formation was reported.[29,18] This can be rationalized in two ways: (i) either the spectral patterns of the complexes **2.1** and **2.2** are very similar to their respective $[Cu^{II}–NO]$ intermediates or (ii) the values of the equilibrium constants, K_{NO} are much lower. Since, in FT-IR studies also, no υ_{NO} frequency corresponding to the formation of $[Cu^{II}–NO]$ was observed, the second option is more logical. The N-nitrosated ligands in both the cases were isolated and characterized completely using various spectroscopic techniques.

2.4 Conclusion

In conclusion, two Cu(II) complexes have been prepared with two tridentate N-donor ligands and their nitric oxide reactivity were studied. The copper(II) centres in complexes **2.1** and **2.2** were found to undergo reduction in the presence of NO in acetonitrile medium. No [Cu^{II}–NO] intermediate was observed in the present cases presumably because of very low value of K_{NO}. In present set of complexes difference in rate of reduction is associated with the effect of substitution present in the ligand framework. The reduction in acetonitrile solvent was found to be accompanied by N-nitrosation of the ligands.

2.5 Experimental section

2.5.1 Materials and methods

All reagents and solvents of reagent grade were purchased from commercial sources and used as received except specified. Ligands $\mathbf{L_1}$ and $\mathbf{L_2}$ were purchased from Sigma-Aldrich and used as received. Acetonitrile was distilled from calcium hydride. Deoxygenation of the solvent and solutions was effected by repeated vacuum/purge cycles or bubbling with nitrogen for 30 min. NO gas was purified by passing through KOH and a P_2O_5 column. UV-visible spectra were recorded on a Perkin Elmer Lambda 25 UV-visible spectrophotometer. FT-IR spectra of the solid samples were taken on a Perkin Elmer spectrophotometer with samples prepared as KBr pellets. Solution electrical conductivity was measured using a Systronic 305 conductivity bridge. ^{1}H-NMR spectra were recorded in a 400 MHz Varian FT spectrometer. Chemical shifts (ppm) were referenced either with an internal standard (Me_4Si) or to the residual solvent peaks. The X-band Electron Paramagnetic Resonance (EPR) spectra were recorded on a JES-FA200 ESR spectrometer, at room temperature and 77 K with microwave power, 0.998 mW; microwave frequency, 9.14 GHz and modulation amplitude, 2.

Elemental analyses were obtained from a Perkin Elmer Series II Analyzer. The magnetic moment of complexes was measured on a Cambridge Magnetic Balance.

2.5.2 Synthesis of complex 2.1

Copper(II) perchlorate hexahydrate, $[Cu(H_2O)_6](ClO_4)_2$ (0.370 g, 1 mmol) was dissolved in 10 ml distilled and degassed acetonitrile and to this solution, 0.160 g (1 mmol) of the ligand **L_1**, was added slowly under nitrogen atmosphere with constant stirring. The color of the solution turned into green from deep blue. The stirring was continued for 1 h. To this, 20 ml of degassed benzene was added and kept in a freezer. This resulted in a green colored precipitate of complex **2.1**. Yield: 0.275 g (~ 60%). Elemental analyses: calcd.(%) C, 26.70; H, 5.60; N, 9.34; found(%): C, 26.57; H, 5.35; N, 9.39. FT-IR (in KBr): 3044, 1621, 1476, 1090, 626 cm^{-1}. Molar conductivity [ΛM (Ω^{-1} cm^2 mol^{-1}), 273]. The EPR data: g_{av}; 2.105. μ_{obs}, 1.83 BM.

2.5.3 Synthesis of complex 2.2

Copper(II) perchlorate hexahydrate, $[Cu(H_2O)_6](ClO_4)_2$ (0.370 g, 1 mmol) was dissolved in 10 ml distilled and degassed acetonitrile and to this solution, 0.187 g (1 mmol) of the ligand **L_2**, was added slowly under nitrogen atmosphere with constant stirring. The color of the solution turned into green from deep blue. The stirring was continued for 1 h. To this, 20 ml of degassed benzene was added and kept in a freezer. This resulted in a green coloured precipitate of complex **2.2**. Yield: 0.320 g (~ 65%). Elemental analyses: calcd.(%) C, 22.78; H, 5.02; N, 9.96; found(%): C, 22.56; H, 5.12; N, 9.88. FT-IR (in KBr): 3056, 1625, 1473, 1115, 621 cm^{-1}. Molar conductivity [ΛM (Ω^{-1} cm^2 mol^{-1}), 243]. The EPR data: g_{av}; 2.105. μ_{obs}, 1.84 BM.

2.5.3 Isolation of modified ligand L_1'

In a 100 ml Schlenk flask, complex **2.1** (~460 mg, 1 mmol) was dissolved in 20 ml degassed acetonitrile. To this, NO gas was purged through a needle for one minute and the mixture was then allowed to stand for 10 min. From the colorless solution, thus obtained, the excess NO was removed by applying several vacuum/nitrogen cycles. To this, 25 ml of degassed benzene was added through a syringe to make a layer. The layered solution was then kept overnight in a freezer. The white crystals of $[Cu(CH_3CN)_4](ClO_4)$ were filtered out from the colorless solution under nitrogen atmosphere using a Schlenk frit. The volume of the filtrate was then reduced to 5 ml and stirred for 1 h in open air in order to allow the residual Cu(I) centre to oxidise to Cu(II). To this, 5 ml saturated aqueous solution of Na_2S was added and stirred for 1/2 h. The black precipitate thus obtained was filtered off and the filtrate was diluted with 50 ml of distilled water. The organic part was then extracted from the mixture using $CHCl_3$ (3 portions × 25 ml). The collected organic layer was then dried under reduced pressure and the residual oil was subjected to column chromatography using silica gel to yield $\mathbf{L_1'}$. Yield: 120 mg (~75%). Elemental analyses: calcd.(%) C, 60.33; H, 13.29; N, 26.38; found(%): C, 60.57; H, 13.35; N, 26.35. FT-IR (in KBr): 3434, 2924, 2853, 1640, 1465, 1086, 909, 811 cm^{-1}. ^{1}H-NMR: (400 MHz, $CDCl_3$): δ_{ppm}: 4.18 (2H, t), 4.12 (2H, t), 3.65 (2H, t), 3.58 (2H, t), 2.76 (1H, t), 2.62 (1H, t), 2.20 (3H, s), 2.16 (3H, s), 1.91 (2H, m), 1.64 (2H, m). ^{13}C-NMR: (100 MHz, $CDCl_3$) $\delta_{ppm:}$ 56.8, 47.2, 46.7, 44.4, 39.2, 32.0, 26.7. Mass $(M+H^+)/z$: calcd: 188.16, found: 189.20.

2.5.4 Isolation of modified ligand L_2'

The same procedure (as in the case of $\mathbf{L_1'}$) was adopted for the isolation of $\mathbf{L_2'}$.Yield, 150 mg (~ 70%). Elemental Analyses: Calcd (%): C, 55.55; H, 11.11; N, 25.92. Found (%) C, 55.59; H, 11.10; N, 25.84. FT-IR (in KBr): 2956, 2868, 1644, 1466 cm^{-1}. ^{1}H-NMR (400 MHz,

$CDCl_3$) δ_{ppm}: 4.09 (2H, t), 3.54 (2H, t), 2.28 (2H, t), 2.11 (14H, m), 1.85 (2H, m), 1.61 (2H, m). ^{13}C-NMR: (100 MHz, $CDCl_3$) δ_{ppm}: 59.0, 48.4, 45.5, 28.0. ESI-Mass: $(M+H^+)/z$ Calcd: 216.30; Found: 217.09.

2.6 References

1. *Nitric Oxide: Biology and Pathobiology*, ed. L. J. Ignarro, Academic Press, San Diego, 2000.
2. (a) Moncada, S.; Palmer, R. M. J. Higgs, E. A. *Pharmacol. Rev*. **1991**, *43*, 109. (b) Butler, A. R.; Williams, D. L. *Chem. Soc. Rev*. **1993**, *22*, 233. (c) *Methods in Nitric Oxide Research*, ed. M. Feelisch and J. S. Stamler, John Wiley and Sons, Chichester, England, 1996.
3. (a) Jia, L.; Bonaventura, C.; Bonaventura, J.; Stamler, J. S. Nature **1996**, *380*, 221. (b) Galdwin, M. T.; Lancaster Jr., J. R.; Freeman, B. A.; Schechter, A. N. *Nat. Med.* **2003**, *9*, 496.
4. (a) Ye, R. W.; Toro-Suarez, I.; Tiedje, J. M.; Averill, B. A. *J. Biol. Chem*. **1991**, *266*, 12848. (b) Hulse, C. L.; Averill, B. A.; Tiedje, J. M. *J. Am. Chem. Soc*. **1989**, *111*, 2322. (c) Jackson, M. A.; Tiedje, J. M.; Averill, B. A. *FEBS Lett*. **1991**, *291*, 41.
5. (a) Godden, J. W.; Turley, S.; Teller, D. C.; Adman, E. T.; Liu, M. Y.; Payne, W. J.; LeGall, J.; Science **1991**, *253*, 438. (b) E. T. Adman and S. Turley, in *Bioinorganic Chemistry of Copper*, ed. K. D. Karlin and Z. Tyekllr, Chapman & Hall, Inc., New York, 1993, p. 397; (c) Ferguson, S. J. *Curr. Opin. Chem. Biol*. **1998**, *2*, 182.
6. (a) Richardson, D. J.; Watmough, N. J. *Curr. Opin. Chem. Biol*. **1999**, *3*, 207. (b) Moura, I.; Moura, J. J. G. *Curr. Opin. Chem. Biol*. **2001**, *5*, 168. (c) Tocheva, E. I.; Rosell, F. I.; Mauk, A. G.; Murphy, M. E. P. *Biochemistry* **2007**, *46*, 12366. (d) Zhou,

X.; Espey, M. G.; Chen, J. X.; Hofseth, L. J.; Miranda, K. M.; Hussain, S. P.; Winks, D. A.; Harris, C. C. *J. Biol. Chem.* **2000**, *275*, 21241.

7. (a) Chien, J. C. W. *J. Am. Chem. Soc*. **1969**, *91*, 2166. (b) Wayland, B. B.; Olson, L. W. *J. Am. Chem. Soc*. **1974**, *96*, 6037. (c) Trofimova, N. S.; Safronov, A. Y.; Ikeda, O. *Inorg. Chem*. **2003**, *42*, 1945.
8. (a) Walker, F. A. *J. Inorg. Biochem.*, **2005**, *99*, 216. (b) Rousseau, D. L.; Li, D.; Couture, M.; Yeh, S. R. *J. Inorg. Biochem.* **2005**, *99*, 306. (c) George, S. J.; Allen, J. W. A.; Ferguson, S. J.; Thorneley, R. N. F. *J. Biol. Chem*. **2000**, *275*, 33231.
9. (a) Pinakoulaki, E.; Gemeinhardt, S.; Saraste, M.; Varotsis, C. *J. Biol. Chem*. **2002**, *277*, 23407. (b) Praneeth, V. K. K.; Paulat, F.; Berto, T. C.; DeBeer George, S.; Nather, C.; Sulok, C. Lehnert, N. *J. Am. Chem. Soc*. **2008**, *130*, 15288.
10. (a) Soldatova, A. V.; Ibrahim, M.; Olson, J. S.; Czernuszewicz, R. S.; Spiro, T. G. *J. Am. Chem. Soc*. **2010**, *132*, 4614. (b) Wasser, I. M.; de Vries, S.; Moënne-Loccoz, P.; Schröder, I.; Karlin, K. D. *Chem. Rev*. **2002**, *102*, 1201.
11. (a) Hoshino, M.; Maeda, M.; Konishi, R.; Seki, H.; Ford, P. C. *J. Am. Chem. Soc*. **1996**, *118*, 5702. (b) Fernandez, B. O.; Lorkovic, I. M.; Ford, P. C. *Inorg. Chem*. **2004**, *43*, 5393. (c) Lehnert, N.; Praneeth, V. K. K.; Paulat, F. *J. Comput. Chem*. **2006**, *27*, 1338.
12. (a) Ellison, M. K.; Scheidt, W. R. *J. Am. Chem. Soc*. **1999**, *121*, 5210. (b) Linder, D. P.; Rodgers, K. R.; Banister, J.; Wyllie, G. R. A.; Ellison, M. K.; Scheidt, W. R. *J. Am. Chem. Soc.*, **2004**, *126*, 14136.
13. (a) Lim, M. D.; Lorkovic, I. M.; Ford, P. C. *J. Inorg. Biochem*. **2005**, *99*, 151. (b) Shamir, D.; Zilbermann, I.; Maimon, E.; Gellerman, G.; Cohen, H.; Meyerstein, D. *Eur. J. Inorg. Chem*. **2007**, *32*, 5029.

14. (a) Torres, J.; Svistunenko, D.; Karlsson, B.; Cooper, C. E.; Wilson, M. T. *J. Am. Chem. Soc*. **2002**, *124*, 963. (b) Torres, J.; Cooper, C. E.; Wilson, M. T. *J. Biol. Chem.* **1998**, *273*, 8756. (c) Martin, C. T.; Morse, R. H.; Kanne, R. M.; Gray, H. B.; Malmstrom, B. G.; Chan, S. I. *Biochemistry* **1981**, *20*, 5147.

15. Gorren, A. C. F.; de Boer, E.; Wever, R. *Biochim. Biophys. Acta, Protein Struct. Mol. Enzymol.* **1987**, *916*, 38.

16. Tran, D.; Ford, P. C. *Inorg. Chem*. **1996**, *35*, 2411.

17. (a) Brown, G. C.; *Biochim. Biophys. Acta, Bioenerg*. **2001**, *46*, 1504. (b) Torres, J.; Sharpe, M. A.; Rosquist, A.; Cooper, C. E.; Wilson, M. T. *FEBS Lett*. **2000**, *475*, 263. (c) Wijma, H. J.; Canters, G. W.; Vries, S. de.; Verbeet, M. P. *Biochemistry* **2004**, *43*, 10467.

18. Tran, D.; Skelton, B. W.; White, A. H.; Laverman, L. E.; Ford, P. C. *Inorg. Chem.* **1998**, *37*, 2505.

19. Lim, M. D.; Capps, K. B.; Karpishin, T. B.; Ford, P. C. *Nitric Oxide* **2005**, *12*, 244.

20. (a) Tsuge, K.; De Rosa, F.; Lim, M. D.; Ford, P. C. *J. Am. Chem. Soc*. **2004**, *126*, 6564. (b) Khin, C.; Lim, M. D.; Tsuge, K.; Iretskii, A.; Wu, G.; Ford, P. C. *Inorg. Chem*. **2007**, *46*, 9323.

21. Pell, S. D.; Armor, J. N. *J. Am. Chem. Soc*. **1973**, *95*, 7625.

22. (a) B. B. Wayland and L. W. Olson, *J. Chem. Soc., Chem. Commun*. **1973**, 897. (b) Choi, I.-K.; Liu, Y.; Wei, Z.; Ryan, M. D.; *Inorg. Chem*. **1997**, *36*, 3113.

23. (a) Sarma, M.; Singh, A.; Gupta, S. G.; Das, G.; Mondal, B. *Inorg. Chim. Acta* **2010**, *363*, 63. (b) Sarma, M.; Kalita, A.; Kumar, P.; Singh, A.; Mondal, B. *J. Am. Chem. Soc*. **2010**, *132*, 7846. (c) Sarma, M.; Mondal, B. *Inorg. Chem*. **2011**, *50*, 3206.

24. Kumar, P.; Kalita, A.; Mondal, B. *Dalton Trans.* **2011**, *40*, 8656.

25. Kalita, A.; Kumar, P.; Deka, R. C.; Mondal, B. *Inorg. Chem.* **2011**, *50*, 11868.

26. Hiroshi, Y.; Taro, I. *Bull. Chem. Soc. Jpn*. **1969**, *42*, 2187.

27. (a) Hathaway, B. J.; Tomlinson, A. A. G. *Coord. Chem. Rev*. **1970**, *5*, 1. (b) Hathway, B. J.; Billing, D. E.; Nicols, P.; Procter, I. M. *J. Chem. Soc. A* **1969**, 312. (c) B. J. Hathway, in *Comprehensive Coordination Chemistry*, ed. G. Wilkinson, R. D. Gillard and J. A. McCleverty, Pergamon, Oxford, 1987, vol. 5, pp. 533–594; (d) Patra, A. K.; Ray, M.; Mukherjee, R. *J. Chem. Soc., Dalton Trans*. **1999**, 2461.

28. R. W. Nims, J. F. Darbyshire, J. E. Saavedra, D. Christodoulou, I. Hanbauer, G. W. Cox, M. B. Grisham, F. Laval, J. A. Cook, M. C. Krishna and D. A. Wink, In *Methods: A Companion to Methods in Enzymology*, Academic Press: San Diego, CA, 1995, Vol. 7, pp 48.

29. Dı'az, A.; Ortiz, M.; Sa'nchez, I.; Cao, R.; Mederos, A.; Sanchiz, J.; Brito, F. *J. Inorg. Biochem.* **2003**, *95*, 283.

30. Reed, C.; Roper, W. J. *J. Chem. Soc., Dalton Trans.* **1972**, 1243.

31. Lim, M. H.; Xu, D.; Lippard, S. J. *Nat. Chem. Biol.* **2006**, *2*, 375.

Chapter 3

Phenol ring nitration induced by unprecedented reduction of the Copper(II) centre by nitrogen dioxide

Abstract

Nitrogen dioxide (NO_2) is known as a nitrating agent in biological systems. It is well accepted that NO_2 induces tyrosine nitration through radical mechanism. Reduction of Cu(II) centre by NO_2 generates nitronium ion (NO_2^+), which also can induce phenol ring nitration. However, the reduction of Cu(II) centre by NO_2 is not exemplified yet. Two Cu(II) complexes, **3.1** and **3.2**, with ligands $\mathbf{L_3}$ and $\mathbf{L_4}$ [$\mathbf{L_3}$ = 2,4-di-*tert*-butyl-6-(((2-(dimethylamino)ethyl)(isopropyl)amino)methyl)phenol; $\mathbf{L_4}$ = 6,6'-(((2-(dimethylamino)ethyl)azanediyl)bis(methylene))*bis*(2,4-di-*tert*-butylphenol)], respectively, have been made to react with NO_2. In both the cases, the reduction of the Cu(II) centre was observed in presence of NO_2 which induced phenol ring nitration.

3.1 Introduction

Reactive nitrogen species (RNS) constitutes a major class of oxidizing agent in biological systems.[1] At low or moderate concentration, they behave as messenger for signal transduction; whereas at high concentration they induce oxidative stress.[2] Tyrosine nitration induced by RNS has attracted a considerable interest of chemists and biochemists as it can alter the protein function as well as can be used as biomarker of several disease states like Alzheimar's and Perkinson's diseases.[3] In biosystems, tyrosine nitration occurs either through peroxynitrite ($OONO^-$) or nitrogen dioxide (NO_2).[4] Peroxynitrite forms in diffusion controlled reaction between superoxide and nitric oxide (NO).[5] NO_2 can be generated by the reaction NO with oxygen, decomposition of $ONOO^-$ or by the oxidation of nitrite (NO_2^-) by hydrogen peroxide (H_2O_2) in presence of peroxidases.[6]

Cu(II) ion is known to favour the generation of radicals and thus causing the oxidative damage of proteins, lipids and nucleic acids; but Cu(II) ion catalyzed nitration is very little known, specially from mechanistic and pathogenesis studies.[7] Known examples of tyrosine nitration involving Cu(II) ion have been focused on Cu-Zn superoxide dismutase where it has been shown to promote the oxidation of NO_2^- to NO_2 in addition to the principal role of scavenging superoxide to form H_2O_2 and oxygen.[8] On the other hand, NO_2, a widely accepted nitrating agent for tyrosine, induces nitration through radical mechanism.[9] Nitronium ion (NO_2^+) is known as the key nitrating agent in nitration reaction generally produced at pH < 0 in concentrated mixture of nitric and sulphuric acid.[10] Transition metal ions like iron and copper can also catalyze two electron oxidation of $OONO^-$ leading to a heterolytic O-O bond cleavage and thus generating a species with similar reactivity like NO_2^+.[10] However, the formation of NO_2^+ from NO_2 in its reaction with Cu(II) is not known in literature. This is perhaps because of high potential barrier. In aqueous medium at pH 7, the NO_2^+/NO_2 potential was found to be 1.6 (±0.2) v relative to NHE.[11] A little lower value (1.51 v) for the

same couple was reported based on the concentration of NO_2^+ in the mixture of concentrated nitric and sulphuric acid.[11]

This chapter discribes two Cu(II) complexes, **3.1** and **3.2**, with two ligands, $\mathbf{L_3}$ and $\mathbf{L_4}$ (Figure 3.1), [$\mathbf{L_3}$ = 2,4-di-*tert*-butyl-6-(((2- dimethylamino)ethyl) (isopropyl)amino) methyl) phenol; $\mathbf{L_4}$ = 6,6'-(((2-(dimethylamino) ethyl) azanediyl) *bis*(methylene))*bis*(2,4-di-*tert*-butylphenol)], respectively, and their reactivity with NO_2 to result in the reduction of Cu(II) centre with a simultaneous phenol ring nitration through NO_2^+ ion formation.

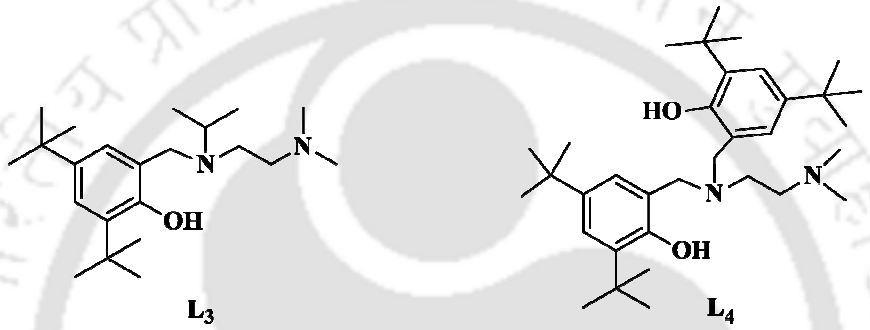

Figure 3.1: Ligands used for the present study.

3.2 Results and discussion

Complexes **3.1** and **3.2** were prepared by the reaction of Cu(II) acetate, monohydrate with equivalent amount of respective ligands. The formation of the mononuclear complexes was authenticated by their X-ray single crystal structure determination. The perspective ORTEP views of the complexes are given in figure 3.2. Cu(II) centre of complex **3.1** is surrounded by two N-donor atoms, one phenolate-oxygen from $\mathbf{L_3}$ and a acetate group. The Cu(II) centre in complex **3.2** also has the same coordination environment with the second phenol ring of $\mathbf{L_4}$ dangling around (Figure 3.2). The metric parameters for both the complexes are found to be similar (Appendix II). Cu-$O_{(phen)}$ distances in complexes **3.1** and **3.2** are 1.863(2) and 1.893(2) Å, respectively and within the range of that in reported mononuclear Cu(II)-phenolato complexes.[12] The crystallographic tables and important bond lengths and angles

are given in appendix II.

In the UV-visible spectroscopy, complexes **3.1** and **3.2** in methanol solutions display phenolato-Cu(II) charge transfer transitions at 478 nm and 485 nm, respectively.[12,13] The weak *d-d* bands were observed at 675 nm and 702 nm in cases of complexes **3.1** and **3.2**, respectively (Figure

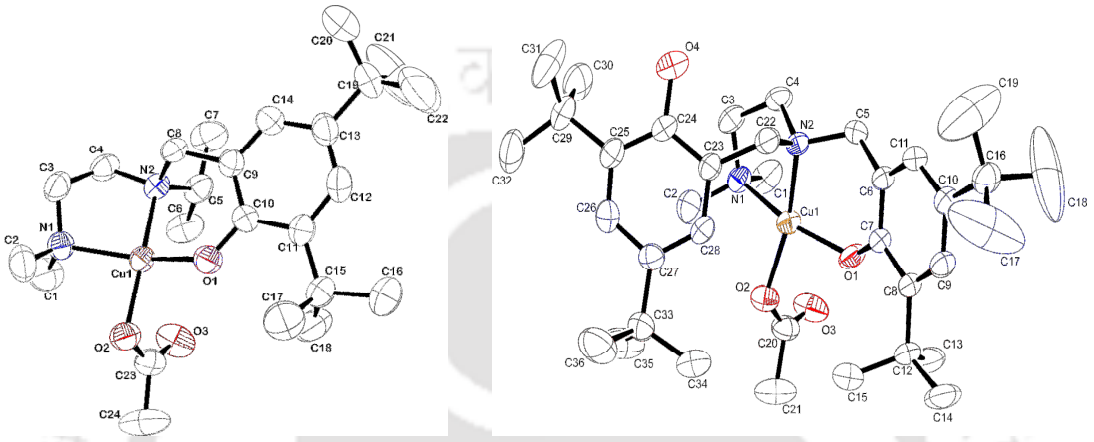

(a) **(b)**

Figure 3.2: ORTEP diagrams of complexes (a) **3.1** and (b) **3.2**. (50% thermal ellipsoid plot, hydrogen atoms are removed for clarity).

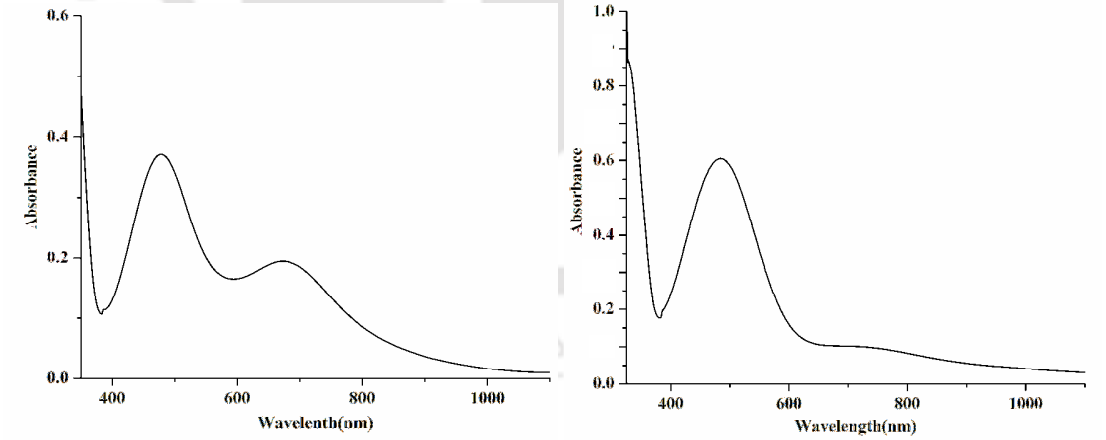

(a) **(b)**

Figure 3.3: UV-visible spectra of complexes (a) **3.1** and (b) **3.2** in methanol.

3.3). In cyclic voltammetric studies in methanol solution, irreversible Cu^{II}/Cu^{I} couple was observed to appear at -1.403 and -1.352 v *versus* Ag/Ag^{+} electrode. Both the complexes

shows characteristic four line X-band EPR spectrum (Appendix II).

3.3 Nitrogen dioxide reactivity

Addition of NO gas in the methanol solution of complex **3.1**, was not found to react. However, addition of oxygen to this reaction mixture immediately results in a colorless solution. This is presumably because of the fact that NO first reacts with O_2 to generate NO_2 which then reacts with Cu(II) centre. To confirm this, NO_2 gas was purged into the degassed methanol solution of complex **3.1**, it was found to result in change the color to light yellow. In UV-visible spectroscopy, the phenolato → Cu(II) charge transfer band at 478 nm as well as the *d-d* band were found to disappear. These are attributed to the reduction of Cu(II) centre by NO_2 (Figure 3.4). The reduction of Cu(II) was further confirmed by the EPR silent nature of the colorless solution (Figure 3.5) as well as by ^{1}H-NMR spectral studies (Figure 3.6). Complex **3.2** was also found to behave similar towards NO_2 (Appendix II).

One could think of the possibility of a NO_2 induced phenoxyl radical formation in the reaction medium. The formation of nitrophenols from phenol by reaction with NO_2 in solution is reported to proceed through a two stage reaction; the abstraction of a hydrogen

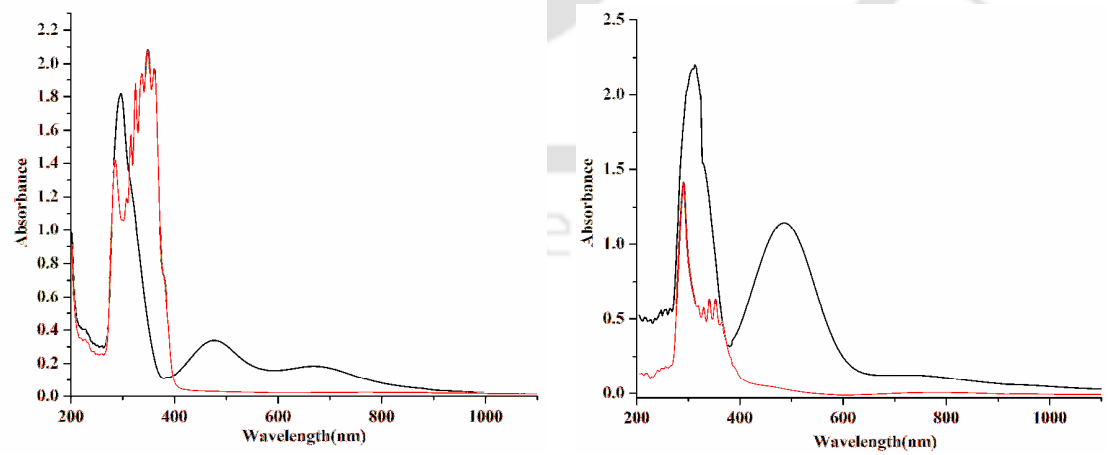

(a) **(b)**

Figure 3.4: UV-visible spectra of complexes (a) **3.1** and (b) **3.2** before (black traces) and after (red traces) reaction with NO_2 in methanol solution.

atom from the phenol-OH group by NO_2 to form phenoxyl radical followed by the reaction of the phenoxyl radical formed with NO_2.[13] However, the absence of characteristic $\pi \rightarrow \pi^*$ transition band at ~440 nm for

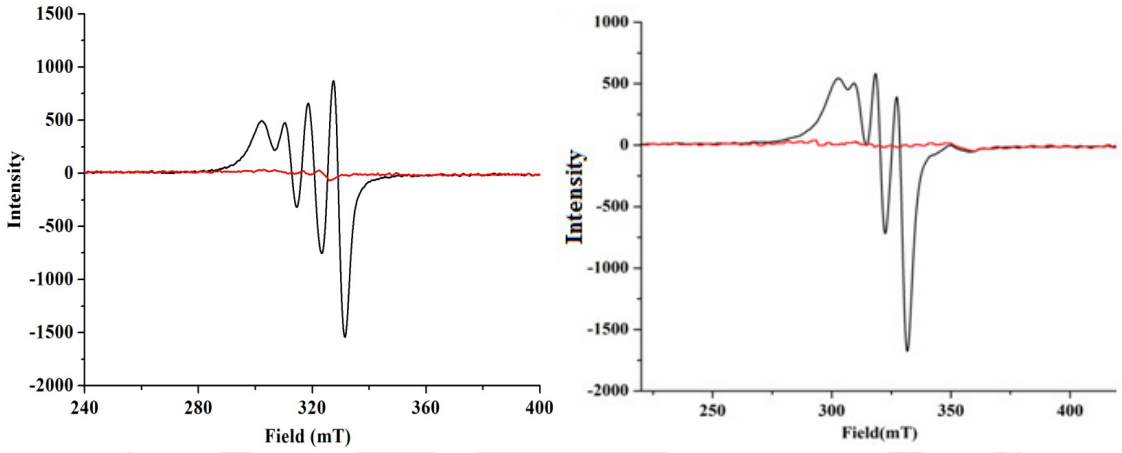

(a) **(b)**

Figure 3.5: X-band EPR spectra of complexes (a) **3.1** and (b) **3.2** before (black traces) and after (red traces) reaction with NO_2 in methanol solution at room temperature.

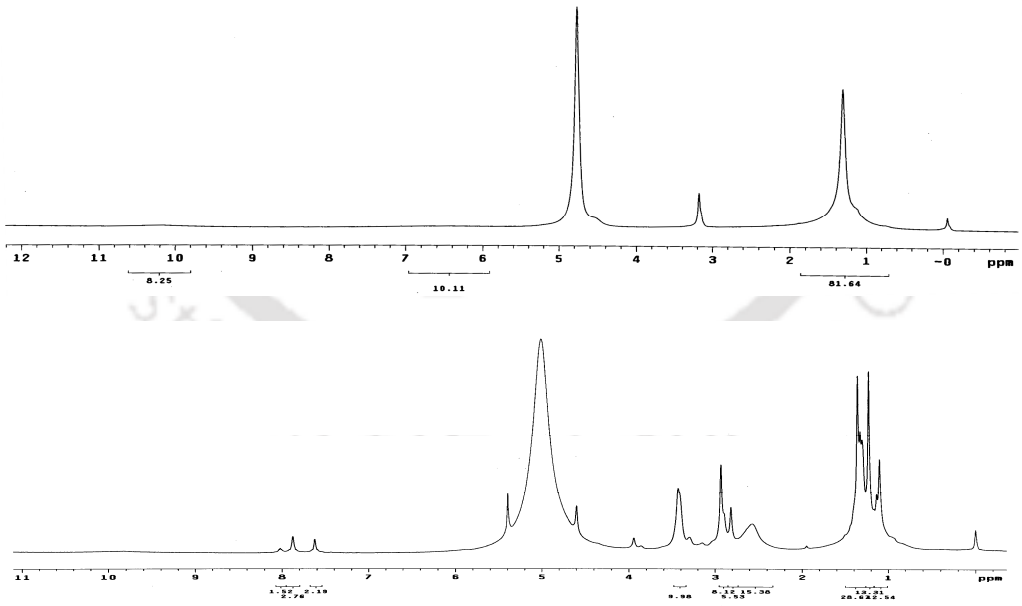

Figure 3.6: ^{1}H-NMR spectra of complex **3.1** before (top) after (bottom) reaction with NO_2 in CD_3OD.

phenoxyl group suggests the non-involvement of phenoxyl radical in the nitration

mechanism.[13] Further, the EPR silent nature of the reaction mixture also supports this. The reduction is found to be associated with a simultaneous phenol ring nitration of the ligand framework (Scheme 3.1). It should be noted that in the present cases, the phenol ring nitration takes place through an *ipso*-mechanism where the nitronium ion (NO_2^+), generated in the reduction of Cu(II) by NO_2, attacks at the 4-position of the phenol ring.[14]

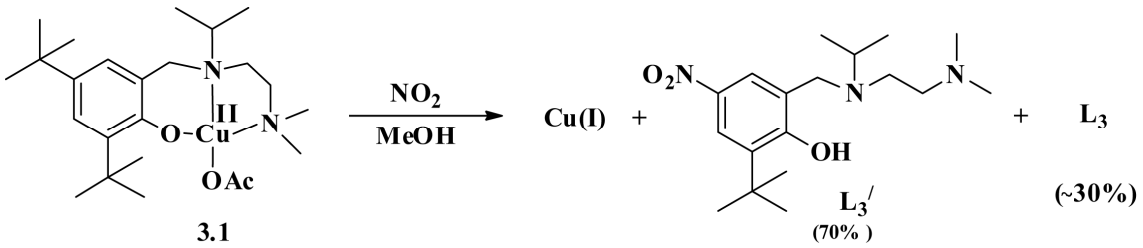

Scheme 3.1

This results into the corresponding 2-*tert*-butyl-4-nitrophenol. The release of *tert*-butyl cation in the process is confirmed from the presence of *tert*-butanol in GC mass spectrum of the reaction mixture (Figure 3.7). However, quantification of this has not been done. The formation of the nitration product in case of complex **3.1** was confirmed from various spectroscopic analyses (Appendix II).

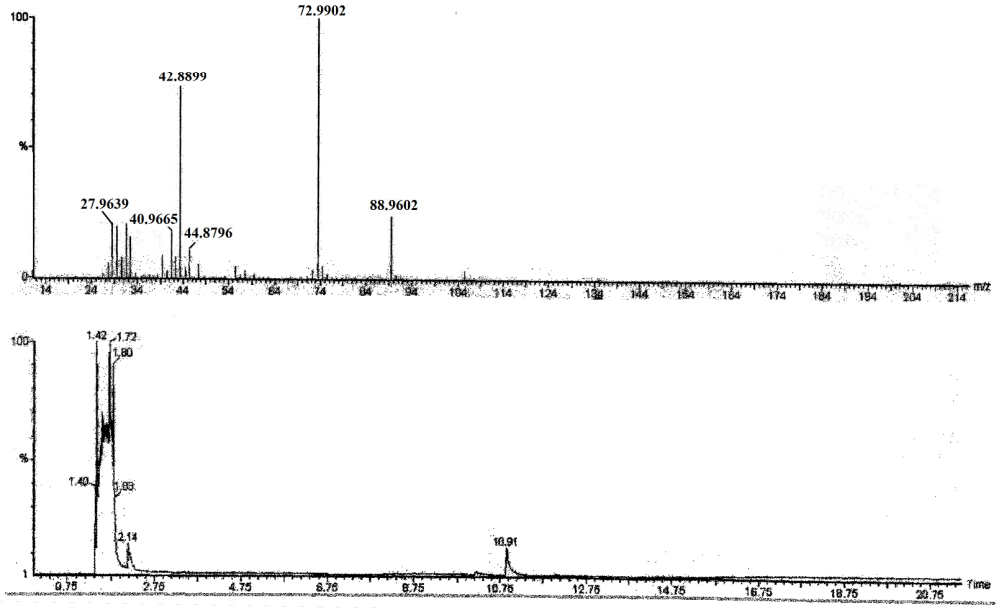

Figure 3.7: GC- mass spectrum of the reaction mixture after the reaction of complex **3.1** with NO_2 in methanol.

In complex **3.2**, interestingly, nitration was observed in both the phenol rings (Scheme 3.2). This has been supported by the single crystal X-ray structure determination (Figure 3.8). The reason for dinitration is not clear. In this connection, it would be worth mentioning here that $[Cu(tiaea)(CH_3CN)]^+$ and $[Cu(teaea)(CH_3CN)]^+$, [tiaea = *tris*-(isopropylaminoethyl)amine and teaea = *tris*-(ethylaminoethyl)amine], in acetonitrile solution upon reaction with NO, trinitrosation at the secondary amine positions of the ligands was observed.[15]

In a recent example, it has been demonstrated that both Cu^{2+} and Cu^{2+}-peptide complexes can catalyze the tyrosine nitration in the presence of NO_2^- and H_2O_2. [9] In this reaction, hydroxyl radicals ($^{\bullet}OH$) and/or copper(II)-bound $^{\bullet}OH$ (Cu^{2+}-$^{\bullet}OH$) are found to be generated from Cu^{2+} and H_2O_2 through a Fenton-like reaction. These radicals may then be scavenged by both NO_2^- to form NO_2 and tyrosine to form tyrosine radicals ($Tyr^{\bullet}$), resulting in to tyrosine nitration. Cu^{2+}/H_2O_2 was found to catalyze the tyrosine nitration induced by NO and oxygen. NO was

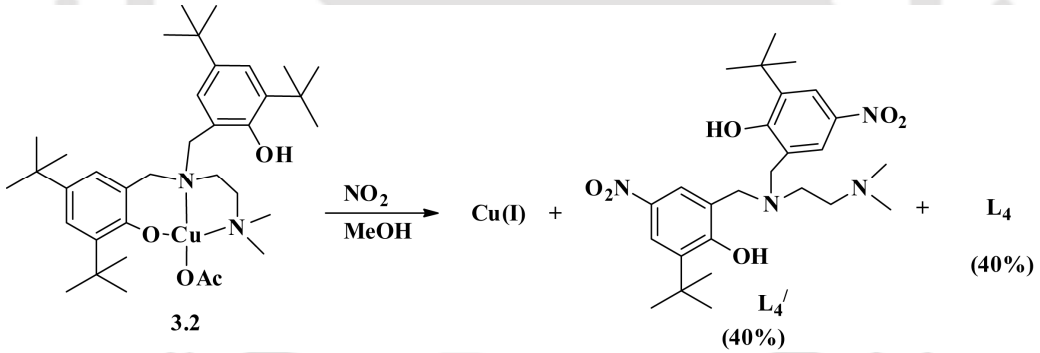

Scheme 3.2

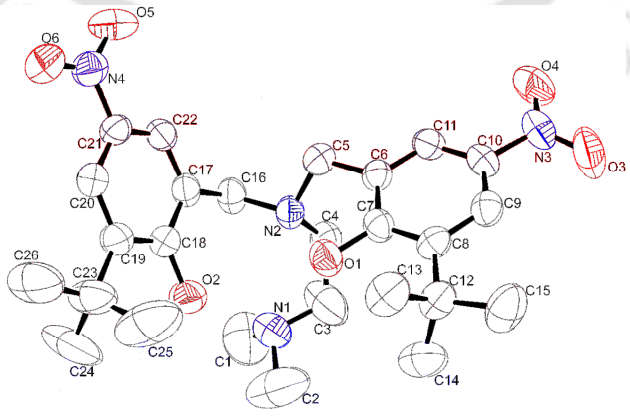

Figure 3.8: ORTEP diagram of $\mathbf{L_4}'$ (50% thermal ellipsoid plot, hydrogen atoms are removed for clarity).

oxidized by O_2 to form NO_2, and the role of Cu^{2+}/H_2O_2 was to generate $^{\bullet}OH/Cu^{2+}$-$^{\bullet}OH$ to promote $Tyr^{\bullet}$ formation.[9] It would be worth mentioning here that in this case, NO/O_2 induced nitration was found to be catalyzed significantly in presence of H_2O_2 and trace amounts of Cu(II); but high concentration of Cu(II) was reported to inhibit the nitration.[9] It should be noted that depending on biological conditions, formation of NO_2^+ as nitrating agent from peroxynitrite $OONO^-$ is reported earlier.[16-18] Superoxide reacts with NO to form strong oxidant peroxynitrite $OONO^-$. This in turn, reacts with superoxide dismutase to result an intermediate like NO_2^+ ion which nitrates tyrosine.[16]

However, there is not even a single example where NO_2 reduces Cu(II) centre to Cu(I) resulting in the formation NO_2^+ which induce phenol ring nitration. It should be noted that for the present study, NO_2 does not induce a significant nitration of the free ligands in the reaction condition.

3.4 Conclusion

The present work demonstrate the reaction of NO_2 with Cu(II) complexes (**3.1** and **3.2**) in methanol medium where NO_2 reduces Cu(II) centre to Cu(I) resulting in the formation NO_2^+ which induce phenol ring nitration.

3.5 Experimental section

3.5.1 Materials and methods

All reagents and solvents of reagent grade were purchased from commercial sources and used as received except specified. Acetonitrile was distilled from calcium hydride. Methanol was dried by refluxing over iodine activated magnesium with a magnesium loading of 5 gm/lit. Then the dried methanol was kept over 20% m/v 3Å molecular sieves for 4-5 days before using. NO_2 gas was prepared by the reaction of purified NO with O_2 in a flask fitted with a

rubber septum. UV-visible spectra were recorded on a Perkin Elmer Lambda 25 UV-visible spectrophotometer. FT-IR spectra of the solid samples were taken on a Perkin Elmer spectrophotometer with samples prepared as KBr pellets. Solution electrical conductivity was measured using a Systronic 305 conductivity bridge. ^{1}H-NMR spectra were recorded in a 400 MHz Varian FT spectrometer. Chemical shifts (ppm) were referenced either with an internal standard (Me_4Si) or to the residual solvent peaks. The X-band Electron Paramagnetic Resonance (EPR) spectra were recorded on a JES-FA200 ESR spectrometer, at room temperature and 77 K with microwave power, 0.998 mW; microwave frequency, 9.14 GHz and modulation amplitude 2. Elemental analyses were obtained from a Perkin Elmer Series II Analyzer. The magnetic moment of complexes was measured on a Cambridge Magnetic Balance. Single crystals were grown by slow diffusion followed by slow evaporation technique. The intensity data were collected using a Bruker SMART APEX-II CCD diffractometer, equipped with a fine focus 1.75 kW sealed tube MoK_α radiation (λ = 0.71073 Å) at 273(3) K, with increasing ω (width of 0.3° per frame) at a scan speed of 3 s/frame. The SMART software was used for data acquisition.[19] Data integration and reduction were undertaken with SAINT and XPREP software.[20] Structures were solved by direct methods using SHELXS-97 and refined with full-matrix least squares on F^2 using SHELXL-97.[21a] All non-hydrogen atoms were refined anisotropically. Structural illustrations have been drawn with ORTEP-3 for Windows.[21b]

3.5.2 Synthesis of ligand L_3

N, N-dimethylethylenediamine (880 mg, 0.1 mol) was added in 20 ml of distilled acetone. The mixture was refluxed for 2 h to give corresponding Schiff's base and excess acetone was completely removed under vacuum. Then the imine was dissolved in 50 ml of methanol and was reduced by slow addition of 2.1 equivalent of $NaBH_4$. After removal of methanol under

reduced pressure, the crude product was dissolved in water and neutralized with dilute acetic acid. N^1-isopropyl-N^2,N^2-dimethylethane-1,2-diamine was extracted from the aqueous solution using dichloromethane (4 × 50 ml portions). Yield: 780 mg (60%). N^1-isopropyl-N^2,N^2-dimethylethane-1,2-diamine (1.30 g, 10 mmol), 2,4-di-*tert*-butylphenol (2.06 g, 10 mmol) and formalin (2.11 g of 37% solution, 26 mmol) were taken in 10 ml of ethanol and the reaction mixture was refluxed for 24 h . Ethanol was removed by using rotary evaporator and 100 ml of water was added to the crude mass. Extraction using dichloromethane (3 × 50 ml portions), followed by column chromatographic purification afforded the ligand **L_3.** Yield: 1.92 g (55%). Elemental analyses: calcd.(%): C, 62.13; H, 11.57; N, 8.04 ; found(%): C, 62.19; H, 11.56; N, 8.11. FT-IR (in KBr): 2964, 1481, 1460, 1241, 1165 cm^{-1}. ^{1}H-NMR: (400 MHz, $CDCl_3$): δ_{ppm}: 7.17 (1H, d), 6.81 (1H, d), 3.76 (2H, s), 3.08 (1H, m), 2.57 (2H, t), 2.44 (2H, t), 2.17 (6H, s), 1.40 (9H, s), 1.26 (9H, s), 1.06 (6H, d). ^{13}C-NMR: (100 MHz, $CDCl_3$) $\delta_{ppm:}$ 154.6, 140.1, 135.3, 123.4, 122.5, 121.5, 58.3, 54.8, 49.7, 46.4, 45.7, 34.8, 34.1, 31.8, 29.6, 17.2. Mass $(M+H^+)$/z: calcd: 349.31; found: 349.36.

3.5.3 Synthesis of ligand L_4

N,N-dimethylethylenediamine (2.19 g, 24.9 mmol), 2,4-di-*tert*-butylphenol (8.19 g, 49.9 mmol) and formalin (8.42 g of 37% solution, 104 mmol) were taken in 50 ml of ethanol and the mixture was refluxed for 24 h while a white precipitate was formed. The precipitate was isolated by filtration and washed with cold ethanol to obtain the ligand **L_4** as a white powder. It was recrystallized from ethanol to obtain pure **L_4**. Yield: 7.8 g (60%). Elemental analyses: calcd.(%): C, 77.81; H, 10.76; N, 5.34; found (%): C, 77.88; H, 10.77; N, 5.43. FT-IR (in KBr): 2959, 1481, 1465, 1361, 1218 cm^{-1}. ^{1}H-NMR: (400 MHz, $CDCl_3$): δ_{ppm}: 9.80 (2H, broad s), 7.22 (2H, d), 6.90 (2H, d), 3.64 (4H, d), 2.60 (4H, m), 2.31 (6H, s), 1.38 (18H, s),

1.27 (18H, s). ^{13}C-NMR: (100 MHz, $CDCl_3$) $\delta_{ppm:}$ 153.5, 140.4, 136.3, 125.0, 123.6, 121.9, 56.8, 56.2, 49.3, 45.1, 35.2, 34.3, 31.9, 29.8. Mass $(M+H^+)/z$: calcd: 525.43; found: 525.25.

3.5.4 Synthesis of complex 3.1

To a stirred solution of $Cu(OAc)_2 \cdot H_2O$ (0.398 g, 2 mmol) in 15 ml methanol was added a solution of ligand **L_1** (0.696 g, 2 mmol) in 10 ml methanol. The reaction mixture was refluxed for 8 h after which it was filtered and the filtrate was reduced under vacuum to obtain the metal complex **3.1** as a dark brown solid. Yield: 0.90 g (80%). Elemental analyses: calcd. (%): C, 61.31; H, 9.00; N, 5.96; found (%): C, 61.26; H, 8.94; N, 6.01. UV-visible (methanol): λ_{max}, 673 nm. FT-IR (in KBr): 2952, 1580, 1470, 1311, 677 cm^{-1}. The complex **3.1** behaves as 1:1 electrolyte in methanol solution [Λ_M ($S\,cm^{-1}$), 154]. μ_{obs}., 1.60 BM.

3.5.5 Synthesis of complex 3.2

To a stirred solution of $Cu(OAc)_2 \cdot H_2O$ (0.398 g, 2 mmol) in 15 ml methanol was added a solution of ligand **L_4** (1.048 g, 2 mmol) in 10 ml methanol. The reaction mixture was refluxed for 8 h; then the solvent was removed under reduced pressure to obtain a dark solid. The residue was washed with 30 ml CH_3CN to obtain the metal complex **3.2** as a dark brown solid. Yield: 0.97 g (75%). Elemental analyses: calcd. (%): C, 66.89; H, 9.04; N, 4.33; found (%): C, 66.93; H, 9.09; N, 4.31. UV-visible (methanol): λ_{max}, 702 nm. FT-IR (in KBr): 2952, 1571, 1411, 1240, 1019 cm^{-1}. The complex **3.2** behaves as 1:1 electrolyte in methanol solution [Λ_M ($S\,cm^{-1}$), 146]. μ_{obs}., 1.52 BM.

3.5.6 Isolation of modified ligand L_3'

To 30 ml of methanol solution of complex **3.1** (470 mg), freshly prepared NO_2 was bubbled for ~1/2 minute. The red color of the solution turned colorless. This solution was allowed to stir for 10 minutes at room temperature. Then the solvent was removed under vacuum using

rotavapour. Then equivalent amount of aqueous solution of Na_2S was added to the solution remove copper ion as its sulphide. The precipitate was filtered off and from the filtrate, the modified ligand $\mathbf{L_3'}$ was extracted using dichloromethane (4 × 50 ml portions). Yield: 235 mg (~70%). Elemental analyses: calcd.(%) C, 64.07; H, 9.26; N, 12.45; found(%): C, 64.11; H, 9.25; N, 12.56. FT-IR (in KBr): 2964, 1589, 1466, 1333, 1167 cm^{-1}. ^{1}H-NMR: (400 MHz, $CDCl_3$): δ_{ppm}: 8.09 (1H, d), 7.80 (1H, d), 3.79 (2H, s), 3.03 (1H, m), 2.59 (2H, t), 2.48 (2H, t), 2.21 (6H, s), 1.39 (9H, s), 1.06 (6H, d). ^{13}C-NMR: (100 MHz, $CDCl_3$) $\delta_{ppm:}$ 164.5, 138.6, 137.4, 123.0, 122.4, 122.4, 57.1, 53.4, 53.2, 49.7, 45.5, 45.2, 34.9, 28.9, 17.0. Mass $(M+H^+)/z$: calcd: 338.23, found: 338.28.

3.5.7 Isolation of modified ligand $\mathbf{L_4'}$

$\mathbf{L_4'}$ has been isolated using same experimental procedure as $\mathbf{L_3'}$. Yield: 195 mg (40%). Elemental analyses: calcd. (%) C, 62.13; H, 7.62; N, 11.15; found(%): C, 62.08; H, 7.62; N, 11.22. FT-IR (in KBr): 2952, 1571, 1465, 1411, 1240 cm^{-1}. ^{1}H-NMR: (400 MHz, $CDCl_3$); δ_{ppm}: 8.13 (2H, d), 7.89 (2H, d), 3.69 (4H, s), 2.68 (4H, s), 2.36(6H, s), 1.37 (18H, s). ^{13}C-NMR: (100 MHz, $CDCl_3$); $\delta_{ppm:}$ 164.8, 138.9, 137.7, 123.3, 122.7, 122.6, 57.4, 53.6, 50.0, 35.2, 29.2, 17.0. Mass $(M+H^+)/z$: calcd: 503.28; found: 503.09.

3.6 References

1. Wiseman, H.; Halliwell, B. *Biochem. J.* **1996**, *313*, 17.
2. (a) Apel, K.; Hirt, H. *Annu. Rev. Plant Biol.* **2004**, *55*, 373. (b) Radi, R. *Proc. Natl. Acad. Sci. U.S.A.* **2004**, *101*, 4003.
3. (a) Shishehbor, M. H.; Aviles, R. J.; Brennan, M. L.; Fu, X. M.; Goormastic, M.; Pearce, G. L.; Gokce, N.; Keaney, J. F.; Penn, M. S.; Sprecher, D. L.; Vita, J. A.; Hazen, S. L. *J. Am. Med. Assoc*. **2003**, *289*, 1675. (b) Good, P. F.; Werner, P.; Hsu,

A.; Olanow, C. W.; Perl, D. P. *Am. J. Pathol.* **1996**, *149*, 21. (c) Danielson, S. R.; Held, J. M.; Schilling, B.; Oo, M.; Gibson, B. W.; Andersen, J. K. *Anal. Chem.* **2009**, *81*, 7823.

4. (a) Gunaydin, H.; Houk, K. N. *Chem. Res. Toxicol*. **2009**, *22*, 894. (b) Vander-Vliet, A.; Eiserich, J. P.; Halliwell, B.; Cross, C. E. *J. Biol. Chem.* **1997**, *272*, 7617.
5. (a) Goldstein, S.; Lind, J.; Merenyi, G. *Chem. Rev*. **2005**, *105*, 2457. (b) Schopfer, M. P.; Wang, J.; Karlin, K. D. *Inorg. Chem.* **2010**, *49*, 6267. (c) Surmeli, N. B.; Litterman, N. K.; Miller, A. F.; Groves, J. T. *J. Am. Chem. Soc.* **2010**, *132*, 17174.
6. (a) Olbregts, J. *Int. J. Chem. Kinet*. **1985**, *17*, 835. (b) Su, J.; Groves, J. T. *J. Am. Chem. Soc.* **2009**, *131*, 12979. (c) Bian, B.; Gao, Z. H.; Weisbrodt, N.; Murad, F. *Proc. Natl. Acad.Sci. U.S.A.* **2003**, *100*, 5712.
7. (a) Thomas, D. D.; Espey, M. G.; Vitek, M. P.; Miranda, K. M.; Wink, D. A. *Proc. Natl. Acad. Sci. U.S.A.* **2002**, *99*, 12691. (b) Gaggelli, E.; Kozlowski, H.; Valensin, D.; Valensin, G. *Chem. Rev*. **2006**, *106*, 1995.
8. (a) Lu, Y.; Prudent, M.; Qiao, L. A.; Mendez, M. A.; Girault, H. H. *Metallomics* **2010**, *2*, 474. (b) Goss, S. P. A.; Singh, R. J.; Kalyanaraman, B. *J. Biol. Chem.* **1999**, *274*, 28233. (c) Singh, R. J.; Goss, S. P. A.; Joseph, J.; Kalyanaraman, B. *Proc. Natl. Acad. Sci. U.S.A.* **1998**, *95*, 12912. (d) Zhang, H.; Joseph, J.; Felix, C.; Kalyanaraman, B. *J. Biol. Chem*. **2000**, *275*, 14038. (e) Bonini, M. G.; Fernandes, D. C.; Augusto, O. *Biochemistry* **2004**, *43*, 344.
9. Qiao, L.; Lu, Y.; Liu, B.; Girault, H. H. *J. Am. Chem. Soc*. **2011**, *133*, 19823.
10. Beckman, J. S.; *Chem. Res. Toxicol*. **1996**, *9*, 836.
11. (a) Tennyson, A. G.; Lippard, S. J. *Cell* **2011**, *18*, 1211. (b) Koppenol, W. H.; Moreno, J.

J.; Pryor, W. A.; Ischiropoulos, H.; Beckman, J. S. *Chem. Res. Toxicol.* **1992**, *5*, 834. (c) Stanbury, D. M. *Adv. Inorg. Chem*. **1989**, *33*, 69.

12. Jazdzewski, B. A.; Tolman, W. B. *Coord. Chem. Rev*. **2000**, *200-202*, 633.
13. (a) Coombes, R. G.; Diggle, A. W. *Tetrahedon Letts*. **1994**, *35*, 6373. (b) Coombes, R. G.; Diggle, A. W. *Tetrahedon Letts*. **1993**, *34*, 8557. (c) Shiri, M.; Zolfigol, M. A.; Kruger, H. G.; Tanbakouchian, Z. *Tetrahedron*, **2010**, *66*, 9077. (d) Halfen, J. A.; Jazdzewski, B. A.; Mahapatra, S.; Berreau, L. M.; Wilkinson, E. C.; Que, Jr. L.; Tolman, W. B. *J. Am. Chem. Soc*. **1997**, *119*, 8217.
14. Verboom, W.; Durie, A.; Egbernik, R. J. M.; Asfari, Z.; Reinhoudt, D. N. *J. Org. Chem.* **1992**, *57*, 1313.
15. Sarma, M.; Kalita, A.; Kumar, P.; Singh, A.; Mondal, B. *J. Am. Chem. Soc*. **2010**, *132*, 7846.
16. Beckman, J. S.; Carson, M.; Smith, C. D.; Koppenol, W. H. *Nature* **1993**, *364*, 584.
17. Beckman, J. S.; Ischiropoulos, H.; Zhu, L.; Vanderwoerd, M.; Smith, C.; Chen, J.; Harrison, J.; Martin, J. C.; Tsai, M. *Arch. Biochem. Biophys.* **1992**, *298*, 438.
18. Ramezanian, M. S.; Padmaja, S.; Koppenol, W. H. *Chem. Res. Toxicol.* **1996**, *9*, 232.
19. SMART, SAINT and XPREP, Siemens Analytical X-ray Instruments Inc., Madison, Wisconsin, USA, **1995**.
20. Sheldrick, G. M. SADABS: Software for Empirical Absorption Correction, University of Gottingen, Institut fur Anorganische Chemieder Universitat, Tammanstrasse 4, D-3400 Gottingen, Germany, **1999–2003**.
21. (a) Sheldrick, G. M. SHELXS-97, Program for solution of crystal structures, University of Göttingen, Germany, **1997**. (b) Farrugia, L. J. *J. Appl. Crystallogr*. **1997**, *30*, 565.

Chapter 4

Copper(II) mediated phenol ring nitration by nitrogen dioxide

Abstract

Cu(II) complexes of N2O2 type ligands, $\mathbf{L_5H_2}$ and $\mathbf{L_6H_2}$ [$\mathbf{L_5H_2}$ = 6,6'-(((pyridin-2-ylmethyl)azanediyl)*bis*(methylene))*bis*(2,4-di-*tert*-butylphenol); $\mathbf{L_6H_2}$ = 2,4-di-*tert*-butyl-6-(((3-(tert-butyl)-2-hydroxy-5-methylbenzyl)(pyridin-2-yl-methyl)amino)methyl)phenol] have been synthesized. Addition of nitrogen dioxide in THF solution of the complexes resulted in the nitration at the 4-position of coordinated equatorial phenolate ring of the ligand frameworks. This nitration did not occur at the phenol ring which is axially coordinated to the metal centre. Spectroscopic evidence suggests that the reaction proceeds through a phenoxyl radical complex formation.

4.1 Introduction

In human physiology, tyrosine nitration has attracted a considerable interest as it can alter the protein functions and thereby, can be used as a biomarker for various disease states caused by oxidative stress.[1-7] Tyrosine nitration is believed to occur in presence of either peroxynitrite ($ONOO^-$) ion or nitrogen dioxide (NO_2).[8,9] NO_2 generation can take place *via* several mechanisms like reaction of NO with O_2, oxidation of nitrite (NO_2^-) by H_2O_2 and peroxydases or by decomposition of $ONOO^-$ ion.[10-15] It is widely accepted that the tyrosine nitration by NO_2 occurs through an initial formation of tyrosine radical.[10] The roles of peroxydases, heme and heme-containing proteins in catalyzing the nitration are well established.[10] A number of examples of tyrosine/phenol nitration assisted by various metal complexes have been reported in recent years.[16] Though copper ion is known to favour the generation of free radicals which cause oxidative damage to proteins and lipids, the role of Cu(II) ion in nitration has not been studied extensively; specially, with respect to the mechanistic studies.[17,18] As such, most of the copper mediated tyrosine nitration studies have focused with copper-zinc superoxide dismutase (Cu-Zn SOD) which, apart from scavenging superoxide anion, has been shown to catalyze the oxidation of NO_2^- to NO_2.[19-22] Earlier studies have shown that Cu(II) can catalyze the decomposition of $ONOO^-$ to oxidize substrates or induce nitration.[23]

Tyrosine nitration by the NO_2^- ions were reported to be induced by Cu-Zn SOD through a Fenton's like mechanism (Scheme 4.1).[24,25] Initially, Cu(II) ion forms the key Cu(II)-hydroperoxo complex in presence of H_2O_2/HO_2^-. The hydroperoxo complex then decomposes to generate Cu(I), which in presence of H_2O_2 produces $^{\bullet}OH$ and/or Cu^{II}-$^{\bullet}OH$ *via* a Fenton like reaction (Scheme 4.1). The $^{\bullet}OH$ and Cu^{II}-$^{\bullet}OH$ radicals then induce the formation of NO_2 and tyrosyl radical from NO_2^- and tyrosine, respectively and lead to the nitration of tyrosine.

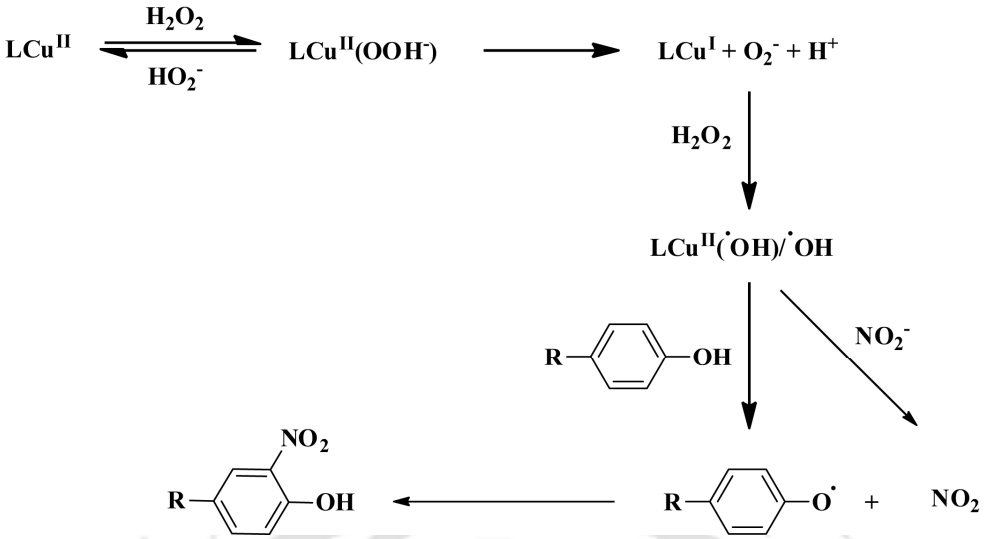

Scheme 4.1: Tyrosine nitration through Fenton's like mechanism (**L** represents ligand framework).

This chapter describes the interaction of NO_2 with Cu(II) complexes of N2O2 type ligands, $\mathbf{L_5H_2}$ and $\mathbf{L_6H_2}$ [$\mathbf{L_5H_2}$ = 6,6'-(((pyridin-2-ylmethyl)azanediyl)*bis*(methylene))*bis*(2,4-di-*tert*-butylphenol); $\mathbf{L_6H_2}$ = 2,4-di-*tert*-butyl-6-(((3-(*tert*-butyl)-2-hydroxy-5-methylbenzyl)(pyridin-2-yl-methyl) amino)methyl)phenol] (Figure 4.1) leading to the nitration of the phenol ring.

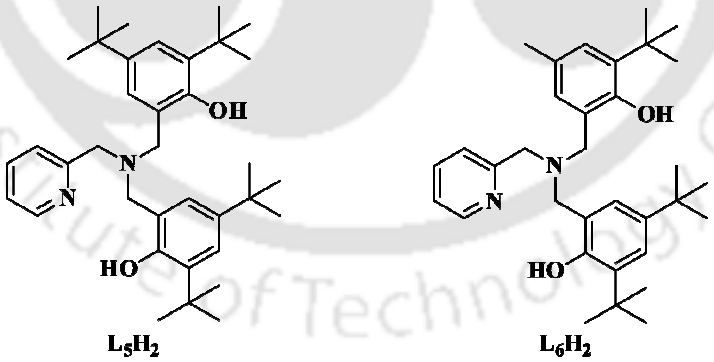

Figure 4.1: Ligands used for the present study.

4.2 Results and discussion

The ligand, $\mathbf{L_5H_2}$ was prepared following an earlier reported procedure.[26] $\mathbf{L_6H_2}$ was prepared

by Mannich reaction involving corresponding amine, phenol and formaldehyde in ethanol (Experimental section). Both the ligands displayed satisfactory elemental analyses (Experimental section). They were characterized by FT-IR, ^{1}H-NMR, ^{13}C-NMR, Mass spectroscopy. The complexes **4.1** and **4.2** were prepared by the reaction of Cu(II) acetate dihydrate with equivalent amount of the respective ligands in acetonitrile:dichloromethane (1:1) mixture (Scheme 4.2). The formation of the complexes **4.1** and **4.2** were established by elemental analyses, UV-visible, FT-IR, X-band EPR spectroscopic studies (Experimental section). Further, single crystal X-ray structure of complex **4.1** was determined (Figure 4.2).

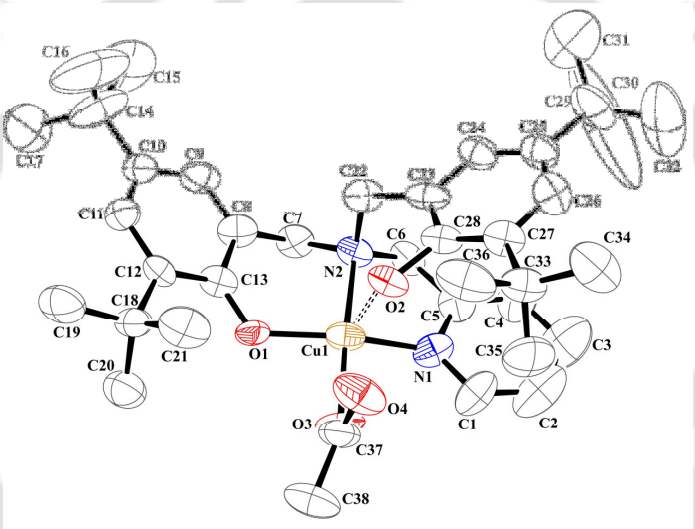

Figure 4.2: ORTEP diagram of complex **4.1** (50% thermal ellipsoid plot, hydrogen atoms and solvent molecules are omitted for clarity).

The structure of complex **4.1** was reported earlier, also. [26] In the mononuclear complex, Cu(II) ion is coordinated to the mono-deprotonated ligand (i.e. $\mathbf{L_5H^-}$) in a distorted square pyramidal geometry. Out of two phenol arms of $\mathbf{L_5H_2}$, one is deprotonated to the corresponding phenolate ion and other remains in the phenol form. The phenol is coordinated to the Cu(II) centre from axial position; whereas the phenolate ion is coordinated equatorially. [26] The axial Cu-O_{phenol} distance is 2.404 Å; whereas, the equatorial Cu-$O_{phenolato}$ distance is 1.900 Å. It is to be noted that

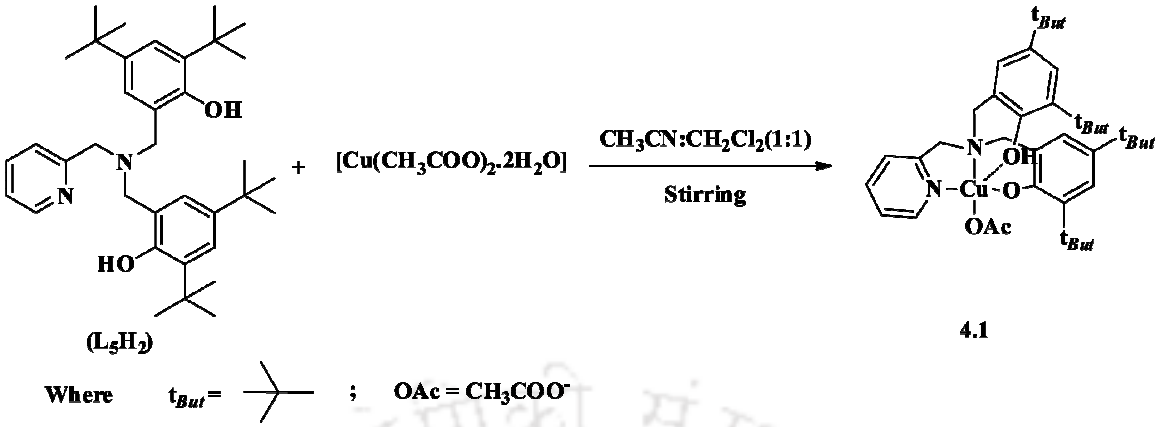

Scheme 4.2: Synthesis of complex **4.1**.

Cu-O_{phenol} distance is more than average Cu-$O_{phenolato}$ distances owing to the (i) axial elongation and (ii) electrostatic interaction between Cu(II) and phenolate ion. The acetate ion is coordinated to the metal centre from an equatorial position in a monodentate fashion. Other two corners of the square plane are occupied by two N-atoms from the ligand framework and thereby, the square pyramidal geometry around the central Cu(II) ion is completed. The discrete Cu(II) unit with the coordinated ligand resembles the structural models of the active site of galactose oxidase enzyme. It should be noted that the average distances for other reported structural models of active sites of galactose oxidase are in good agreement with the observed metric parameters in cases of complex **4.1**.[27-39]

In the UV-visible spectroscopy, complex **4.1** displays an intense absorption band centred at ~ 470 nm with a weaker *d-d* transition near 675 nm in acetonitrile solution. The band centred at 470 nm is assigned as the phenolato → Cu(II) charge transfer; while the bands at lower are attributed to the intra-ligand transitions. [26,40] The λ_{max} of the phenolato → Cu(II) charge transfer in acetonitrile was shifted to 458 nm in methanol (Figure 4.3). In case of complex **4.2**, the transitions were appeared at 480 and 680 nm in acetonitrile. In methanol, the phenolato → Cu(II) charge transfer band of complex **4.2** appeared at 470 nm (Appendix III).

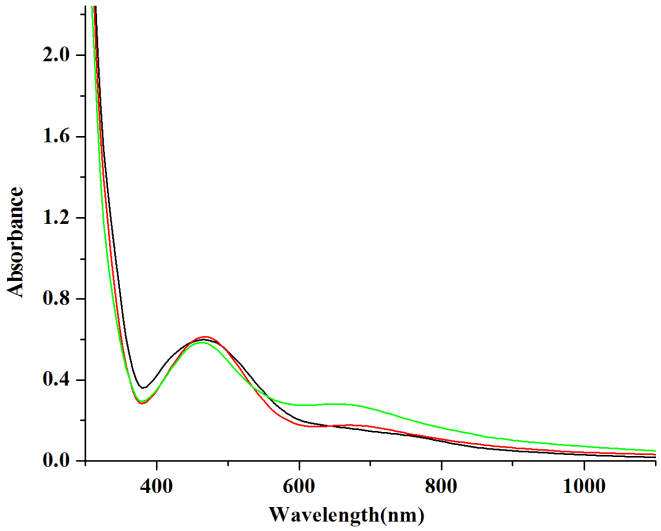

Figure 4.3: UV-visible spectra of complex **4.1** in THF (black trace), acetonitrile (red trace) and methanol (green trace) solvents.

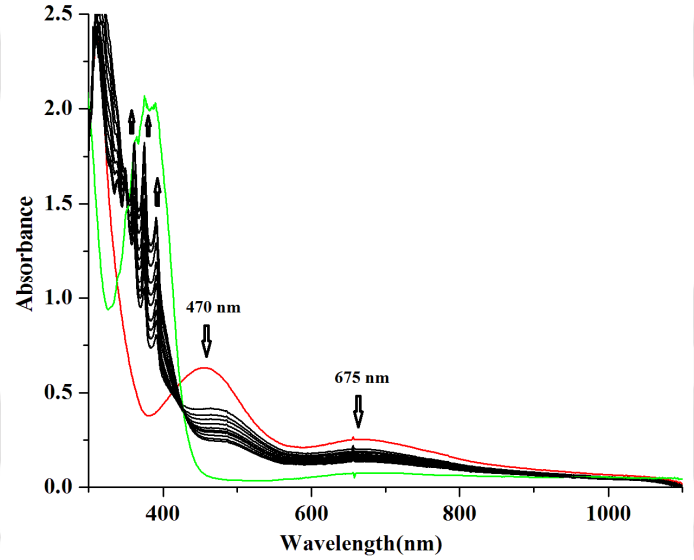

Figure 4.4: UV-visible spectra of complex **4.1** before (red trace) and after purging NO_2 (black traces and green trace) in dry THF at -80 °C.

The X-band EPR spectra of the complexes were recorded both in solid state and solution at 77 K. The crystalline complexes **4.1** and **4.2** are dissolved in methanol and the EPR spectra were recorded. The calculated values for $g_{\parallel}$ and $g_{\perp}$ are 2.329, 2.072, respectively. For complex **4.2**, these values are 2.316, 2.065, respectively. The g_{zz}/A_{zz} ratio is found to be characteristic for a copper centre within a square-pyramidal geometry with axial coordination. [26,40] It also reveals the presence of only one species in the solution.

4.3 Nitrogen dioxide reactivity

Addition of NO_2 in methanol solution of complexes **4.1** and **4.2**, resulted in green complexes, **4.3** and **4.4**, respectively. The complexes **4.3** and **4.4** were isolated as pure solid and characterized structurally. The ORTEP diagrams are shown in figure 4.5. The crystallographic data and the metric parameters are given in tables 4.1, 4.2 and 4.3, respectively. Characterization reveals that in complexes **4.3** and **4.4**, the equatorial phenolate ring of the ligands has undergone nitration at 4-position. Phenols are known to afford nitrophenols in their reaction with NO_2 in solution in two steps; the abstraction of a hydrogen atom from the phenolic OH group by NO_2 to form phenoxyl radical followed by the reaction of the phenoxyl radical with NO_2.[16] However, the free ligands in the reaction condition are not found to afford corresponding nitrophenols significantly (< 5%). On the other hand, the reactions of NO_2 with Cu(II) complexes of 2,4-di-*tert*-butyl-6-(((2-dimethylamino)ethyl)(isopropyl)amino)methyl)phenol and 6,6'-(((2-(dimethylamino)ethyl) azanediyl) *bis*(methylene))*bis*(2,4-di-*tert*-butylphenol)], respectively, were reported recently to result in the reduction of Cu(II) centre.[41] In these cases, UV-visible, EPR and ^{1}H-NMR spectroscopic studies unambiguously confirmed the reduction of Cu(II) centre in presence of NO_2. The reduction resulted in the nitration of phenol ring of the ligand frameworks in a mechanism where the nitronium ion (NO_2^+) generated, which attacks at the 4-position of the phenol ring.

However, in the present case, UV-visible, EPR spectroscopic studies did not show any indication of reduction of Cu(II) centre in the reaction of complexes **4.1** and **4.2** in methanol with NO_2 (Appendix III). Thus, the possibility of a mechanism involving the reduction of Cu(II) by NO_2 followed by the formation of NO_2^+ can be ruled out. In that case, one could think of the possibility of a NO_2 induced phenoxyl radical formation in the reaction medium.

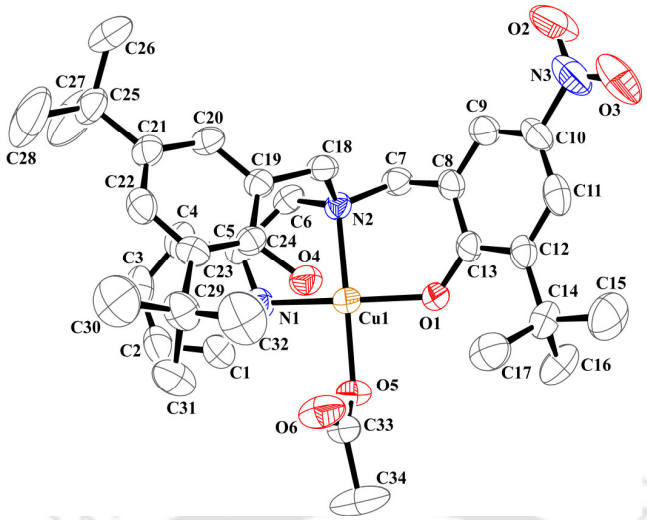

(a)

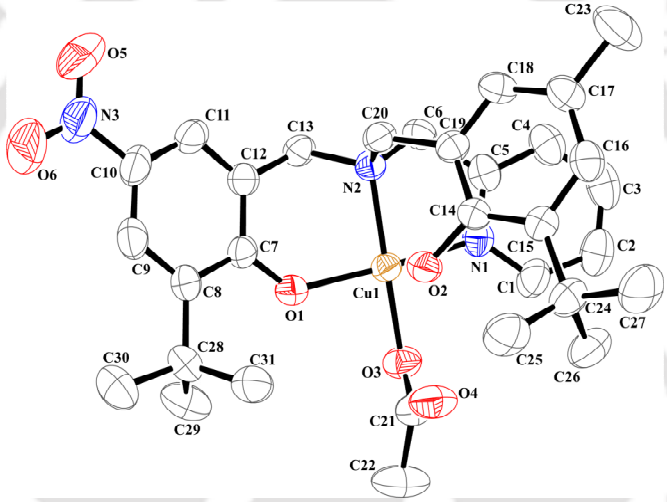

(b)

Figure 4.5: ORTEP diagram of complexes (a) **4.3** and (b) **4.4** (50% thermal ellipsoid plot, hydrogen atoms are omitted for clarity).

In methanol solution, no intermediate was trapped in UV-visible spectroscopy even at -80 °C or in X-band EPR spectral study of the frozen reaction mixture even at the very early stage of reaction. But in dry and degassed THF solution of complex **4.1** at -80 °C temperature, addition of NO_2 resulted in a transient pale brown intermediate. The phenolato →Cu(II) charge transfer transition band centred at ~470 nm gradually disappears with a concomitant appearance of bands at 365, 380 and 395 nm. These have been assigned as the charge transfer

bands for 2,4-ditertiarybutyl phenoxyl radical.[40] The intensity of the band centreed at ~675 nm decreases, but not disappeared indicating the existence of Cu(II) state in the intermediate. It would be worth mentioning here that addition of NO_2 gas in THF at -80 °C does not show similar absorption bands (Appendix III). The intermediate decomposes to the complex **4.3** with a strong absorption band at ~385 nm which is attributed to the π→π* of nitrophenol moiety (Figure 4.3).[40] On the other hand, addition of NO_2 in the THF solution of complex **4.1** at -80 °C followed by immediate freezing of the reaction mixture at 77 K, the solution became silent in X-band EPR spectroscopy suggesting the formation of a diamagnetic intermediate (Figure 4.6). This has been attributed to the significant overlap between $d_{x^2-y^2}$ magnetic orbital of Cu(II) with half occupied π-orbital of phenoxyl radical leading to S = 0 ground state.[40] The intermediate was found to be decomposed instantaneously at room temperature to result complex **4.3**. It is to be noted that in methanol solution even at -80 °C, the intermediate was not observed; reaction of complex **4.1** with NO_2 resulted to complex **4.3**. Since the formation of Cu(I) species in the reaction *via* reduction by NO_2 has already been ruled out, it is more logical to believe that NO_2 is promoting the formation of phenoxyl radical in the

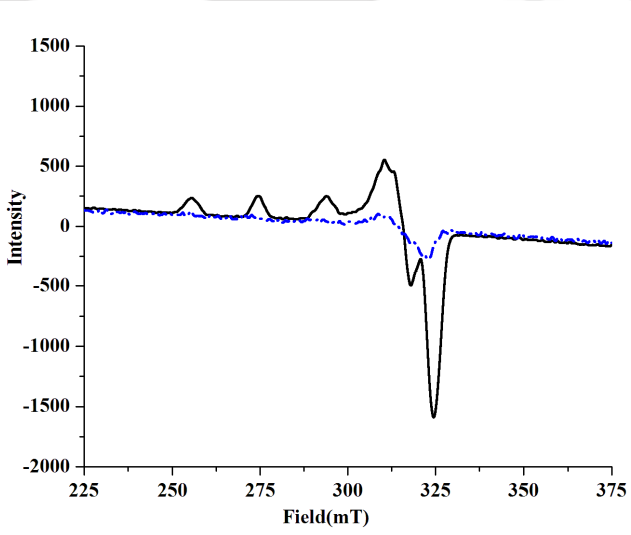

Figure 4.6: X-band EPR spectra of complex **4.1** (black trace) and phenoxyl radical intermediate (blue trace) in dry THF at 77 K.

one of the phenol ring of the complex. Moreover, analysis of the reaction mixture reveals the presence of tertiarybutyl nitrite (Appendix III). During the reaction, tertiarybutyl radical is formed and this resulted in the formation of tertiarybutyl nitrite upon combination with NO_2 (Appendix III). The presence of tertiarybutyl nitrite also supports the involvement of the radical mechanism. It should be noted that in biological systems, peroxynitrite and hemeperoxidase pathways are the two most widely acceptable mechanisms leading to the simultaneous formation of tyrosyl radical and NO_2; these then combine at a diffusion controlled rate to afford 3-nitrotyrosine. Though, other oxidants such as carbonate radical, oxo-metal complexes and hydroxyl radicals can lead tyrosyl radical formation; NO_2 alone is found to be insufficient to promote tyrosine nitration.[16] This is because the initial reaction of NO_2 with tyrosine leading to the formation of tyrosyl radical is slower than the other processes that NO_2 undergoes.

The thermal instability did not allow further characterization of the intermediate complex. Complex **4.2** also found to behave similar. In dry and degassed THF solution, addition of NO_2 resulted in the appearance of absorption bands at ~ 365, 380 and 395 nm with the decay of phenolato → Cu(II) charge transfer (Appendix III). The intermediate was found silent in X-band EPR spectroscopy at 77 K (Appendix III). Upon warming up, the radical complex led to the formation of complex **4.4** (Experimental section). It is to be noted that while oxidizing phenolate moiety to phenoxyl radical, NO_2 is expected to be reduced to NO_2^-. In the FT-IR spectrum of the crude reaction mixtures obtained from complexes **4.1** and **4.2**, respectively a stretching frequency at 1384 cm^{-1} was observed (Appendix III). This is attributed to the NO_3^- stretching. However, no frequency corresponding to the NO_2^- was observed in any case. On the other hand, while the reaction mixture from complex **4.1** was allowed to stand for few days, a small crop (~10 %) of the Cu(II) complex of corresponding nitrated ligand crystallized out as nitrate (NO_3^-) salt, complex **4.5**. The ORTEP diagram is shown in figure

4.7. The crystallographic data and metric parameters are listed in tables 4.1, 4.2 and 4.3, respectively. Presumably, NO_2^- ion formed during the reaction resulted in HNO_2 after taking up one H^+ from the solvent methanol. HNO_2 is known to decompose to NO_3^- at room temperature. Thus, instead of NO_2^-, stretching frequency corresponding to NO_3^- was observed in the FT-IR spectrum of the crude reaction mixture.

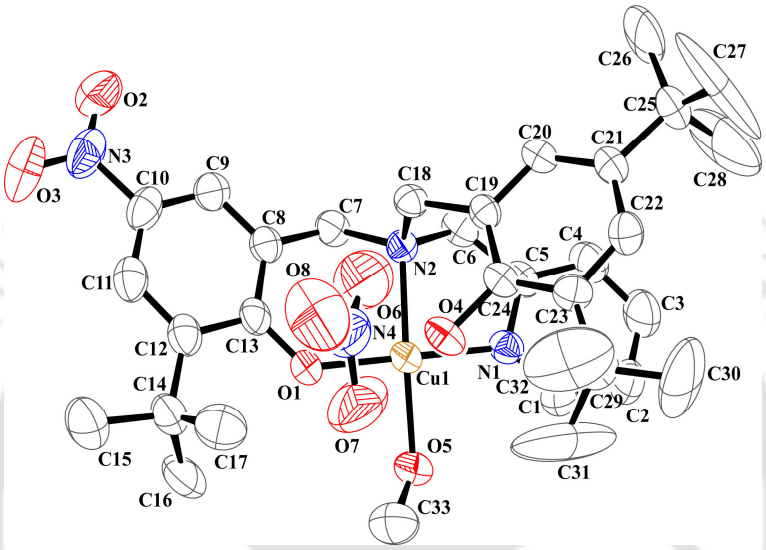

Figure 4.7: ORTEP diagram of complex **4.5** (50% thermal ellipsoid plot, hydrogen atoms are omitted for clarity).

It is to be noted that the phenolato → Cu(II) charge transfer band at 470 nm of complex **4.1** was reported to disappear on oxidation with Ce(IV) in dichloromethane/actonitrile solution at -40 °C though the phenoxyl radical could not be detected.[26,40] But, copper(II) perchlorate, hexahydrate was found to undergo a rapid reaction with $\mathbf{L_5H_2}$ in CH_2Cl_2/CH_3CN leading to the formation of Cu(II)-phenoxyl radical intermediate. However, no such reactions are observed in methanol.[26,40]

Table 4.1: Crystallographic table for complex **4.3, 4.4** and **4.5**.

	Complex **4.3**	Complex **4.4**	Complex **4.5**
Formulae	$C_{34}\ H_{45}\ N_3\ O_6\ Cu$	$C_{31}\ H_{39}\ N_3\ O_6\ Cu$	$C_{34}\ H_{50}\ N_4\ O_9\ Cu$
Mol. wt.	655.27	613.19	722.32
Crystal system	Monoclinic	Monoclinic	Monoclinic
Space group	P2(1)/n	P2(1)/n	P2(1)/n
Temperature /K	293(2)	150(2)	293(2)
Wavelength /Å	0.71073	1.5418	0.71073
a /Å	14.4864(7)	13.3750(2)	15.7058(9)
b /Å	13.9322(5)	14.3438(3)	10.0428(6)
c /Å	17.6786(6)	17.9158(4)	23.1982(13)
α/°	90.00	90.00	90.00
β/°	100.459(4)	95.880(2)	92.868(5)
γ/°	90.00	90.00	90.00
V/ $Å^3$	3508.7(2)	3419.03(12)	3654.5(4)
Z	4	4	4
Density/Mgm^{-3}	1.240	1.191	1.313
Abs. co-eff. /mm^{-1}	0.667	1.243	0.654
Abs. correction	multi-scan	multi-scan	multi-scan
F(000)	1388	1292	1532
Total no. of reflections	6181	6580	6419
Reflections, $I > 2\sigma(I)$	4840	5488	4434
Max. 2θ/°	25.00	71.39	25.00
Ranges (h, k, l)	-17≤h ≤17 -11≤ k ≤16 -21≤ l ≤ 19	-11≤h ≤16 -17≤ k ≤16 -21≤ l ≤ 20	-18≤h ≤16 -11≤ k ≤11 -27≤ l ≤ 22
Complete to 2θ (%)	99.8	98.9	99.8
Refinement method	Full-matrix least-squares on F^2	Full-matrix least-squares on F^2	Full-matrix least-squares on F^2
Goof (F^2)	1.837	1.103	1.085
R indices [$I > 2\sigma(I)$]	0.0493	0.0652	0.0688
R indices (all data)	0.0671	0.0732	0.1025

Table 4.2: Complex **4.3, 4.4** and **4.5** selected bond angles (°).

Complex **4.3**		Complex **4.4**		Complex **5.5**	
Atoms	Angles (°)	Atoms	Angles (°)	Atoms	Angles (°)
O1 - Cu1 - O5	87.98(8)	O1 - Cu1 - N1	174.8(1)	O1 - Cu1 - O2	99.04(8)
O1 - Cu1 - O4	101.81(7)	O1 - Cu1 - O4	95.4(1)	O1 - Cu1 - O3	87.54(9)
O5 - Cu1 - N2	172.33(9)	N1 - Cu1 - N2	84.7(1)	O1 - Cu1 - N1	169.20(9)
O5 - Cu1 - N1	92.78(9)	N1 - Cu1 - O5	90.0(1)	O1 - Cu1 - N2	94.06(9)
N2 - Cu1 -N1	83.81(9)	N2 - Cu1 - O5	167.6(1)	O2 - Cu1 - O3	98.84(8)
Cu1 - O1 - C13	126.7(2)	Cu1 - O1 - C13	130.3(3)	O2 - Cu1 - N1	91.40(8)
Cu1 - N2 - C6	106.4(2)	Cu1 - N1 - C1	127.8(3)	O2 - Cu1 - N2	87.69(8)
Cu1 - N2 - C18	112.2(2)	Cu1 - N2 - C18	112.5(2)	O3 - Cu1 - N1	93.62(9)
Cu1 - O4 - C24	113.8(2)	Cu1 - N2 - C6	106.6(2)	O3 - Cu1 - N2	172.96(9)
Cu1 - N1 - C1	127.2(2)	Cu1 - O4 - C24	110.3(3)	N1 - Cu1 - N2	83.54(9)
O1 - Cu1 - N2	93.97(9)	O1 - Cu1 - N2	94.9(1)	Cu1 - O1 - C7	127.0(2)
O1 - Cu1 - N1	168.22(9)	O1 - Cu1 - O5	89.4(1)	Cu1 - O2 - C14	114.8(2)
O5 - Cu1 - O4	100.06(8)	N1 - Cu1 - O4	89.8(1)	Cu1 - O3 - C21	124.0(2)
N2 - Cu1 - O4	86.82(8)	N2 - Cu1 - O4	89.1(1)	Cu1 - N1 - C1	126.2(2)
O4 - Cu1 - N1	89.64(8)	O4 - Cu1 - O5	102.1(1)	Cu1 - N1 - C5	114.1(2)
Cu1 - O5 - C33	123.7(2)	Cu1 - N1 - C5	113.6(3)	Cu1 - N2 - C6	106.5(2)
Cu1 - N2 - C7	109.0(2)	Cu1 - N2 - C7	108.3(2)	Cu1 - N2 - C13	108.9(2)
Cu1 - N1 - C5	113.9(2)	-	-	Cu1 - N2 - C20	112.3(2)

Table 4.3: Complex **4.3, 4.4** and **4.5** selected bond distances (Å).

Complex **4.3**		Complex **4.4**		Complex **4.5**	
Atoms	Distances (Å)	Atoms	Distances (Å)	Atoms	Distances (Å)
Cu1 - O1	1.903(2)	Cu1 - O1	1.885(3)	Cu1 - O1	1.908(2)
Cu1 - N2	2.018(2)	Cu1 - N2	2.008(3)	Cu1 - O2	2.393(2)
Cu1 - N1	1.993(2)	Cu1 - O5	2.007(3)	Cu1 - O3	1.943(2)
O5 - C33	1.278(4)	N1 - C5	1.352(6)	Cu1 - N1	1.995(2)
N2 - C7	1.494(3)	N1 - C1	1.339(6)	Cu1 - N2	2.022(2)
O4 - C24	1.382(4)	N2 - C6	1.494(5)	O1 - C7	1.307(3)
N1 - C1	1.342(4)	O2 - N3	1.218(7)	O2 - C14	1.378(3)
O6 - C33	1.223(5)	C24 - O4	1.391(6)	O2 - H111	0.80(3)
Cu1 - O5	1.934(2)	O7 - N4	1.215(7)	O3 - C21	1.269(3)
Cu1 - O4	2.482(2)	N4 - O6	1.217(8)	O4 - C21	1.232(3)
O1 - C13	1.306(3)	Cu1 - N1	1.977(3)	O5 - N3	1.221(6)
N2 - C6	1.483(3)	Cu1 - O4	2.429(4)	O6 - N3	1.230(5)
N2 - C18	1.503(4)	O1 - C13	1.302(5)	N1 - C1	1.345(4)
N1 - C5	1.337(4)	N2 - C18	1.490(5)	N1 - C5	1.333(4)
O2 - N3	1.233(4)	-	-	N2 - C6	1.492(4)
O3 - N3	1.225(5)	-	-	N2 - C13	1.506(3)

Another analogous tripodal ligand, $\mathbf{LH_2}$ [$\mathbf{LH_2}$ = 2-(*tert*-butyl)-6-(((3-(*tert*-butyl)-2-hydroxy-5-methoxybenzyl)(pyridin-2-ylmethyl)amino)methyl)-4-nitrophenol] with two phenolic arms was reported to allow the formation of phenoxyl radical in equatorial phenolate moiety.[40] The corresponding Cu(II) complex, [Cu(LH)(OAc)] was characterized structurally. In mononuclear complex the Cu(II) ion is surrounded in a square pyramidal geometry like complex **4.1**. One electron oxidation of [Cu(LH)(OAc)] results in the formation of $[Cu(LH)(OAc)]^{\bullet+}$ radical complex which is EPR silent.[40] In the UV-visible spectra the formation of a sharp band at 410 nm was observed. This was attributed to the absorption of the phenoxyl radical.[40]

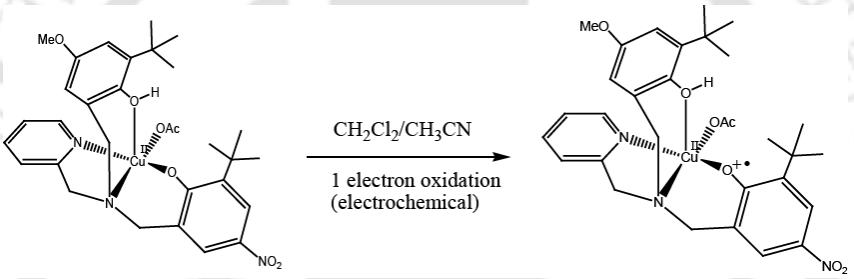

Scheme 4.3

In the present case, the nitration was observed only at one phenol ring of the ligands. The crystal structures of the products i.e. complexes **4.3** and **4.4** revealed that in both the cases nitration occurred at the 4-position of the phenolate ring which is coordinated to the Cu(II) centre at equatorial position. Interestingly, the nitration through NO_2^+ ion formation mechanism was reported to occur at the 4-position of all the available phenol rings of the ligand frameworks. Since the free ligands were not observed to afford appreciable nitration in presence of NO_2, this indirectly supports the involvement of the Cu(II) centre in the radical formation mechanism; though exact role is not yet known. The selective nitration is perhaps because of the higher probability of Cu(II) induced formation of phenoxyl radical at the equatorial phenolate ring.

It would be worth to mention here that the tyrosine nitration promoted by peroxynitrites in presence of transition metal centres may undergo through NO_2^+ ion formation. However, it is not yet confirm that electrophilic aromatic nitration pathway involving NO_2^+ ion is a biologically relevant mechanism though reported recently in model systems.

4.4 Conclusion

In conclusion, the present work demonstrates the NO_2 reactivity of two Cu(II) complexes of N2O2 type ligands. The reaction leads to the nitration at the 4-position of coordinated equatorial phenolate ring of the ligand frameworks. This nitration did not occur at the phenol ring which is axially coordinated to the metal centre. Spectroscopic evidence suggests that the reaction proceeds through a phenoxyl radical complex formation in presence of NO_2. In contrast, NO_2 reactivity of Cu(II) complexes of 2,4-di-*tert*-butyl-6-(((2- dimethylamino) ethyl)(isopropyl) amino) methyl) phenol and 6,6'-(((2-(dimethylamino)ethyl)azanediyl)*bis*(methylene))*bis*(2,4-di-*tert*-butylphenol)] was reported to induce reduction of Cu(II) centres leading to the nitration of the phenol ring of the ligand through NO_2^+ ion.

4.5 Experimental section

4.5.1 Materials and methods

All reagents and solvents of reagent grade were purchased from commercial sources and used as received except specified. Acetonitrile was distilled from calcium hydride. Methanol was dried by refluxing over iodine activated magnesium with a magnesium loading of 5 gm/lit. Then the dried methanol was kept over 20% m/v 3Å molecular sieves for 4-5 days before using. THF was dried by refluxing over sodium metal in presence of benzophenone. Deoxygenation of the solvent and solutions was effected either by repeated vacuum/purge

cycles or bubbling with argon for 30 minutes or using freeze-pump-thaw cycles. NO_2 gas was prepared by the reaction of purified NO with O_2 followed by passing through an oxygen trap [Model 1000 oxygen trap; Z290246 Aldrich] to remove extra oxygen, if any. UV-visible spectra were recorded on a Perkin Elmer Lambda 25 UV-visible spectrophotometer. FT-IR spectra of the solid samples were taken on a Perkin Elmer spectrophotometer with samples prepared as KBr pellets. Solution electrical conductivity was measured using a Systronic 305 conductivity bridge. ^{1}H-NMR spectra were recorded in a 400 MHz Varian FT spectrometer. Chemical shifts (ppm) were referenced either with an internal standard (Me_4Si) or to the residual solvent peaks. The X-band Electron Paramagnetic Resonance (EPR) spectra were recorded on a JES-FA200 ESR spectrometer, at room temperature and 77 K with microwave power, 0.998 mW; microwave frequency, 9.14 GHz and modulation amplitude, 2. Elemental analyses were obtained from a Perkin Elmer Series II Analyzer. The magnetic moment of complexes was measured on a Cambridge Magnetic Balance. Single crystals were grown by slow diffusion followed by slow evaporation technique. The intensity data were collected using a Bruker SMART APEX-II CCD diffractometer, equipped with a fine focus 1.75 kW sealed tube MoKa radiation (λ = 0.71073 Å) at 273(3) K, with increasing w (width of 0.3° per frame) at a scan speed of 3 s/frame. The SMART software was used for data acquisition.[42] Data integration and reduction were undertaken with SAINT and XPREP software.[43] Structures were solved by direct methods using SHELXS-97 and refined with full-matrix least squares on F^2 using SHELXL-97.[44] Structural illustrations have been drawn with ORTEP-3 for Windows.[45]

4.5.2 Synthesis of ligand L_5H_2

2-picolylamine (1.08 g, 10 mmol), 2, 4-di *tert*-butylphenol (4.12 g, 20 mmol) and formaldehyde (2 g of 37% solution, 21 mmol) were taken in 50 ml of ethanol and the mixture

was refluxed for 12 h during which a white precipitate was formed. The precipitate was isolated by filtration and washed with cold ethanol to obtain the ligand **L_5H_2** as white powder. It was recrystallized from methanol to obtain pure **L_5H_2**. Yield: 4.35 g (~ 80%). Elemental analyses: calcd. (%): C, 79.36; H, 9.62; N, 5.14; found (%): C, 79.39; H, 9.65; N, 5.07. FT-IR (in KBr): 2958, 2866, 1597, 1232,

1201, 757 cm^{-1}. ^{1}H-NMR: (400 MHz, $CDCl_3$): δ_{ppm}: 10.60 (2H, s), 8.71 (1H, d), 7.71 (1H, t), 7.29 (1H, t), 7.24 (2H, s), 7.14 (1H, d), 6.95 (2H, s), 3.86 (2H, s), 3.82 (4H, s), 1.42 (18H, s), 1.30 (18H, s). ^{13}C-NMR: (100 MHz, $CDCl_3$) δ_{ppm}: 156.4, 154.0, 148.3, 140.6, 137.4, 136.5, 125.3, 123.8, 123.6, 122.6, 121.5, 57.1, 55.6, 35.3, 34.3, 31.9, 29.8. Mass $(M+H^+)/z$: calcd: 545.40; found: 545.41.

4.5.3 Synthesis of ligand L_6H_2

2-picolylamine (1.08 g, 10 mmol) and 3,5-di-*tert*-butyl-2-hydroxybenzaldehyde (2.34, 10 mmol) was added in 50 ml of methanol. The mixture was stirred for 1 h at room temperature to give corresponding imine. The imine was then reduced by 2.1 equivalent of $NaBH_4$ to give corresponding amine. The solvent was dried under vacuum. 50 ml water was added to the crude mass and it was neutralized with acetic acid. The organic component was extracted from the crude solution using chloroform (50 ml × 3 portions). The solvent was dried under vacuum. The crude mass was then dissolved in 50 ml of ethanol and made to react with 2-*tert*-butyl-4- methylphenol (1.64g, 10 mmol) and formaldehyde (1 g of 37% solution, 11 mmol); the reaction mixture was refluxed for 12 h to give a white precipitate. The precipitate was isolated by filtration and washed with cold ethanol to obtain the ligand **L_6H_2** as white powder. It was recrystallized from methanol to obtain pure **L_6H_2**. Yield: 3.50 g (~70%). Elemental analyses: calcd. (%): C, 78.84; H, 9.22; N, 5.57; found (%): C, 78.90; H, 9.24; N, 5.48. FT-IR (in KBr): 3417, 2958, 1599, 1479, 1232, 790 cm^{-1}. ^{1}H-NMR: (400 MHz, $CDCl_3$):

δ_{ppm}: 10.56 (2H, s), 8.70 (1H, s), 7.70 (1H, t), 7.28 (2H, d), 7.13 (1H, d), 7.00 (1H, d), 6.91 (1H, s), 6.77 (1H, s), 3.82 (2H, s), 3.79 (2H, s), 3.77 (2H, s), 2.24 (3H, s), 1.40 (18H, s), 1.28 (9H, s). ^{13}C-NMR: (100 MHz, $CDCl_3$) δ_{ppm}: 156.3, 154.0, 154.0, 148.3, 140.5, 137.5, 137.3, 136.5, 129.2, 127.3, 127.2, 123.9, 123.5, 122.6, 122.3, 121.4, 57.0, 56.2, 55.4, 35.2, 34.9, 34.3, 31.9, 29.8, 29.8, 20.9. Mass $(M+H^+)/z$: calcd: 503.36; found: 503.37.

4.5.4 Synthesis of complex 4.1

To a stirred solution of copper(II) acetate dihydrate, $Cu(OAc)_2 \cdot H_2O$ (0.398 g, 2 mmol) in 50 ml acetonitrile was added to a solution of ligand **L_5H_2** (1.09 g, 2 mmol) in 50 ml dichloromethane. The reaction mixture was stirred for 2 h. The volume of the solution was reduced under vacuum to ~10 ml and kept in freezer for 12 h to obtain complex **4.1** as a dark brown solid. Yield: 1.2 g (~90%). Elemental analyses: calcd. (%): C, 68.49; H, 8.17; N, 4.20; found (%): C, 68.12; H, 8.34; N, 4.31. UV-visible (methanol): λ_{max}, 675 and 458 nm. FT-IR (in KBr): 3428, 2953, 1565, 1442, 1411, 1237, 757 cm^{-1}. The complex **4.1** behaves as 1:1 electrolyte in methanol solution [ΛM (S cm^{-1}), 151]. μ_{obs},1.57 BM.

4.5.5 Synthesis of complex 4.2

Complex **4.2** was prepared using same protocol used for complex **4.1**. Yield: 1.05 g (~85%). Elemental analyses: calcd. (%): C, 67.33; H, 7.75; N, 4.49; found (%): C, 67.41; H, 7.87; N, 4.41. UV-visible (methanol): λmax, 680 and 470 nm. FT-IR (in KBr): 3425, 2956, 1569, 1438, 1413, 1237, 757 cm^{-1}. The complex **4.2** behaves as 1:1 electrolyte in methanol solution [ΛM (S cm^{-1}), 148]. μ_{obs}, 1.63 BM.

4.5.6 Synthesis of complex 4.3

To a degassed solution of complex **4.1** (500 mg) in methanol (or in THF, 20 ml), excess NO_2

gas was purged at room temperature. The brown colored solution becomes greenish. The volume of the solution was reduced to ~ 5 ml and kept in freezer afforded crystals of complex **4.3**. Yield: (~60%). Elemental analyses: calcd. (%): C, 62.32; H, 6.92; N, 6.41; found (%): C, 62.90; H, 7.13; N, 6.48. UV-visible (methanol): λ_{max}, 690 and 390 nm. FT-IR (in KBr): 3416, 2957, 1583, 1281, 1104, 728 cm^{-1}. X-band EPR data: $g_{\parallel}$, 2.332; $g_{\perp}$, 2.085 and $A_{\parallel}$, 166.984×10^{-4} cm^{-1}. The complex **4.3** behaves as 1:1 electrolyte in methanol solution [ΛM (S cm^{-1}), 155]. μ_{obs}, 1.58 BM.

4.5.7 Synthesis of complex 4.4

It was prepared from complex **4.2** (500 mg) using same protocol used for the preparation of complex **4.3** from complex **4.1**. Yield: ~65%. Elemental analyses: calcd. (%): C, 60.72; H, 6.41; N, 6.85; found (%): C, 60.68; H, 6.44; N, 6.83. UV-visible (methanol): λmax, 688 and 390 nm. FT-IR (in KBr): 3405, 2965, 1607, 1434, 1092, 708 cm^{-1}. X-band EPR data: $g_{\parallel}$, 2.334; $g_{\perp}$, 2.086 and $A_{\parallel}$, 167.447×10-4 cm^{-1}. The complex **4.4** behaves as 1:1 electrolyte in methanol solution [ΛM (S cm^{-1}), 156]. μ_{obs}., 1.64 BM.

4.5.8 Isolation of tertiarybutyl nitrite

For both the cases of complex **4.1** and **4.2**, same protocol was used to isolate tertiarybutyl nitrite. The details are given for complex **4.1**. 500 mg of complex **4.1** was dissolved in dry and degassed THF (or methanol, 10 ml). To this, excess NO_2 gas was purged at room temperature. The brown colored solution becomes greenish. The reaction mixture was allowed to stand at room temperature for 1 h. Then the after removing the excess NO_2, the reaction mixture was subjected column chromatography using neutral alumina. Yield, ~ 50%. The formation of tertiarybutyl nitrite was confirmed by ESI-Mass spectroscopy as well as by comparing the other spectral data with the commercially available one. Elemental analyses:

calcd. (%): C, 46.59; H, 8.80; N, 13.58; found (%): C, 46.56; H, 8.81; N, 13.66. Mass ($M+H^+$)/z: calcd: 104.06; found: 103.95.

4.5.8 Synthesis of complex 4.5

To a degassed solution of complex **4.1** in methanol (20 ml), excess NO_2 gas was purged at room temperature. The brown colored solution becomes greenish. The volume of the solution was reduced to ~ 5 ml and kept at room temperature for 5-6 days to afforded crystals of complex **4.5**. Yield: (~10 %).

4.6 References

1. Wattanapitayakul, S. K.; Weinstein, D. M.; Holycross, B. J.; Bauer, J. A. *FASEB J.* **2000**, *14*, 271.
2. Ferdinandy, P.; Danial, H.; Ambrus, I.; Rothery, R. A.; Schulz, R. *Circ. Res.* **2000**, *87*, 241.
3. Oyama, J.; Shimokawa, H.; Momii, H.; Cheng, X.; Fukuyama, N.; Arai, Y.; Egashira, K.; Nakazawa, H.; Takeshita, A. *J. Clin. Invest.* **1998**, *101*, 2207.
4. Kondo, S.; Toyokuni, S.; Tsuruyama, T.; Ozeki, M.; Tachibana, T.; Echizenya, M.; Hiai, H.; Onodera, H.; Imamura, M. *Cancer Lett*. **2002**, *179*, 87.
5. Mendes, R. V.; Martins, A. R.; de Nucci, G.; Murad, F.; Soares, F. A. *Histopathology* **2001**, *39*, 172.
6. Fukuyama, N.; Takebayashi, Y.; Hida, M.; Ishida, H.; Ichimori, K.; Nakazawa, H. *Free Radical Biol. Med.* **1997**, *22,* 771.
7. Liu, J. S.; Zhao, M. L.; Brosnan, C. F.; Lee, S. C. *Am. J. Pathol.* **2001**, *158*, 2057.
8. Gunaydin, H.; Houk, K. N. *Chem. Res. Toxicol*. **2009**, *22*, 894.

9. Van der Vliet, A.; Eiserich, J. P.; Halliwell, B.; Cross, C. E. *J. Biol. Chem.* **1997**, *272*, 7617.

10. Radi, R. *Proc. Natl. Acad. Sci. U.S.A.* **2004**, *101*, 4003.

11. Radi, R. *Acc. Chem. Res*. **2013**, *46*, 550.

12. Surmeli, N. B.; Litterman, N. K.; Miller, A. F.; Groves, J. T. *J. Am. Chem. Soc.* **2010**, *132*, 17174.

13. Olbregts, J. *Int. J. Chem. Kinet.* **1985**, *17*, 835.

14. Su, J.; Groves, J. T. *J. Am. Chem. Soc.* **2009**, *131*, 12979.

15. Bian, K.; Gao, Z. H.; Weisbrodt, N.; Murad, F. *Proc. Natl. Acad. Sci. U.S.A.* **2003**, *100*, 5712.

16. (a) Su, J.; Groves, J. T. *Inorg. Chem.* **2010**, *49*, 6317. (b) Schopfer, M. P.; Mondal, B.; Lee, D.-H.; Narducci Sarjeant, A. A.; Karlin, K. D. *J. Am. Chem. Soc.* **2009**, *131*, 11304. (c) Park, G. Y.; Deepalatha, S.; Puiu, S. C.; Lee, D.-H.; Mondal, B.; Narducci Sarjeant, A. A.; del Rio, D.; Pau, M. Y. M.; Solomon, E. I.; Karlin, K. D. *J. Biol. Inorg. Chem*. **2009**, *14*, 1301. (d) Maiti, D.; Lee, D.- H.; Narducci Sarjeant, A. A.; Pau, M. Y. M.; Solomon, E. I.; Gaoutchenova, K.; Sundermeyer, J.; Karlin, K. D. *J. Am. Chem. Soc.* **2008**, *130*, 6700. (e) Yokoyama, A.; Cho, K.-B.; Karlin, K. D.; Nam, W. *J. Am. Chem. Soc*., **2013**, *135*, 14900.

17. Reddy, P. V. B.; Rao, K. V. R.; Norenberg, M. D. *Lab. Invest.* **2008**, *88*, 816.

18. Thomas, D. D.; Espey, M. G.; Vitek, M. P.; Miranda, K. M.; Wink, D. A. *Proc. Natl. Acad. Sci. USA.* **2002**, *99*, 12691.

19. Goss, S. P. A.; Singh, R. J.; Kalyanaraman, B. *J. Biol. Chem.* **1999**, *274*, 28233.

20. Singh, R. J.; Goss, S. P. A.; Joseph, J.; Kalyanaraman, B. *Proc. Natl. Acad. Sci. USA.* **1998**, *95*, 12912.

21. Zhang, H.; Joseph, J.; Felix, C.; Kalyanaraman, B. *J. Biol. Chem.* **2000**, *275*, 14038.

22. Bonini, M. G.; Fernandes, D. C.; Augusto, O. *Biochemistry* **2004**, *43*, 344.

23. Beckman, J. S.; Carson, M.; Smith, C. D.; Koppenol, W. H. *Nature* **1993**, *364*, 584.

24. Thomas, D. D.; Espey, M. G.; Vitek, M. P.; Miranda, K. M.; Wink, D. A. *Pro. Natl. Acad. Sci. U.S.A.* **2002**, *99*, 12691.

25. Qiao, L.; Lu, Y.; Liu, B.; Girault, H. H. *J. Am. Chem. Soc.* **2011**, *133*, 19823.

26. Shimazaki, Y.; Huth, S.; Odani, A.; Yamauchi, O. *Angew. Chem. Int. Ed.* **2000**, *39*, 1666.

27. Halfen, J. A.; Young Jr.; V. G.; Tolman, W. B. *Angew. Chem. Int. Ed.* **1996**, *35*, 1687.

28. Wang, Y.; Stack, T. D. P. *J. Am. Chem. Soc.* **1996**, *118*, 13097.

29. Whittaker, M. M.; Duncan, W. R.; Whittaker, J. W. *Inorg. Chem.* **1996**, *35*, 382.

30. Halfen, A.; Jazdzewski, B. A.; Mahapatra, S.; Berreau, L. M.; Wilkinson, E. C.; Que Jr, L.; Tolman, W. B. *J. Am. Chem. Soc.* **1997**, *119*, 8217.

31. Sokolowski, A.; Leutbecher, H.; Weyhermuller, T.; Schnepf, R.; Bothe, E.; Bill, E.; Hildebrandt, P.; Wieghardt, K. *J. Biol. Inorg. Chem.* **1997**, *2*, 444.

32. Zurita, D.; Gautier-Luneau, I.; Menage, S.; Pierre, J.-L.; Saint-Aman, E. *J. Biol. Inorg. Chem.* **1997**, *2*, 46.

33. Wang, Y.; DuBois, J. L.; Hedman, B.; Hodgson, K. O.; Stack, T. D. P. *Science* **1998**, *279*,537.

34. Itoh, S.; Takayama, S.; Arakawa, R.; Furuta, A.; Komatsu, M.; Ishida, A.; Takamuku, S.; Fukuzumi, S. *Inorg. Chem.* **1997**, *36*, 1407.

35. Muller, J.; Weyhermuller, T.; Bill, E.; Hildebrandt, P.; Ould-Moussa, L.; Glaser, T.; Wieghardt, K. *Angew. Chem. Int. Ed.* **1998**, *37*, 616.

36. Jazdzewski, B. A.; Young Jr. V. G.; Tolman, W. B. *Chem. Commun*. **1998**, 2521.

37. Chaudhuri, P.; Hess, M.; Florke, U.; Wieghardt, K. *Angew. Chem. Int. Ed.* **1998**, *110*, 2217.

38. Chaudhuri, P.; Hess, M.; Weyhermuller, T.; Wieghardt, K. *Angew. Chem. Int. Ed.* **1999**, *38*, 1095.

39. Chaudhuri, P.; Hess, M.; Muller, J.; Hildebrandt, K.; Bill, E.; Weyhermuller, T.; Wieghardt, K. *J. Am. Chem. Soc.* **1999**, *119*, 9599.

40. Thomas, F.; Gellon, G.; Gautier- Luneau, I.; Saint-Aman, E.; Pierre, J. L. *Angew. Chem. Int. Ed.* **2002**, *41*, 3047.

41. Kumar, V.; Kalita, A.; Mondal, B. *Dalton Trans.* **2013**, *42,* 16264.

42. SMART, SAINT and XPREP, Siemens Analytical X-ray Instruments Inc., Madison, Wisconsin, USA. **1995**.

43. Sheldrick, G. M. SADABS: Software for Empirical Absorption Correction, University of Gottingen, Institut fur Anorganische Chemieder Universitat, Tammanstrasse 4, D-3400 Gottingen, Germany, 1999–2003.

44. Sheldrick, G. M. SHELXS-97, University of Gottingen, Germany, **1997**.

45. Farrugia, L. J. *J. Appl. Crystallogr.* **1997**, *30*, 565.

Chapter 5

A fluorescence turn-on probe for selective detection of nitrogen dioxide

Abstract

Two copper(II) complexes, **5.1** and **5.2**, of two ligands, $\mathbf{L_7}$ and $\mathbf{L_8}$ [$\mathbf{L_7}$ = 2- {[anthracen-9-ylmethyl-(2-dimethylamino-ethyl)-amino]-methyl}-4,6-di-tert-butyl-phenol; $\mathbf{L_8}$ = 5-dimethylamino-naphthalene-1-sulfonicacid (3,5-di-tert-butyl-2-hydroxy-benzyl)-(2-dimethylamino-ethyl)-amide, were synthesized and characterized. In methanol solution, the quenched fluorescence intensity of the ligands in complexes **5.1** and **5.2** was found to restore upon exposure to nitrogen dioxide (NO_2). This is attributed to the reduction of the paramagnetic Cu(II) centre by NO_2 to diamagnetic Cu(I). The reduction was accompanied by simultaneous nitration in the phenol ring of the ligands.

5.1 Introduction

Nitric oxide (NO) is known to play important roles in physiological functions such as vasodilation and neurotransmission. It is also known that NO could participate as a cytotoxic effector and/or a pathogenic mediator when produced at high concentration.[1] NO mediated pathogenicity mostly depends on the formation of secondary intermediates like peroxynitrite ($ONOO^-$) and nitrogen dioxide (NO_2) that are more reactive and toxic than NO itself.[2] The formation of these reactive nitrogen species requires the presence of oxidants such as superoxide radicals, hydrogen peroxide, and transition metal centres. Nitrogen dioxide can also be formed in hydrophobic environments from the reactions of NO with molecular oxygen.[3,4] These reactive nitrogen species are known to induce nitration of protein tyrosine residues to 3-nitrotyrosine.[5] This modification has attracted considerable interest to biomedical research as it can alter protein function and is associated to disease states. Though the capacity of $ONOO^-$ to cause protein tyrosine nitration in *vitro* and *vivo* has been demonstrated, the role of $ONOO^-$ as a central species in biological nitration is not yet confirmed beyond doubt.[6–10] An alternative pathway involving on the formation of NO_2 from nitrite (NO_2^-) ; the main metabolism product from NO by the action of hemeperoxidases and/or transition metal complexes has been proposed recently.[11–15] Thus, a probe which could selectively identify the NO_2, would be of immense importance to establish the tyrosine nitration mechanism. There have not been many examples of sensor which could detect NO_2 selectively.[16]

In chapter 3, we have demonstrated that the reduction of Cu(II) centre by NO_2 gas in the complexes of the 2,4-di-*tert*-butyl-6-(((2- dimethylamino)ethyl)(isopropyl)amino)methyl-phenol (**L_3**) and 6,6'-(((2-(dimethylamino)ethyl)azanediyl)*bis*(methylene))- *bis*(2,4-di-*tert*-butylphenol) (**L_4**) ligands.[17]

This instigate us to develop selective fluorescent NO_2 sensors based on Cu(II) complexes by attaching fluorophore to the same ligand frameworks. This chapter describes the example of Cu(II) complexes of two such fluorophore ligands as selective sensors for NO_2 (Figure 5.1).

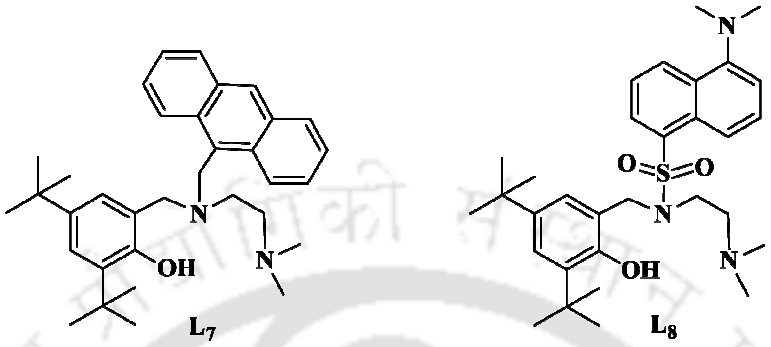

Figure 5.1: Ligands used for the present study.

5.2 Results and discussion

Ligand $\mathbf{L_7}$ has been synthesized in a three step procedure: (i) the condensation of *N,N*-dimethylethylenediamine with anthracene aldehyde; (ii) reduction of the imine by $NaBH_4$ to get the corresponding amine and (iii) subsequent Mannich reaction with 2,4-di-*tert*-butyl phenol in presence of formaldehyde (Experimental section). $\mathbf{L_8}$ has been prepared by the reaction of corresponding *N,N*-dimethylethylenediamine with dansyl chloride to get the corresponding sulphonamide. In the next step, the sulphonamide was treated with 2,4-di-*tert*-butyl-6-chloromethylphenol (Experimental section). The ligands were characterized by various spectral analyses and micro analyses (Appendix IV). $\mathbf{L_7}$ has been further characterized by its X-ray single crystal structure determination. The perspective ORTEP view of $\mathbf{L_7}$ is shown in figure 5.2. The crystallographic table, bond angles and lengths are listed in the appendix IV.

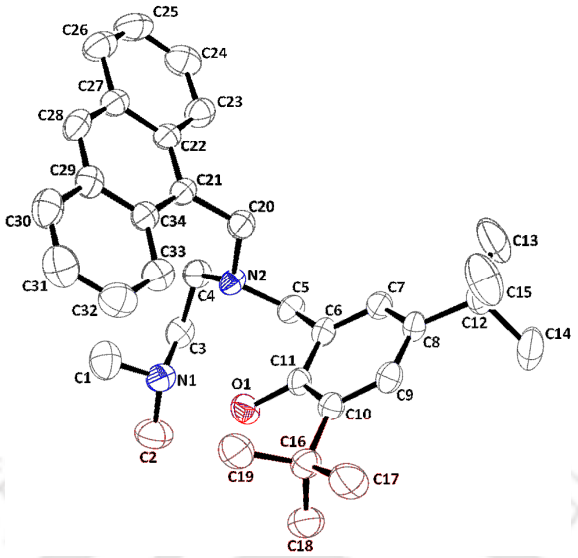

Figure 5.2: ORTEP diagram of ligand $\mathbf{L_7}$ (50% thermal ellipsoid plot, hydrogen atoms are removed for clarity).

The complexes **5.1** and **5.2** were synthesized by the reaction of copper(II) acetate dihydrate with equivalent amount of the respective ligands. The complexes were characterized by various analytic techniques and elemental analyses (Experimental section; Appendix IV). Complex **5.1** has been further characterized by single crystal X-ray structure determination. The ORTEP view is shown in figure 5.3. Even after several attempts, we could not grow the X-ray quality crystals of the complex **5.2**. It should be noted that the structure of the Cu(II) complex with similar framework but isopropyl substitution at N_{amine} position is reported in chapter 3 (complex **3.1** and **3.2**).[17]

In UV-visible spectroscopy, complexes **5.1** and **5.2** in methanol solutions display phenolato → Cu(II) charge transfer transitions at 485 nm and 470 nm, respectively. The weak *d-d* bands were observed at 665 nm and 685 nm in cases of complex **5.1** and **5.2**, respectively (Appendix IV). In X-band EPR both the complex shows characteristic four line spectrum for Cu(II) centre (Figure 5.4).

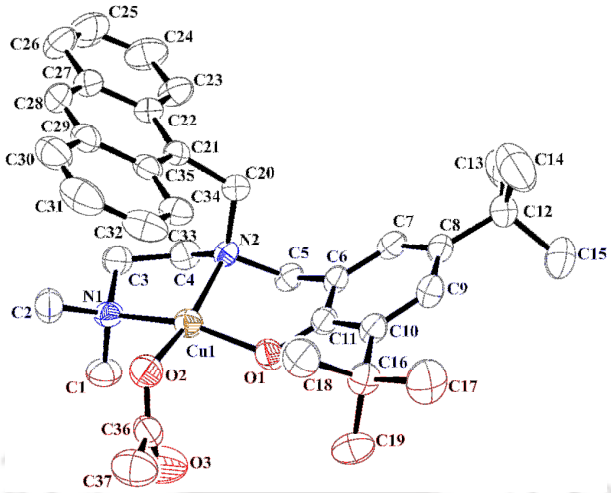

Figure 5.3: ORTEP diagram of complex **5.1** (50% thermal ellipsoid plot, hydrogen atoms are omitted for clarity).

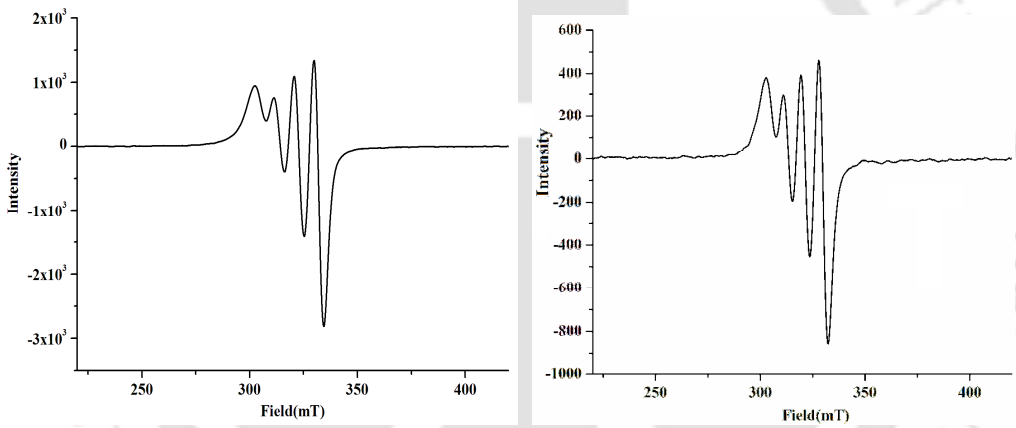

(a) **(b)**

Figure 5.4: X-band EPR spectrum of complexes (a) **5.1** and (b) **5.2** in methanol at room temperature.

5.3 Nitrogen dioxide reactivity

In methanol solution, the Cu(II) centre in the complex **5.1** was found to undergo rapid reduction in presence of NO_2. Addition of NO to the methanol solution did not result in the reduction of the Cu(II) centre (Appendix IV) in the complex. Similar observation was observed with Cu(II) complexes of $\mathbf{L_3}$ and $\mathbf{L_4}$ ligands. In UV-visible spectroscopy of methanol solution of complex **5.1**, the phenolato → Cu(II) charge transfer as well as the *d-d*

bands were found to disappear upon addition of NO_2. These are attributed to the reduction of Cu(II) centre by NO_2 (Figure 5.5). The reduction of Cu(II) was further confirmed by the EPR silent nature of the colorless solution (Figure 5.6). Complex **5.2** was also found to behave similar towards NO_2.

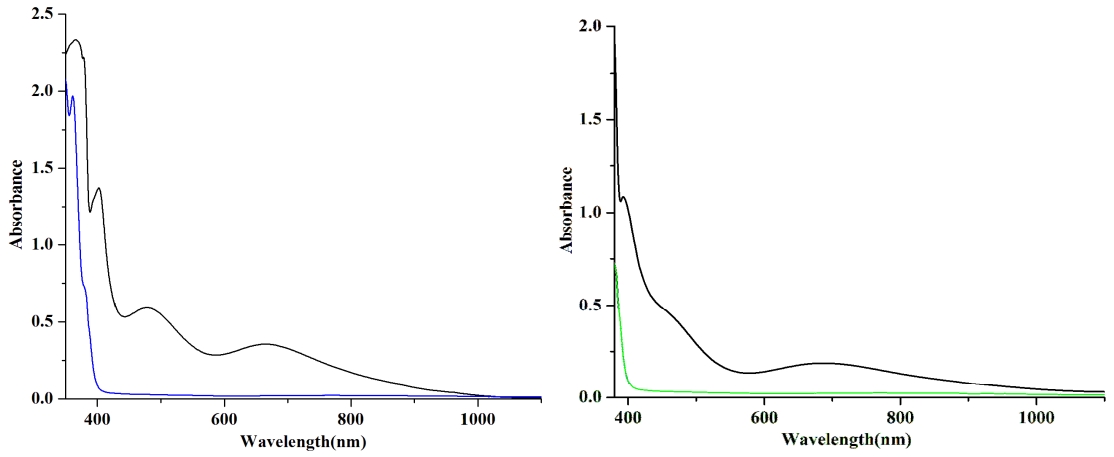

(a) **(b)**

Figure 5.5: UV-visible spectra of complexes (a) **5.1** before (black) and after (blue) and (b) **5.2** before (black) and after (green) addition of NO_2 in methanol solution.

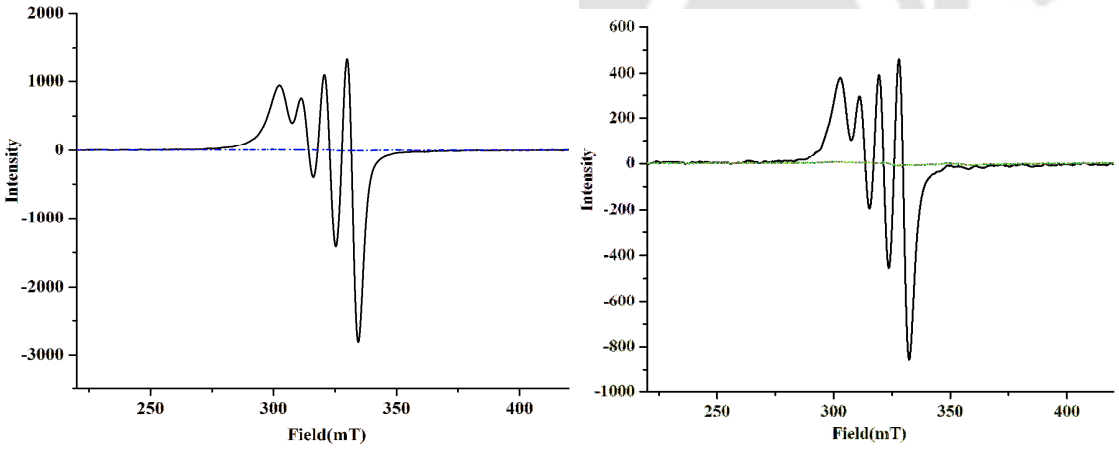

(a) **(b)**

Figure 5.6: X-band EPR spectra of complexes (a) **5.1** before (black trace) and after (blue trace) (b) **5.2** before (black trace) and after (green trace) addition of NO_2 in methanol solution at room temperature.

The reduction of Cu(II) centres in complexes by NO_2 resulted in simultaneous nitration of the phenol ring present in the ligand frameworks (Scheme 5.1).

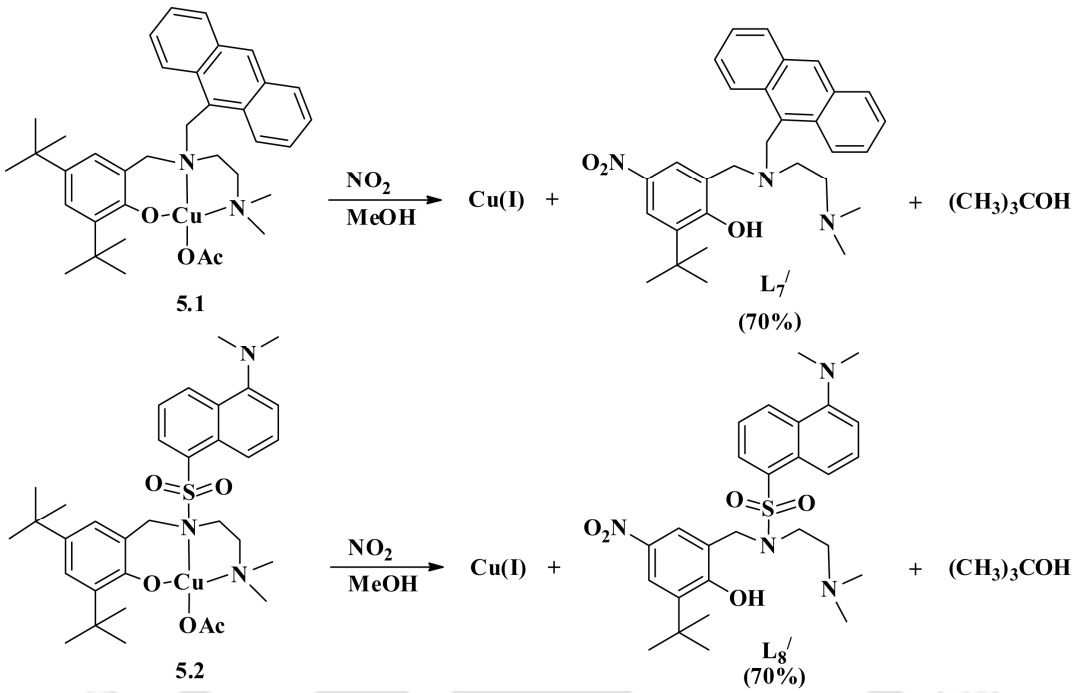

Scheme 5.1

The nitration products of $\mathbf{L_7}$ and $\mathbf{L_8}$ were isolated in a good yield (~70%) and characterized by various spectral techniques (Appendix IV). The phenol ring nitration takes place through an electrophilic substitution where *tert*-butyl group is being substituted by nitronium ion (NO_2^+). The NO_2^+ formed during the reduction of Cu(II) by NO_2, attacks at the 4-position of the phenol ring resulting in the corresponding 2-*tert*-butyl-4-nitrophenol. The release of *tert*-butyl cation during the reaction is confirmed from the presence of *tert*-butanol in GC mass spectrum of the reaction mixture (Appendix IV). In cases of earlier reported Cu(II) complexes of $\mathbf{L_3}$ and $\mathbf{L_4}$ ligands (Chapter 3), the similar nitration was observed. The nitration was reported to proceed through a NO_2^+ species which is formed in the reduction of Cu(II) to Cu(I) by NO_2.

5.4 Fluorescence study

Fluorescence studies of the ligands at 298 K in methanol solution exhibited a significant quenching of the intensity in presence of equivalent amount of Cu(II) ion (Appendix IV).

This is attributed to the paramagnetic effect of Cu(II) centres.[18] When NO is purged to the degassed methanol solution of the complexes, no change in fluorescence behaviour was observed (Appendix IV). This is in accord with the observation that the Cu(II) centre in these complexes does not undergo reduction by NO unlike other reported ones.[19] However, addition of NO_2 to the degassed methanol solution of complexes **5.1** and **5.2** restored the quenched fluorescence intensity of the ligands (Figure 5.7). The restored emission intensity was found to be more in case of dansyl fluorophore ($\mathbf{L_8}$) compared to $\mathbf{L_7}$. In case of complex **5.1**, the restored intensity was 3 ± 0.2 fold and in case complex **5.2**, it was 5 ± 0.2 fold. The detection was observed even at 10 nmol concentration. Though addition of NO or O_2 alone in the degassed methanol solution of complexes did not make any difference, when NO was added in presence of O_2, the quenched fluorescence intensity of the respective ligands was restored. This is because of the fact that NO reacts first with O_2 to yield NO_2 and thus formed NO_2 reacts with the Cu(II) centre of the complexes. Addition of H_2O_2, KO_2 also found to be not reactive. As such, there is only one fluorescence sensor for NO_2 is known which is based on Ni(II) complex of dithiocarbamate ligand derived from sulforhodamine B fluorophore.[16] The quenching of ligand fluorescence is attributed to the photoinduced electron transfer from Ni(II) to the sulforhodamine B excited state. The reaction of NO_2 with the complex results in to the photoinduced electron transfer from Ni(II) to the sulforhodamine B excited state. The reaction of NO_2 with the complex results in oxidation and decomplexation of the ligand from Ni(II). This leads to dimerization of the dithiocarbamate ligand to yield strong fluorescence.[16] In the present case, the turn-on of fluorescence intensity in presence of NO_2 is attributed to the reduction of Cu(II) centre to diamagnetic Cu(I). The reduction has been authenticated by UV-visible, X-band EPR and ^{1}H-NMR spectroscopic studies.

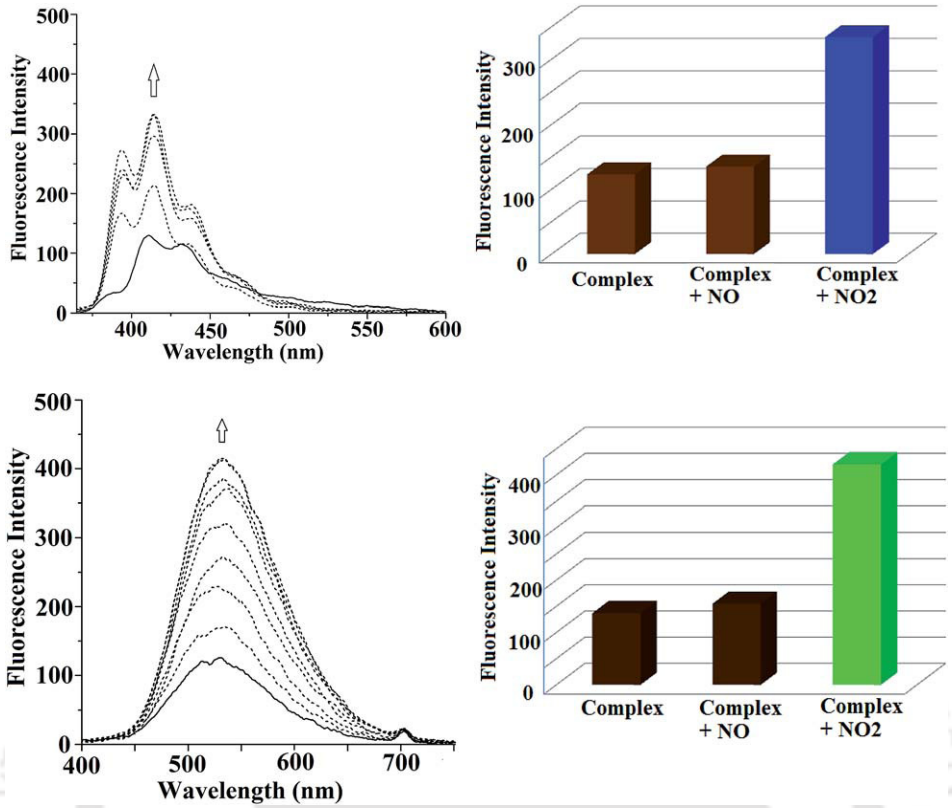

Figure 5.7: Fluorescence response of complexes **5.1** (Top) and **5.2** (Bottom) in methanol solution after addition of NO_2. The respective bar-diagram shows the fluorescence responses of the complexes, after addition of NO and NO_2, respectively.

5.5 Conclusion

The present set of complexes demonstrate the example where NO_2 induces the reduction of Cu(II) centre and thus, turns on the quenched fluorescence intensity of the fluorophore ligands. The reaction results in the simultaneous nitration of the phenol ring present in the ligand framework. The reaction was not observed with NO alone.

5.6 Experimental section

5.6.1 Materials and methods

All reagents and solvents of reagent grade were purchased from commercial sources and used as received except specified. Methanol was dried by heating over iodine activated magnesium

with a magnesium loading of 5 gm/lit. Then the dried methanol was kept over 20% m/v 3Å molecular sieves for 4-5 days before using. Deoxygenation of the solvent and solutions was effected either by repeated vacuum/purge cycles or bubbling with argon for 30 minutes or using freeze-pump-thaw cycles. NO_2 gas was prepared by the reaction of purified NO with O_2 followed by passing through an oxygen trap to remove extra oxygen, if any. UV-visible spectra were recorded on a Perkin Elmer Lambda 25 UV visible spectrophotometer. FT-IR spectra of the solid samples were taken on a Perkin Elmer spectrophotometer with samples prepared as KBr pellets. Solution electrical conductivity was measured using a Systronic 305 conductivity bridge. ^{1}H-NMR spectra were recorded in a 400 MHz Varian FT spectrometer. Chemical shifts (ppm) were referenced either with an internal standard (Me_4Si) or to the residual solvent peaks. The X-band Electron Paramagnetic Resonance (EPR) spectra were recorded on a JES-FA200 ESR spectrometer, at room temperature and 77 K with microwave power, 0.998 mW; microwave frequency, 9.14 GHz and modulation amplitude 2. Elemental analyses were obtained from a Perkin Elmer Series II Analyzer. The magnetic moment of complexes was measured on a Cambridge Magnetic Balance. Single crystals were grown by slow diffusion followed by slow evaporation technique. The intensity data were collected using a Bruker SMART APEX-II CCD diffractometer, equipped with a fine focus 1.75 kW sealed tube MoKa radiation (l = 0.71073 Å) at 273(3) K, with increasing ω (width of 0.3° per frame) at a scan speed of 3 s/frame. The SMART software was used for data acquisition.[20] Data integration and reduction were undertaken with SAINT and XPREP software.[21] Structures were solved by direct methods using SHELXS-97 and refined with full-matrix least squares on F^2 using SHELXL-97.[22] All non-hydrogen atoms were refined anisotropically. Structural illustrations have been drawn with ORTEP-3 for Windows.[23]

5.6.2 Synthesis of ligand L_7

N, N-dimethylethylenediamine (880 mg, 0.01 mol) and anthracene-10-carbaldehyde (2.06 g, 0.01 mol) were added in 20 ml of distilled ethanol in a round bottom flask fitted with a stir bar. The mixture was stirred for 12 h at room temperature to result corresponding Schiff's base. Then the imine was reduced by slow addition of 2.1 equivalent of $NaBH_4$. After removal of methanol under reduced pressure, the crude product was dissolved in water and neutralized with dilute acetic acid. The corresponding amine was extracted from the aqueous solution by dichloromethane (4 × 50 ml portions). The organic layer was dried over rotary evaporator to get the amine. The amine thus obtained was then purified by column chromatography using neutral aluminum oxide. Then the purified amine (2.5 g, 0.009 mol), 2,4-di-*tert*-butylphenol (1.85 g, 0.009 mol) and formalin (1.09g of 37% solution, 0.0135 mol) were taken in 50 mol of methanol and the mixture was stirred for 8 h. The solution was removed under reduced pressure to get the crude product. The compound was purified by column chromatography to get ligand **L_7**. Yield: ~75%. Elemental analyses: calcd.(%): C, 82.21; H, 8.93; N, 5.64 ; found(%): C, 82.26; H, 8.94; N,5.71. FT-IR (in KBr): 3183, 2959, 1479, 1361, 1223, 729 cm-1. ^{1}H-NMR: (400 MHz, $CDCl_3$): δ_{ppm}: 8.38 (1H, s), 8.34 (2H, d), 7.97 (1H, s), 7.95 (1H, d), 7.48 (4H, m), 7.29 (1H, d), 7.06 (1H, d), 4.55 (2H,s), 3.78 (2H, s), 2.53 (2H, t), 2.39 (2H, t), 1.86 (6H, s), 1.53 (9H, s), 1.30 (9H, s). ^{13}C-NMR: (100 MHz, CDCl3) δ_{ppm}: 154.0, 140.1, 136.0, 131.7, 131.5, 129.5, 129.0, 127.8, 125.9, 125.3, 125.2, 125.0, 123.3, 122.7, 57.3, 55.9, 50.9, 49.4, 44.5, 35.4, 34.3, 31.9, 30.0. Mass $(M+H^+)/z$: calcd: 497.345; found: 497.366.

5.6.3 Synthesis of ligand L_8

N, N-dimethylethylenediamine (440 mg, 5 mmol) and dansyl chloride (1.35 g, 5 mmol) was added in 20 ml of acetonitrile. The mixture was stirred for 1 h at room temperature to give

corresponding sulphonamide. To the reaction mixture, 100 ml water was added. Then the sulphonamide was extracted with dichloromethane (50 ml × 3 portions) and dried under vacuum. The solid thus obtained was dissolved in 20 ml of methanol and to this 2,4-di-*tert*-butyl-6-chloromethylphenol (1.27 g, 5 mmol), equivalent amount of triethylamine was added and the reaction mixture was refluxed for 24 h. After removal of methanol under reduced pressure, the crude product was dissolved in water and neutralized with dilute acetic acid and was extracted from the aqueous solution by dichloromethane (50 ml × 3 portions). The organic layer was dried over rotary evaporator to get the crude mass. The ligand **L_8** thus obtained was then purified by column chromatography using neutral aluminum oxide. Yield: ~60%. Elemental analyses: calcd.(%): C, 68.98; H, 8.40; N, 7.78; found(%): C, 68.94; H, 8.40; N, 7.89. FT-IR (in KBr): 3417, 2955, 1611, 1482, 1434, 1140, 790 cm^{-1}. ^{1}H-NMR: (400 MHz, CDCl3): δ_{ppm}: 8.57 (1H, d), 8.26 (2H, t), 7.54 (2H, m), 7.27 (1H, d), 7.13 (1H, d), 6.31 (1H, d), 4.38 (2H, s), 3.47 (2H, t), 2.89 (6H, s), 2.67 (2H, t), 2.26 (6H, s), 1.28 (9H, s), 0.98 (9H, s). ^{13}C-NMR: (100 MHz, CDCl3) δ_{ppm}: 152.7, 152.0, 141.7, 137.9, 134.4, 130.8, 130.6, 130.3, 130.1, 128.4, 125.7, 124.1, 123.2, 121.3, 119.8, 115.5, 60.1, 47.4, 45.9, 45.5, 44.0, 35.3, 34.0, 31.5, 29.9. Mass $(M+H^+)$/z: calcd: 540.35; found: 540.35.

5.6.4 Synthesis of complex 5.1

To a stirred solution of $Cu(OAc)_2 \cdot H_2O$ (0.398 g, 2 mmol) in 15 ml methanol was added a solution of ligand **L_7** (0.992 g, 2 mmol) in 50 ml methanol. The reaction mixture was stirred for 2 h. Then solvent was reduced to 5 ml under vacuum and 20 ml of diethyl ether was added. Then it was kept in freezer for 12 h to obtain the complex **5.1** as a dark brown precipitate. Yield: 0.97 g (~80%). Elemental analyses: calcd.(%): C, 69.93; H, 7.50; N, 4.53; found(%): C, 69.99; H, 7.52; N, 4.61. UV-visible (methanol): λ_{max}, 485 and 665 nm. FT-IR

(in KBr): 2954, 1576, 1467, 1441, 735 cm^{-1}. The complex **5.1** behaves as 1:1 electrolyte in methanol solution [Λ_M (S cm^{-1}), 151]. μ_{obs}., 1.58 BM.

5.6.5 Synthesis of complex 5.2

To a stirred solution of $Cu(OAc)_2 \cdot H_2O$ (0.398 g, 2 mmol) in 10 ml methanol was added a solution of ligand $\mathbf{L_8}$ (1.080 g, 2 mmol) in 50 ml methanol. The reaction mixture was stirred for 2 h. The solvent was reduced under vacuum to 5 ml and 20 ml of diethylether was added to this. The mixture was kept in freezer for 12 h to obtain the complex **5.2** as a brown precipitate. Yield: 1.20 g (~70%). Elemental analyses: calcd.(%): C, 59.94; H, 7.16; N, 6.35; found(%): C, 59.98; H, 7.16; N, 6.42. UV-visible (methanol): λ_{max}, 685 nm. FT-IR (in KBr): 2954, 1480, 1460, 1140, 791 cm^{-1}. The complex **5.2** behaves as 1:1 electrolyte in methanol solution [Λ_M (S cm^{-1}), 148]. μ_{obs}., 1.56 BM.

5.6.6 Isolation of modified ligand L_7'

To 30 ml of methanol solution of complex **5.1** (620 mg), NO_2 was bubbled till the brown color of the solution becomes colorless. This solution was allowed to stir for 10 minutes at room temperature. The excess NO_2 was removed by application several cycles of vacuum and argon purging. Then the solvent was reduced to 5 ml under vacuum using rotavapour. Then equivalent amount of aqueous solution of Na_2S was added to the solution remove copper ion as its sulphide. The precipitate was filtered off and from the filtrate, the modified ligand $\mathbf{L_7'}$ was extracted with dichloromethane (4 × 50 ml portions) and purified using column chromatography. Yield: 350 mg. (~70%). Elemental analyses: calcd.(%): C, 74.20; H, 7.26; N, 8.65 ; found(%): C, 74.26; H, 7.25; N, 8.74. FT-IR (in KBr): 2964, 1589, 1466, 1333, 1167 cm^{-1}. ^{1}H-NMR: (400 MHz, $CDCl_3$): δ_{ppm}: 8.35 (1H, s), 8.22 (2H, d), 8.11 (3H, m), 7.94(1H, d), 7.91 (1H, s), 7.40 (4H, m), 4.51 (2H,s), 3.75 (2H, s), 2.50 (4H, s), 1.87 (6H, s),

1.51 (9H, s). ^{13}C-NMR: (100 MHz, $CDCl_3$) δ_{ppm}: 165.0, 138.3, 134.3, 131.7, 131.5, 129.2, 127.4, 126.1, 125.3, 125.1, 124.7, 124.26, 123.4, 55.4, 54.9, 50.6, 48.0, 43.8, 35.6, 29.6. Mass ($M+H^+$)/z: calcd: 486.27; found: 486.27.

5.6.7 Isolation of modified ligand $L_8^/$

Same procedure was followed as in case of $\mathbf{L_7^/}$. Yield: 200 mg (~70%). Elemental analyses: calcd.(%): C, 61.34; H, 6.86; N, 10.60; found(%): C, 61.39; H, 6.87; N, 10.71. FT-IR (in KBr): 3444, 2955, 1642, 1460, 1315, 1140, 733 cm^{-1}. ^{1}H-NMR: (400 MHz, $CDCl_3$): δ_{ppm}: 8.51 (1H, d), 8.23 (2H, t), 8.02 (1H, d), 7.84 (1H, d), 7.53 (2H, m), 7.12 (1H, d), 4.08 (2H, s), 2.86 (6H, s), 2.79 (2H, t), 2.51 (2H, t), 2.23 (6H, s), 1.34 (9H, s). ^{13}C-NMR: (100 MHz, $CDCl_3$) δ_{ppm}: 164.5, 151.9, 141.6, 138.6, 137.8, 137.4, 134.3, 130.7, 130.6, 130.2, 128.3, 125.7, 124.0, 123.2, 123.0, 122.4, 122.3. Mass ($M+H^+$)/z: calcd: 529.40; found: 529.27.

5.7 References

1. Ignarro, L. J. *Annu. Rev. Pharmacol. Toxicol.* **1990**, *30*, 535.
2. R. Radi, A. Denicola, B. Alvarez, G. Ferrer-Sueta and H. Rubbo, in *Nitric Oxide*, ed. L. Ignarro, Academic, San Diego, 2000, pp. 57.
3. Liu, X.; Miller, M. J.; Joshi, M. S.; Thomas D. D.; Lancaster Jr, J. R. *Proc. Natl. Acad. Sci. U. S. A.* **1998**, *95*, 2175.
4. Denicola, A.; Batthyany, C.; Lissi, E.; Freeman, B. A.; Rubbo H.; Radi, R. *J. Biol. Chem.* **2002**, *277*, 932.
5. Sokolovsky, M.; Riordan, J. F.; Vallee, B. L. *Biochemistry*, **1966**, *5*, 3582. (b) Radi, R. *Proc. Natl. Acad. Sci. U. S. A*. **2004**, *101*, 4003.
6. Beckman, J. S.; Ischiropoulos, H.; Zhu, L.; Vander-Woerd, M.; Smith, C.; Chen, J.; Harrison, J.; Martin, J. C.; Tsai, M. *Arch. Biochem. Biophys*. **1992**, *298*, 438.

7. Ischiropoulos, H.; Zhu, L.; Chen, J.; Tsai, M.; Martin, J. C.; Smith, C. D.; Beckman, J. S. *Arch. Biochem. Biophys.* **1992**, *298*, 431.

8. Ischiropoulos, H.; Zhu, L.; Beckman, J. S. *Arch. Biochem. Biophys*. **1992**, *298*, 446.

9. Beckmann, J. S.; Ye, Y. Z.; Anderson, P. G.; Chen, J.; Accavitti, M. A.; Tarpey, M. M.; White, C. R. *Biol. Chem.* **1994**, *375*, 81.

10. Ohshima, H.; Friesen, M.; Brouet, I.; Bartsch, H. *Food Chem. Toxicol*. **1990**, *28*, 647.

11. Pfeiffer, S.; Schmidt, K.; Mayer, B. *J. Biol. Chem*. **2000**, *275*, 6346.

12. Thomas, D. D.; Espey, M. G.; Vitek, M. P.; Miranda, K. M.; Wink, D. A. *Proc. Natl. Acad. Sci. U. S. A*. **2002**, *99*, 12691.

13. Eiserich, J. P.; Hristova, M.; Cross, C. E.; Jones, A. D.; Freeman, B. A.; Halliwell, B.; Vander Vliet, A. Nature **1998**, *391*, 393.

14. Bian, K.; Gao, Z.; Weisbrodt, N. Murad, F. *Proc. Natl. Acad. Sci. U.S.A*. **2003**, *100*, 5712.

15. Brennan, M. L.; Wu, W.; Fu, X.; Shen, Z.; Song, W.; Frost, H.; Vadseth, C.; Narine, L.; Lenkiewicz, E.; Borchers, M. T.; Lusis, A. J.; Lee, J. J.; Lee, N. A.; Abu-Soud, H. M.; Ischiropoulos, H.; Hazen, S. L. *J. Biol. Chem*. **2002**, *277*, 17415.

16. Yan, Y.; Krishnakumar, S.; Yu, H.; Ramishetti, S.; Deng, L. W.; Wang, S.; Huang, L.; Huang, D. *J. Am. Chem. Soc*. **2013**, *135*, 5312.

17. Kumar, V.; Kalita, A.; Mondal, B. *Dalton Trans*. **2013**, *42*, 16264.

18. Lim, M. H.; Wong, B. A.; Pitcock Jr, W. H.; Mokshagundam, D.; Baik, M. H.; Lippard, S. J. *J. Am. Chem. Soc.* **2006**, *128*, 14364.

19. Kumar, P.; Kalita, A.; Mondal, B. *Dalton Trans*. **2013**, *42*, 5731.

20. SMART, SAINT and XPREP, Siemens Analytical X-ray Instruments Inc., Madison, Wisconsin, USA, **1995**.

21. Sheldrick, G. M. SADABS: Software for Empirical Absorption Correction, University of Gottingen, Institut fur Anorganische Chemieder Universitat, Tammanstrasse 4, D-3400 Gottingen, Germany, 1999–2003.
22. Sheldrick, G. M. SHELXS-97, Program for solution of crystal structures, University of Göttingen, Germany, **1997**.
23. Farrugia, L. J. *J. Appl. Crystallogr*. **1997**, *30*, 565.

Chapter 6

A new NBD-based fluorogenic turn-on probe for selective detection of NO_2

Abstract

A copper(II) complex, **6.1** with a NBD-based tridentate ligand $\mathbf{L_9}$ [7-nitro-N-(2-(pyridin-2-yl)ethyl)-N-((pyridin-2-yl)methyl)benzo(c)(1,2,5)oxadiazol-4-amine] was synthesised and its highly selective reaction with nitrogen dioxide (NO_2) has been demonstrated. Complex **6.1**, due to paramagnetic quenching, does not display any fluorescence; however, on addition of NO_2 to acetonitrile solution of complex **6.1**, the fluorescence intensity has been found to be restored and enhanced. This is attributed to the reduction of the Cu(II) centre by NO_2 to diamagnetic Cu(I).

6.1 Introduction

The selective and sensitive detection of NO_X (X = 1, 2) is one of the most promising application of optical probes. In this context NO_2 is a major air pollutant as well as the roles of NO_2 in mammalian biology are drawing increasing attention.[1-4] NO_2 is a strong lipophilic oxidant; it can trigger lipid auto-oxidation[5] and oxidative nitration of aromatic amino acids, particularly tyrosine.[6] Protein tyrosine nitration has been observed in connection with numerous human diseases including neurodegenerative conditions, cardiovascular disorders, diabetes, and Alzheimer's disease.[7-14] In human physiology NO_2 can be generated *via* several mechanisms, including the oxidation of NO by oxygen,[18] the decomposition of $ONOO^-$,[19] and the oxidation of NO_2^- ions by hydrogen peroxide (H_2O_2) catalyzed with peroxidases.[20] However, most of the reported probes are for NO detection. Most of the transition-metal based probes where metal is quite reactive towards NO and used as a fluorescence quencher.[21-25] Thus to establish the tyrosine nitration mechanism, a probe which can selectively detect NO_2 would be of great importance. Recently, Huang et al has reported the first example of a Ni(II) based fluorescent probe where NO_2 selectively reacts with metal centre and gives maximum fluorescence enhancement after 5 minute.[26] This chapter discusses a Cu(II) complex of NBD-based fluorophoric ligand **L_9** as a selective turn-on probe for fast detection of NO_2 in acetonitrile medium.

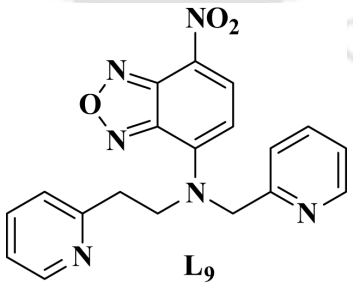

Figure 6.1: Ligand used for the present study.

6.2 Results and discussion

The ligand **L_9** was synthesized by the reaction of NBD-Cl [4-chloro-7-nitrobenzo(c)(1,2,5)oxadiazole] and 2-(pyridin-2-yl)-N-((pyridin-2-yl)methyl)ethanamine in dichloromethane medium (Experimental section). Ligand **L_9** was characterized by various spectral analysis and was further authenticated by elemental analysis (Experimental section). The complex **6.1** was prepared by the reaction of copper(II) chloride dihydrate with equivalent amount of ligand **L_9**. Complex **6.1** has been characterized by various analytic techniques (Experimental section) and also by single crystal X-ray structure determination. The ORTEP diagram is shown in figure 6.2. The crystallographic data, important bond angles and distances are listed in tables 6.1, 6.2 and 6.3, respectively.

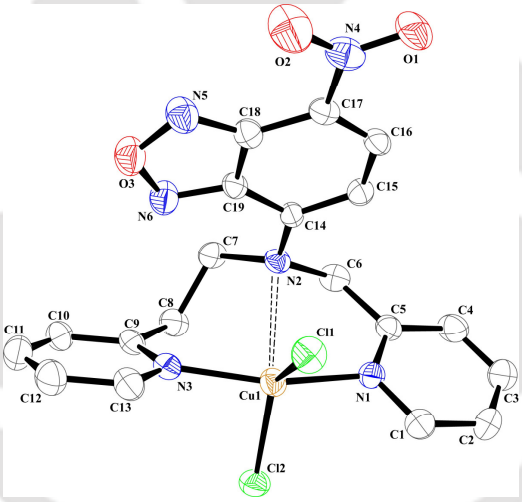

Figure 6.2: ORTEP diagram of complex **6.1** (50% thermal ellipsoid plot, hydrogen atoms and solvent molecules are omitted for clarity).

In acetonitrile solution, complex **6.1** shows absorption at 420 nm (ε = 14495 $M^{-1}cm^{-1}$) and 768 nm (ε = 495 $M^{-1}cm^{-1}$). The absorption band at 420 nm is ligand based charge transfer transition which is clear from the spectrum of free ligand (Appendix V) and the band at 768 nm is due to *d-d* transition. In X-band EPR spectrum, complex **6.1** shows characteristic signal for Cu(II) centre at room temperature (Figure 6.3).

Table 6.1: Crystallographic table for complex **6.1**.

	Complex **6.1**
Formulae	C_{23} H_{22} N_8 O_3 Cu Cl_2
Mol. wt.	592.93
Crystal system	Monoclinic
Space group	Cc
Temperature /K	296(2)
Wavelength /Å	0.71073
a /Å	11.4903(11)
b /Å	31.533(3)
c /Å	7.7272(7)
α/°	90.00
β/°	110.019(6)
γ/°	90.00
V/ $Å^3$	2630.6(4)
Z	4
Density/Mgm^{-3}	1.497
Abs. co-eff. /mm^{-1}	1.075
Abs. correction	none
F(000)	1212
Total no. of reflections	3183
Reflections, $I > 2\sigma(I)$	2678
Max. 2θ/°	22.03
Ranges (h, k, l)	$-12 \leq h \leq 12$ $-33 \leq k \leq 32$ $-8 \leq l \leq 8$
Complete to 2θ (%)	99.4
Refinement method	Full-matrix least-squares on F^2
Goof (F^2)	1.021
R indices [$I > 2\sigma(I)$]	0.0386
R indices (all data)	0.0501

Table 6.2: Selected bond angles (°) for complex **6.1**.

Atoms	Angles (°)	Atoms	Angles (°)
Cl(1) – Cu(1) – Cl(2)	134.57(6)	Cl(1) - Cu(1) – N(3)	98.2(2)
Cl(1) – Cu(1) – N(2)	103.2(1)	Cl(1) – Cu(1) – N(1)	92.4(1)
Cl(2) – Cu(1) – N(3)	91.3(1)	Cl(2) – Cu(1) – N(2)	121.6(1)
Cl(2) – Cu(1) – N(1)	91.8(1)	N(3) – Cu(1) – N(2)	87.0(2)
N(3) – Cu(1) – N(1)	161.6(2)	N(2) – Cu(1) – N(1)	76.0(2)
Cu(1) – N(3) – C(9)	120.0(4)	Cu(1) – N(3) – C(13)	120.7(4)
C(9) – N(3) – C(13)	119.2(5)	N(2) – C(14) – C(19)	122.1(5)
N(2) – C(14) – C(15)	124.1(5)	N(5) – O(3) – N(6)	111.9(5)
C(18) – N(5) – O(3)	105.0(5)	N(5) – C(18) – C(19)	109.3(5)
C(18) – C(17) – (N4)	121.9(6)	Cu(1) – N(2) – C(14)	99.1(3)
N(5) – C(18) – C(17)	131.4(6)	Cu(1) – N(2) – C(6)	97.6(3)
Cu(1) – N(2) – C(7)	107.2(3)	C(14) – N(2) – C(6)	116.6(4)
C(14) – N(2) – C(7)	120.1(4)	N(1) – C(1) – C(2)	121.5(6)
C(7) – N(2) – C(6)	111.9(4)	N(2) – C(6) – C(5)	115.9(5)
C(19) – N(6) – O(3)	105.4(5)	N(2) – C(7) – C(8)	112.7(5)
N(3) – C(9) – C(8)	117.8(5)	N(3) – C(9) – C(10)	119.7(6)
C(8) – C(9) – C(10)	122.5(6)	N(3) – C(13) – C(12)	122.8(6)
Cu(1) – N(1) – C(1)	117.9(4)	Cu(1) – N(1) – C(5)	122.5(4)
C(17) – N(4) – O(1)	119.5(6)	C(5) – N(1) – C(1)	119.5(5)
O(1) – N(4) – O(2)	124.2(6)	C(17) – N(4) – O(2)	116.3(6)
N(1) – C(5) – C(6)	118.8(5)	N(1) – C(5) – C(4)	120.2(6)

Table 6.3: Selected bond distances (Å) for complex **6.1**.

Atoms	Distances (Å)	Atoms	Distances (Å)
Cu(1) - Cl(1)	2.277(2)	Cu(1) - Cl(2)	2.272(2)
Cu(1) - N(3)	1.984(5)	Cu(1) - N(2)	2.603(5)
Cu(1) - N(1)	1.984(5)	N(3) - C(9)	1.360(8)
N(3) - C(13)	1.346(9)	C(14) - N(2)	1.390(6)
C(14) - C(19)	1.452(8)	C(14) - C(15)	1.376(8)
N(5) - C(18)	1.323(8)	N(5) - O(3)	1.368(7)
C(17) - N(4)	1.455(8)	C(18) - C(19)	1.432(7)
N(2) - C(7)	1.485(6)	N(2) - C(6)	1.469(7)
C(7) - C(8)	1.526(9)	N(6) - O(3)	1.389(6)
C(3) - C(4)	1.364(9)	C(3) - C(2)	1.35(1)
C(9) - C(8)	1.50(1)	C(9) - C(10)	1.373(9)
C(13) - C(12)	1.393(9)	N(1) - C(5)	1.339(9)
N(1) - C(1)	1.334(8)	N(4) - O(1)	1.218(8)
N(4) - O(2)	1.234(8)	C(5) - C(4)	1.383(9)

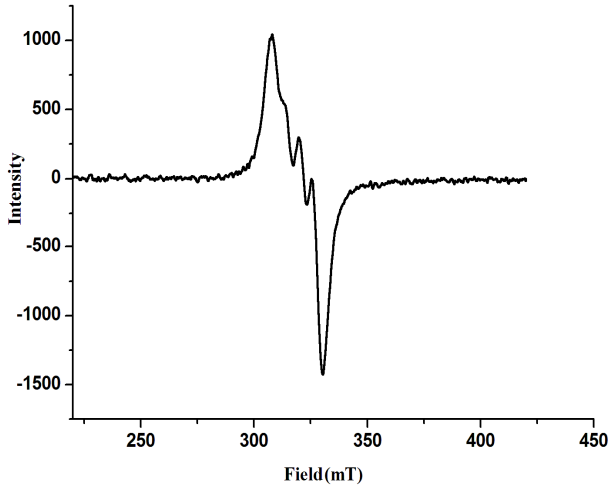

Figure 6.3: X-band EPR spectrum of complex **6.1** in acetonitrile at room temperature.

6.3 Nitrogen dioxide reactivity

Addition of NO_2 in degassed acetonitrile solution of complex **6.1** results in rapid reduction of Cu(II) centre. The reduction of Cu(II) centre has been monitored by UV-visible spectroscopy. The *d-d* band centered at 768 nm disappears upon addition of NO_2 suggesting the formation of Cu(I) (Figure 6.4). It was supported by the EPR silent nature of reaction mixture in X-band EPR study at room temperature (Figure 6.5).

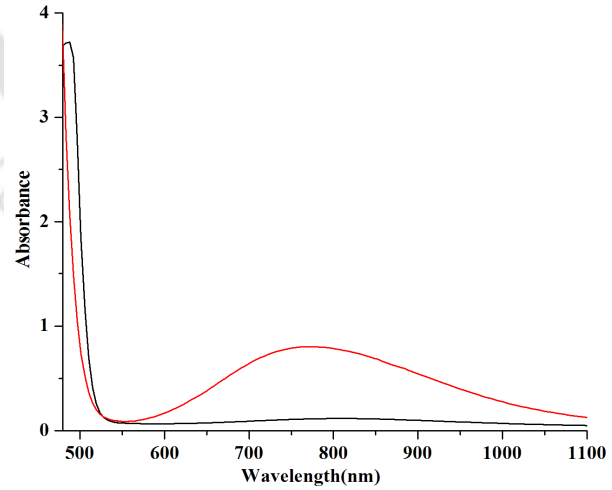

Figure 6.4: UV-visible spectra of complex **6.1** before (red trace) and after (black trace) addition of NO_2 in acetonitrile medium.

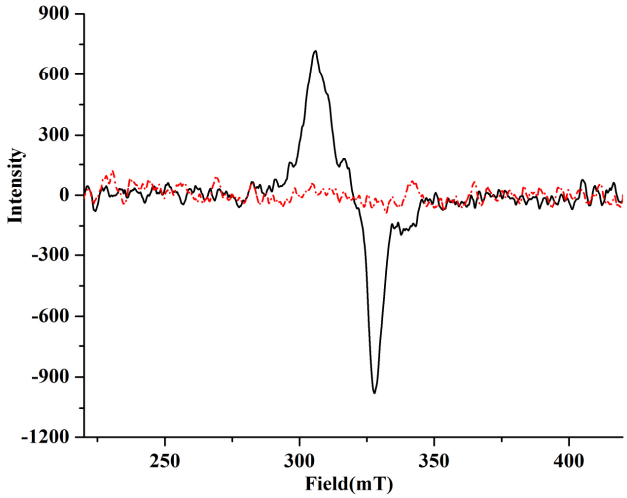

Figure 6.5: X-band EPR spectrum of complex **6.1** before (black trace) and after addition of NO_2 (red trace) in acetonitrile medium at room temperature.

To check, whether the complex **6.1** is sensitive toward NO or NO_2, NO in the absence of O_2 was purged in the solution of complex **6.1** and it did not result the reduction of the Cu(II) centre (Appendix V). However, addition of O_2 to this reaction mixture resulted in the reduction of Cu(II) centre. This is attributed to the fact that NO first reacts with O_2 to form NO_2 and this then reduces Cu(II) centre. Earlier, it was observed that reduction of Cu(II) by NO_2 leads to formation of nitronium ion (NO_2^+) and induces nitration of phenol ring present in the ligand framework.[27]

But in present case NO_2^+ decomposes to give NO_3^- ions (Experimental section). Further we tried to study the reaction of complex **6.1** with NO_2 in aqueous medium, however in aqueous medium complex **6.1** is quite unstable and we found that in aqueous medium for appreciable quenching in fluorescence intensity we needed to add about 400 equivalent of Cu(II) ions.[29]

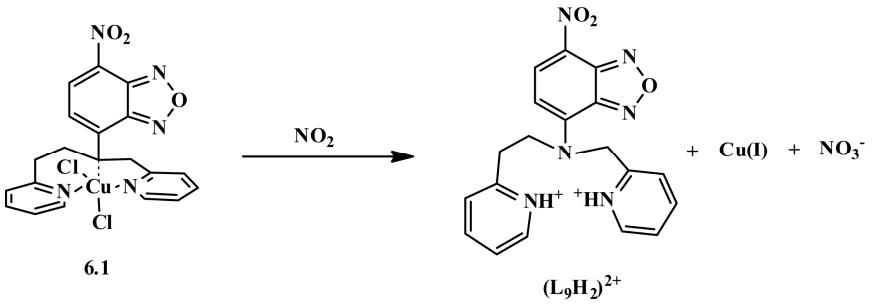

Scheme-6.1

6.4 Fluorescence study

The emission profile of ligand **L_9** shows typical NBD based fluorescence at 536 nm. The fluorescence emission of **L_9** centered at 536 nm is found to decrease significantly (>90%) upon the addition of equivalent amount of Cu(II) ion in acetonitrile medium as shown in figure 6.6.

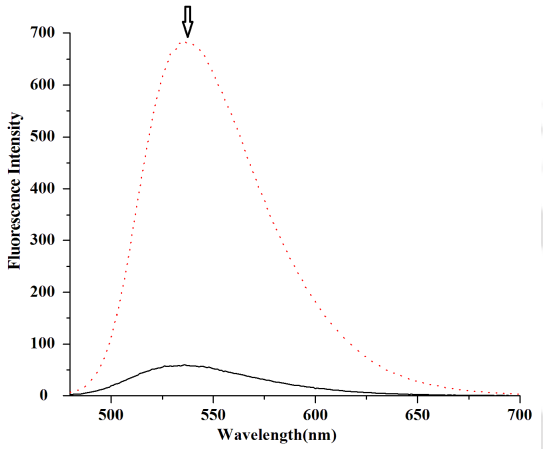

Figure 6.6: Fluorescence response (λ_{ex}, 470nm) for 5 µM solution of ligand **L_9** (dotted trace), and after addition of one equivalent of $CuCl_2.2H_2O$ (solid trace) in acetonitrile medium.

The selective quenching of fluorescence of ligand **L_9** by Cu(II) ions was checked for other metal ions like Ca(II), Mg(II), Ni(II), Zn(II), Hg(II), Mn(II) and Co(II) and was found to have

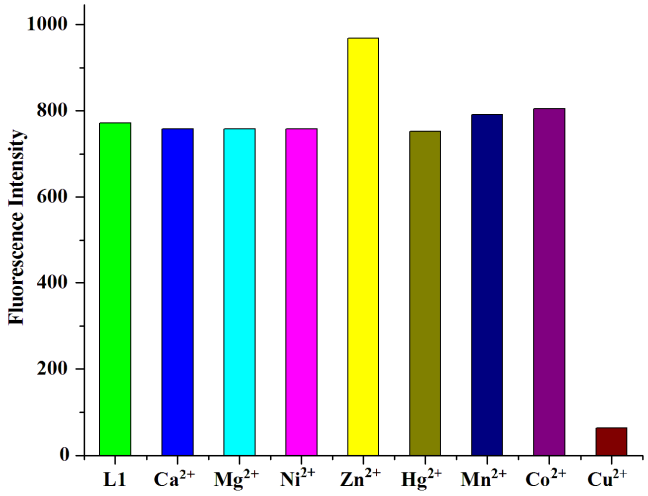

Figure 6.7: Selectivity of ligand **L_9** (5 µM) for Cu^{2+}. Fluorescence response of **L_9** following the addition of 1 equivalent of different metal ions in acetonitrile medium.

negligible effects on fluorescence quenching (Figure 6.7).

Addition of NO_2 gas in the 5 µM acetonitrile solution of complex **6.1** immediately resulted the enhancement in fluorescence intensity, the fluorescence intensity reaches up to 40 (±1) folds. The emission spectrum is centered around 525 nm within a second time. The blue shift of the emission wave length as well as the increased fluorescence intensity is due to the reduction of Cu(II) centre with the concominant protonation of the ligand $\mathbf{L_9}$. Initially the fluorofhoric ligand $\mathbf{L_9}$ was weakly fluorofhore due to intramolicular photoinduced electron transfer (PET) but after protonation PET has removed and it becomes highly fluorophore. It should be noted that, for earlier reported complexes such as $[Ni(RCNS_2)_2]$(where R= *ortho* and *para* isomer of sulphorhodamine B fluorophore) and [Cu(DMABP)oac](where DMABP = 6,6'-(((2-(dimethylamino)ethyl)azanediyl)*bis*(methylene))-*bis*(2,4-di-*tert*-butylphenol), the quenched fluorescence intensity enhances significantly up to 12 fold and 5 (±0.2) fold, respectively.[26a,b] In the present case enhancement in emission intensity is found to be 40 (±1) fold in acetonitrile medium (Figure 6.8).

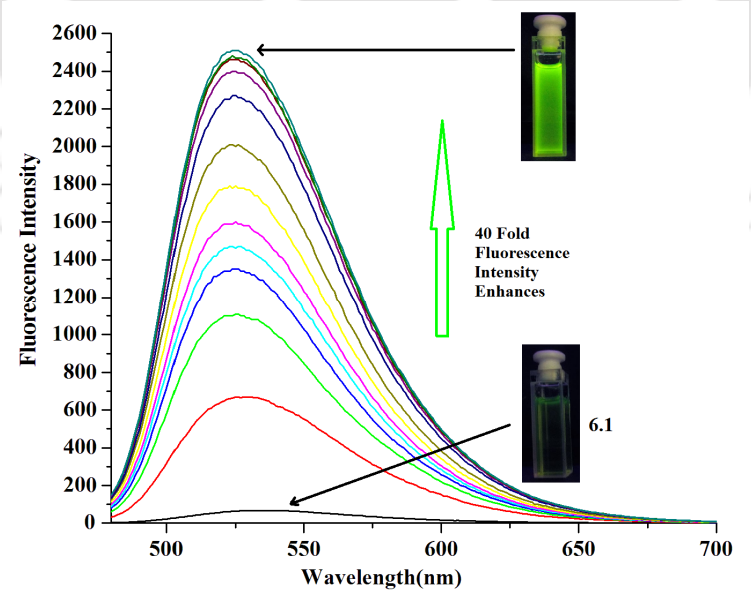

Figure 6.8: Fluorescence response (λ_{ex}, 470 nm) for 5 µM solution of complex **6.1** (black trace) before and after addition of NO_2 in acetonitrile medium.

We evaluated the selectivity of complex **6.1** towards common reactive nitrogen and oxygen species (NO, NO_2, OH^-, O_2^-, O_2, NO_2^- and NO_3^-) in acetonitrile medium (Figure 6.9). Only NO_2 was found to increase the fluorescence intensity up to 40(±1) fold.

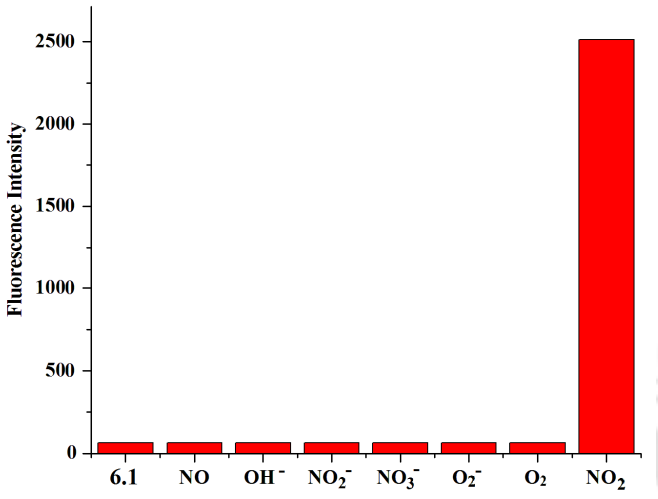

Figure 6.9: Fluorescence response of complex **6.1** towards NO_2 in acetonitrile medium.

6.5 Conclusion

In conclusion, a Cu(II) complex has been synthesized with NBD-based tridentate N-donar ligand. Addition of NO_2 to acetonitrile solution of Cu(II) complex resulted in the reduction of Cu(II) centre and thus, turns on the quenched fluorescence intensity of the fluorogenic ligand. The reaction was not found with NO alone. In the present case, fluorescence enhancement is attributed to formation of diamagnetic Cu(I).

6.6 Experimental section

6.6.1 Materials and methods

All reagents and solvents of reagent grade were purchased from commercial sources and used as received except specified. Acetonitrile was distilled from calcium hydride. Deoxygenation of the solvent and solutions was effected by repeated vacuum/purge cycles or bubbling with nitrogen for 30 minutes. NO_2 gas was prepared by the reaction of purified NO with O_2 in a

flask fitted with a rubber septum. UV-visible spectra were recorded on a Perkin Elmer Lambda 25 UV visible spectrophotometer. FT-IR spectra of the solid samples were taken on a Perkin Elmer spectrophotometer with samples prepared as KBr pellets. Solution electrical conductivity was measured using a Systronic 305 conductivity bridge. ^{1}H-NMR spectra were recorded in a 400 MHz Varian FT spectrometer. Chemical shifts (ppm) were referenced either with an internal standard (Me4Si) or to the residual solvent peaks. The X-band Electron Paramagnetic Resonance (EPR) spectra were recorded on a JES-FA200 ESR spectrometer, at room temperature and 77 K with microwave power, 0.998 mW; microwave frequency, 9.14 GHz and modulation amplitude, 2. Elemental analyses were obtained from a Perkin Elmer Series II Analyzer. The magnetic moment of complexes was measured on a Cambridge Magnetic Balance.

Single crystals were grown by slow diffusion followed by slow evaporation technique. The intensity data were collected using a Bruker SMART APEX-II CCD diffractometer, equipped with a fine focus 1.75 kW sealed tube MoKa radiation (l = 0.71073 Å) at 273(3) K, with increasing w (width of 0.3° per frame) at a scan speed of 3 s/frame. The SMART software was used for data acquisition.[30] Data integration and reduction were undertaken with SAINT and XPREP software.[31] Structures were solved by direct methods using SHELXS-97 and refined with full-matrix least squares on *F*2 using SHELXL-97.[32] Structural illustrations have been drawn with ORTEP-3 for Windows.[33]

6.6.2 Synthesis of ligand L_9

Pyridine-2-ethylamine (1.22 g, 10 mmol) and pyridine-2-carboxaldehyde (1.07 g, 10 mmol) were taken in 50 ml of ethanol and the mixture was refluxed for 5 h during which leads to the formation of schiff's base. This schiff's base was further reduced by $NaBH_4$ to give respective amine. This amine was further extracted by dichloromethane water mixture (4×50

ml). After that 4-chloro-7-nitrobenzofurazane (2.0 g, 10 mmol) was dissolved in dry dichloromethane and added drop wise to the stirring amine solution at ~0 °C. The reaction mixture was allowed to react with in dry dichloromethane for 24 hr at room temperature. The crude mixture was purified by column chromatography to obtain pure ligand **L_9**. Yield: 2.63 g (70%). Elemental analyses: calcd. (%): C, 60.63; H, 4.28; N, 22.23; found (%): C, 60.74; H, 4.33; N, 22.29. FT-IR (in KBr): 1609, 1548, 1209, 916, 757 cm^{-1}. ^{1}H-NMR: (400 MHz, $CDCl_3$): δ_{ppm}: 8.56 (2H, t), 8.40 (1H, d), 7.70 (2H, m), 7.31 (1H, d), 7.24 (3H, m), 6.32 (1H, b s), 5.21 (2H, s), 4.54 (2H, s), 3.36 (2H, t). ^{13}C-NMR: (100 MHz, $CDCl_3$): $\delta_{ppm:}$ 157.7, 155.1, 150.1, 149.8, 145.5, 145.0, 144.7, 137.3, 137.1, 135.5, 123.9, 123.1, 122.3, 121.4, 102.6, 58.7, 54.7, 35.9. Mass $(M+H^+)/z$: calcd: 376.128; found: 377.138.

6.6.3 Synthesis of complex 6.1

To a stirred solution of $CuCl_2 \cdot 2H_2O$ (0.340 g, 2 mmol) in 25 ml acetonitrile was added a solution of ligand **L_9** (0.752 g, 2 mmol) in 25 ml acetonitrile. The reaction mixture was stirred for 2 h after that it was filtered and the filtrate was reduced under vacuum to obtain the metal complex **6.1** as a green solid. Yield: 0.91 g (90%). Elemental analysis: calcd.(%) C, 44.67; H, 3.16; N, 16.45; found(%): C, 44.71; H, 3.18; N, 16.39. FT-IR (in KBr): 1606, 1518, 1445, 1318, 1239, 949, 767 cm^{-1}. UV-visible (acetonitrile): λ_{max}, 768, 420 nm. The complex **6.1** behaves as 1:2 electrolyte in methanol solution [ΛM (S cm^{-1}), 256]. μ_{obs} 1.58 BM.

6.7 References

1. (a) Kirsch, M.; Korth, H. G.; Sustmann, R.; Groot, H. D. *Biol. Chem.* **2002**, *383*, 389. (b) Pfeiffer, S.; Mayer, B.; Hemmens, B. *Angew. Chem.* **1999**, *111*, 1824; *Angew. Chem.* **1999,** *38,* 1714.

2. Espey, M. G.; Xavier, S.; Thomas, D. D.; Miranda, K. M.; Wink, D. A. *Proc. Natl. Acad. Sci. U.S.A.* **2002**, *99,* 3481.

3. Pfeiffer, S.; Lass, A.; Schmidt, K.; Mayer, B. *FASEB J.* **2001**, *15,* 2355.

4. (a) Bryan, N. S.; Rassaf, T.; Maloney, R. E.; Rodriguez, C. M.; Saijo, F.; Rodriguez, J. R.; Feelisch, M. *Proc. Natl. Acad. Sci. U.S.A.* **2004**, *101,* 4308. (b) Rassaf, T.; Feelisch, M.; Kelm, M. *Free Radical Biol. Med.* **2004**, *36,* 413.

5. Cosby, K.; Partovi, K. S.; Crawford, J. H.; Patel, R. P.; Reiter, C. D.; Martyr, S.; Yanq, B. K.; Waclawiw, M. A.; Zalos, G.; Xu, X.; Huang, K. T.; Shields, H.; Kim-Shapiro, D. B.; Schechter, A. N.; Cannon, R. O.; Gladvin, M. T. *Nat. Med.* **2003**, *9,* 1498.

6. Kirsch, M.; Korth, H. G.; Sustmann, R.; De Groot, H. *Biol. Chem*. **2002**, *383*, 389.

7. Beckman, J. S. *Arch. Biochem. Biophys.* **2009**, *484*, 114.

8. Ischiropoulos, H. *Arch. Biochem. Biophys*. **2009**, *484*, 117.

9. Ferrer-Sueta, G.; Radi, R. *ACS Chem. Biol.* **2009**, *4*, 161.

10. Abello, N.; Kerstjens, H. A. M.; Postma, D. S.; Bischoff, R. *J. Proteome Res.* **2009**, *8*, 3222.

11. Radi, R. *Proc. Natl. Acad. Sci. U.S.A.* **2004**, *101*, 4003.

12. Ischiropoulos, H. *Arch. Biochem. Biophys.* **1998**, *356*, 1.

13. Reynolds, M. R.; Berry, R. W.; Binder, L. I. *Biochemistry* **2007**, *46*, 7325.

14. Ascenzi, P.; Di Masi, A.; Sciorati, C.; Clementi, E. *BioFactors* **2010**, *36*, 264.

15. Reyes, J. F.; Reynolds, M. R.; Horowitz, P. M.; Fu, Y. F.; Guillozet- Bongaarts, A. L.; Berry, R.; Binder, L. I. *Neurobiol. Dis.* **2008**, *31*, 198.

16. Wattanapitayakul, S. K.; Weinstein, D. M.; Holycross, B. J.; Bauer, J. A. *FASEB J.* **2000**, *14*, 271.

17. Cruthirds, D. L.; Novak, L.; Akhi, K. M.; Sanders, P. W.; Thompson, J. A.; MacMillan-Crow, L. A. *Arch. Biochem. Biophys.* **2003**, *412*, 27.

18. Olbregts, J. *Int. J. Chem. Kinet.* **1985**, *17,* 835.

19. Su, J.; Groves, J. T. *J. Am. Chem. Soc.* **2009**, *131,* 12979.

20. Bian, K.; Gao, Z. H.; Weisbrodt, N.; Murad, F. *Proc. Natl. Acad. Sci. U.S.A.* **2003**, *100,* 5712.

21. Mondal, B.; Kumar, P.; Ghosh, P.; Kalita, A. *Chem. Commun.* **2011**, *47*, 2964.

22. Hu, X.; Wang, J.; Zhu, X.; Dong, D.; Zhang, X.; Wu, S.; Duan, C. *Chem. Commun.* **2011**, *47*, 11507.

23. Rosenthal, J.; Lippard, S. J. *J. Am. Chem. Soc.* **2010**, *132*, 5536.

24. Lim, M. H.; Lippard, S. *J. Acc. Chem. Res.* **2007**, *40*, 41.

25. Wang, S. H.; Han, M. Y.; Huang, D. J. *J. Am. Chem. Soc.* **2009**, *131*, 11692.

26. (a) Yan, Y.; Krishnakumar, S.; Yu, H.; Ramishetti, S.; Deng, L.; Wang, S.; Huang, L.; Huang, D. *J. Am. Chem. Soc.* **2013**, *135*, 5312. (b) Mondal, B.; Kumar, V. *RSC Adv.* **2014**, *4*, 61944.

27. (a) Kumar, V.; Kalita, A.; Mondal, B. *Dalton Trans.* **2013**, *42*, 16264. (b) Gogoi, K.; Deka, H.; Kumar, V.; Mondal, B. *Inorg. Chem.* **2015**, *54*, 4799.

28. Lymar, S. V.; Hurst, J. K. *Chem. Res. Toxicol*. **1996**, *9*, 845.

29. Banthia, S.; Samanta, A. *New. J. Chem*. **2005**, *29*, 1007.

30. SMART, SAINT and XPREP, Siemens Analytical X-ray Instruments Inc., Madison, Wisconsin, USA, **1995**.

31. Sheldrick, G. M. SADABS: Software for Empirical Absorption Correction, University of Gottingen, Institut fur Anorganische Chemieder Universitat, Tammanstrasse 4, D-3400 Gottingen, Germany, **1999–2003**.

32. Sheldrick, G. M. SHELXS-97, Program for solution of crystal structures, University of Göttingen, Germany, **1997**.

33. Farrugia, L. J. *J. Appl. Crystallogr*. **1997**, *30*, 565.

Appendix

Appendix I

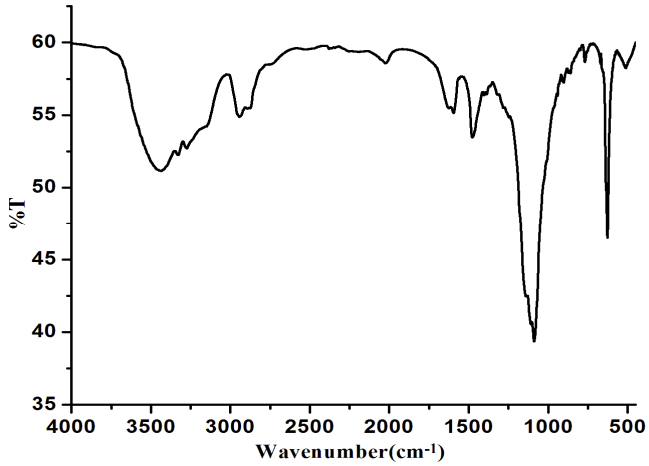

Figure A1.1 FT-IR spectrum of complex **2.1** in KBr pellet.

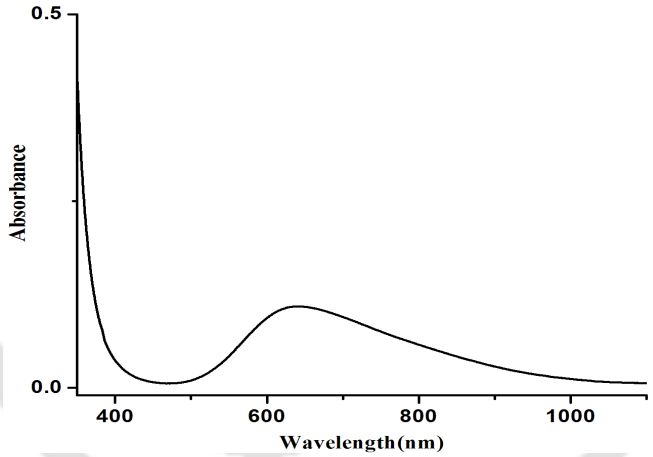

Figure A1.2 UV-visible spectrum of complex **2.1** in acetonitrile.

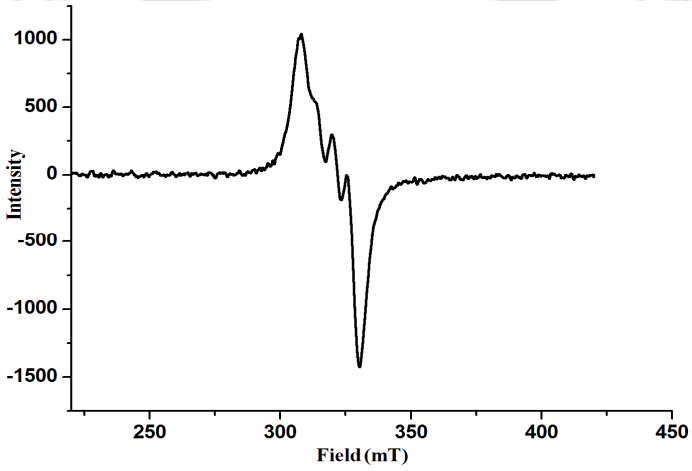

Figure A1.3 X-band EPR spectrum of complex **2.1** in acetonitrile at room temperature.

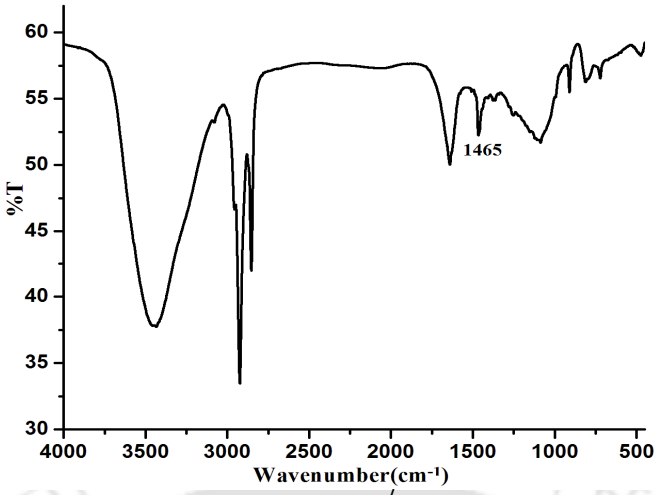

Figure A1.4 FT-IR spectrum of modified ligand $\mathbf{L_1}'$ in KBr pellet.

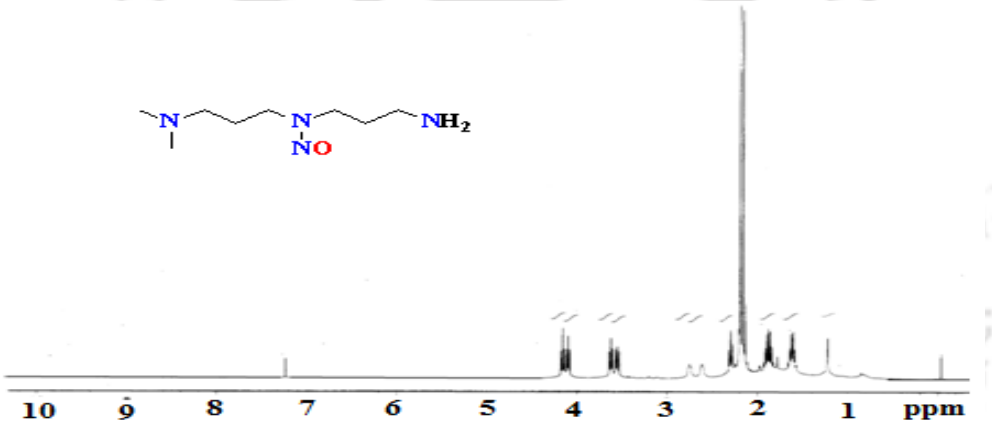

Figure A1.5 ^{1}H-NMR spectrum of modified ligand $\mathbf{L_1}'$ in $CDCl_3$.

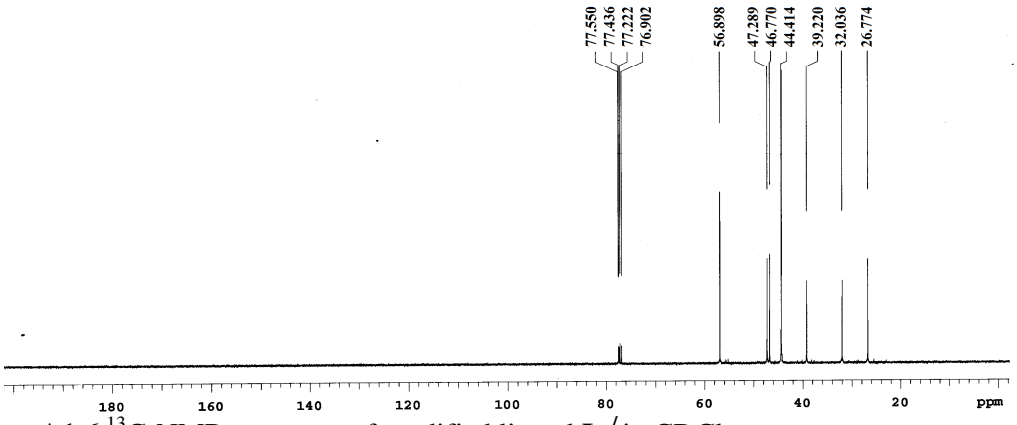

Figure A1.6 ^{13}C-NMR spectrum of modified ligand $\mathbf{L_1}'$ in $CDCl_3$.

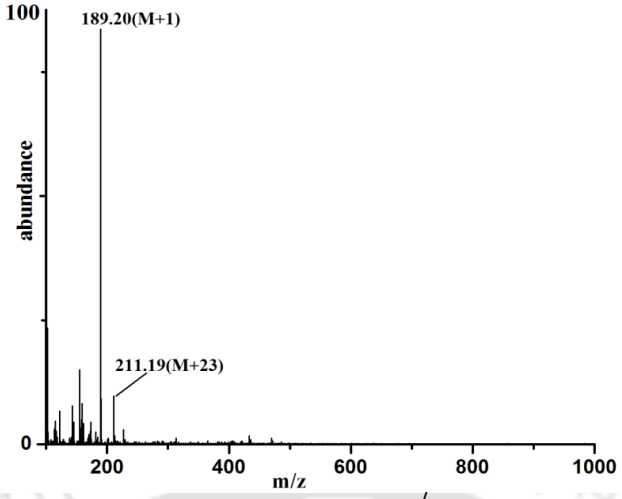

Figure A1.7 ESI- Mass spectrum of modified ligand $\mathbf{L_1'}$ in methanol.

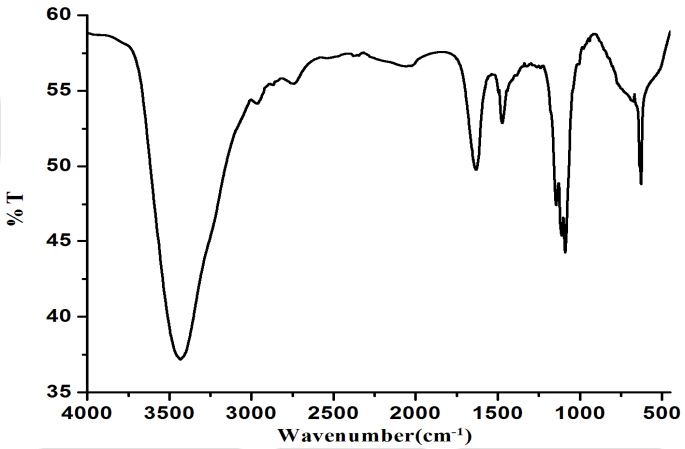

Figure A1.8 FT-IR spectrum of complex **2.2** in KBr pellet.

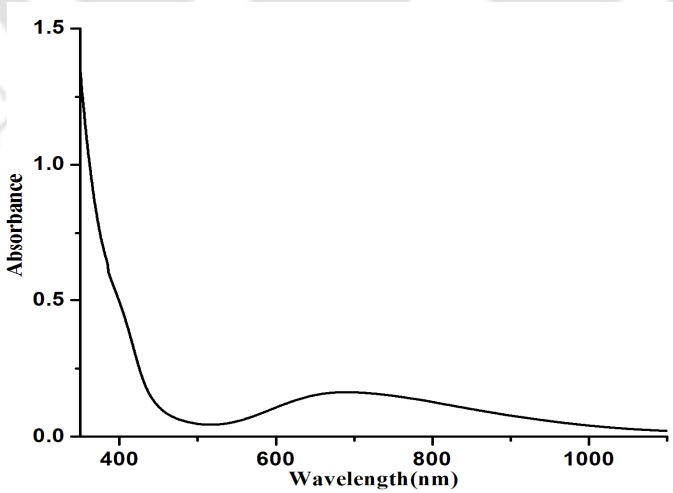

Figure A1.9 UV-visible spectrum of complex **2.2** in acetonitrile.

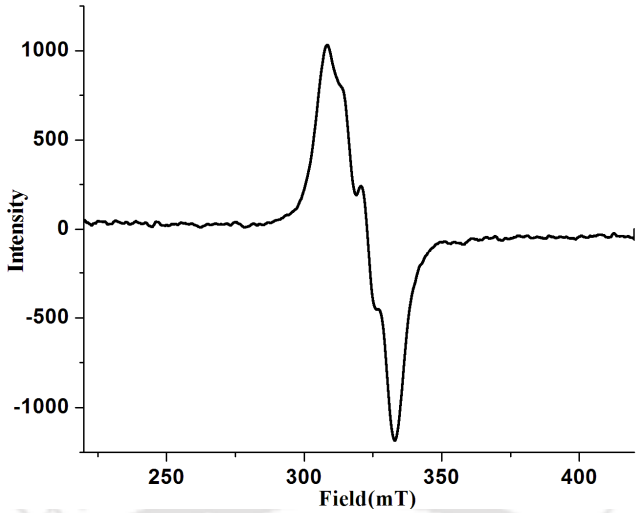

Figure A1.10 X-band EPR spectrum of complex **2.2** in acetonitrile at room temperature.

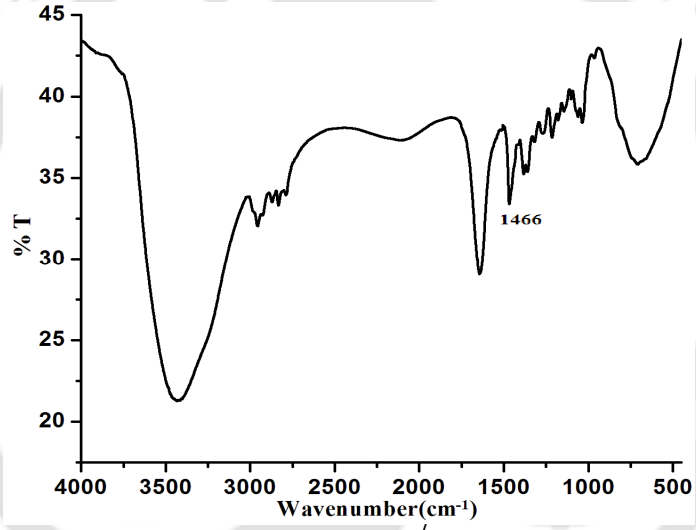

Figure A1.11 FT-IR spectrum of modified ligand $\mathbf{L_2}'$ in KBr pellet.

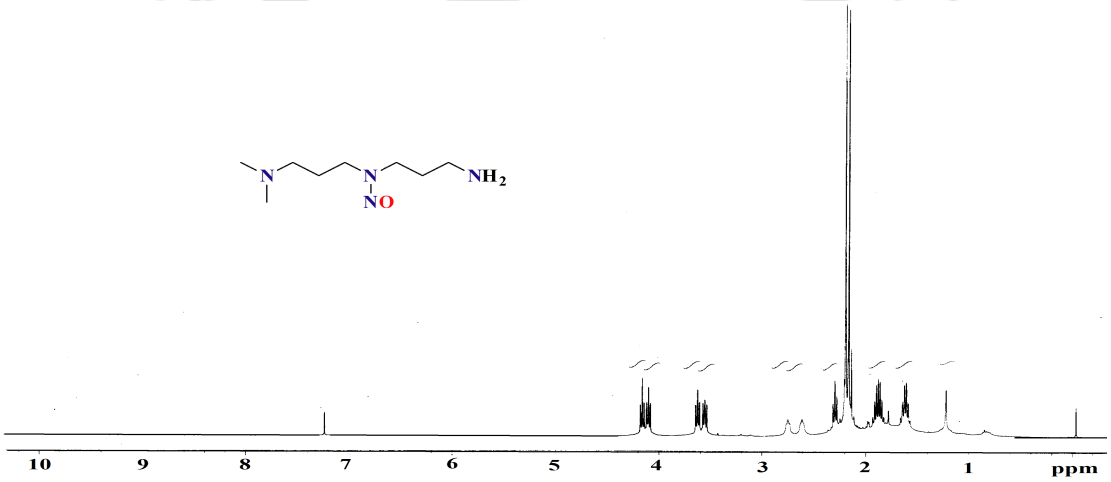

Figure A1.12 ^{1}H-NMR spectrum of modified ligand $\mathbf{L_2}'$ in $CDCl_3$.

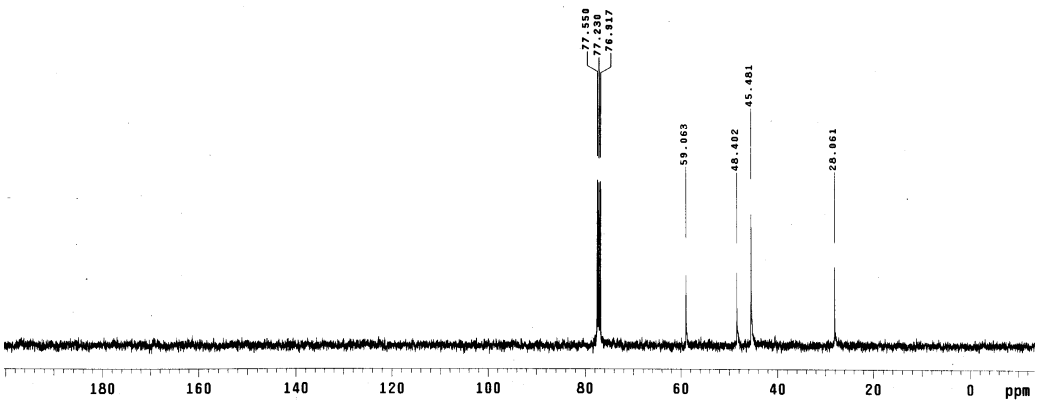

Figure A1.13 ^{13}C-NMR spectrum of modified ligand $\mathbf{L_2'}$ in $CDCl_3$.

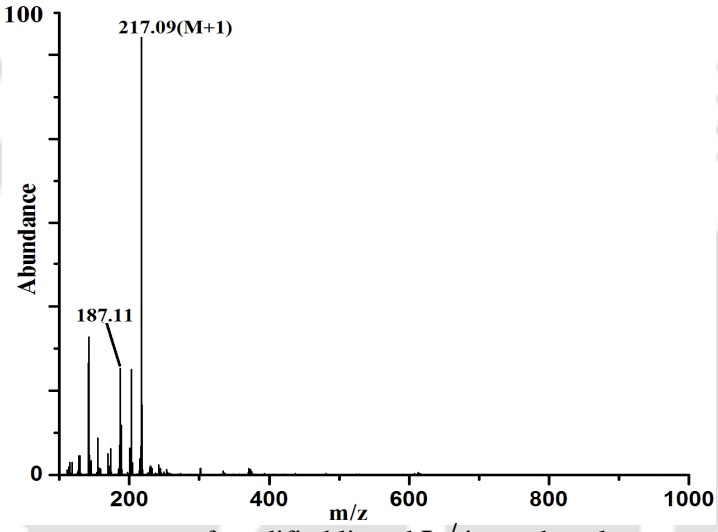

Figure A1.14 ESI- mass spectrum of modified ligand $\mathbf{L_2'}$ in methanol.

Appendix II

Table A2.1 Crystallographic data for complexes **3.1** and **3.2**.

	Complex **3.1**	Complex **3.2**
Formulae	C_{24} H_{42} Cu N_2 O_3	C_{36} H_{58} Cu_1 N_2 O_4
Mol. wt.	470.15	646.38
Crystal system	Monoclinic	Triclinic
Space group	P 21/n	P-1
Temperature /K	293(2)	296(2)
Wavelength /Å	0.71073	0.71073
a /Å	10.1575(3)	9.8751(13)
b /Å	24.1596(8)	13.671(2)
c /Å	11.0644(3)	14.078(2)
α/°	90.00	98.778(8)
β/°	103.211(3)	104.531(8)
γ/°	90.00	96.777(8)
V/ $Å^3$	2643.36(14)	1793.8(4)
Z	4	2
Density/Mgm^{-3}	1.181	1.197
Abs. co-eff. /mm^{-1}	0.850	0.647
Abs. correction	None	None
F(000)	1265	698
Total no. of reflections	4650	6345
Reflections, $I > 2\sigma(I)$	3374	4341
Max. 2θ/°	25	25.24
Ranges (h, k, l)	-12≤h ≤11 -28≤ k ≤16 -8≤ l ≤ 13	-11≤h ≤11 -16≤ k ≤14 -15≤ l ≤ 16
Complete to 2θ (%)	99.8	97.9
Refinement method	Full-matrix least-squares on F^2	Full-matrix least-squares on F^2
Goof (F^2)	0.955	0.986
R indices [$I > 2\sigma(I)$]	0.0460	0.0477
R indices (all data)	0.0677	0.0671

Table A2.2 Selected bond lengths (Å) for complexes **3.1** and **3.2**.

	Complex **3.1**	Complex **3.2**
Cu(1) – O(2)	1.973(2)	1.922(3)
Cu(1) – O(1)	1.863(2)	1.893(2)
Cu(1) - O(3)	2.565(2)	-
Cu(1) - N(2)	2.045(2)	2.026(3)
Cu(1) - N(1)	2.046(3)	2.059(3)
O(2) - C(23)	1.264(4)	-
N(2) - C(8)	1.502(4)	-
N(2) - C(5)	1.502(4)	1.496(3)
N(2) - C(4)	1.482(4)	1.488(5)
N(1) - C(1)	1.477(5)	1.478(5)
N(1) - C(3)	1.477(4)	1.489(6)
N(1) - C(2)	1.490(5)	1.469(5)

Table A2.3 Selected bond angles (°) for complexes **3.1** and **3.2**.

	Complex **3.1**	Complex **3.2**
O(2)-Cu(1)-O(1)	91.6(1)	90.0(1)
O(2)-Cu(1)-O(3)	55.74(9)	-
O(2)-Cu(1)-N(2)	169.5(1)	162.1(1)
O(2)-Cu(1)-N(1)	90.2(1)	94.6(1)
O(1)-Cu(1)-O(3)	89.84(9)	-
O(1)-Cu(1)-N(2)	94.90(9)	94.3(1)
O(1)-Cu(1)-N(1)	156.8(1)	160.0(1)
O(3)-Cu(1)-N(2)	115.92(9)	-
O(3)-Cu(1)-N(1)	110.1(1)	-
N(2)-Cu(1)-N(1)	87.0(1)	87.2(1)

Table A2.4 Crystallographic data for modified ligand $\mathbf{L_4'}$.

	$\mathbf{L_4'}$
Formulae	$C_{26}\ H_{38}\ N_4\ O_6$
Mol. wt.	502.60
Crystal system	Monoclinic
Space group	P2(1)/c
Temperature /K	293(2)
Wavelength /Å	0.71073
a /Å	15.5224(11)
b /Å	9.7342(9)
c /Å	19.2871(12)
α/°	90.00
β/°	105.076(7)
γ/°	90.00
V/ $Å^3$	2813.9(4)
Z	4
Density/Mgm^{-3}	1.186
Abs. co-eff. /mm^{-1}	0.085
Abs. correction	none
F(000)	1080
Total no. of reflections	4824
Reflections, $I > 2\sigma(I)$	2465
Max. 2θ/°	25.00
Ranges (h, k, l)	-18≤h ≤14 -11≤ k ≤8 -22≤ l ≤ 22
Complete to 2θ (%)	97.3
Refinement method	Full-matrix least-squares on F^2
Goof (F^2)	1.434
R indices [$I > 2\sigma(I)$]	0.0895
R indices (all data)	0.1532

Table A2.5 Selected bond lengths (Å) for modified ligand $\mathbf{L_4'}$.

Atoms	Bond Angle
N(2) - C(16)	1.478(5)
N(2) - C(5)	1.493(5)
N(2) - C(4)	1.470(6)
N(4) - O(6)	1.224(5)
N(4) - O(5)	1.228(5)
N(4) - C(21)	1.462(5)
N(3) - O(3)	1.237(5)
N(3) - O(4)	1.220(5)
N(3) - C(10)	1.470(6)
N(1) - C(3)	1.412(7)
N(1) - C(1)	1.448(8)
N(1) - C(2)	1.451(6)
O(1) - C(7)	1.356(5)
O(2) - C(18)	1.371(5)
C(6) - C(7)	1.407(4)
C(6) - C(11)	1.369(5)
C(6) - C(5)	1.503(5)

Table A2.6 Selected bond angles (°) for modified ligand $\mathbf{L_4'}$.

Atoms	Bond Angle
C(16)-N(2)-C(5)	109.5(3)
C(16)-N(2)-C(4)	112.0(3)
C(5)-N(2)-C(4)	112.6(3)
O(6)-N(4)-O(5)	123.4(4)
O(6)-N(4)-C(21)	118.5(4)
O(5)-N(4)-C(21)	118.1(4)
O(3)-N(3)-O(4)	124.1(4)
O(3)-N(3)-C(10)	117.4(4)
O(4)-N(3)-C(10)	118.5(4)
C(3)-N(1)-C(1)	111.5(4)
C(3)-N(1)-C(2)	111.3(4)
C(1)-N(1)-C(2)	107.0(4)
O(2)-C(18)-C(17)	120.3(4)
O(2)-C(18)-C(19)	117.1(4)
N(2)-C(4)-C(3)	110.7(4)
N(1)-C(3)-C(4)	116.5(4)
O(1)-C(7)-C(6)	118.9(3)
O(1)-C(7)-C(8)	118.9(3)

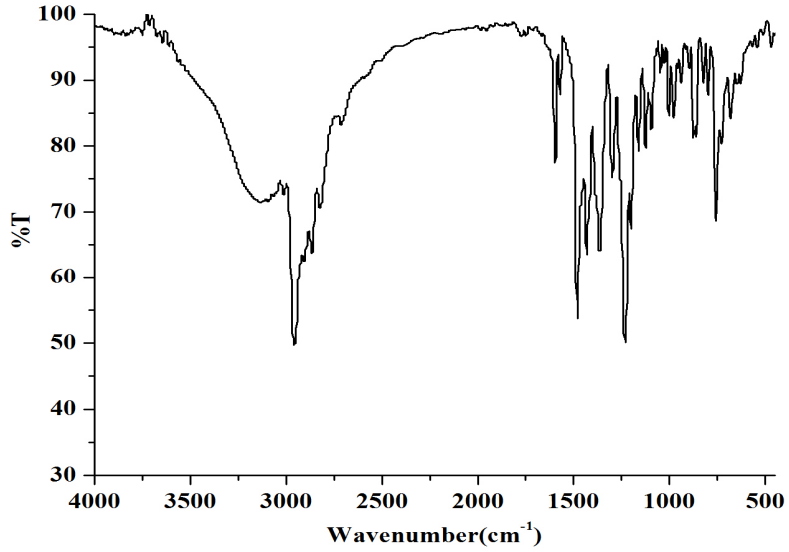

Figure A2.1 FT-IR spectrum of ligand $\mathbf{L_3}$ in KBr pellet.

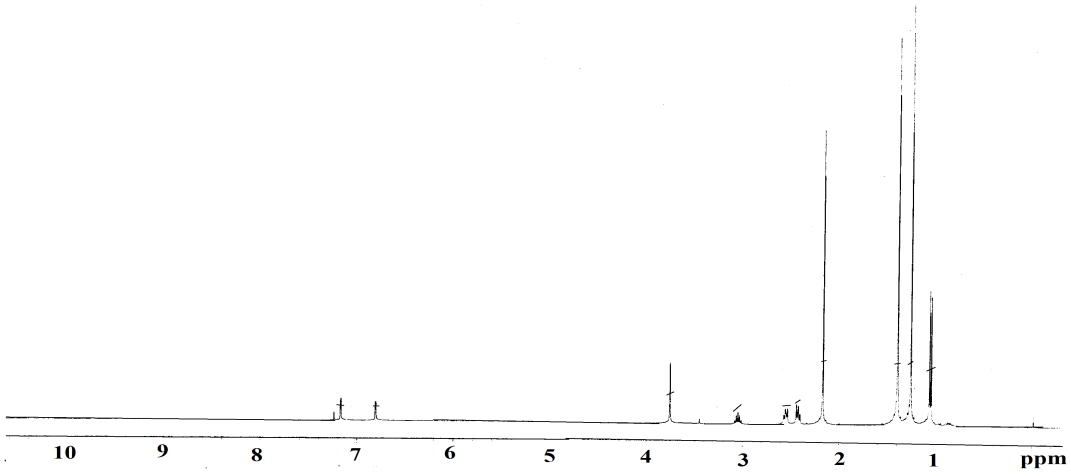

Figure A2.2 ^{1}H-NMR spectrum of ligand $\mathbf{L_3}$ in $CDCl_3$.

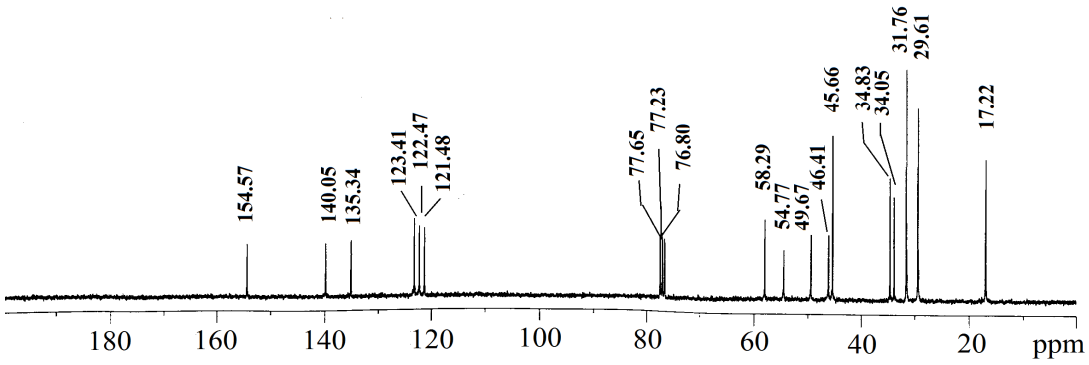

Figure A2.3 ^{13}C-NMR spectrum of ligand $\mathbf{L_3}$ in $CDCl_3$.

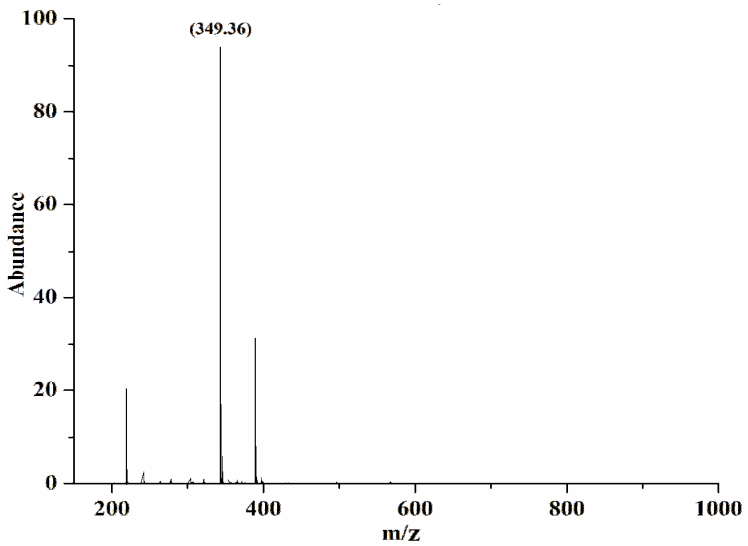

Figure A2.4 ESI- mass spectrum of ligand $\mathbf{L_3}$ in methanol.

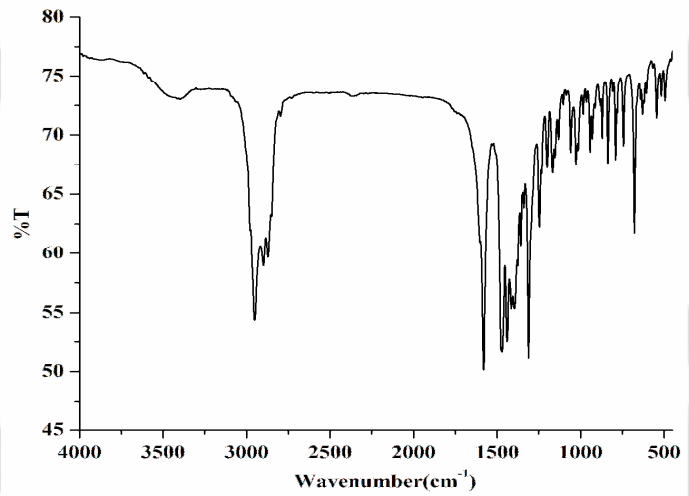

Figure A2.5 FT-IR spectrum of complex **3.1** in KBr pellet.

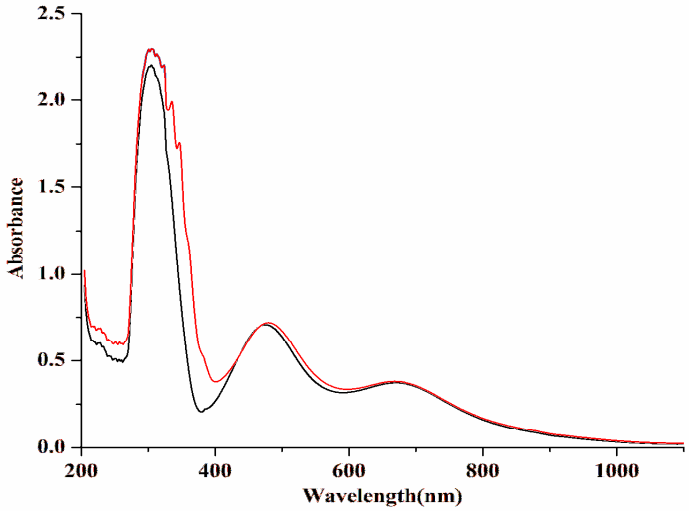

Figure A2.6 UV-visible spectra of complex **3.1** before (black trace) and after purging excess NO (red trace) in methanol.

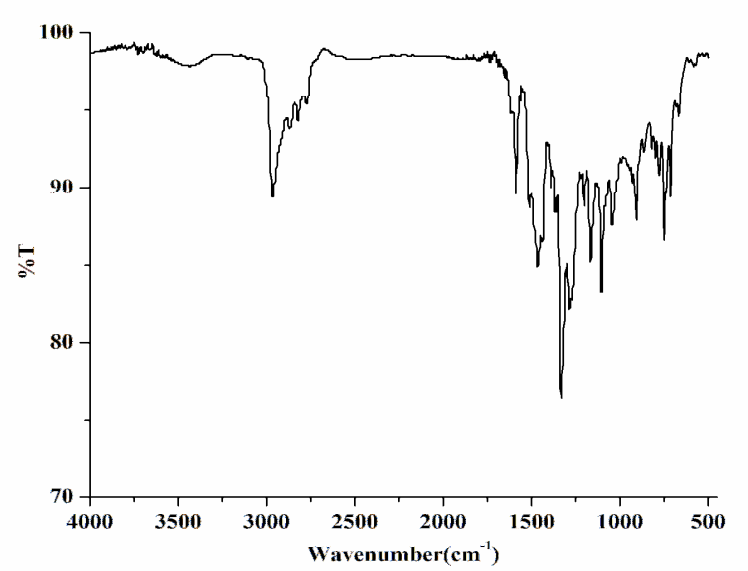

Figure A2.7 FT-IR spectrum of modified ligand $\mathbf{L_3'}$ in KBr pellet.

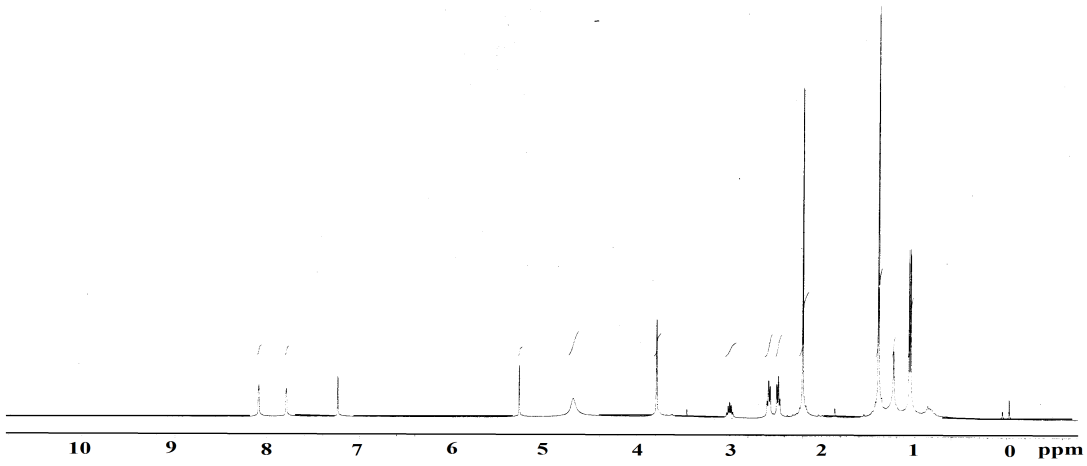

Figure A2.8 ^{1}H-NMR spectrum of modified ligand $\mathbf{L_3'}$ in $CDCl_3$.

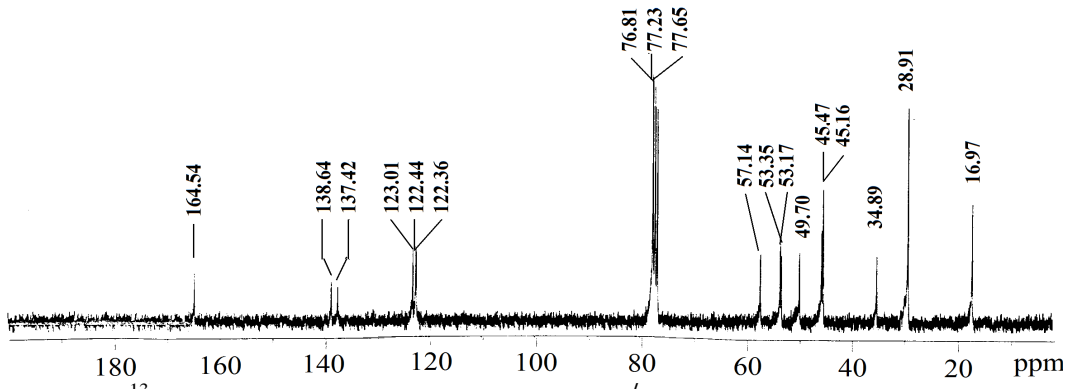

Figure A2.9 ^{13}C-NMR spectrum of modified ligand $\mathbf{L_3'}$ in $CDCl_3$.

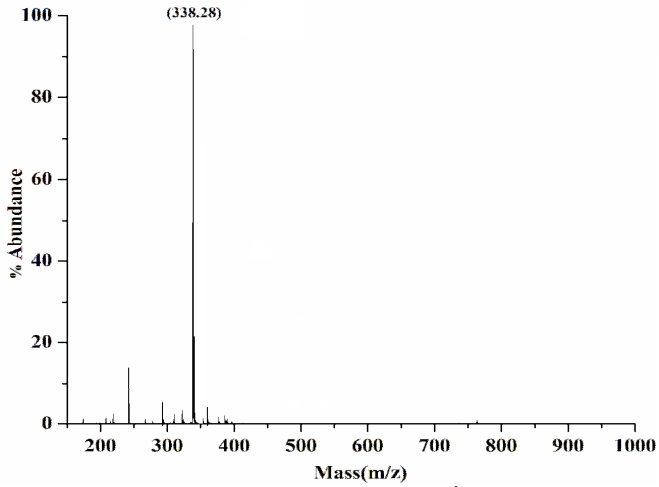

Figure A2.10 ESI- mass spectrum of modified ligand $\mathbf{L_3'}$ in methanol.

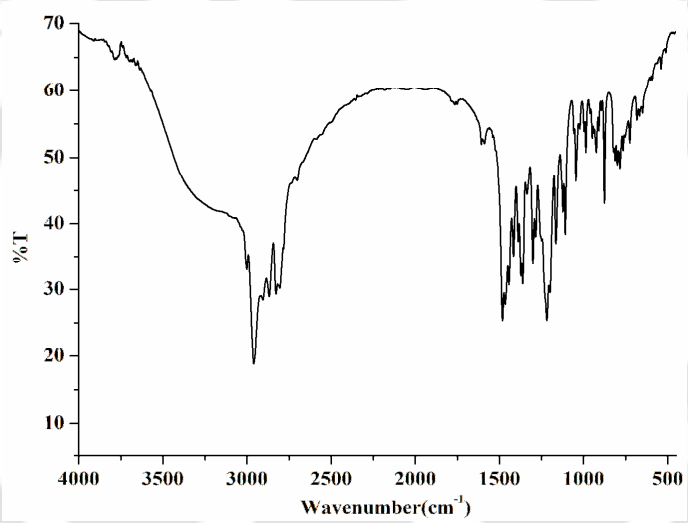

Figure A2.11 FT-IR spectrum of ligand $\mathbf{L_4}$ in KBr pellet.

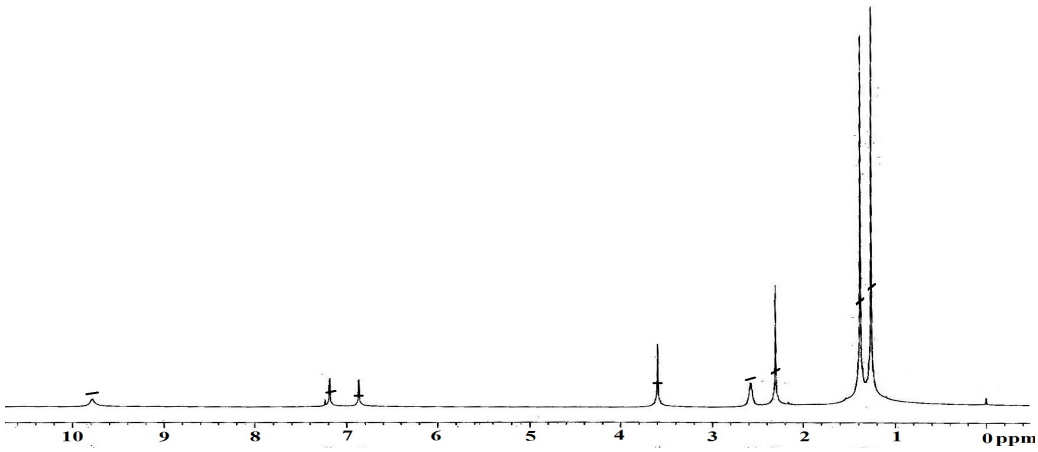

Figure A2.12 ^{1}H-NMR spectrum of ligand $\mathbf{L_4}$ in $CDCl_3$.

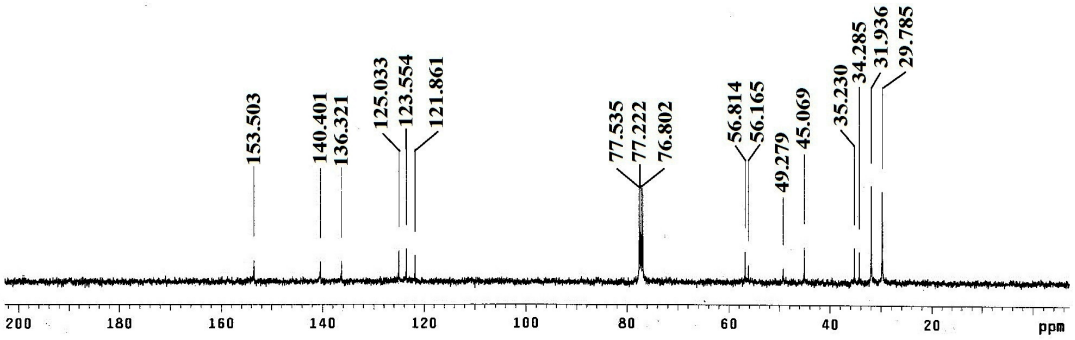

Figure A2.13 ^{13}C-NMR spectrum of ligand **L$_4$** in $CDCl_3$.

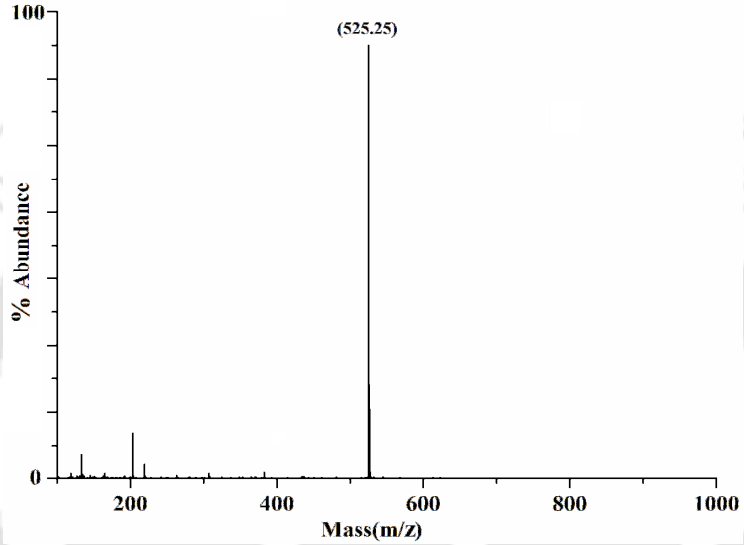

Figure A2.14 ESI- mass spectrum of ligand **L$_4$** in methanol.

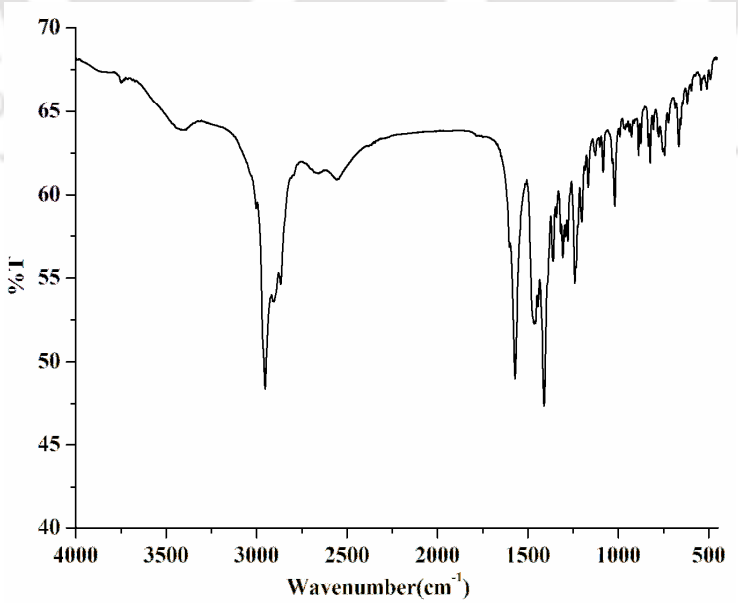

Figure A2.15 FT-IR spectrum of complex **3.2** in KBr pellet.

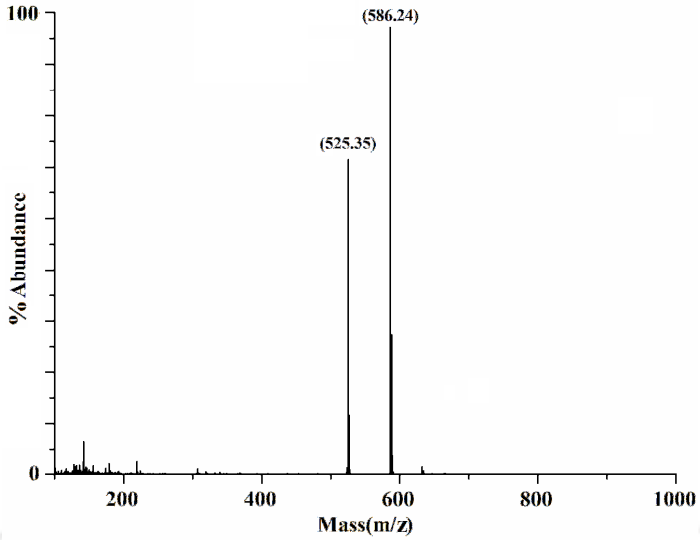

Figure A2.16 ESI- mass spectrum of complex **3.2** in methanol.

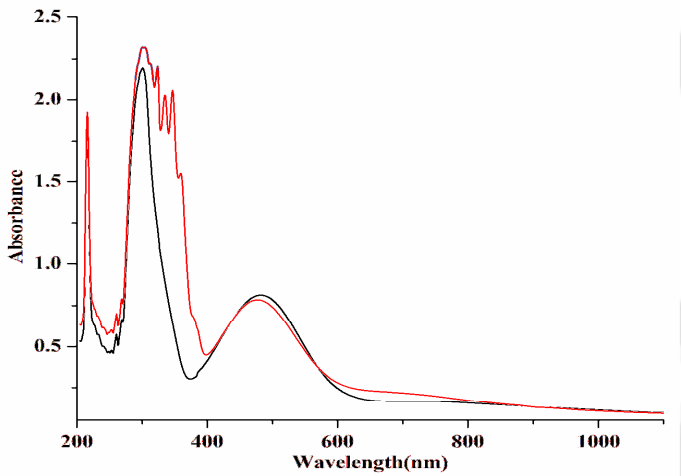

Figure A2.17 UV-visible spectra of complex **3.2** before (black trace) and after purging excess NO (red trace) in methanol.

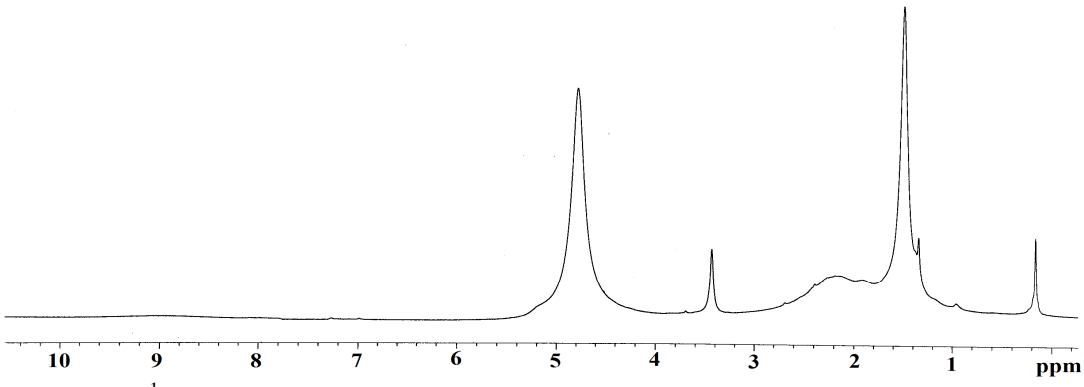

Figure A2.18 ^{1}H-NMR spectrum of complex **3.2** in CD_3OD.

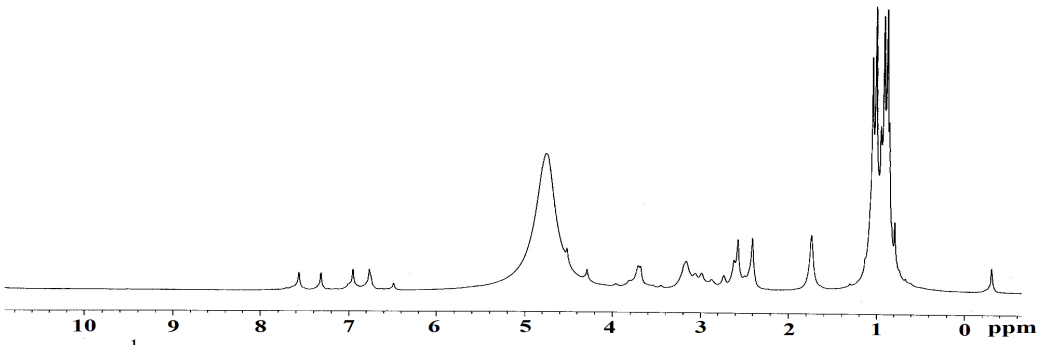

Figure A2.19 ^{1}H-NMR spectrum of complex **3.2** after purging NO_2 in CD_3OD.

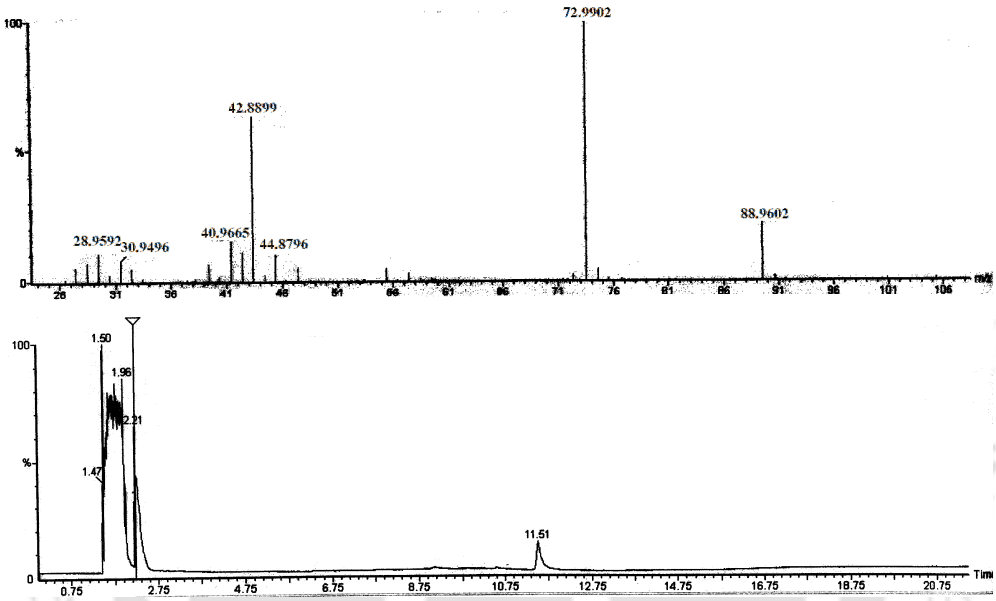

Figure A2.20 GC- mass spectrum of complex **3.2** after purging NO_2 in methanol.

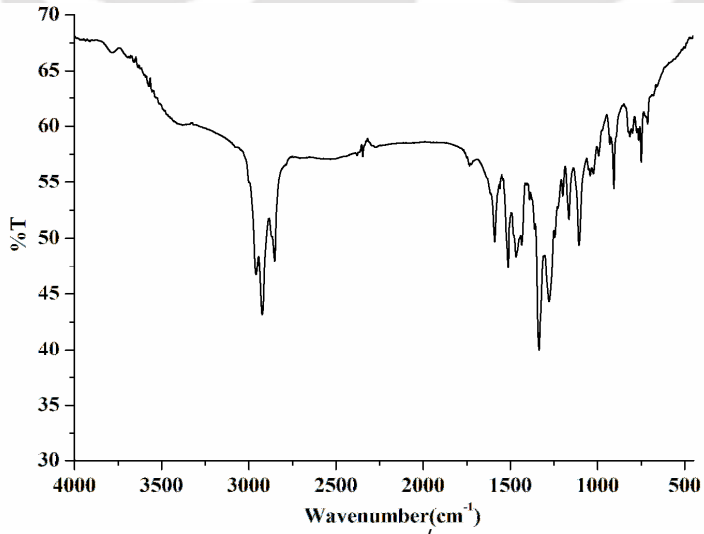

Figure A2.21 FT-IR spectrum of modified ligand $\mathbf{L_4'}$ in KBr pellet.

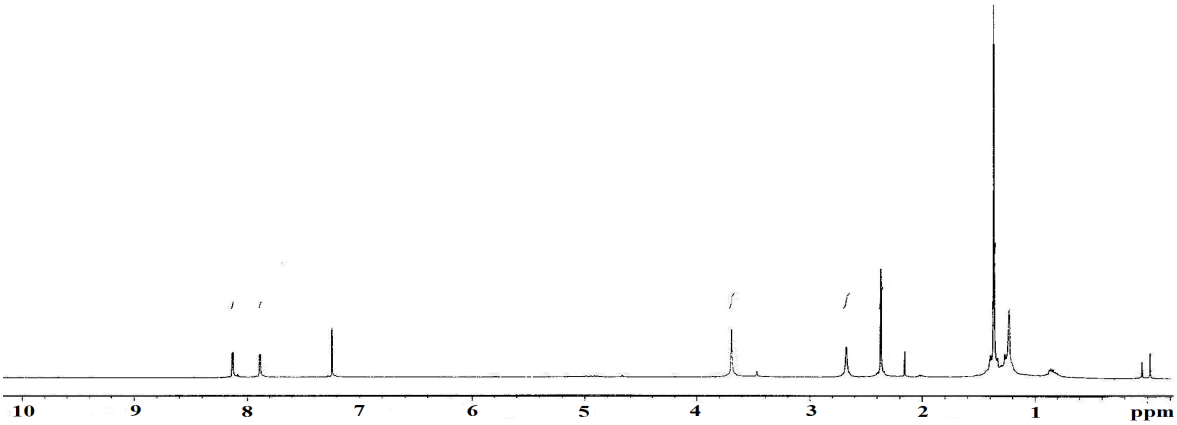

Figure A2.22 ^{1}H-NMR spectrum of modified ligand $\mathbf{L_4'}$ in $CDCl_3$.

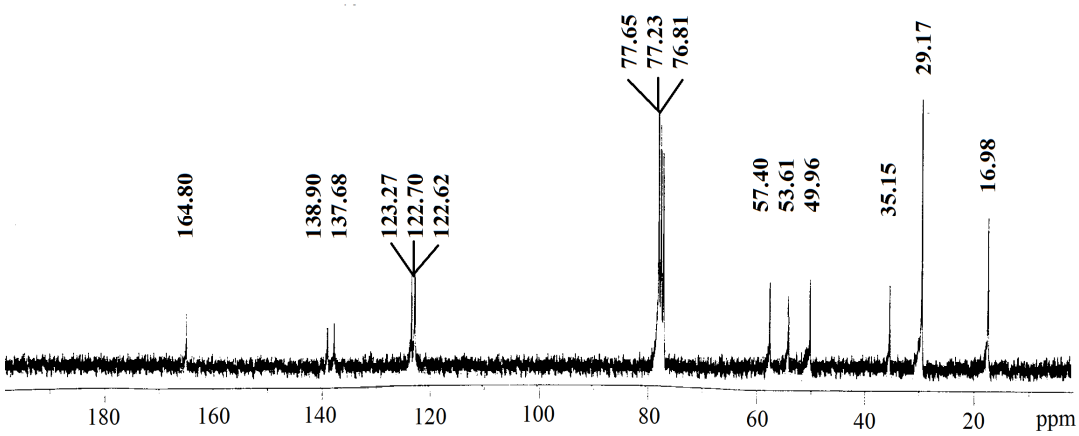

Figure A2.23 ^{13}C-NMR spectrum of modified ligand $\mathbf{L_4'}$ in $CDCl_3$.

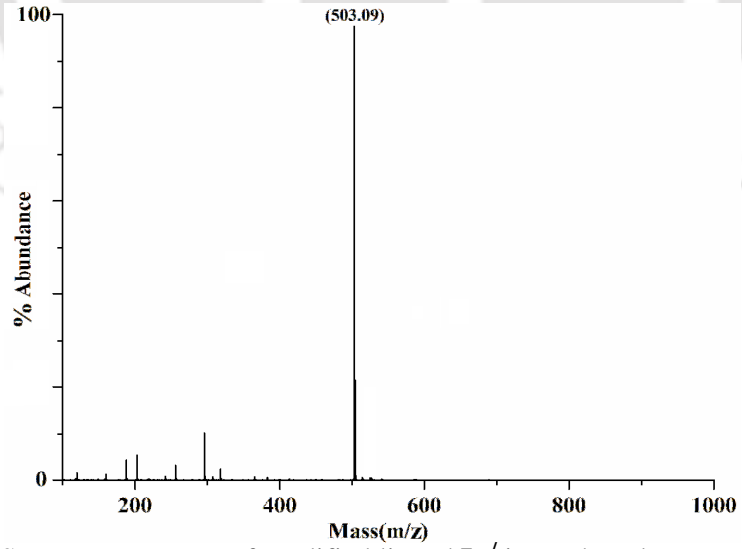

Figure A2.24 ESI- mass spectrum of modified ligand $\mathbf{L_4'}$ in methanol.

Appendix III

Table A3.1 Crystallographic data for complex **4.1**.

	Complex **4.1**
Formulae	C_{39} H_{57} N_2 O_5 Cu
Mol. wt.	697.41
Crystal system	Monoclinic
Space group	P21/n
Temperature /K	296(2)
Wavelength /Å	0.71073
a /Å	26.8261(11)
b /Å	10.7728(4)
c /Å	27.9227(17)
α/°	90.00
β/°	96.304(4)
γ/°	90.00
V/ Å^3	8020.6(7)
Z	8
Density/Mgm^{-3}	1.155
Abs. co-eff. /mm^{-1}	0.585
Abs. correction	multi-scan
F(000)	2992
Total no. of reflections	18185
Reflections, $I > 2\sigma(I)$	7961
Max. 2θ/°	28.75
Ranges (h, k, l)	-34≤h ≤35 -14≤ k ≤13 -37≤ l ≤ 33
Complete to 2θ (%)	87.2
Refinement method	Full-matrix least-squares on F^2
Goof (F^2)	1.270
R indices [$I > 2\sigma(I)$]	0.1204
R indices (all data)	0.2014

Table A3.2 Selected bond length (Å) for complex **4.1**.

Atoms	Bond Distances (Å)	Atoms	Bond Distances (Å)
Cu(1) - N(1)	1.993(5)	O(3) - C(37)	1.25(1)
Cu(1) - N(2)	2.047(4)	N(1) - C(1)	1.340(9)
Cu(1) - O(1)	1.900(4)	N(2) - C(7)	1.498(8)
Cu(1) - O(2)	2.404(5)	N(2) - C(6)	1.485(8)
Cu(1) - O(3	1.959(4)	N(2) - C(22)	1.47(1)
N(1) - C(5)	1.342(8)	O(1) - C(13)	1.335(8)
C(8) - C(7)	1.506(9)	O(2) - C(28)	1.348(9)

Table A3.3 Selected bond angles (°) for complex **4.1**.

Atoms	Bond Angles (°)	Atoms	Bond Angles (°)
N(1) - Cu(1) - N(2)	83.7(2)	O(2) - Cu(1) - O(3)	95.1(2)
N(1) - Cu(1) - O(1)	162.8(2)	Cu(1) - N(1) - C(5)	115.3(4)
N(1) - Cu(1) - O(2)	90.9(2)	Cu(1) - N(1) - C(1)	126.3(5)
N(1) - Cu(1) - O(3)	93.8(2)	Cu(1) - N(2) - C(7)	107.8(4)
N(2) - Cu(1) - O(1)	94.5(2)	Cu(1) - N(2) - C(22)	111.8(4)
N(2) - Cu(1) - O(2)	86.7(2)	Cu(1) - O(1) - C(13)	127.9(4)
N(2) - Cu(1) - O(3)	177.0(2)	Cu(1) - O(3) - C(37)	126.3(5)
O(1) - Cu(1) - O(2)	106.1(2)	Cu(1) - N(2) - C(6)	106.8(4)
O(1) - Cu(1) - O(3)	87.4(2)	-	-

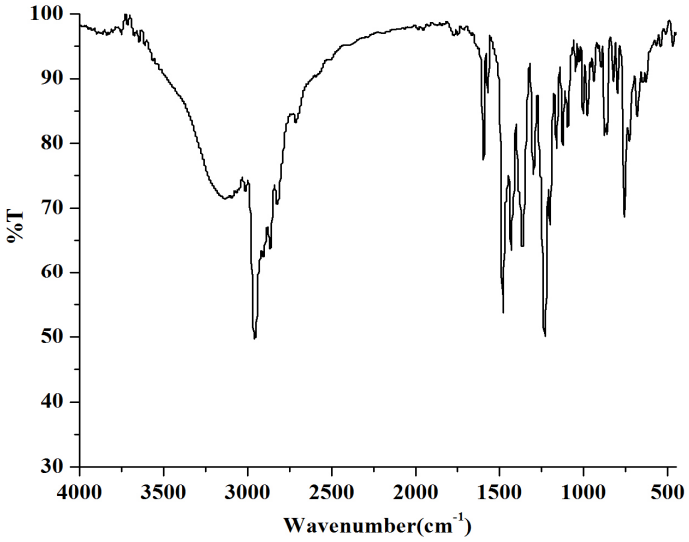

Figure A3.1 FT-IR spectrum of ligand $\mathbf{L_5H_2}$ in KBr pellet.

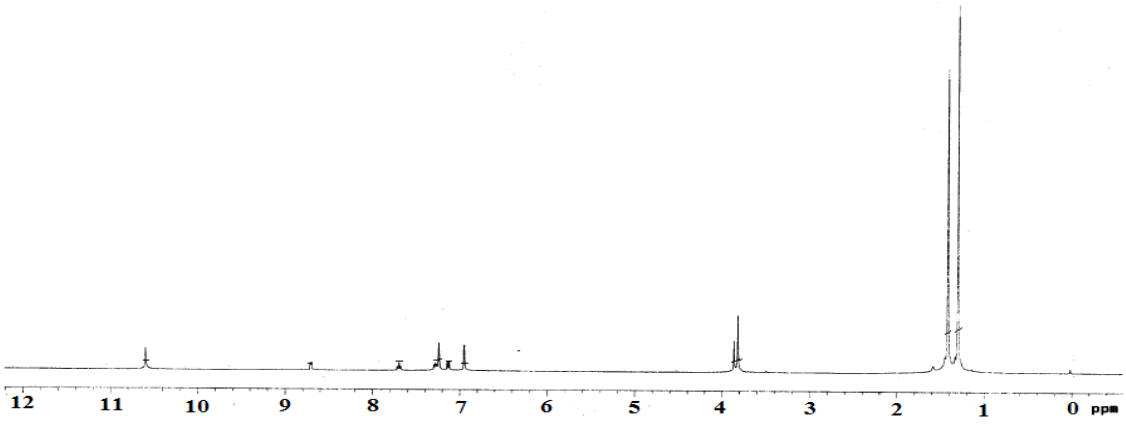

Figure A3.2 ^{1}H-NMR spectrum of ligand $\mathbf{L_5H_2}$ in $CDCl_3$.

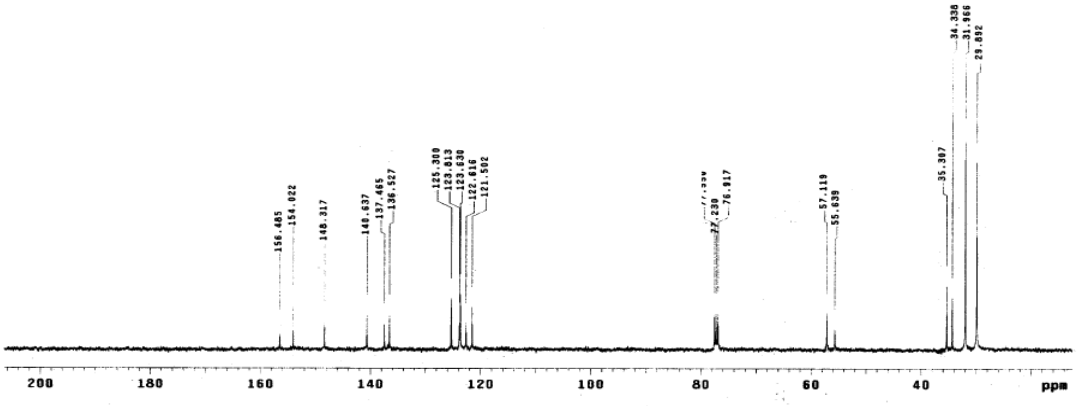

Figure A3.3 ^{13}C-NMR spectrum of ligand $\mathbf{L_5H_2}$ in $CDCl_3$.

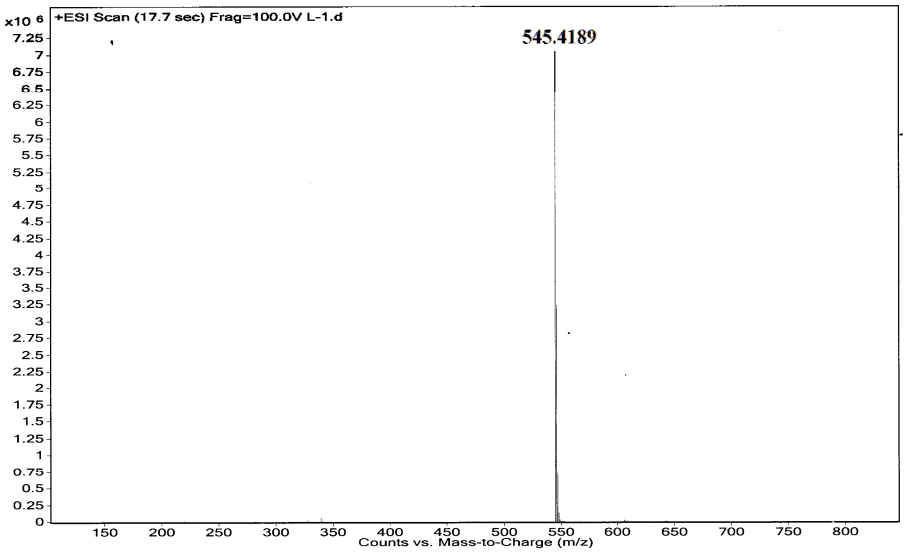

Figure A3.4 ESI mass spectrum of ligand $\mathbf{L_5H_2}$ in methanol.

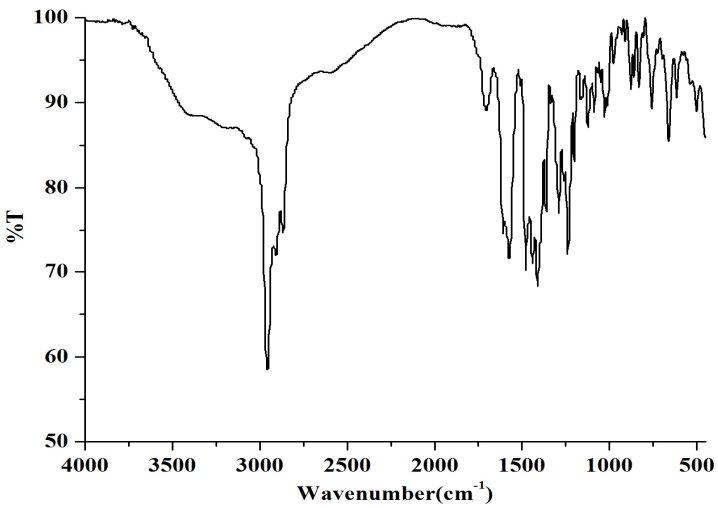

Figure A3.5 FT-IR spectrum of complex **4.1** in KBr pellet.

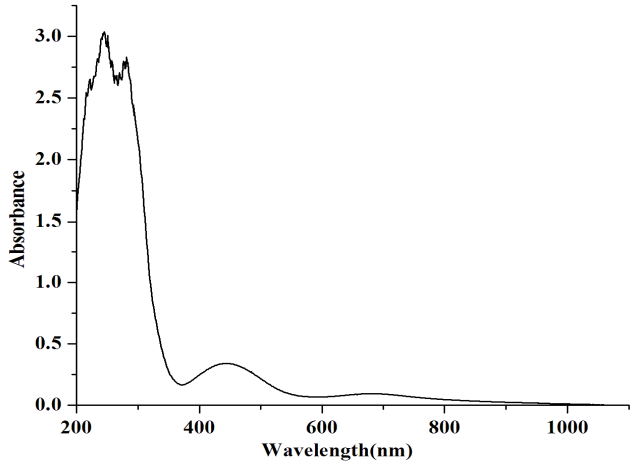

Figure A3.6 UV-visible spectrum of complex **4.1** in methanol.

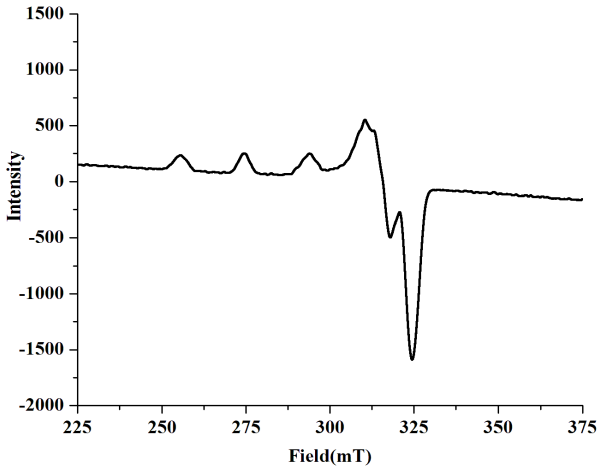

Figure A3.7 X-band EPR spectrum of complex **4.1** in THF at 77 K.

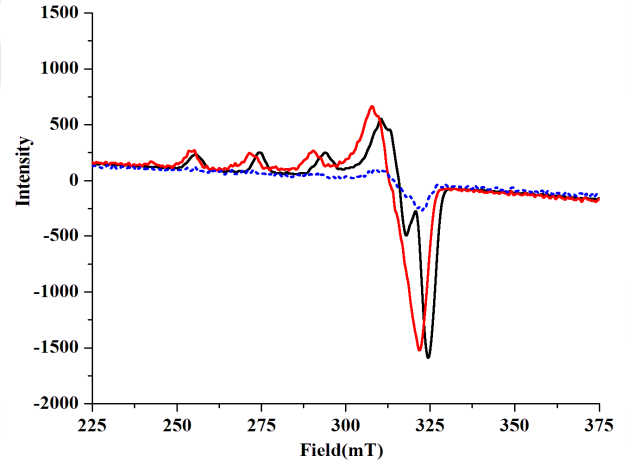

Figure A3.8 X-band EPR spectra of complex **4.1** (black trace), phenoxyl radical intermediate (blue trace) and complex **4.3** (red trace) at 77 K in THF.

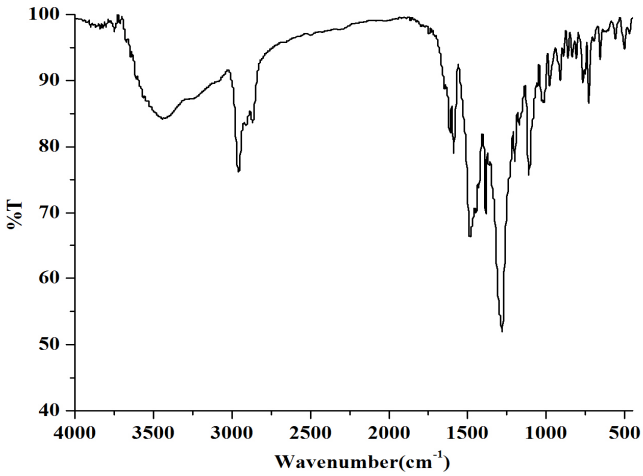

Figure A3.9 FT-IR spectrum of complex **4.3** in KBr pellet.

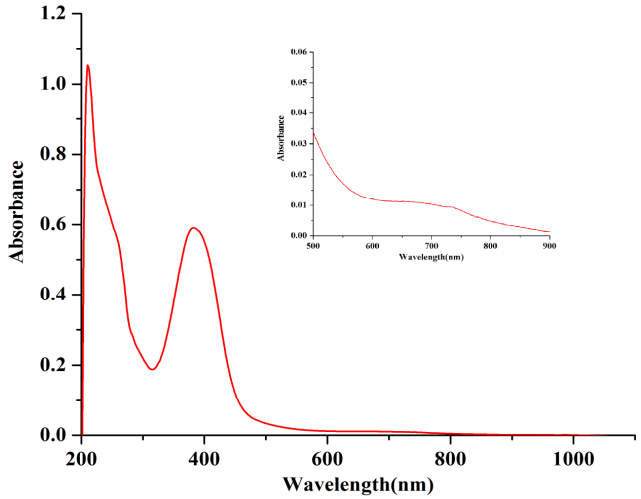

Figure A3.10 UV-visible spectrum of complex **4.3** in methanol at room temperature.

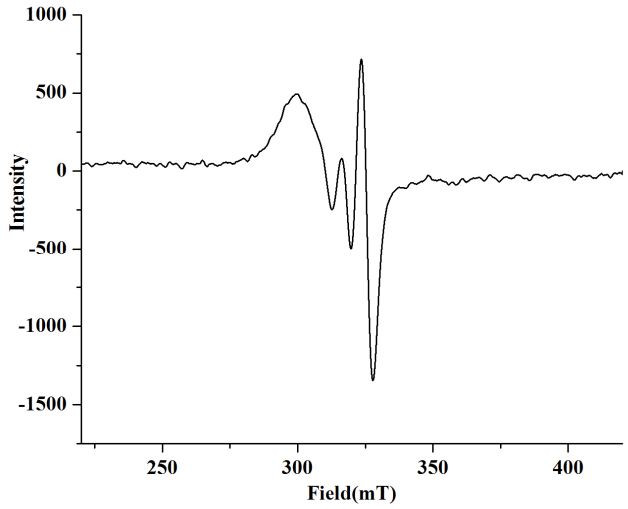

Figure A3.11 X-band EPR spectrum of complex **4.5** in methanol at room temperature.

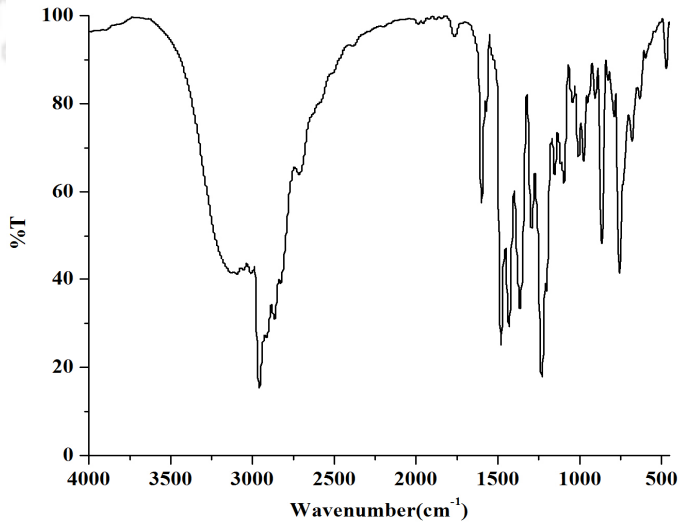

Figure A3.12 FT-IR spectrum of ligand $\mathbf{L_6H_2}$ in KBr pellet.

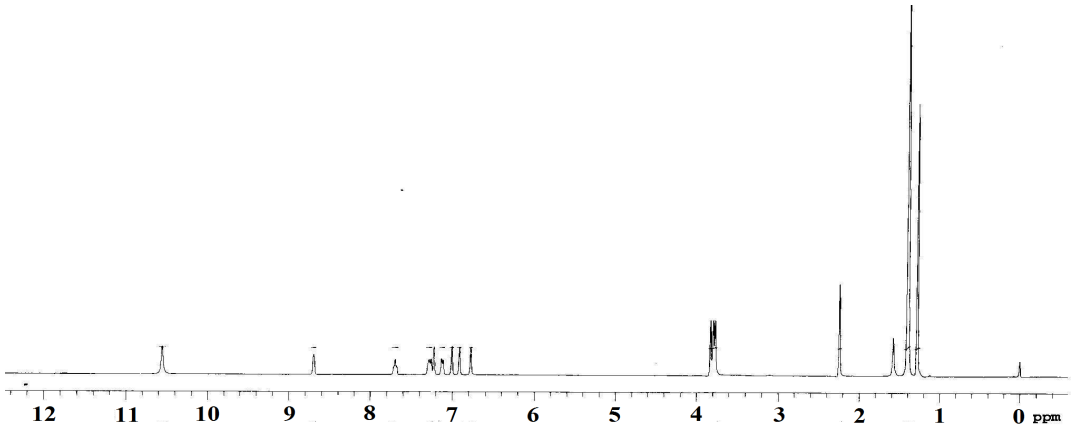

Figure A3.13 ^{1}H-NMR spectrum of ligand $\mathbf{L_6H_2}$ in $CDCl_3$.

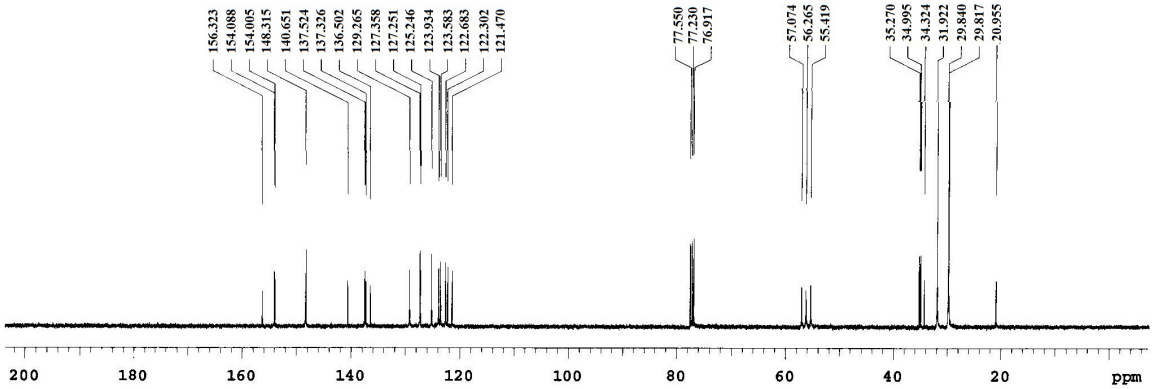

Figure A3.14 ^{13}C-NMR spectrum of ligand $\mathbf{L_6H_2}$ in $CDCl_3$.

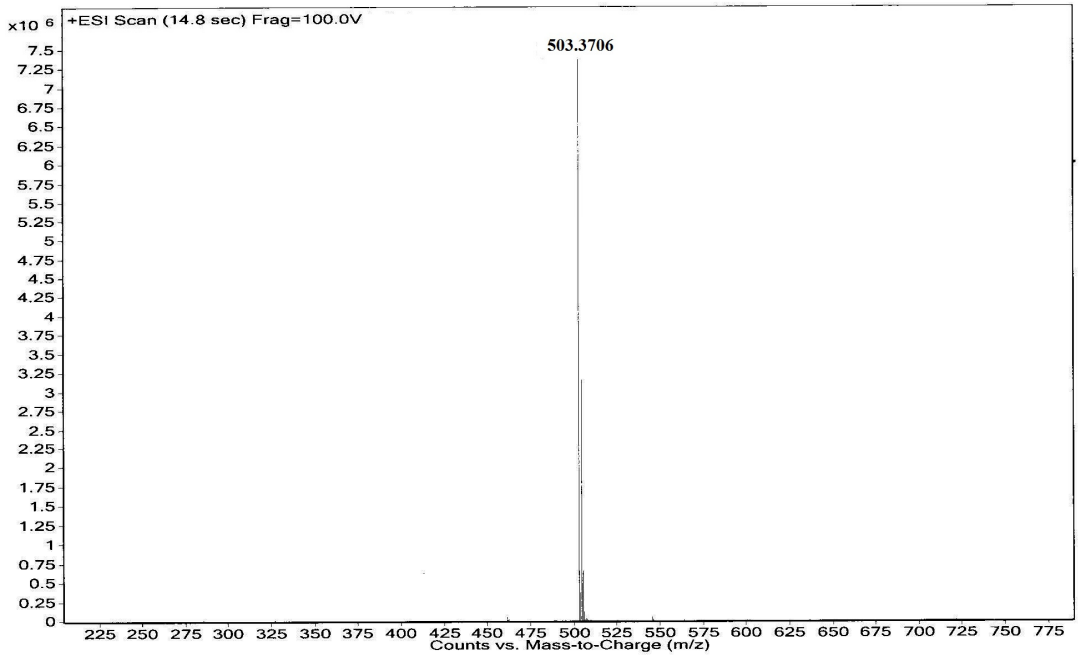

Figure A3.15 ESI mass spectrum of ligand $\mathbf{L_6H_2}$ in methanol.

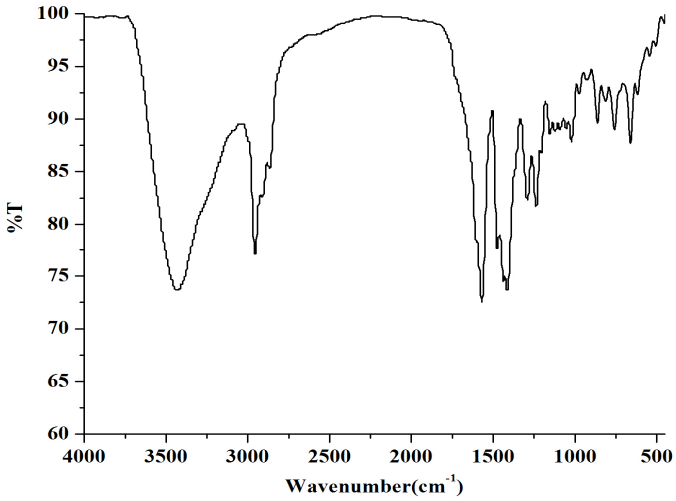

Figure A3.16 FT-IR spectrum of complex **4.2** in KBr pellet.

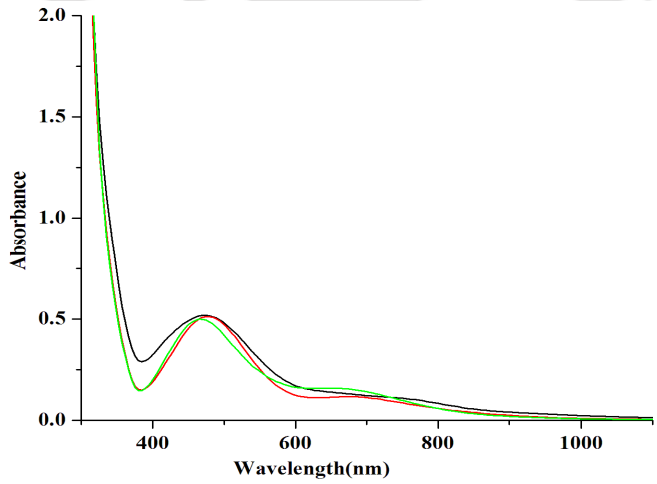

Figure A3.17 UV-visible spectra of complex **4.2** in different solvents as THF (black trace), acetonitrile (red trace) and methanol (green trace) at room temperature.

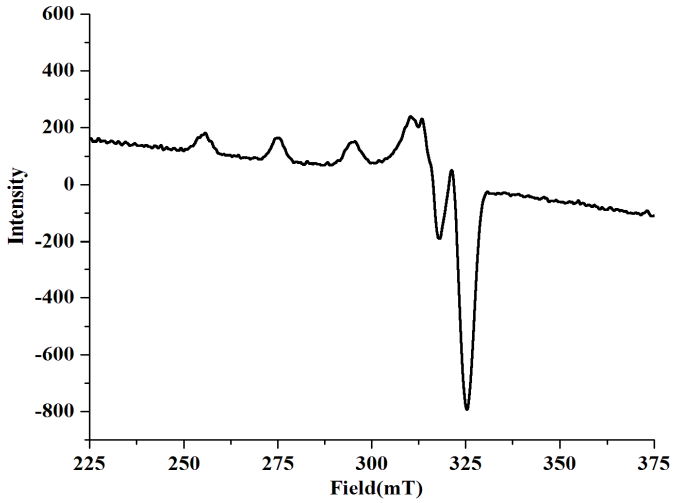

Figure A3.18 X-band EPR spectrum of complex **4.2** in dry THF at 77 K.

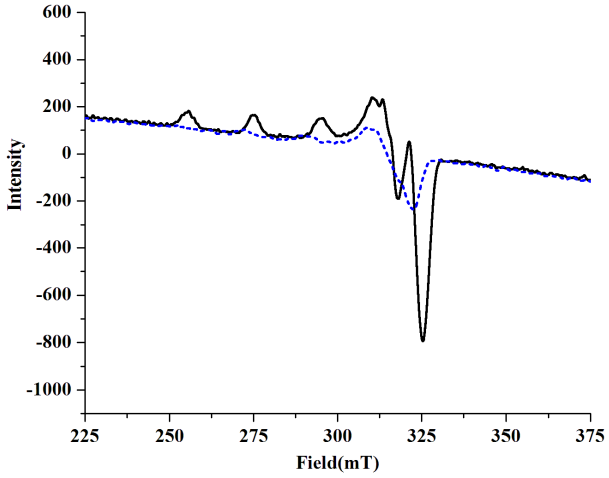

Figure A3.19 X-band EPR spectra of complex **4.2** (black trace) and phenoxyl radical intermediate (blue dotted trace) at 77 K in THF.

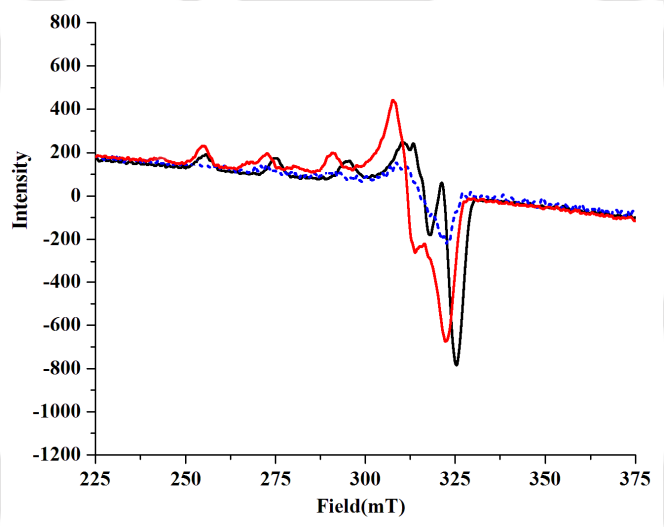

Figure A3.20 X-band EPR spectra of complex **4.2** (black trace), phenoxyl radical intermediate (blue dotted trace) and complex **4.4** (red trace) in THF at 77 K.

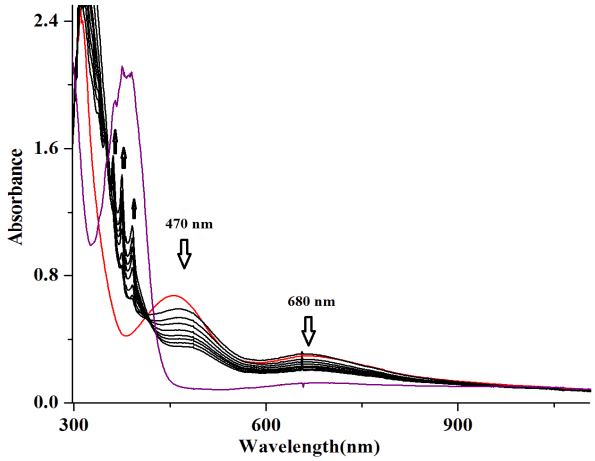

Figure A3.21 UV-visible spectra of complex **4.2** (red trace), phenoxyl radical (black traces) and final product (violet trace) in THF at -80 °C.

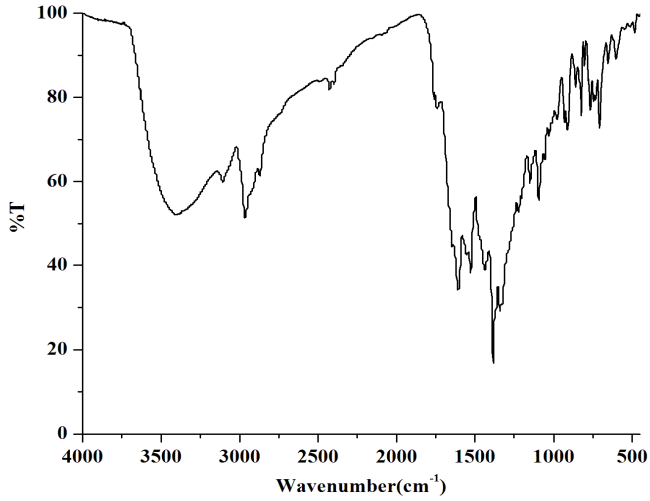

Figure A3.22 FT-IR spectrum of complex **4.4** in KBr pellet.

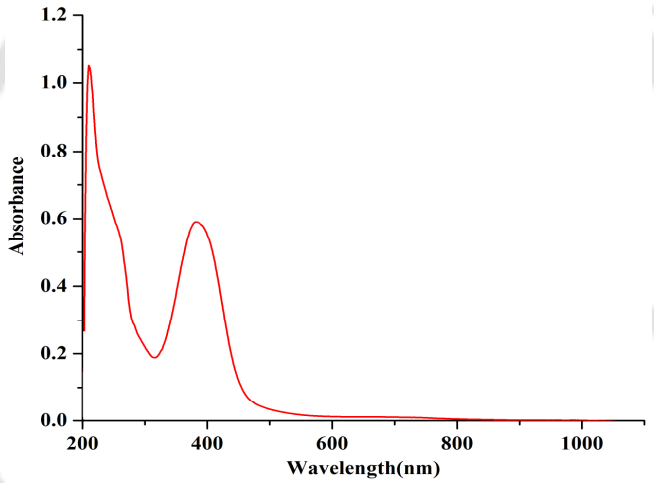

Figure A3.23 UV-visible spectrum of complex **4.4** in methanol at room temperature.

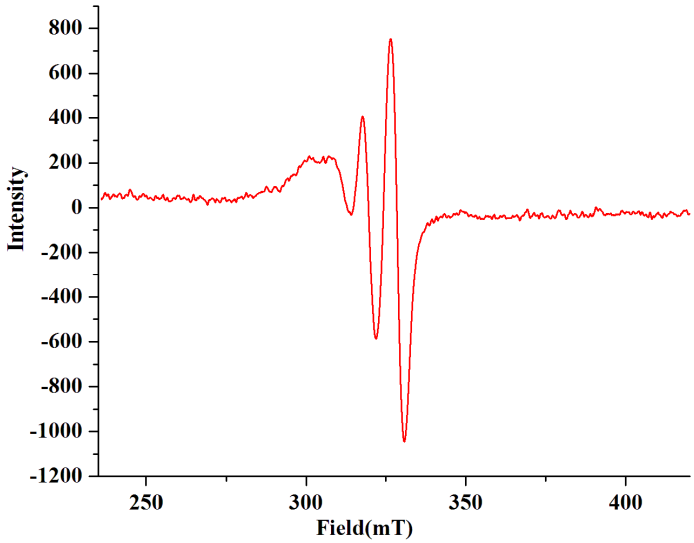

Figure A3.24 X-band EPR spectrum of complex **4.4** in methanol at room temperature.

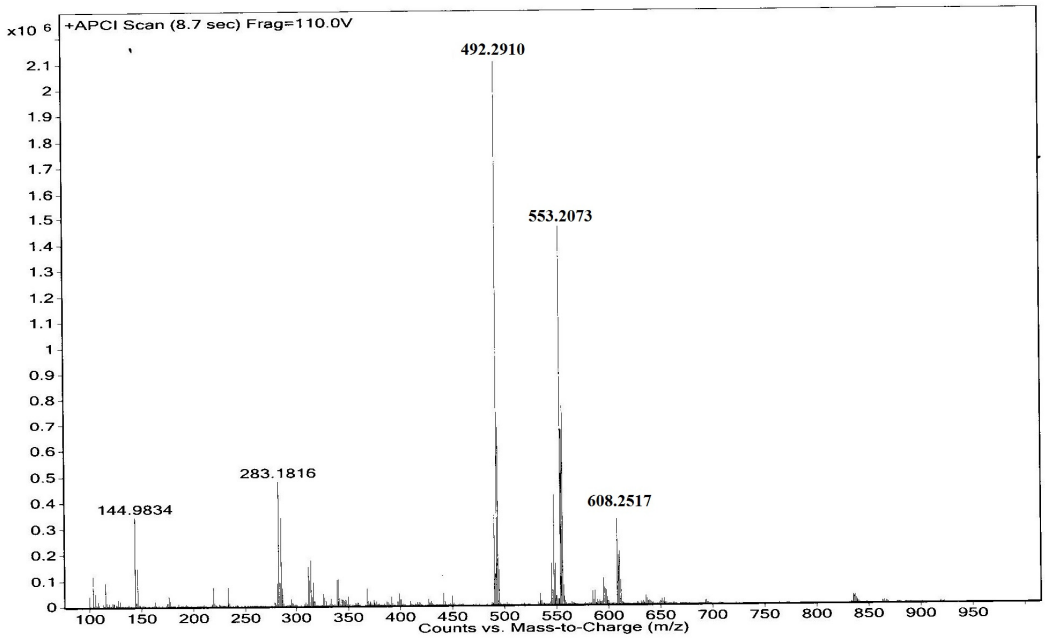

Figure A3.25 ESI-mass spectrum of complex **4.4** in methanol.

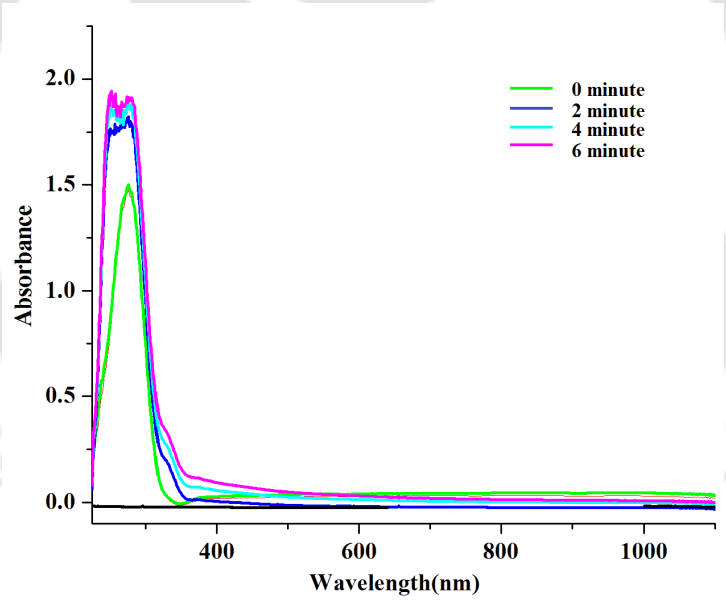

Figure A3.26 UV-visible spectra of NO_2 purged in THF at -80 °C at various time after purging.

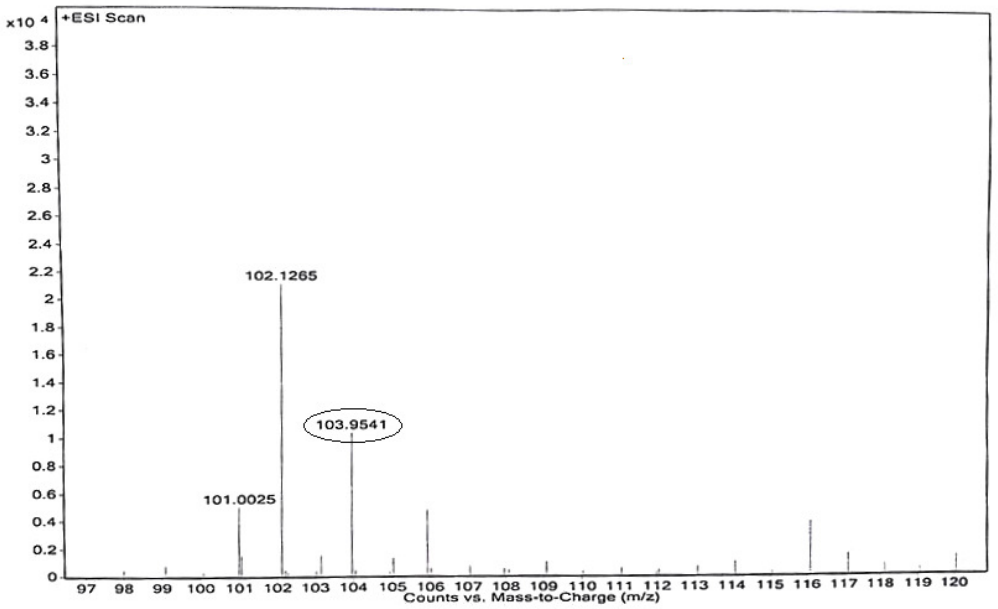

Figure A3.27 ESI-mass of $(CH_3)_3NO_2$ from the reaction of complex **4.1** with NO_2**.**

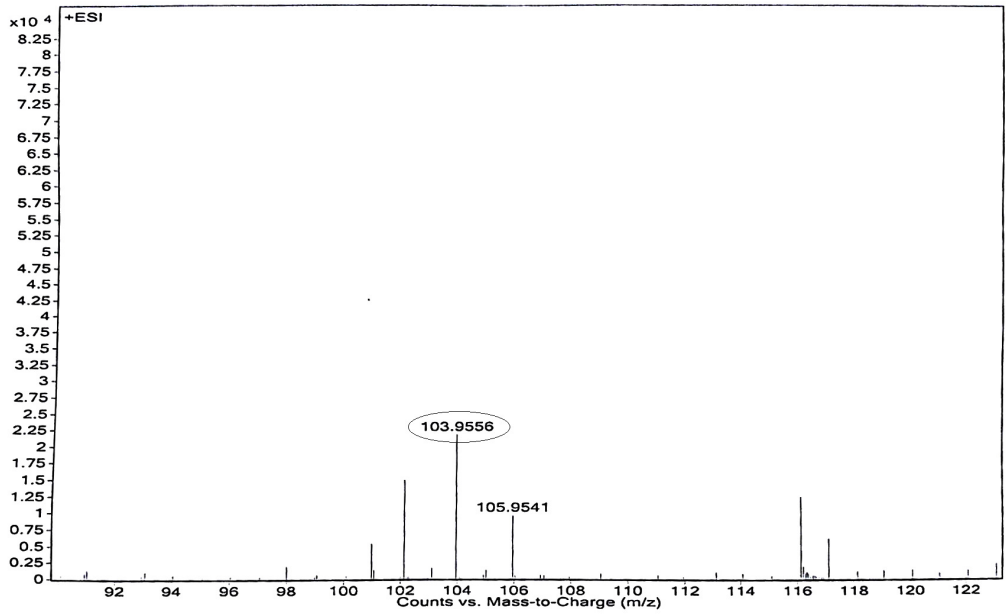

Figure A3.28 ESI-mass of $(CH_3)_3NO_2$ from the reaction of complex **4.2** with NO_2**.**

Appendix IV

Table A4.1 Crystallographic data for ligand $\mathbf{L_7}$.

	Ligand $\mathbf{L_7}$
Formulae	$C_{34}\ H_{44}\ N_2\ O$
Mol. wt.	496.71
Crystal system	Monoclinic
Space group	P2(1)/c
Temperature /K	293(2)
Wavelength /Å	0.71073
a /Å	11.4955(11)
b /Å	10.9564(13)
c /Å	23.216(2)
α/°	90.00
β/°	95.880(9)
γ/°	90.00
V/ $Å^3$	2908.7(5)
Z	4
Density/Mgm^{-3}	1.134
Abs. co-eff. /mm^{-1}	0.067
Abs. correction	multi-scan
F(000)	1080
Total no. of reflections	5110
Reflections, $I > 2\sigma(I)$	2500
Max. 2θ/°	25.00
Ranges (h, k, l)	$-13 \le h \le 13$ $-13 \le k \le 9$ $-27 \le l \le 24$
Complete to 2θ (%)	99.8
Refinement method	Full-matrix least-squares on F^2
Goof (F^2)	1.174
R indices [$I > 2\sigma(I)$]	0.0701
R indices (all data)	0.1488

Table A4.2 Selected bond lengths (Å) for ligand $\mathbf{L_7}$.

Atoms	Bond Distances (Å)	Atoms	Bond Distances (Å)
N(1) – C(1)	1.461(5)	C(27) – C(22)	1.427(5)
N(1) – C(2)	1.467(4)	O(1) – C(11)	1.375(4)
N(1) – C(3)	1.464(4)	C(31) – C(32)	1.418(6)
N(2) – C(4)	1.463(4)	C(29) – C(28)	1.389(5)
N(2) – C(20)	1.470(4)	C(6) – C(11)	1.400(5)
N(2) – C(5)	1.470(4)	C(8) – C(7)	1.376(4)
C(21) – C(22)	1.414(4)	C(8) – C(12)	1.540(5)
C(23) – C(22)	1.437(5)	C(12) – C(14)	1.524(5)

Table A4.3 Selected bond angles (°) for ligand $\mathbf{L_7}$.

Atoms	Bond Angles (°)	Atoms	Bond Angles (°)
C(2) - N(1) - C(1)	110.9(3)	C(8) - C(9) - C(10)	123.7(3)
C(1) - N(1) - C(3)	111.8(3)	C(21) - C(22) - C(23)	123.5(3)
C(4) - N(2) - C(20)	112.4(2)	C(25) - C(24) - C(23)	120.9(3)
C(4) - N(2) - C(5)	112.1(2)	C(24) - C(25) - C(26)	120.2(4)
O(1) - C(11) - C(10)	118.5(3)	C(25) - C(26) - C(27)	120.8(3)
C(11) - C(10) - C(16)	122.1(3)	C(26) - C(27) - C(28)	120.2(3)
C(17) - C(16) - C(18)	107.2(3)	C(29) - C(28) - C(27)	121.6(3)
N(2) - C(20) - C(21)	115.2(2)	C(29) - C(34) - C(21)	119.7(3)
C(20) - C(21) - C(22)	120.7(3)	C(34) - C(29) - C(28)	119.4(3)
C(5) - C(6) - C(7)	120.9(3)	C(34) - C(29) - C(30)	118.9(3)
C(11) - C(6) - C(5)	120.1(3)	-	-

Table A4.4 Crystallographic data for complex **5.1**.

	Complex **5.1**
Formulae	C_{36} H_{46} N_2 O_3 Cu
Mol. wt.	618.29
Crystal system	Monoclinic
Space group	C2/c
Temperature /K	296(2)
Wavelength /Å	0.71073
a /Å	28.2038(9)
b /Å	12.6258(4)
c /Å	22.7579(8)
α/°	90.00
β/°	128.0360(10)
γ/°	90.00
V/ Å^3	6382.9(4)
Z	8
Density/Mgm^{-3}	1.287
Abs. co-eff. /mm^{-1}	0.722
Abs. correction	none
F(000)	2632
Total no. of reflections	5622
Reflections, $I > 2\sigma(I)$	4006
Max. 2θ/°	25.00
Ranges (h, k, l)	-32≤h ≤33 -12≤ k ≤15 -26≤ l ≤ 27
Complete to 2θ (%)	100
Refinement method	Full-matrix least-squares on F^2
Goof (F^2)	1.473
R indices [$I > 2\sigma(I)$]	0.0410
R indices (all data)	0.0596

Table A4.5 Selected bond lengths (Å) for complex **5.1**.

Atoms	Bond Distances (Å)	Atoms	Bond Distances (Å)
Cu(1) - N(2)	2.079(3)	Cu(1) - N(1)	2.044(2)
Cu(1) - O(2)	1.935(2)	Cu(1) - O(1)	1.888(2)
N(2) - C(5)	1.511(3)	N(2) - C(4)	1.492(3)
N(2) - C(20)	1.510(4)	N(1) - C(3)	1.485(5)
C(4) - C(3)	1.530(4)	C(5) - C(6)	1.491(3)
C(11) - C(6)	1.399(5)	C(11) -C(10)	1.423(3)
O(2) - C(35)	1.231(6)	N(1) - C(1)	1.488(4)
N(1) - C(2)	1.494(3)	O(1) - C(11)	1.334(4)

Table A4.6 Selected bond angles (°) for complex **5.1**.

Atoms	Bond Angles (°)	Atoms	Bond Angles (°)
N(2) - Cu(1) - N(1)	86.41(9)	N(2) - Cu(1) - O(2)	165.15(9)
N(2) - Cu(1) - O(1)	94.16(9)	N(1) - Cu(1) - O(2)	94.52(9)
N(1) - Cu(1) - O(1)	159.58(9)	O(2) - Cu(1) - O(1)	90.11(9)
Cu(1) - N(1) - C(2)	113.1(2)	Cu(1) - N(1) - C(1)	106.4(2)
Cu(1) - N(1) - C(3)	108.2(2)	Cu(1) - O(1) - C(11)	125.6(2)
N(1) - C(3) - C(4)	109.7(2)	N(2) - C(4) - C(3)	110.3(2)
O(1) - C(11) - C(6)	120.1(3)	Cu(1) - N(2) - C(5)	106.2(2)
Cu(1) - N(2) - C(4)	104.6(2)	Cu(1) - O(2) - C(35)	119.0(2)

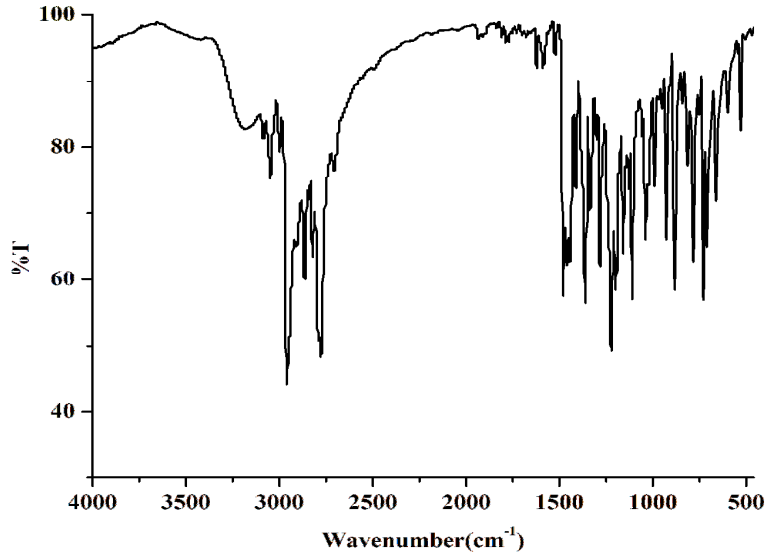

Figure A4.1 FT-IR spectrum of ligand $\mathbf{L_7}$ in KBr pellet.

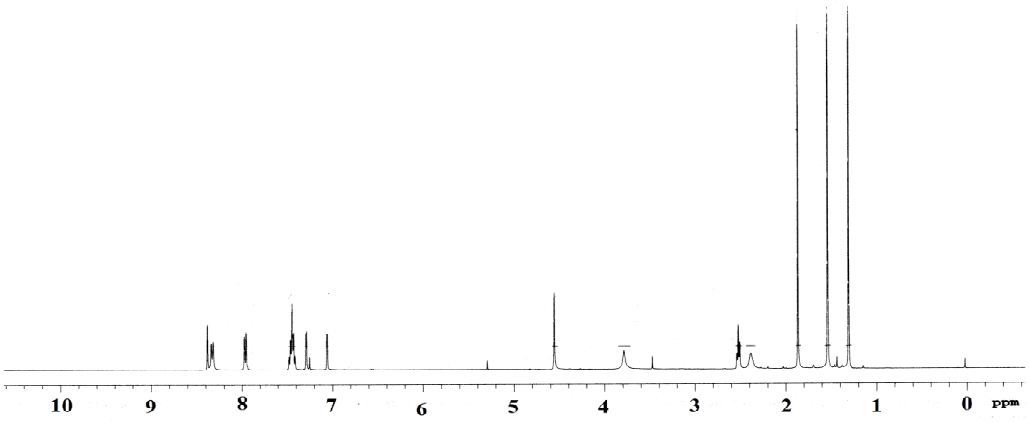

Figure A4.2 ^{1}H-NMR spectrum of ligand $\mathbf{L_7}$ in $CDCl_3$.

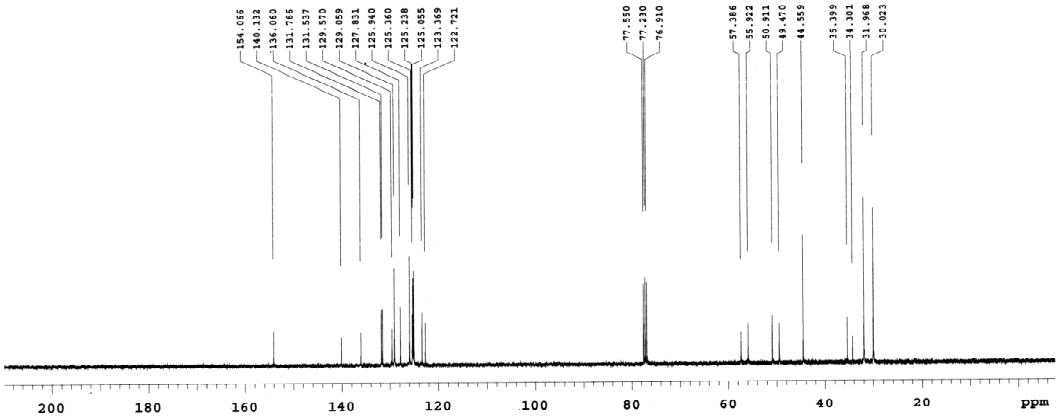

Figure A4.3 ^{13}C-NMR spectrum of ligand $\mathbf{L_7}$ in $CDCl_3$.

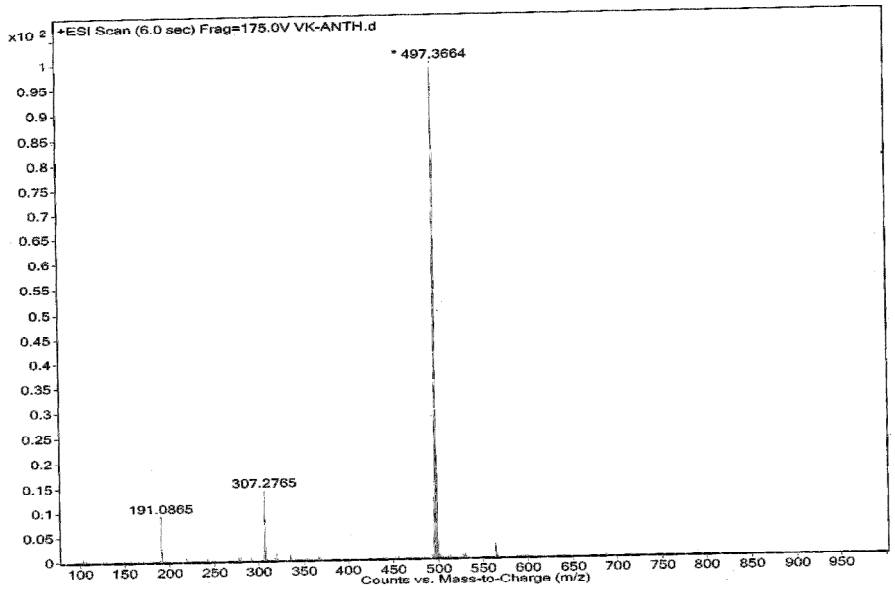

Figure A4.4 ESI-mass spectrum of ligand $\mathbf{L_7}$ in methanol.

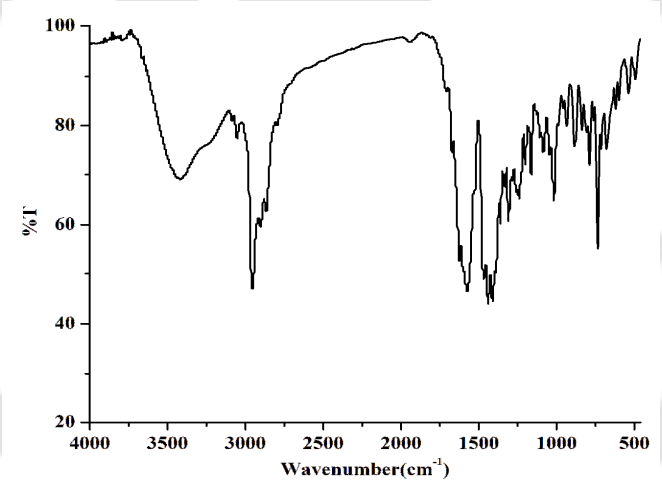

Figure A4.5 FT-IR spectrum of complex **5.1** in KBr pellet.

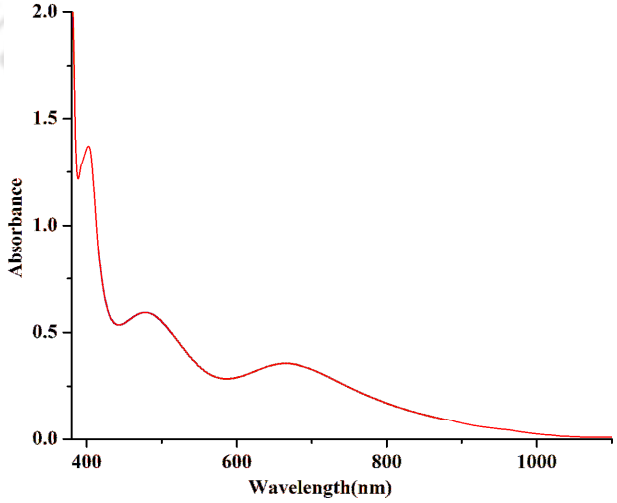

Figure A4.6 UV-visible spectrum of complex **5.1** in methanol.

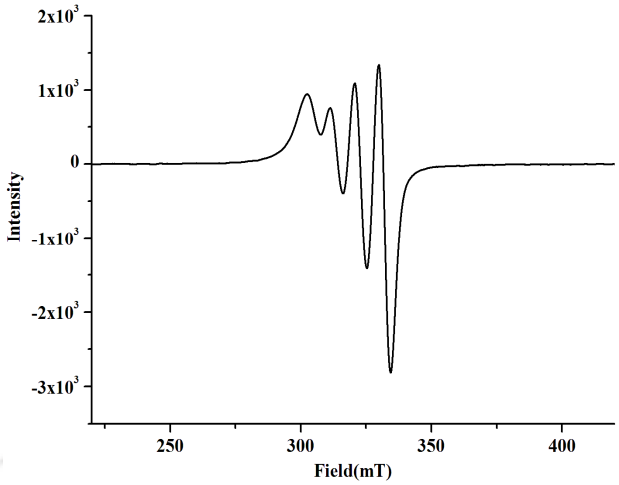

Figure A4.7 X-band EPR spectrum of complex **5.1** in methanol at room temperature.

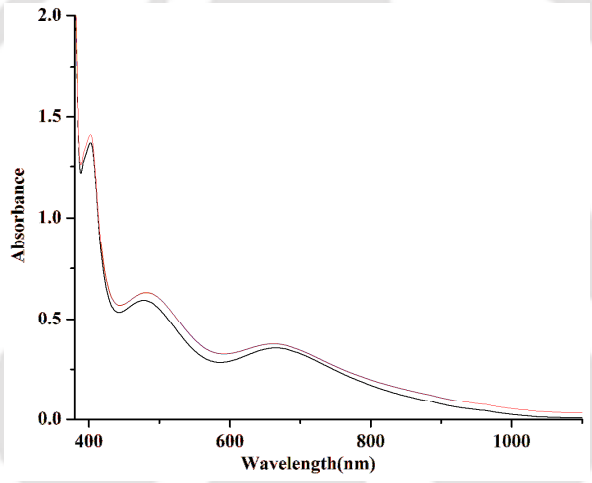

Figure A4.8 UV-visible spectra of complex **5.1** before (black trace) and after (red trace) addition of NO in methanol.

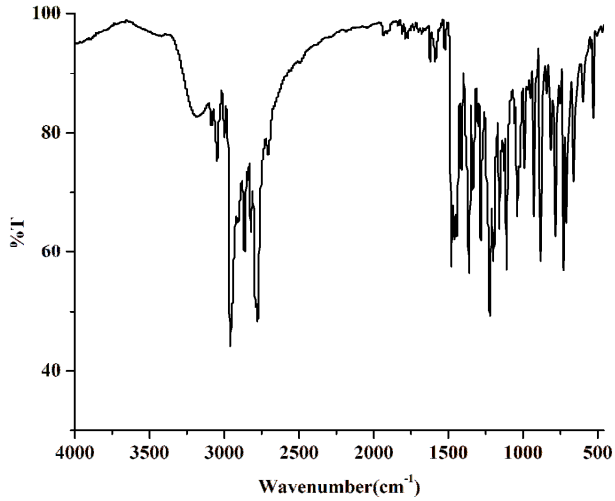

Figure A4.9 FT-IR spectrum of modified ligand $\mathbf{L_7'}$ in KBr pellet.

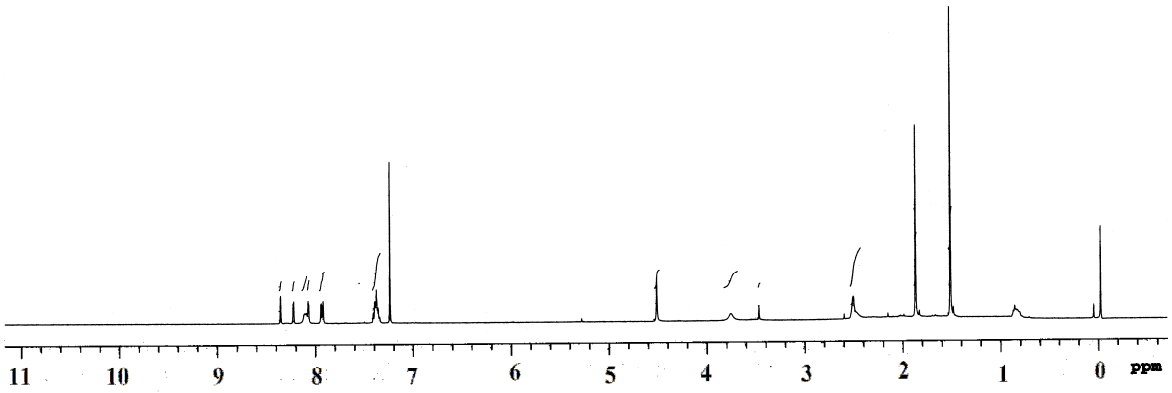

Figure A4.10 ^{1}H-NMR spectrum of modified ligand $\mathbf{L_7'}$ in $CDCl_3$.

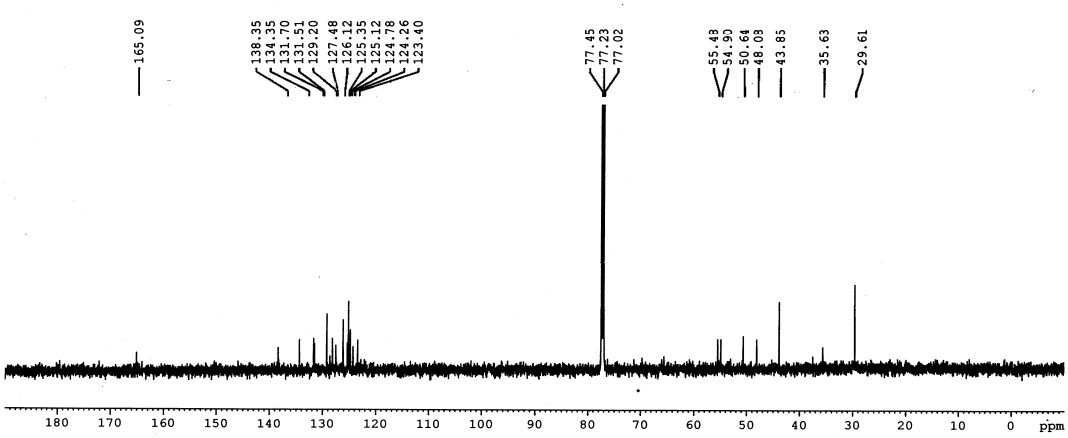

Figure A4.11 ^{13}C-NMR spectrum of modified ligand $\mathbf{L_7'}$ in $CDCl_3$.

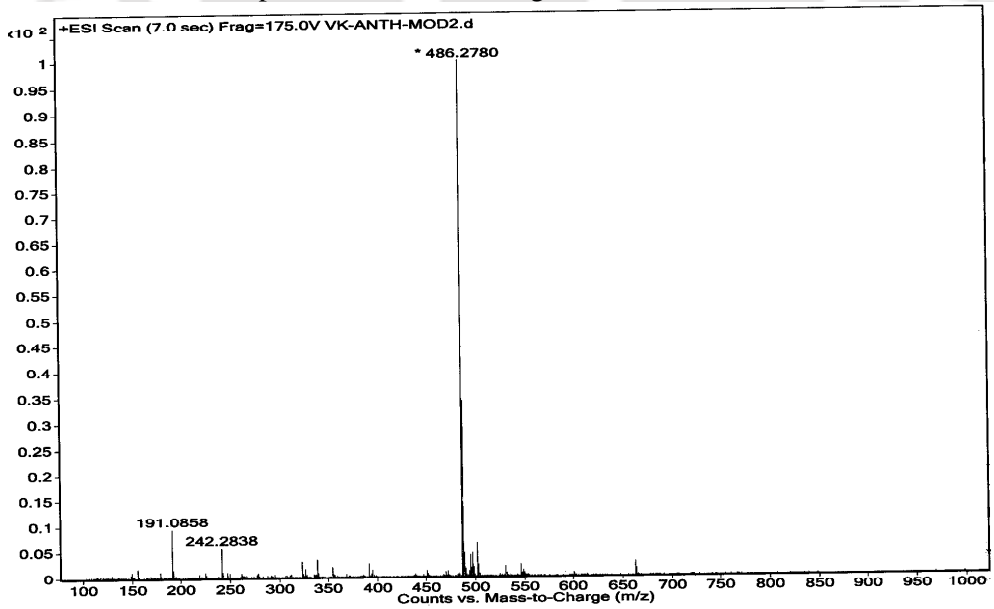

Figure A4.12 ESI-mass spectrum of modified ligand $\mathbf{L_7'}$ in methanol.

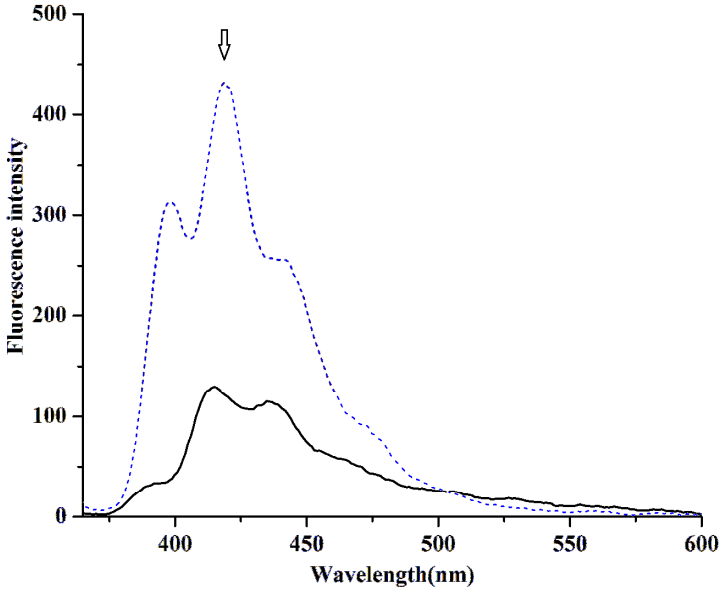

Figure A4.13 Fluorescence responses (λ_{ex}, 350 nm) for 40 μM solution of free ligand, $\mathbf{L_7}$ (dotted trace) and after addition of one equivalent of $[Cu(CH_3COO)_2.2H_2O]$ in methanol (solid trace).

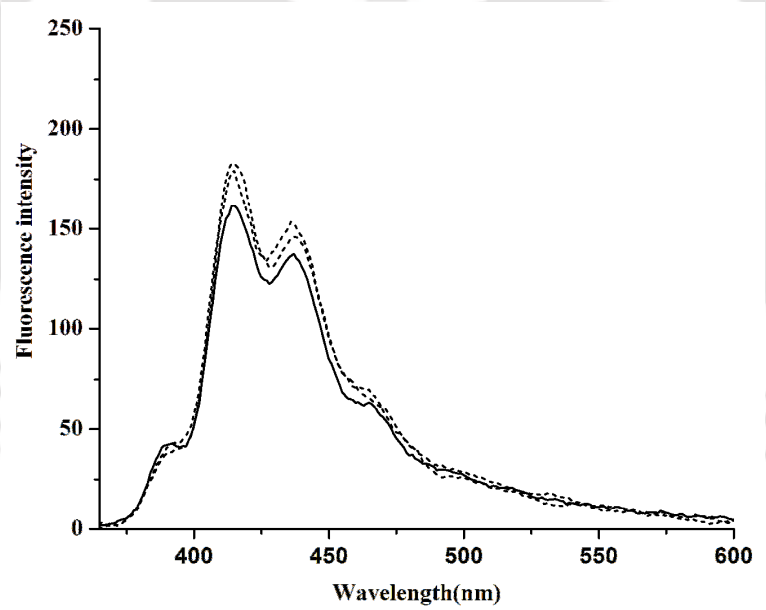

Figure A4.14 Fluorescence responses (λ_{ex}, 350 nm) of deoxygenated methanol solution (40 μM) of complex **5.1** before (solid trace) and after (dotted traces) addition of 5 equivalent of NO at 298 K.

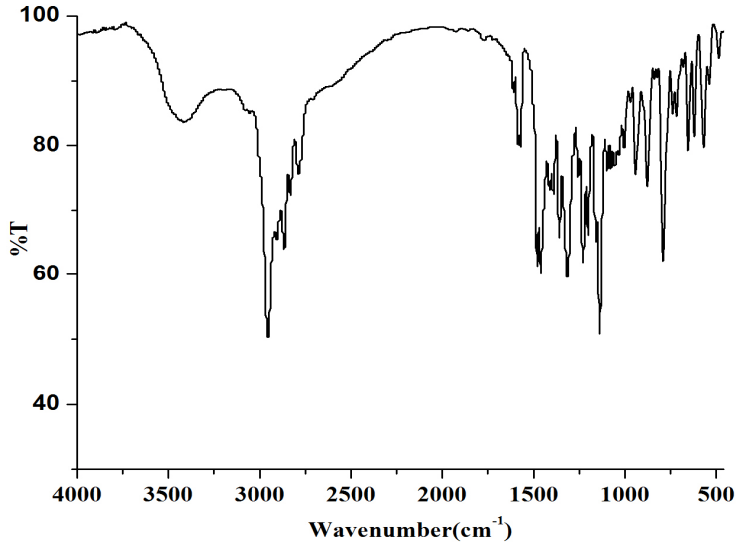

Figure A4.15 FT-IR spectrum of ligand $\mathbf{L_8}$ in KBr pellet.

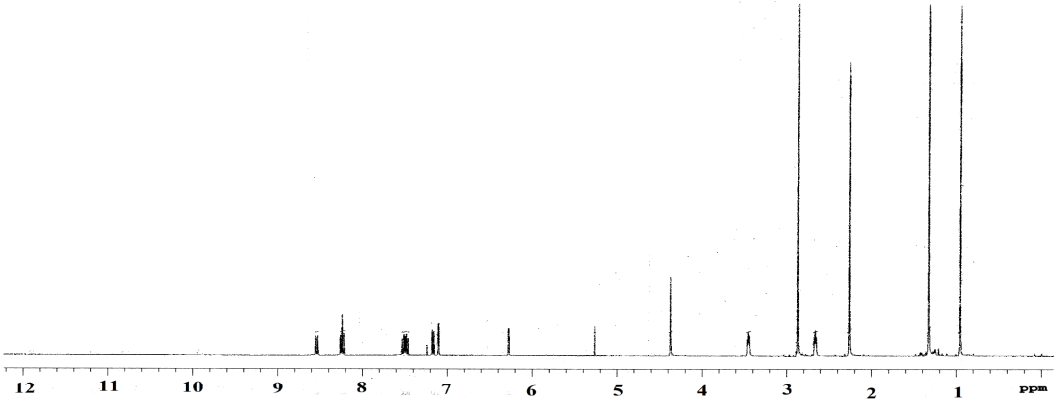

Figure A4.16 ^{1}H-NMR spectrum of ligand $\mathbf{L_8}$ in $CDCl_3$.

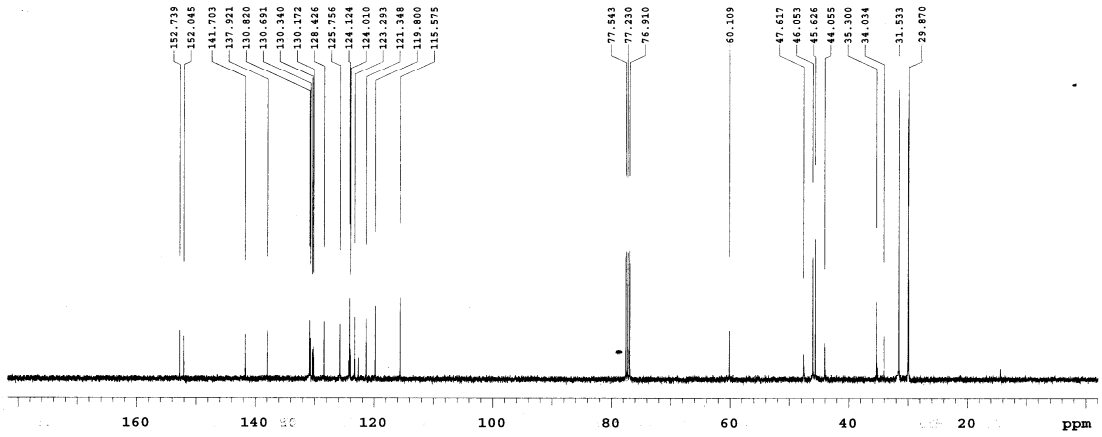

Figure A4.17 ^{13}C-NMR spectrum of ligand $\mathbf{L_8}$ in $CDCl_3$.

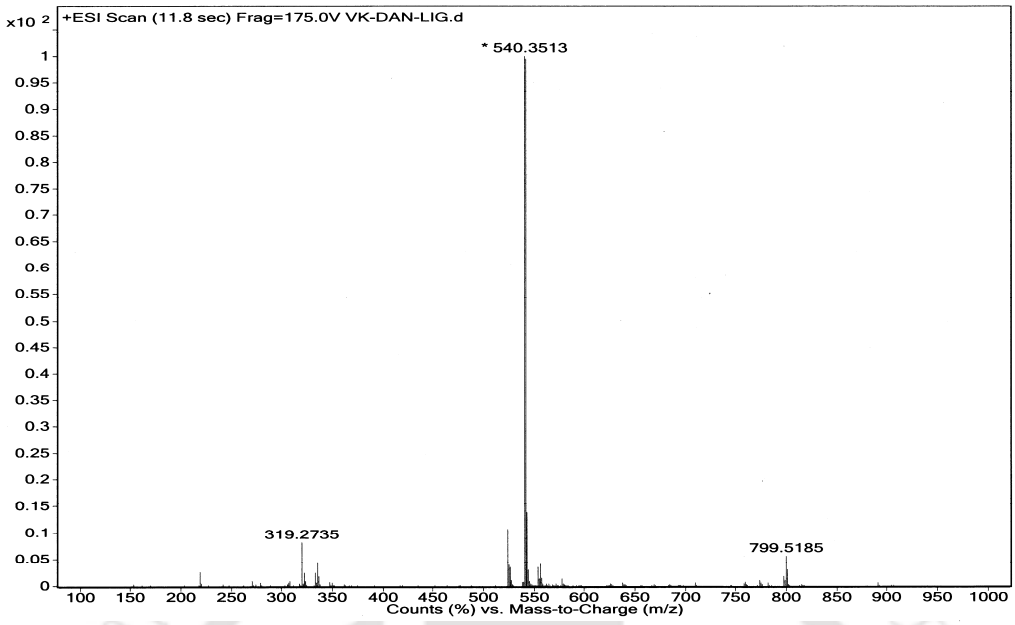

Figure A4.18 ESI-mass spectrum of ligand $\mathbf{L_8}$ in methanol.

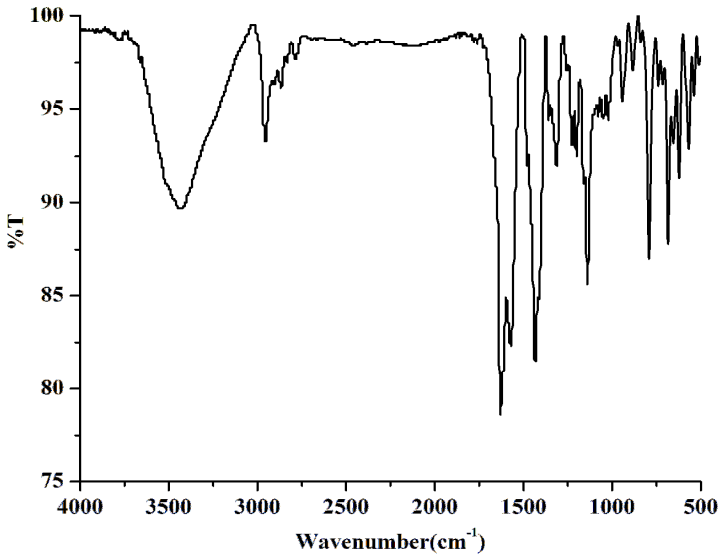

Figure A4.19 FT-IR spectrum of complex **5.2** in KBr pellet.

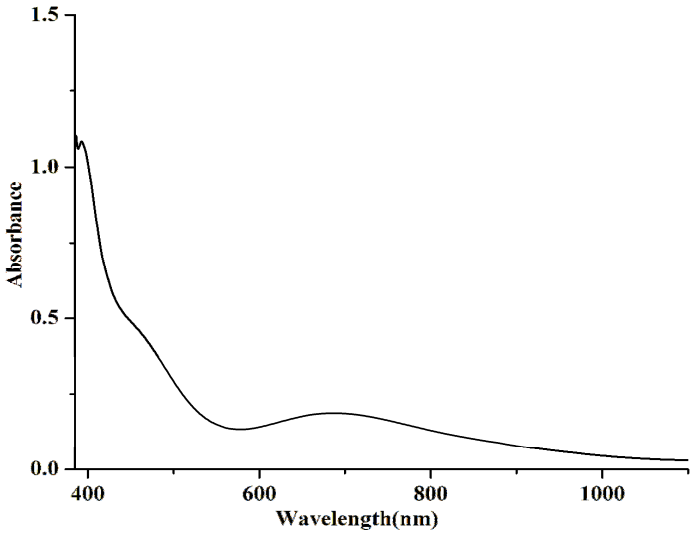

Figure A4.20 UV-visible spectrum of complex **5.2** in methanol.

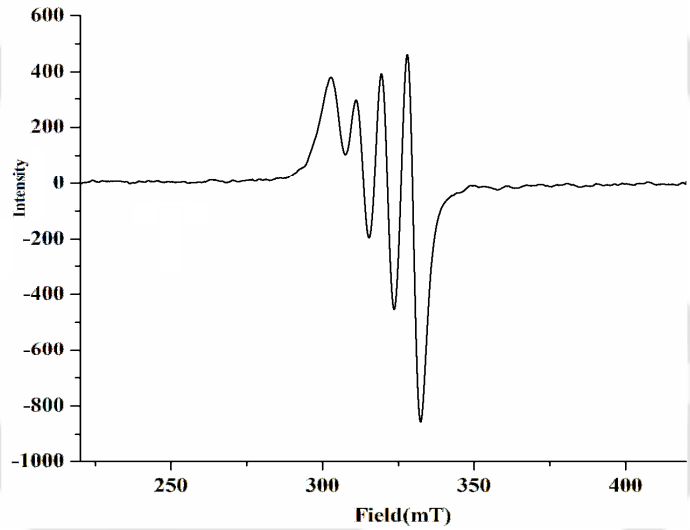

Figure A4.21 X-band EPR spectrum of complex **5.2** in methanol at room temperature.

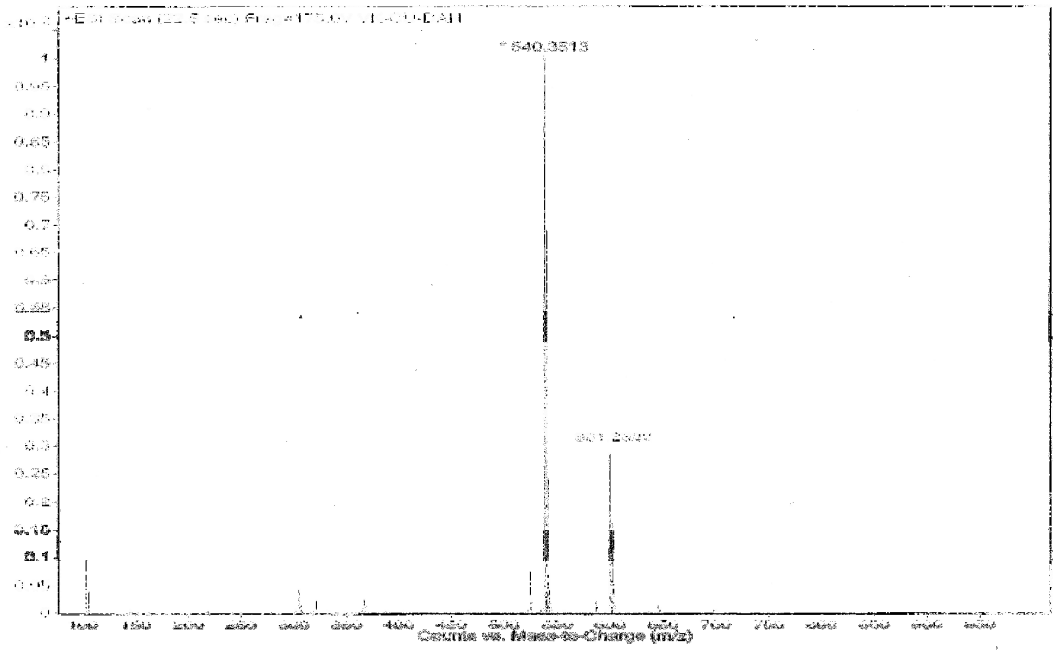

Figure A4.22 ESI-mass spectrum of complex **5.2** in methanol.

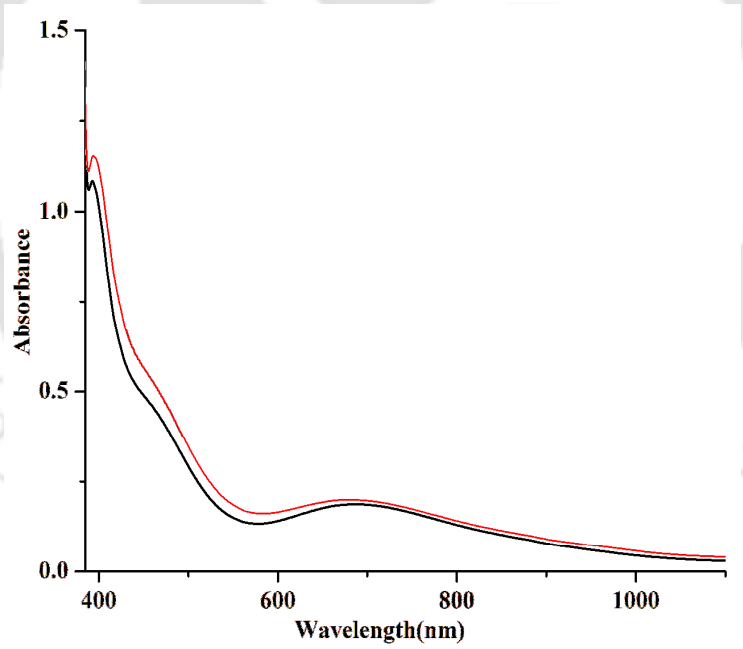

Figure A4.23 UV-visible spectra of complex **5.2** before (black trace) and after (red trace) addition of NO in methanol.

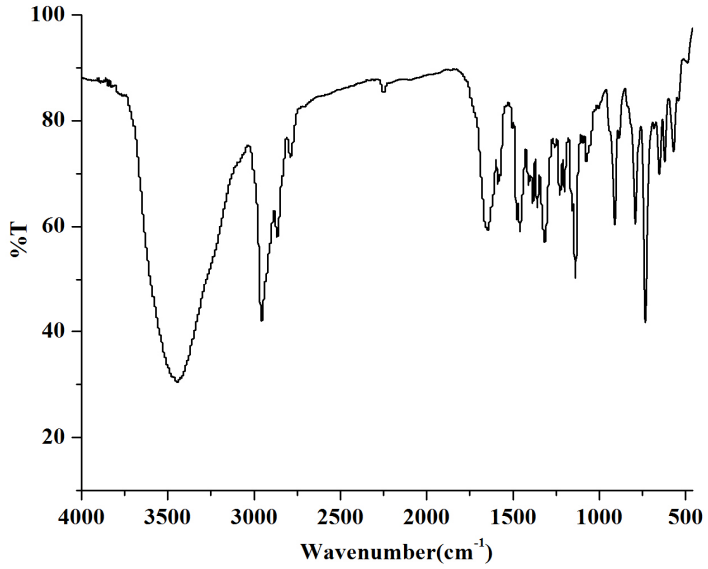

Figure A4.24 FT-IR spectrum of modified ligand $\mathbf{L_8}'$ in KBr pellet.

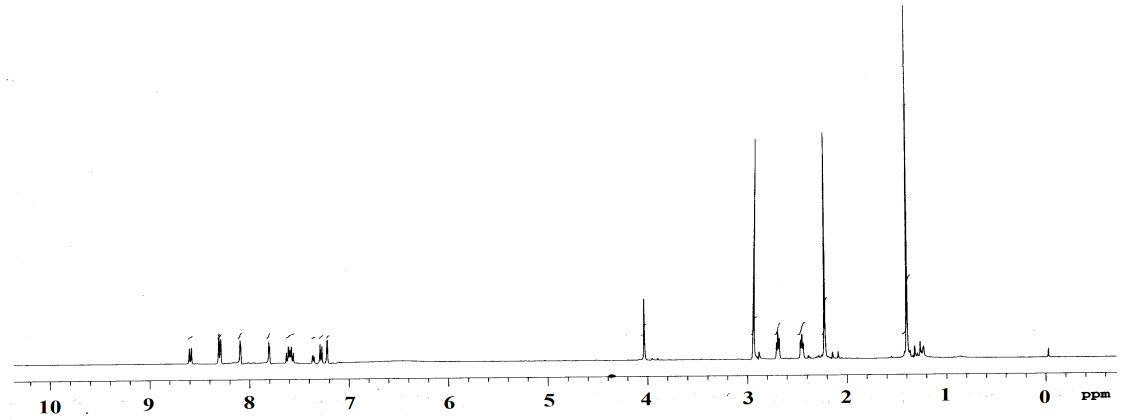

Figure A4.25 ^{1}H-NMR spectrum of ligand $\mathbf{L_8}'$ in $CDCl_3$.

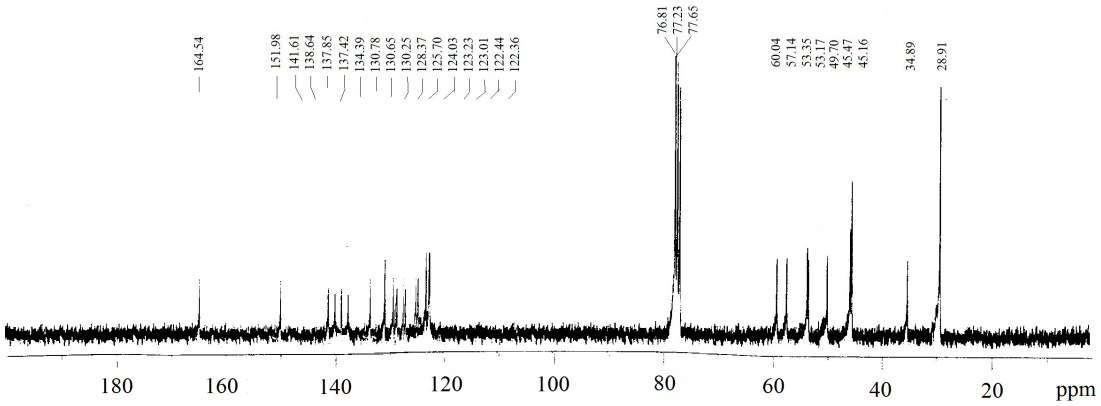

Figure A4.26 ^{13}C-NMR spectrum of ligand $\mathbf{L_8}'$ in $CDCl_3$.

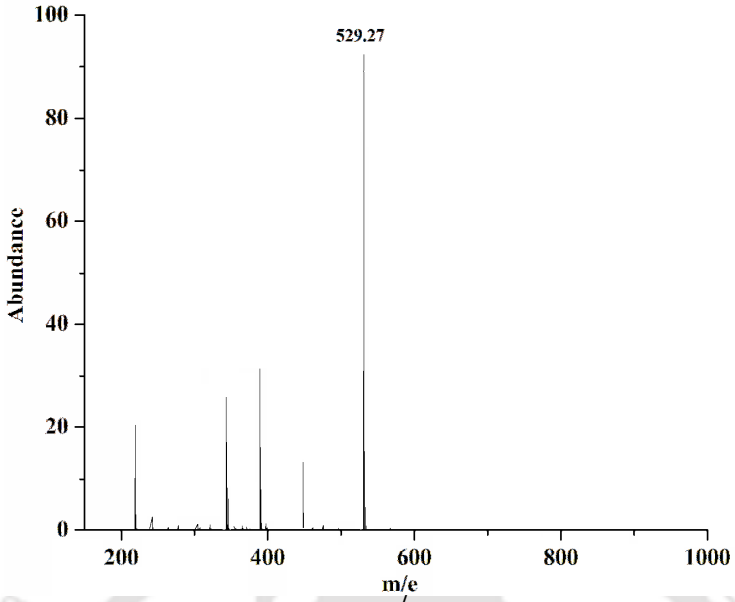

Figure A4.27 ESI-mass spectrum of ligand $\mathbf{L_8'}$ in methanol.

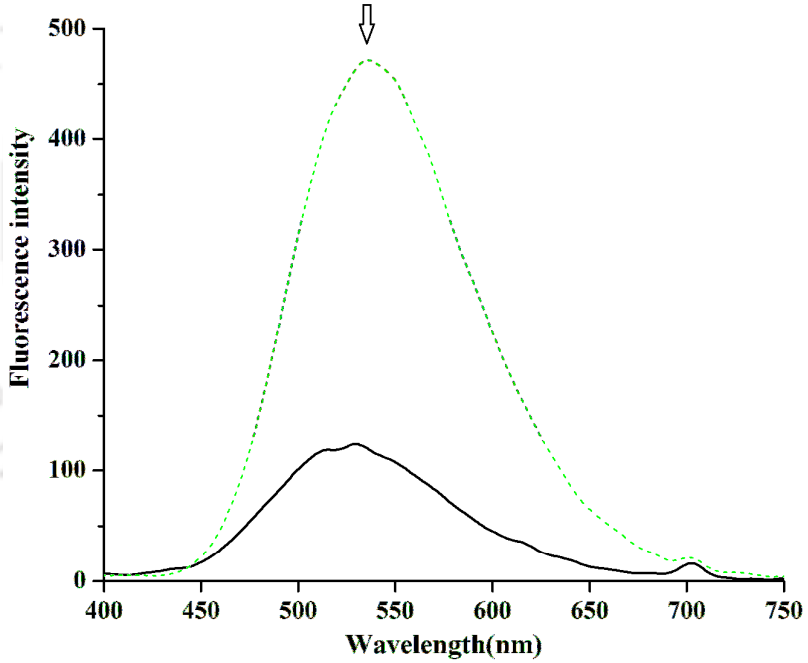

Figure A4.28 Fluorescence responses (λ_{ex}, 354 nm) for 20 μM solution of free ligand, $\mathbf{L_8}$ (dotted trace) and after addition of one equivalent of $[Cu(CH_3COO)_2.2H_2O]$ in methanol(solid trace).

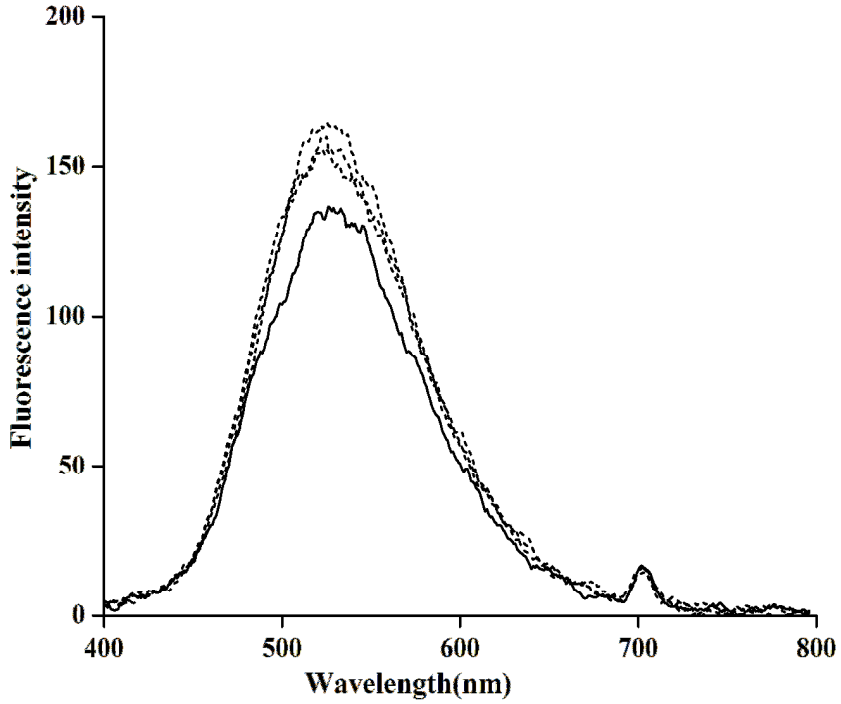

Figure A4.29 Fluorescence responses (λ_{ex}, 354 nm) of deoxygenated methanol solution (20 μM) of complex **5.2** before (solid trace) and after (dotted traces) addition of 5 equivalent of NO at 298 K.

Appendix V

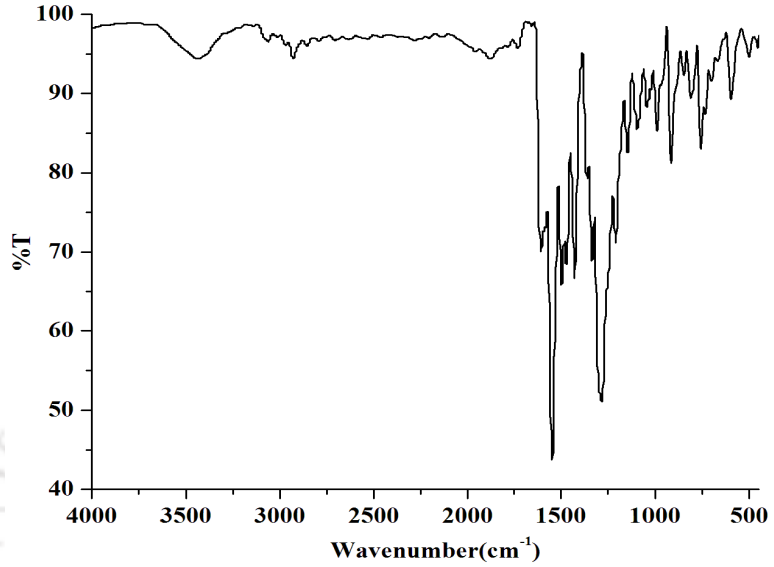

Figure A5.1 FT-IR spectrum of ligand **L_9** in KBr pellet.

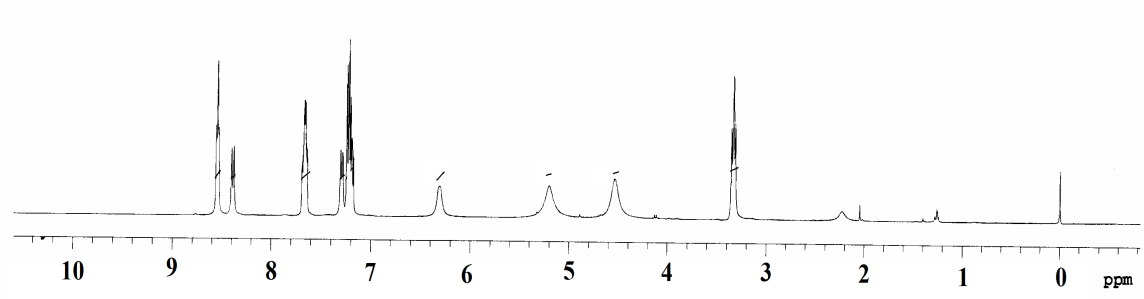

Figure A5.2 ^{1}H-NMR spectrum of ligand **L_9** in $CDCl_3$.

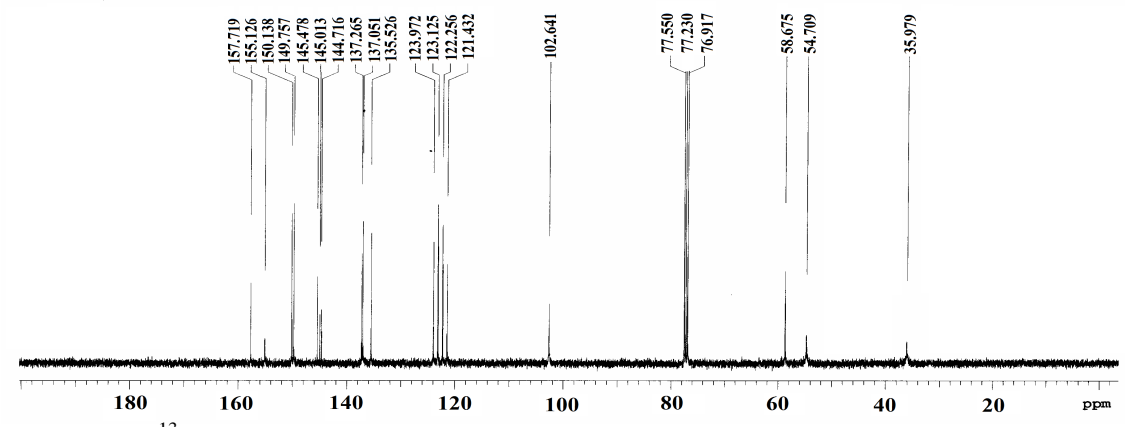

Figure A5.3 ^{13}C-NMR spectrum of ligand **L_9** in $CDCl_3$.

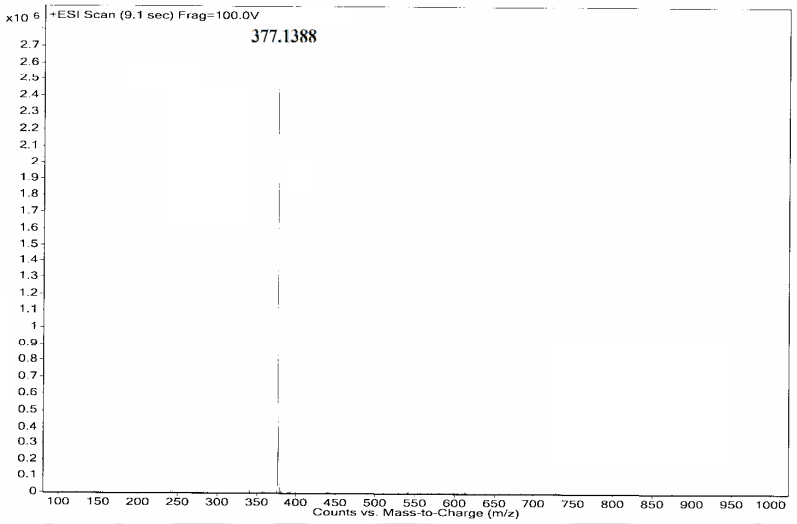

Figure A5.4 ESI mass spectrum of ligand **L_9** in methanol.

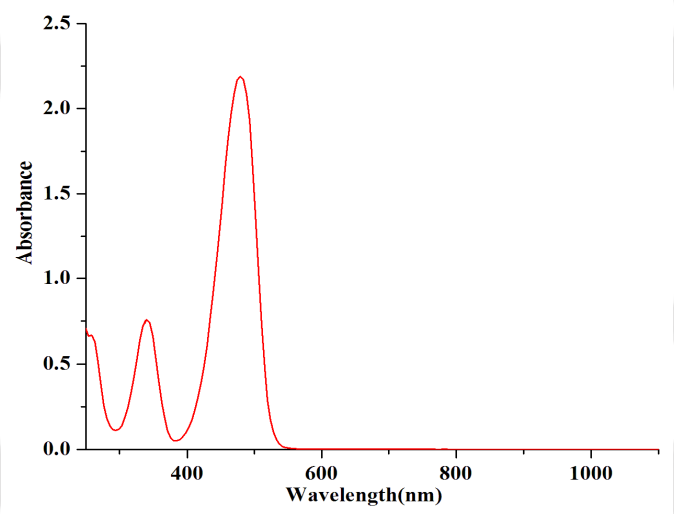

Figure A5.5 UV-visible spectrum of ligand **L_9** in acetonitrile medium.

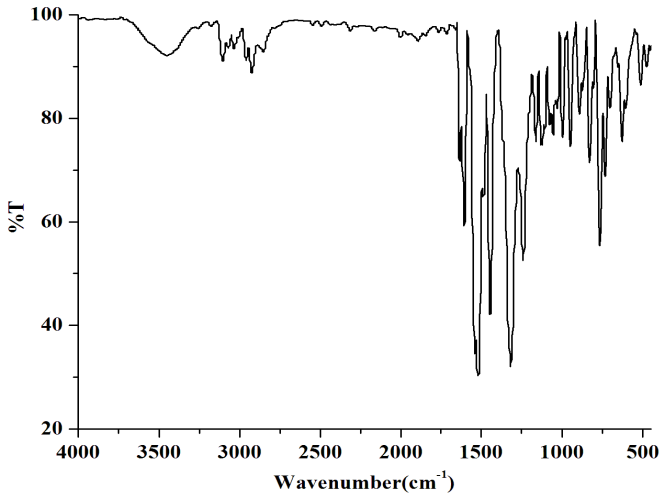

Figure A5.6 FT-IR spectrum of complex **6.1** in KBr pellet.

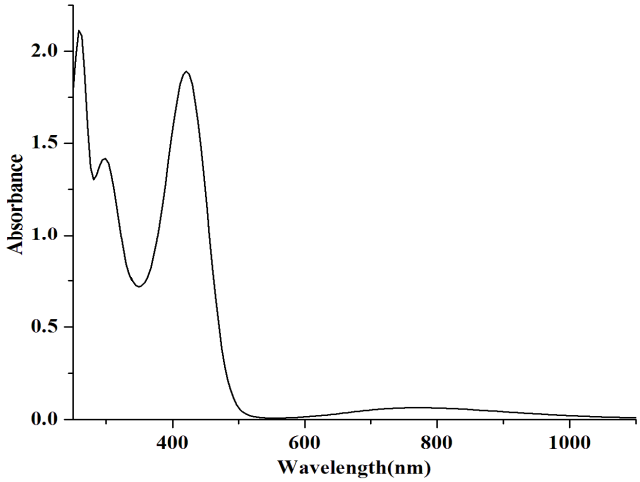

Figure A5.7 UV-visible spectrum of complex **6.1** in acetonitrile.

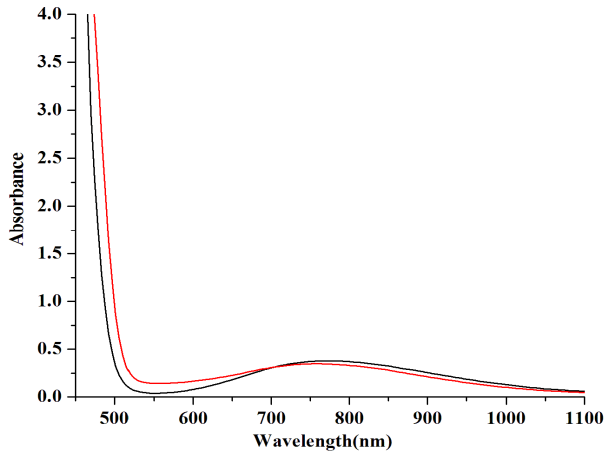

Figure A5.8 X-band EPR spectra of complex **6.1** (black trace) and after addition of excess NO (red trace) in acetonitrile medium.

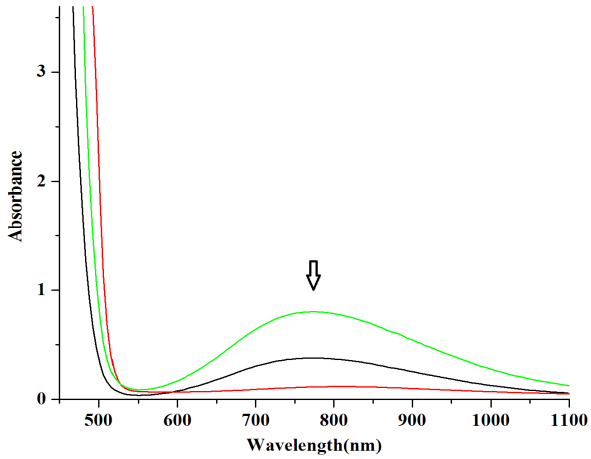

Figure A5.9 UV-visible spectra of complex **6.1** (green trace) and after addition of NO in presence of oxygen at in acetonitrile medium.

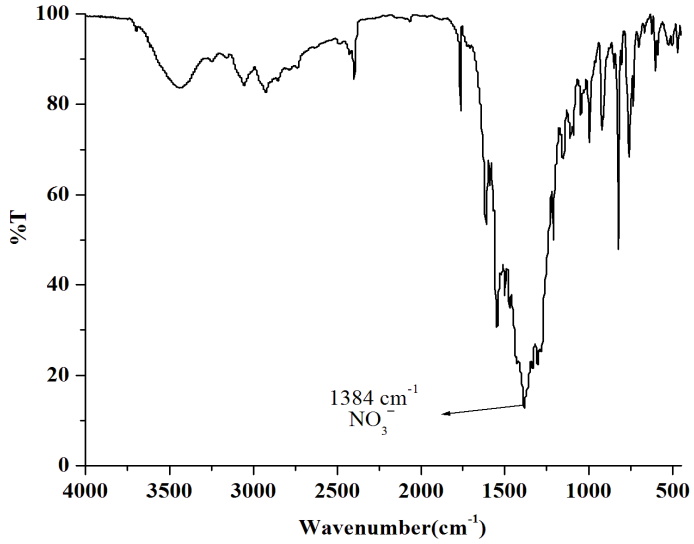

Figure A5.10 FT-IR spectrum of complex **6.1** after addition of NO_2 in acetonitrile medium in KBr pellet.

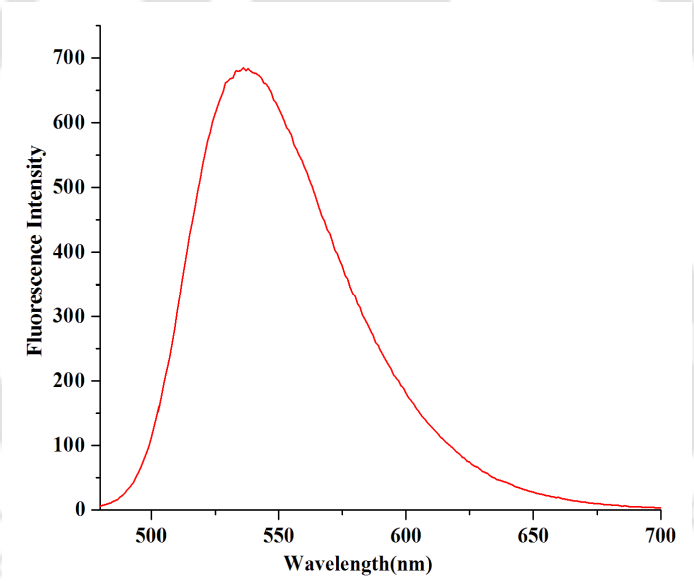

Figure A5.11 Fluorescence response (λ_{ex}, 470 nm) for 5 μM solution of ligand **L_9** in acetonitrile medium.

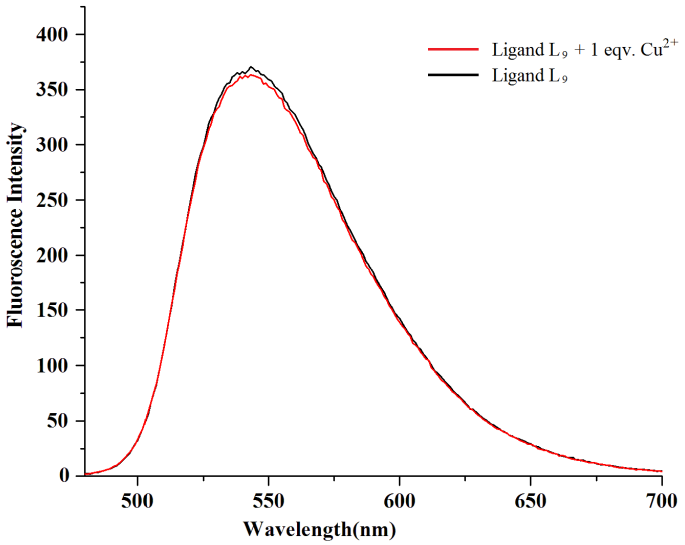

Figure A5.12 Fluorescence response (λ_{ex}, 470 nm) for 5 μM solution of ligand **L_9** (black trace), and after addition of one equivalent of $CuCl_2.2H_2O$ (red trace) in water medium.

Lists of Publications

1. **Nitric oxide reactivity of copper(II) complexes of bidentate amine ligands: effect of chelate ring size on the stability of a [Cu^{II}–NO] intermediate**

Sharma, M.; **Kumar**, **V**.; Kalita, A.; Deka, R.C.; Mondal, B.
Dalton Trans. **2012**, 41, 9543

2. **Phenol ring nitration induced by the unprecedented reduction of the Cu(II) centre by nitrogen dioxide**

Kumar, **V**.; Kalita, A.; Mondal, B.
Dalton Trans. **2013**, 42, 16264

3. **A fluorescence turn-on probe for selective detection of nitrogen dioxide**

Kumar, **V**.; Mondal, B.
RSC Adv. **2014**, *4*, 61944

4. **C-Nitrosation of a β-diketiminate ligand incopper(II) complex**

Kalita, A.; **Kumar**, **V**.; Mondal, B.
RSC Adv. **2015**, *5*, 643

5. **First Nitric oxide reactivity of copper(II) complexes of bidentate amine ligands**

Kalita, A.; **Kumar**, **V**.; Mondal, B.
Inorganica Chemica Acta. **2015**, *430*, 55

6. **Oxo transfer from nitrogen dioxide to nitrito group in a copper(II) complex**

Gogoi, K.; Deka, H.; **Kumar**, **V**.; Mondal, B.
Inorg. Chem. **2015**, *54,* 4799.

7. **Copper(II) mediated phenol ring nitration by nitrogen dioxide**
Kumar, **V.**; Ghosh, S.; Mondal, B.
Dalton Trans. **2015***, xx,* xxxx.

8. **A new NBD-based fluorogenic turn-on probe for selective detection of NO_2**

Kumar, **V**.; Mondal, B.
(communicated)